

2016-01-01

# National Evaluation For Development And Exploration Potential Of Mineral Commodities In Produced Waters

Stephanie Ray

*University of Texas at El Paso*, [stephanieray6@yahoo.com](mailto:stephanieray6@yahoo.com)

Follow this and additional works at: [https://digitalcommons.utep.edu/open\\_etd](https://digitalcommons.utep.edu/open_etd)



Part of the [Civil Engineering Commons](#), [Geochemistry Commons](#), and the [Geology Commons](#)

---

## Recommended Citation

Ray, Stephanie, "National Evaluation For Development And Exploration Potential Of Mineral Commodities In Produced Waters" (2016). *Open Access Theses & Dissertations*. 931.  
[https://digitalcommons.utep.edu/open\\_etd/931](https://digitalcommons.utep.edu/open_etd/931)

This is brought to you for free and open access by DigitalCommons@UTEP. It has been accepted for inclusion in Open Access Theses & Dissertations by an authorized administrator of DigitalCommons@UTEP. For more information, please contact [lweber@utep.edu](mailto:lweber@utep.edu).

NATIONAL EVALUATION FOR DEVELOPMENT AND EXPLORATION POTENTIAL OF  
MINERAL COMMODITIES IN PRODUCED WATERS

STEPHANIE RAY

Masters Program in Geological Sciences

APPROVED:

---

Philip Goodell, Ph.D., Chair

---

Mark Engle, Ph.D.

---

Shane Walker, Ph.D.

---

Charles Ambler, Ph.D.  
Dean of the Graduate School

Copyright ©

by

Stephanie Ray

2016

## **Dedication**

To my children: Andrea and John, “with hard work and dedication, everything is possible”.

NATIONAL EVALUATION FOR DEVELOPMENT AND EXPLORATION  
POTENTIAL OF MINERAL COMMODITIES IN PRODUCED WATERS

by

STEPHANIE RAY, B.S in Geological Sciences

THESIS

Presented to the Faculty of the Graduate School of

The University of Texas at El Paso

in Partial Fulfillment

of the Requirements

for the Degree of

Master of Science

Geological Sciences

THE UNIVERSITY OF TEXAS AT EL PASO

May 2016

## **Acknowledgements**

Dr. Mark Engle and the United States Geological Survey Energy Resources Program for funding. Dr. Philip Goodell, Professor in Geological Sciences; my advisor and Dr. Shane Walker, Professor in Civil Engineering; my advisor.

## **Abstract**

The U.S. Geological Survey recently updated a geochemical database consisting of data for approximately 160,000 produced waters samples, primarily from petroleum and geothermal reservoirs. Using major and trace elements from conventional and unconventional well types from the database, this thesis provides a comprehensive, national evaluation for mineral commodity potential in produced waters. Produced waters contain virtually every naturally occurring element and can range in salinity to several times that of seawater. Despite the typical outlook to view produced waters as a waste, they have potential for natural resource development.

This thesis provides, for each mineral commodity found in the produced waters database, maps showing the distribution of concentration, economic values of mineral commodities, and statistical analysis, for the contiguous United States. The maps identify areas of interest for both resource potential and show the largest priority for future mineral exploration; as well as to identify data gaps and needs for future exploration. Identified constituents in concentrations at some locations exceed disposal costs and hold the greatest potential for profit: cesium, bromine, lithium carbonate, iodine, lithium chloride, magnesium, potash, soda ash, rubidium formate, and rubidium chloride. From these commodities, further data exploration would be required for rubidium formate, rubidium chloride and cesium. To maximize potential for development of produced waters is grouping minerals commodities to increase revenues. Either through selective or grouped removal for commodities, produced waters have potential for economic development. It may be possible to no longer consider produced waters as a waste product and a new viable resource.

## Table of Contents

Acknowledgements.....	v
Abstract.....	vi
Table of Contents.....	vii
List of Tables .....	xvii
List of Figures.....	xviii
Chapter 1: Introduction and Statement of the Problem .....	1
1.2 Objectives: .....	6
Chapter 2. Background .....	7
2.2 Geochemistry of Basinal Brines .....	8
2.2.1 Subsurface basinal brine origins and evolution .....	8
2.2.2 Characterization of Brines .....	9
2.2.3 Localized sources of salinity:.....	11
2.2.4 pH and Alkalinity.....	12
2.2.5 Basin Lithology.....	13
2.2.5.1 Carbonate Lithologies.....	13
2.2.5.2. Silicate Lithologies .....	13
Chapter 3.0 Disposal Costs .....	15
Chapter 4.0 Methods.....	19
Chapter 5.0 Mineral Commodities.....	23
5.1 Barium.....	25
5.1.1 Commodity: .....	25
5.1.2 Geochemical Statistics:.....	25
5.1.3 Summary Statistics: .....	26
5.1.4 Kendall Tau:.....	26
5.1.5 Maps:.....	27
5.1.5.1 Spatial Data .....	27
5.1.5.2 Estimated Economic Values for Barium.....	28
5.1.6 Summary:.....	29

5.2 Boron.....	30
5.2.1 Commodity: .....	30
5.2.2 Geochemical Statistics: .....	30
5.2.3 Summary Statistics: .....	31
5.2.4 Kendall Tau:.....	31
5.2.5 Maps:.....	32
5.2.5.1 Spatial Data.....	32
5.2.5.2 Estimated Economic Values for Boron.....	33
5.2.6 Summary: .....	34
5.3 Bromine.....	35
5.3.1 Commodity: .....	35
5.3.2 Geochemical Statistics: .....	35
5.3.3 Summary Statistics: .....	36
5.3.4 Kendall Tau correlation: .....	36
5.3.5 Maps:.....	38
5.3.5.1 Spatial Distribution: .....	38
5.3.5.2 Estimated Economic Values: .....	39
5.3.6 Summary: .....	40
5.4 Cadmium.....	42
5.4.1 Commodity: .....	42
5.4.2 Geochemical Statistics: .....	42
5.4.3 Summary Statistics: .....	43
5.4.4 Kendall Tau correlation: .....	43
5.4.5 Maps:.....	44
5.4.5.1 Spatial Distribution: .....	44
5.4.5.2 Estimated Economic Values: .....	45
5.4.6 Summary: .....	46
5.5 Calcium.....	47
5.5.1 Commodity: .....	47
5.5.2 Geochemical Statistics: .....	47
5.5.3 Summary Statistics: .....	48
5.5.4 Kendall Tau correlation: .....	48
5.5.5 Maps:.....	49

5.5.5.1 Spatial Distribution: .....	49
5.5.5.2 Estimated Economic Values: .....	50
5.5.6 Summary: .....	51
5.6 Cesium .....	53
5.6.1 Commodity: .....	53
5.6.2 Geochemical Statistics: .....	53
5.6.3 Summary Statistics: .....	54
5.6.4 Kendall Tau correlation: .....	54
5.6.5 Maps: .....	55
5.6.5.1 Spatial Distribution: .....	55
5.6.5.2 Estimated Economic Values: .....	56
5.6.6 Summary: .....	57
5.7 Chromium .....	58
5.7.1 Commodity: .....	58
5.7.2 Geochemical Statistics: .....	58
5.7.3 Summary Statistics: .....	59
5.7.4 Kendall Tau correlation: .....	59
5.7.5 Maps: .....	60
5.7.5.1 Spatial Distribution: .....	60
5.7.5.2 Estimated Economic Values: .....	61
5.7.6 Summary: .....	62
5.8 Cobalt .....	63
5.8.1 Commodity: .....	63
5.8.2 Geochemical Statistics: .....	63
5.8.3 Summary Statistics: .....	64
5.8.4 Kendall Tau correlation: .....	64
5.8.5 Maps: .....	65
5.8.5.1 Spatial Distribution: .....	65
5.8.5.2 Estimated Economic Values: .....	66
5.8.6 Summary: .....	67
5.9 Copper .....	68
5.9.1 Commodity: .....	68
5.9.2 Geochemical Statistics: .....	68

5.9.3 Summary Statistics: .....	69
5.9.4 Kendall Tau correlation: .....	69
5.9.5 Maps:.....	70
5.9.5.1 Spatial Distribution: .....	70
5.9.5.2 Estimated Economic Values: .....	71
5.9.6 Summary:.....	72
5.10 Fluorspar .....	73
5.10.1 Commodity: .....	73
5.10.2 Geochemical Statistics: .....	73
5.10.3 Summary Statistics: .....	74
5.10.4 Kendall Tau correlation: .....	74
5.10.5 Maps:.....	75
5.10.5.1 Spatial Distribution: .....	75
5.10.5.2 Estimated Economic Values: .....	76
5.10.6 Summary:.....	77
5.11 Iodine .....	78
5.11.1 Commodity: .....	78
5.11.2 Geochemical Statistics: .....	78
5.11.3 Summary Statistics: .....	79
5.11.4 Kendall Tau correlation: .....	79
5.11.5 Maps:.....	80
5.11.5.1 Spatial Distribution: .....	80
5.11.5.2 Estimated Economic Values: .....	81
5.11.6 Summary:.....	82
5.12 Lead.....	83
5.12.1 Commodity: .....	83
5.12.2 Geochemical Statistics: .....	83
5.12.3 Summary Statistics: .....	84
5.12.4 Kendall Tau correlation: .....	84
5.12.5 Maps:.....	85
5.12.5.1 Spatial Distribution: .....	85
5.12.5.2 Estimated Economic Values: .....	86
5.12.6 Summary:.....	87

5.13 Lithium.....	88
5.13.1 Commodity: .....	88
5.13.2 Geochemical Statistics: .....	88
5.13.3 Summary Statistics: .....	89
5.13.4 Kendall Tau correlation: .....	89
5.13.5 Maps:.....	90
5.13.5.1 Spatial Distribution: .....	90
5.13.5.2 Estimated Economic Values: .....	91
5.13.6 Summary: .....	93
5.14 Magnesium.....	94
5.14.1 Commodity: .....	94
5.14.2 Geochemical Statistics: .....	94
5.14.3 Summary Statistics: .....	95
5.14.4 Kendall Tau correlation: .....	95
5.14.5 Maps:.....	96
5.14.5.1 Spatial Distribution: .....	96
5.14.5.2 Estimated Economic Values: .....	97
5.14.6 Summary: .....	98
5.15 Manganese .....	99
5.15.1 Commodity: .....	99
5.15.2 Geochemical Statistics: .....	99
5.15.3 Summary Statistics: .....	100
5.15.4 Kendall Tau correlation: .....	100
5.15.5 Maps:.....	101
5.15.5.1 Spatial Distribution: .....	101
5.15.5.2 Estimated Economic Values: .....	102
5.15.6 Summary: .....	103
5.16 Mercury.....	104
5.16.1 Commodity: .....	104
5.16.2 Geochemical Statistics: .....	104
5.16.3 Summary Statistics: .....	105
5.16.4 Kendall Tau correlation: .....	105
5.16.5 Maps:.....	106

5.16.5.1 Spatial Distribution: .....	106
5.16.5.2 Estimated Economic Values: .....	107
5.16.6 Summary: .....	108
5.17 Molybdenum .....	109
5.17.1 Commodity: .....	109
5.17.2 Geochemical Statistics: .....	109
5.17.3 Summary Statistics: .....	110
5.17.4 Kendall Tau: .....	110
5.17.5.1 Spatial Data .....	111
5.17.5.2 Estimated Economic Values for Molybdenum .....	112
5.17.6 Summary: .....	113
5.18 Nickel .....	114
5.18.1 Commodity: .....	114
5.18.2 Geochemical Statistics: .....	114
5.18.3 Summary Statistics: .....	115
5.18.4 Kendall Tau correlation: .....	115
5.18.5 Maps: .....	117
5.18.5.1 Spatial Distribution: .....	117
5.18.5.2 Estimated Economic Values: .....	118
5.18.6 Summary: .....	119
5.19 Potash .....	120
5.19.1 Commodity: .....	120
5.19.2 Geochemical Statistics: .....	120
5.19.3 Summary Statistics: .....	121
5.19.4 Kendall Tau correlation: .....	121
5.19.5 Maps: .....	122
5.19.6.1 Spatial Distribution: .....	122
5.19.5.2 Estimated Economic Values: .....	123
5.19.6 Summary: .....	124
5.20 Rubidium .....	125
5.20.1 Commodity: .....	125
5.20.2 Geochemical Statistics: .....	125
5.20.3 Summary Statistics: .....	126

5.20.4 Kendall Tau correlation: .....	126
5.20.5 Maps:.....	127
5.20.5.1 Spatial Distribution: .....	127
5.20.5.2 Estimated Economic Values: .....	128
5.20.6 Summary: .....	130
5.21 Salt .....	131
5.21.1 Commodity: .....	131
5.21.2 Geochemical Statistics: .....	131
5.21.3 Summary Statistics: .....	132
5.21.4 Kendall Tau correlation: .....	132
5.21.5 Maps:.....	133
5.21.5.1 Spatial Distribution: .....	133
5.21.5.2 Estimated Economic Values: .....	134
5.21.6 Summary: .....	135
5.22 Soda Ash .....	136
5.22.1 Commodity: .....	136
5.22.2 Geochemical Statistics: .....	136
5.22.3 Summary Statistics: .....	137
5.22.4 Kendall Tau correlation: .....	137
5.22.5 Maps:.....	138
5.22.5.1 Spatial Distribution: .....	138
5.22.5.2 Estimated Economic Values: .....	139
5.22.6 Summary: .....	140
5.23 Strontium.....	141
5.23.1 Commodity: .....	141
5.23.2 Geochemical Statistics: .....	141
5.23.3 Summary Statistics: .....	142
5.23.4 Kendall Tau correlation: .....	142
5.23.5 Maps:.....	143
5.23.5.1 Spatial Distribution: .....	143
5.23.5.2 Estimated Economic Values: .....	144
5.23.6 Summary: .....	145
5.24 Sulfur.....	146

5.24.1 Commodity: .....	146
5.24.2 Geochemical Statistics: .....	146
5.24.3 Summary Statistics: .....	147
5.24.4 Kendall Tau correlation: .....	147
5.24.5 Maps:.....	148
5.24.5.1 Spatial Distribution: .....	148
5.24.5.2 Estimated Economic Values: .....	149
5.24.6 Summary: .....	150
5.25 Zinc .....	151
5.25.1 Commodity: .....	151
5.25.2 Geochemical Statistics: .....	151
5.25.3 Summary Statistics: .....	152
5.25.4 Kendall Tau correlation: .....	152
5.25.5 Maps:.....	153
5.25.5.1 Spatial Distribution: .....	153
5.25.5.2 Estimated Economic Values: .....	154
5.25.6 Summary: .....	155
Chapter 6. Grouped Commodities .....	156
6.1 Alkali Metals.....	157
Summary: .....	158
6.2 Alkaline Earth Metals .....	159
Summary: .....	160
6.3 Transition Metals .....	161
Summary: .....	162
6.4 Halogens .....	163
Summary: .....	164
Chapter 7. Permian Basin Case Study .....	165
7.1 Permian Basin background .....	166
7.2 Bromine in the Permian Basin .....	168
7.2.1 Geochemical Statistics: .....	169
7.2.2 Maps:.....	170
7.2.2.1 Spatial Distribution: .....	170

7.2.2.2 Estimated Economic Values: .....	171
Summary: .....	172
7.3 Iodine in the Permian Basin .....	173
7.3.1 Geochemical Statistics: .....	174
7.3.2 Maps: .....	175
7.3.2.1 Spatial Distribution: .....	175
7.3.2.2 Estimated Economic Values: .....	176
7.3.3 Summary: .....	177
7.4 Lithium in the Permian Basin .....	178
7.4.1 Geochemical Statistics: .....	179
7.4.2 Maps: .....	180
7.4.2.1 Spatial Distribution: .....	180
7.4.2.2 Estimated Economic Values: .....	181
7.4.3 Summary: .....	183
7.5 Magnesium in the Permian Basin .....	184
7.5.1 Geochemical Statistics: .....	185
7.5.2 Maps: .....	186
7.5.2.1 Spatial Distribution: .....	186
7.5.2.2 Estimated Economic Values: .....	187
7.5.3 Summary: .....	188
7.6 Potash in the Permian Basin .....	189
7.6.1 Geochemical Statistics: .....	190
7.6.2 Maps: .....	191
7.6.2.1 Spatial Distribution: .....	191
7.6.2.2 Estimated Economic Values: .....	192
7.6.3 Summary: .....	193
7.7 Maximizing Potential .....	194
7.8 Regulation and Policies .....	196
7.9 Permian Basin Summary .....	199

Chapter 8. Conclusion.....	201
References .....	207
Appendix A- Potential Mineral Commodities of Produced Waters .....	213
Appendix B- Kendall Tau Correlation Table.....	215
Appendix C - Comparison of available treatment technologies .....	216
Appendix D– National Summary Statistics .....	217
Vita	218

## List of Tables

Table 1: Estimated produced water costs, by state, for six regions. ....	18
Table 2. Univariate data analysis for barium. ....	26
Table 3. Univariate data analysis for boron. ....	31
Table 4. Univariate data analysis for bromine. ....	36
Table 5. Univariate data analysis for cadmium. ....	43
Table 6. Univariate data analysis for calcium. ....	48
Table 7. Univariate data analysis for cesium. ....	54
Table 8. Univariate data analysis for chromium. ....	59
Table 9. Univariate data analysis for cobalt. ....	64
Table 10. Univariate data analysis for copper. ....	69
Table 11. Univariate data analysis for fluorine. ....	74
Table 12. Univariate data analysis for iodine. ....	79
Table 13. Univariate data analysis for lead. ....	84
Table 14. Univariate data analysis lithium. ....	89
Table 15. Univariate data analysis magnesium. ....	95
Table 16. Univariate data analysis for manganese. ....	100
Table 17. Univariate data analysis for mercury. ....	105
Table 18. Univariate data analysis molybdenum. ....	110
Table 19. Univariate data analysis for nickel. ....	115
Table 20. Univariate data analysis for potassium. ....	121
Table 21. Univariate data analysis for rubidium. ....	126
Table 22. Univariate data analysis for sodium. ....	132
Table 23. Univariate data analysis for gross carbonate. ....	137
Table 24. Univariate data analysis for strontium. ....	142
Table 25. Univariate data analysis for sulfate. ....	147
Table 26. Univariate data analysis for zinc. ....	152
Table 27. Univariate data analysis for all available constituents. ....	166

## List of Figures

Figure 1: National spatial concentration map for total dissolved solids. Black triangles identify locations where total dissolved solids concentration data exist but are below the 75th percentile. Color ramped symbols applied to the sites where concentrations exceed the 75th percentile. ....	4
Figure 2: National EDA-plot in log scale, barium concentrations are bi-modal with small sub-populations at 0.15 and 2.0 mg/L.....	26
Figure 3: National spatial concentration map for barium. Black triangles identify locations where Ba concentration data exist but are below the 75th percentile. Color ramped symbols applied to the sites where concentrations exceed the 75th percentile.....	27
Figure 4: Economic concentration map identifying highest areas of interest: The Appalachian Basin .....	28
Figure 5: Tukey boxplot of economic values for barium in produced waters. ....	28
Figure 6: National EDA-plot in log scale, boron concentrations that is slightly right skewed with multiple populations with breaks at 1 mg/L and 250 mg/L. The EDCF plot on the right presents a sigmodal distribution curve.....	31
Figure 7: National spatial concentration map for boron. Black triangles identify locations where B concentration data exist but are below the 75th percentile. Color ramped symbols applied to the sites where concentrations exceed the 75th percentile.....	32
Figure 8: Economic concentration map identifying highest areas of value: The Smackover Formation, Williston Basin, Woodward Basin, Permian Basin and the Gulf Coast. ....	33
Figure 9: Tukey boxplot of economic values for boron in produced waters. ....	33
Figure 10: National EDA-plot in log scale, which includes a combination of a histogram, density trace, boxplot, and one-dimensional scatterplot (left side) and Empirical Cumulative Distribution Function (ECDF)-plot (right side). Bromine concentrations have a bimodal distribution and the EDCF plot has a sigmoidal distribution curve. ....	36
Figure 11: National spatial concentration map for bromine. Black triangles identify locations where Br concentration data exist but are below the 75th percentile. Color ramped symbols applied to the sites where concentrations exceed the 75th percentile.....	38
Figure 12: Economic concentration map identifying highest areas of interest: The Gulf Coast Basin, Smackover Formation and the Appalachian Basin.....	39
Figure 13: Tukey boxplot of economic values for bromine in produced waters. ....	39
Figure 14: National EDA-plot in log scale, which includes a combination of a histogram, density trace, boxplot, and one-dimensional scatterplot (left side) and Empirical Cumulative Distribution Function (ECDF)-plot (right side). Cadmium concentrations shows a multi-modal distribution. ....	43
Figure 15: National spatial concentration map for cadmium. Black triangles identify locations where Cd concentration data exist but are below the 75th percentile. Color ramped symbols applied to the sites where concentrations exceed the 75th percentile.....	44
Figure 16: Economic concentration map identifying highest areas of interest; The Western Region, the Gulf Coast Basin (Black Warrior Basin) and Northeastern Region (the Appalachian Basin). ....	45
Figure 17: Tukey boxplot of economic values for boron in produced waters. ....	45
Figure 18: National EDA-plot in log scale, which includes a combination of a histogram, density trace, boxplot, and one-dimensional scatterplot (left side) and Empirical Cumulative Distribution	

Function (ECDF)-plot (right side). Calcium concentrations graph shows a multiple distribution.	48
Figure 19: National spatial concentration map for calcium. Black triangles identify locations where Ca concentration data exist but are below the 75th percentile. Color ramped symbols applied to the sites where concentrations exceed the 75th percentile.	49
Figure 20: Economic concentration map for calcium identifying highest areas of interest; The Williston Basin, The Permian Basin, The Gulf Coast Basin, Smackover Formation and the Appalachian Basin.	50
Figure 21: Tukey boxplot of economic values for calcium carbonate in produced waters.	50
Figure 22: National EDA-plot in log scale, which includes a combination of a histogram, density trace, boxplot, and one-dimensional scatterplot (left side) and Empirical Cumulative Distribution Function (ECDF)-plot (right side). Cesium concentrations are skewed to the right.	54
Figure 23: National spatial concentration map for cesium. Black triangles identify locations where Cs concentration data exist but are below the 75th percentile. Color ramped symbols applied to the sites where concentrations exceed the 75th percentile.	55
Figure 24: Economic concentration map for Cs identifying highest areas of interest: The Gulf Coast Basin.	56
Figure 25: Tukey boxplot of economic values for cesium in produced waters.	56
Figure 26: National EDA-plot in log scale, which includes a combination of a histogram, density trace, boxplot, and one-dimensional scatterplot (left side) and Empirical Cumulative Distribution Function (ECDF)-plot (right side). Chromium concentrations are right skewed and the graph shows a slight bi modal distribution.	59
Figure 27: National spatial concentration map for chromium. Black triangles identify locations where Cr concentration data exist but are below the 75th percentile. Color ramped symbols applied to the sites where concentrations exceed the 75th percentile.	60
Figure 28: Economic concentration map identifying highest areas of interest: The Williston Basin.	61
Figure 29: Tukey boxplot of economic values for chromium in produced waters.	61
Figure 30: National EDA-plot in log scale, which includes a combination of a histogram, density trace, boxplot, and one-dimensional scatterplot (left side) and Empirical Cumulative Distribution Function (ECDF)-plot (right side). Cobalt concentrations are bimodal with a right skewed tail.	64
Figure 31: National spatial concentration map for cobalt. Black triangles identify locations where Co concentration data exist but are below the 75th percentile. Color ramped symbols applied to the sites where concentrations exceed the 75th percentile.	65
Figure 32: Economic map for Co identifying highest areas of interest: California, Nevada and upper Appalachian Basin.	66
Figure 33: Tukey boxplot of economic values for cobalt in produced waters.	66
Figure 34: National EDA-plot in log scale, which includes a combination of a histogram, density trace, boxplot, and one-dimensional scatterplot (left side) and Empirical Cumulative Distribution Function (ECDF)-plot (right side). Copper concentrations are right skewed.	69
Figure 35: National spatial concentration map for copper. Black triangles identify locations where Cu concentration data exist but are below the 75th percentile. Color ramped symbols applied to the sites where concentrations exceed the 75th percentile.	70
Figure 36: Economic map for copper identifying highest areas of interest: California, Nevada and the Smackover Formation.	71
Figure 37: Tukey boxplot of economic values for copper in produced waters.	71

Figure 38: National EDA-plot in log scale, which includes a combination of a histogram, density trace, boxplot, and one-dimensional scatterplot (left side) and Empirical Cumulative Distribution Function (ECDF)-plot (right side). Fluorine concentrations are right skewed. ....	74
Figure 39: National spatial concentration map for fluoride. Black triangles identify locations where F concentration data exist but are below the 75th percentile. Color ramped symbols applied to the sites where concentrations exceed the 75th percentile. ....	75
Figure 40: Economic map for fluorine identifying highest areas of interest: The Michigan Basin .....	76
Figure 41: Tukey boxplot of economic values for fluorspar in produced waters. ....	76
Figure 42: National EDA-plot in log scale, which includes a combination of a histogram, density trace, boxplot, and one-dimensional scatterplot (left side) and Empirical Cumulative Distribution Function (ECDF)-plot (right side). Iodine concentrations are skewed to the left and the graph shows a bimodal distribution. ....	79
Figure 43: National spatial concentration map for iodine. Black triangles identify locations where iodine concentration data exist but are below the 75th percentile. Color ramped symbols applied to the sites where concentrations exceed the 75th percentile. ....	80
Figure 44: Economic map for iodine identifying highest areas of interest: The Anadarko Basin and the Gulf Coast Basin. ....	81
Figure 45: Tukey boxplot of economic values for iodine in produced waters. ....	81
Figure 46: National EDA-plot in log scale, which includes a combination of a histogram, density trace, boxplot, and one-dimensional scatterplot (left side) and Empirical Cumulative Distribution Function (ECDF)-plot (right side). Lead concentrations are skewed to the left and the graph shows a bimodal distribution. ....	84
Figure 47: National spatial concentration map for lead. Black triangles identify locations where lead concentration data exist but are below the 75th percentile. Color ramped symbols applied to the sites where concentrations exceed the 75th percentile. ....	85
Figure 48: Economic map for lead identifying highest areas of interest: The Gulf Coast Basin, Smackover Formation and the Appalachian Basin. ....	86
Figure 49: Tukey boxplot of economic values for lead in produced waters. ....	86
Figure 50: National EDA-plot in log scale, which includes a combination of a histogram, density trace, boxplot, and one-dimensional scatterplot (left side) and Empirical Cumulative Distribution Function (ECDF)-plot (right side). Lithium concentrations are left skewed and the graph shows a multiple distribution. ....	89
Figure 51: National spatial concentration map for lithium. Black triangles identify locations where Li concentration data exist but are below the 75th percentile. Color ramped symbols applied to the sites where concentrations exceed the 75th percentile. ....	90
Figure 52: Economic map for lithium carbonate identifying highest areas of interest: the Gulf Coast Basin, areas where the Smackover is present, and the northern Appalachian Basin. ....	91
Figure 53: Tukey boxplot of economic values for lithium carbonate in produced waters .....	91
Figure 54: Economic map for lithium hydroxide identifying highest areas of interest: the Gulf Coast Basin, areas where the Smackover Formation is present, the Central Midwest Region, and the northern Appalachian Basin. ....	92
Figure 55: Tukey boxplot of economic values for lithium hydroxide in produced waters. ....	92
Figure 56: National EDA-plot in log scale, which includes a combination of a histogram, density trace, boxplot, and one-dimensional scatterplot (left side) and Empirical Cumulative Distribution	

Function (ECDF)-plot (right side). Magnesium concentrations are left skewed and the graph shows a multiple distribution. ....	95
Figure 57: National spatial concentration map for magnesium. Black triangles identify locations where Mg concentration data exist but are below the 75th percentile. Color ramped symbols applied to the sites where concentrations exceed the 75th percentile. ....	96
Figure 58: Economic map for magnesium identifying highest areas of interest: the northern Appalachian Basin, Gulf Coast Region, Permian Basin, and the Williston Basin. ....	97
Figure 59: Tukey boxplot of economic values for magnesium in produced waters. ....	97
Figure 60: National EDA-plot in log scale, which includes a combination of a histogram, density trace, boxplot, and one-dimensional scatterplot (left side) and Empirical Cumulative Distribution Function (ECDF)-plot (right side). Manganese concentrations are slightly right and the graph shows a multiple distribution. ....	100
Figure 61: National spatial concentration map for manganese. Black triangles identify locations where Mn concentration data exist but are below the 75th percentile. Color ramped symbols applied to the sites where concentrations exceed the 75th percentile. ....	101
Figure 62: Economic map for Mn identifying highest areas of interest: the Anadarko Basin. ..	102
Figure 63: Tukey boxplot of economic values for manganese in produced waters. ....	102
Figure 64: National EDA-plot in log scale, which includes a combination of a histogram, density trace, boxplot, and one-dimensional scatterplot (left side) and Empirical Cumulative Distribution Function (ECDF)-plot (right side). Fluorine concentrations are right skewed. ....	105
Figure 65: National spatial concentration map for mercury. Black triangles identify locations where Hg concentration data exist but are below the 75th percentile. Color ramped symbols applied to the sites where concentrations exceed the 75th percentile. ....	106
Figure 66: Economic map for mercury identifying highest areas of interest: Nevada. ....	107
Figure 67: Tukey boxplot of economic values for mercury in produced waters. ....	107
Figure 68: National EDA-plot in log scale, molybdenum concentrations that is left skewed with multiple populations at 0.25 mg/L and 50 mg/L. ....	110
Figure 69: National spatial concentration map for molybdenum. Black triangles identify locations where Mo concentration data exist but are below the 75th percentile. Color ramped symbols applied to the sites where concentrations exceed the 75th percentile. ....	111
Figure 70: Economic map for molybdenum identifying highest area of interest: Nevada. ....	112
Figure 71: Tukey boxplot of economic values for molybdenum in produced waters. ....	112
Figure 72: National EDA-plot in log scale, which includes a combination of a histogram, density trace, boxplot, and one-dimensional scatterplot (left side) and Empirical Cumulative Distribution Function (ECDF)-plot (right side). Nickel concentrations are skewed to the right and the graph shows a bimodal distribution. ....	115
Figure 73: National spatial concentration map for nickel. Black triangles identify locations where Ni concentration data exist but are below the 75th percentile. Color ramped symbols applied to the sites where concentrations exceed the 75th percentile. ....	117
Figure 74: Economic map for nickel identifying highest areas of interest: northern Appalachian Basin. ....	118
Figure 75: Tukey boxplot of economic values for nickel in produced waters. ....	118
Figure 76: National EDA-plot in log scale, which includes a combination of a histogram, density trace, boxplot, and one-dimensional scatterplot (left side) and Empirical Cumulative Distribution Function (ECDF)-plot (right side). Potassium concentrations are right skewed. ....	121

Figure 77: National spatial concentration map for potassium. Black triangles identify locations where K concentration data exist but are below the 75th percentile. Color ramped symbols applied to the sites where concentrations exceed the 75th percentile.....	122
Figure 78: Economic map for potassium identifying highest areas of interest: The Williston and Permian basins. ....	123
Figure 79: Tukey boxplot of economic values for potash in produced waters. ....	123
Figure 80: National EDA-plot in log scale, which includes a combination of a histogram, density trace, boxplot, and one-dimensional scatterplot (left side) and Empirical Cumulative Distribution Function (ECDF)-plot (right side). Rubidium concentrations are left skewed.....	126
Figure 81: National spatial concentration map for rubidium. Black triangles identify locations where Rb concentration data exist but are below the 75th percentile. Color ramped symbols applied to the sites where concentrations exceed the 75th percentile.....	127
Figure 82: Economic map for rubidium chloride identifying areas of highest interest: The Anadarko Basin, the Gulf Coast Basin and the Western Region.....	128
Figure 83: Tukey boxplot of economic values for rubidium chloride in produced waters.....	128
Figure 84: Economic for rubidium formate identifying areas of highest interest: the Anadarko Basin, the Gulf Coast Basin and the Western Region. ....	129
Figure 85: Tukey boxplot of economic values for rubidium formate in produced waters. ....	129
Figure 86: National EDA-plot in log scale, which includes a combination of a histogram, density trace, boxplot, and one-dimensional scatterplot (left side) and Empirical Cumulative Distribution Function-plot (right side). Sodium concentrations are left skewed and the graph shows a multiple distribution. ....	132
Figure 87: National spatial concentration map for sodium. Black triangles identify locations where Na concentration data exist but are below the 75th percentile. Color ramped symbols applied to the sites where concentrations exceed the 75th percentile.....	133
Figure 89: Tukey boxplot of economic values for sodium chloride in produced waters. ....	134
Figure 90: National EDA-plot in log scale, which includes a combination of a histogram, density trace, boxplot, and one-dimensional scatterplot (left side) and Empirical Cumulative Distribution Function (ECDF)-plot (right side). Sodium concentrations are left skewed. ....	137
Figure 91: National spatial concentration map for total available carbonate. Black triangles identify locations where Na concentration data exist but are below the 75th percentile. Color ramped symbols applied to the sites where concentrations exceed the 75th percentile. ....	138
Figure 92: Economic map for soda ash identifying highest areas of interest: Anadarko Basin, Appalachian Basin, Gulf Coast Basin, Permian Basin, San Juan Basin and Williston Basin. ...	139
Figure 93: Tukey boxplot of economic values for sodium carbonate in produced waters. ....	139
Figure 94: National EDA-plot in log scale, which includes a combination of a histogram, density trace, boxplot, and one-dimensional scatterplot (left side) and Empirical Cumulative Distribution Function (ECDF)-plot (right side). Strontium concentrations are left skewed.....	142
Figure 95: National spatial concentration map for strontium. Black triangles identify locations where Sr concentration data exist but are below the 75th percentile. Color ramped symbols applied to the sites where concentrations exceed the 75th percentile.....	143
Figure 96: Economic concentration map for strontium identifying highest areas of interest: The Central Midwest Region and Northeast Region. ....	144
Figure 97: Tukey boxplot of economic values for strontium in produced waters. ....	144

Figure 98: National EDA-plot in log scale, which includes a combination of a histogram, density trace, boxplot, and one-dimensional scatterplot (left side) and Empirical Cumulative Distribution Function (ECDF)-plot (right side). Sulfur concentrations are right skewed. ....	147
Figure 99: National spatial concentration map for sulfur. Black triangles identify locations where sulfate concentration data exist but are below the 75th percentile. Color ramped symbols applied to the sites where concentrations exceed the 75th percentile. ....	148
Figure 100: Economic concentration map identifying highest areas of interest; The Permian Basin and the Black Hills Region. ....	149
Figure 101: Tukey boxplot of economic values for sulfate in produced waters. ....	149
Figure 102: National EDA-plot in log scale, which includes a combination of a histogram, density trace, boxplot, and one-dimensional scatterplot (left side) and Empirical Cumulative Distribution Function (ECDF)-plot (right side). Zinc concentrations have a bimodal distribution with a slight right skew. ....	152
Figure 103: National spatial concentration map for zinc. Black triangles identify locations where Zn concentration data exist but are below the 75th percentile. Color ramped symbols applied to the sites where concentrations exceed the 75th percentile. ....	153
Figure 104: Economic map for zinc identifying highest areas of interest: The Gulf Coast Region. ....	154
Figure 105: Tukey boxplot of economic values for zinc in produced waters. ....	154
Figure 106: Grouped economic value map for alkali metals, identifying areas of interest; The Gulf Coast Basin, Smackover Formation and the Williston Basin. ....	157
Figure 107: Tukey boxplot of economic values for alkali metals in produced waters. Left: All alkali metals. Right: Alkali metals excluding Rb and Cs. ....	157
Figure 108: Grouped economic value map for alkaline earth metals, identifying areas of interest: the Gulf Coast, Permian and Appalachian Basins. ....	159
Figure 109: Tukey boxplot of economic values for alkaline earth metals in produced waters. Left: All alkali earth metals. Right: Barium and Strontium only. ....	159
Figure 110: Grouped economic value map for transition metals, identifying areas of interest: The Gulf Coast Basin. ....	161
Figure 111: Tukey Boxplot of economic values for transition metals in produced waters. ....	161
Figure 112: Grouped economic value map for halogens, identifying areas of interest: the Anadarko Basin, Smackover Formation and the Appalachian Basin. ....	163
Figure 113: Tukey boxplot of economic values for halogens in produced waters. ....	163
Figure 114: National EDA-plot in log scale, which includes a combination of a histogram, density trace, boxplot, and one-dimensional scatterplot (left side) and Empirical Cumulative Distribution Function (ECDF)-plot (right side). Bromine concentrations have a bimodal distribution and the EDCF plot has a sigmoidal distribution curve. ....	169
Figure 115: National spatial concentration map for bromine. Black triangles identify locations where Br concentration data exist but are below the 75th percentile. Color ramped symbols applied to the sites where concentrations exceed the 75th percentile. ....	170
Figure 116: Magnified view of the Permian Basin spatial concentration map for bromine. Black triangles identify locations where Br concentration data exist but are below the 75th percentile. Color ramped symbols applied to the sites where concentrations exceed the 75th percentile. ..	170
Figure 117: Magnified economic bromine Permian Basin concentration map identifying highest areas of interest. ....	171

Figure 118: Tukey boxplot of economic values for identifying bromine in Permian Basin produced waters. ....	172
Figure 119: Permian Basin EDA-plot in log scale, which includes a combination of a histogram, density trace, boxplot, and one-dimensional scatterplot (left side) and Empirical Cumulative Distribution Function (ECDF)-plot (right side). Iodine concentrations have a multi-modal distribution. ....	174
Figure 120: Permian Basin spatial concentration map for bromine. Black triangles identify locations where iodine concentration data exist but are below the 75th percentile. Color ramped symbols applied to the sites where concentrations exceed the 75th percentile. ....	175
Figure 121: Magnified view of the Permian Basin spatial concentration map for iodine. Black triangles identify locations where Br concentration data exist but are below the 75th percentile. Color ramped symbols applied to the sites where concentrations exceed the 75th percentile. ..	175
Figure 122: Permian Basin economic map for iodine identifying highest areas of interest. ....	176
Figure 123: Magnified economic iodine Permian Basin concentration map identifying highest areas of interest. ....	176
Figure 124: Tukey boxplot of economic values for identifying iodine in Permian Basin produced waters. ....	177
Figure 125: Permian Basin EDA-plot in log scale, which includes a combination of a histogram, density trace, boxplot, and one-dimensional scatterplot (left side) and Empirical Cumulative Distribution Function (ECDF)-plot (right side). Lithium concentrations are right skewed and the graph shows a multiple distribution. ....	179
Figure 126: Permian Basin spatial concentration map for lithium. Black triangles identify locations where Li concentration data exist but are below the 75th percentile. Color ramped symbols applied to the sites where concentrations exceed the 75th percentile. ....	180
Figure 127: Magnified view of the Permian Basin spatial concentration map for lithium. Black triangles identify locations where Br concentration data exist but are below the 75th percentile. Color ramped symbols applied to the sites where concentrations exceed the 75th percentile. ..	180
Figure 128: Permian Basin economic map for lithium carbonate identifying highest areas of interest. ....	181
Figure 129: Magnified economic lithium carbonate Permian Basin concentration map identifying highest areas of interest. ....	181
Figure 130: Tukey boxplot of economic values for identifying lithium carbonate in Permian Basin produced waters. ....	182
Figure 131: Economic concentration map identifying highest areas of interest. ....	182
Figure 132: Magnified economic lithium hydroxide Permian Basin concentration map identifying highest areas of interest. ....	182
Figure 133: Boxplot of economic values for identifying lithium hydroxide in Permian Basin produced waters. ....	183
Figure 134: Permian Basin EDA-plot in log scale, which includes a combination of a histogram, density trace, boxplot, and one-dimensional scatterplot (left side) and Empirical Cumulative Distribution Function (ECDF)-plot (right side). Magnesium concentrations are left skewed and the graph shows a multiple distribution. ....	185
Figure 135: Permian Basin spatial concentration map for magnesium. Black triangles identify locations where Mg concentration data exist but are below the 75th percentile. Color ramped symbols applied to the sites where concentrations exceed the 75th percentile. ....	186

Figure 136: Magnified view of the Permian Basin spatial concentration map for magnesium. Black triangles identify locations where Br concentration data exist but are below the 75th percentile. Color ramped symbols applied to the sites where concentrations exceed the 75th percentile.....	186
Figure 137: Permian Basin economic map for magnesium identifying highest areas of interest.....	187
Figure 138: Magnified economic magnesium Permian Basin concentration map identifying highest areas of interest.....	187
Figure 139: Tukey boxplot of economic values for identifying magnesium in Permian Basin produced waters.....	188
Figure 140: Permian Basin EDA-plot in log scale, which includes a combination of a histogram, density trace, boxplot, and one-dimensional scatterplot (left side) and Empirical Cumulative Distribution Function (ECDF)-plot (right side). Potassium concentrations are slightly left skewed.....	190
Figure 141: Permian Basin spatial concentration map for potassium. Black triangles identify locations where K concentration data exist but are below the 75th percentile. Color ramped symbols applied to the sites where concentrations exceed the 75th percentile. ....	191
Figure 142: Magnified view of the Permian Basin spatial concentration map for potassium. Black triangles identify locations where Br concentration data exist but are below the 75th percentile. Color ramped symbols applied to the sites where concentrations exceed the 75th percentile. ..	191
Figure 143: Permian Basin economic map for potassium identifying highest areas of interest.	192
Figure 144: Magnified economic potash Permian Basin concentration map identifying highest areas of interest. ....	192
Figure 145: Tukey boxplot of economic values for identifying potash in Permian Basin produced waters. ....	192
Figure 142: Boxplot of economic values for identifying bromine, iodine, lithium, magnesium, and potash values in Permian Basin produced waters. ....	194
Figure 137. Complete analysis of available commodities in produced water compared to disposal costs.....	204

## **Chapter 1: Introduction and Statement of the Problem**

Produced waters, waters which are co-generated from hydrocarbon wells, are the most voluminous byproduct of the oil and gas industry. On average, in the United States seven to ten barrels of water are produced for every barrel of crude oil (Guerra, 2011) and a major expense for the oil and gas industry is the treatment and/or disposal of produced waters (Clark and Veil, 2009; Mantell 2011). Veil (2015) estimated that in 2012, 21.2 billion barrels [1 bbl=42 gallons] of produced water were generated through on-shore and offshore U.S. oil and gas production. Oil production increased by 29% and gas production increased by 22% between 2007 through 2012, but estimated produced water volumes increased less than 1% over this same period (Veil, 2015). Despite mineral resource potential, only 0.6% of produced water by volume, in 2012, was used for a beneficial purpose. The remaining 99% volume was disposed of either through injection, surface discharge, commercial treatment, or other methods (Veil, 2015). These patterns exist because the most cost effective manner to handle produced waters by the oil and gas industry is typically disposal via subsurface injection.

Costs of produced water management for both beneficial reuse and disposal depend on technology, regulations, and intended usage (e.g. municipal or agricultural application such as water for parks; Theodori et al., 2007), along with transportation, logistics and management (Boschee, 2014). Moreover, water management practices and costs also depend on produced water composition, which affects available treatments/disposal technologies. Regulations control costs; can the water be injected on-site or does it have to be trucked to another location? In some areas, on-site commercial treatment facilities are available to treat produced waters for uses including agricultural application, chemical production, injection to maintain reservoir pressure, and other beneficial uses (Guerra et al., 2011). Geologic constraints and state regulations often limit methods

for disposal or reuse (Boschee, 2014; Skalak et al., 2014). Restrictions that require off site trucking for injection often results in higher disposal costs (Guerra et al., 2011). In response to disposal costs, states often support practices that offer beneficial recycling methods for drilling re-use, road deicing along with other common practices that include land application or injection for enhanced hydrocarbon recovery (e.g., water flooding secondary recovery) (ICF Consulting, 2000).

The typical outlook views produced waters as a waste. However, there are many instances where the waters can and are being utilized as a natural resource. Commodities currently generated from produced waters and basin brines include: 1) livestock drinking water, typically after desalination or other treatment methods (Tao et al., 1993); 2) minerals commodities, of which sodium chloride is the leading product (46% of domestic sodium chloride production comes from basinal brines and produced waters; U.S. Geological Survey, 2014); and 3) oil, grease and other organic compounds (Horner et al., 2011).

Three mineral commodities generated in abundance from produced waters are bromine, lithium and iodine. In Arkansas, bromine and lithium are extracted and commercially produced from produced waters and basinal brines from the Smackover Formation (Warren, 2000). U.S. bromine extraction from sedimentary basin brines, accounts for one-third of world production (U.S. Geological Survey, 2014). Bromine's world market value is approximately \$800 million dollars a year and is dominated by imports sources from the Dead Sea (U.S. Geological Survey, 2014). The Anadarko Basin in Oklahoma is home to the largest domestic production site for iodine (Johnson, 1994). Ninety-nine percent of all U.S import for iodine is from Chile or Japan. Sources include seaweed, organic marine deposits and basinal brines. The Anadarko Basin is an ideal location for iodine U.S. production (Krukowski, 2008) as the region is a remnant oceanic shelf

where iodine was concentrated in marine rocks, at a beyond those in other sedimentary basins in the United States (Collins, 1975).

Many constituents in produced waters have high economic values and may potentially be a resource of domestic mineral commodities, as defined by the U.S. Geological Survey National Minerals Information Center (Appendix A). Mineral commodities present in produced waters include, but are not limited to, barite (as barium), boron, bromine (as bromide), calcium (as lime), carbon (as inorganic and organic carbon), cesium, chlorine (as chloride), iodine (as iodide), lithium, magnesium, potash (as potassium), rubidium, silicon, sodium, strontium, sulfate, and zinc.

Commodity prices are subject to the rise and fall of the worldwide economics. These values are partly determined by industry trades, removal processing and/or availability for the commodity. Also, multiple products of differing value can be produced from the same element. For instance, lithium hydroxide is valued at \$7.43 per kilogram (\$25.63 per kg of lithium) while lithium carbonate is valued at \$5.64 per kilogram (\$30.15 per kg of lithium) (USGS, 2015). Additional variation in pricing occurs due to international differences. For instance, in China, battery grade lithium carbonate averages \$6.38 per kilogram compared to the U.S. values listed above (U.S. Geological Survey, 2014). Thus, the “true” value of any commodity is variable and dependent upon its final form and market. To simplify, the focus here is on domestic values for the most common commodity forms with an understanding that any commodity considered valuable, its value must, at a minimum, exceed the disposal costs of the water.

Despite knowledge that produced waters are a known domestic source for valuable mineral resources, there has been no attempt to construct a national-scope evaluation of that potential. Lack of previous efforts may have been partly due a paucity of data. Recently, the U.S Geological

Survey compiled and released a revised geochemical database containing results for more 165,000 produced waters samples across the United States (Blondes et al., 2016). The database, is restricted primarily to produced water samples from on-shore hydrocarbon and geothermal wells, and contains chemical results for major ions, trace elements and isotopes (Figure 1). The release of the new produced waters database, includes, for the first time, results for minor and trace constituents. This inclusion of new elements allows for a tool to evaluate the potential for a broad spectrum of mineral commodities in produced water and basin brines at a national level.

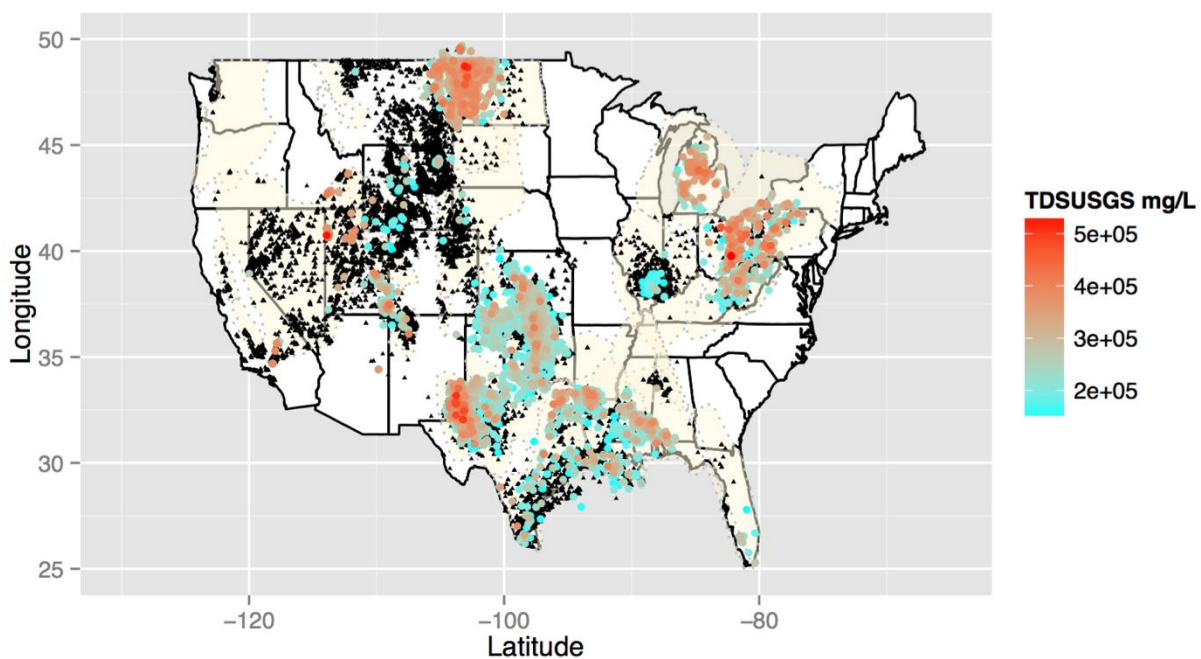


Figure 1: National spatial concentration map for total dissolved solids. Black triangles identify locations where total dissolved solids concentration data exist but are below the 75th percentile. Color ramped symbols applied to the sites where concentrations exceed the 75th percentile.

As noted above, in addition to mineral commodities, the water itself also has value. As a result of reoccurring droughts and increasing demand for freshwater in western United States, oil and gas operations are under pressure to reduce their dependence on freshwater sources. To help

minimize freshwater use for hydrocarbon development, desalination of produced water allows for re-use or recycling while removing mineral commodities from produced waters provides dual benefits (Coday et al., 2015).

This thesis identifies some of the engineering methods that combine water treatment and mineral commodity removal from produced waters. Engineering applications can be modified per basin and per commodity desired but would require detailed analysis from an engineering, which is beyond the scope of this thesis. For commercial success, methods to treat produced waters for reuse/recycling in drilling and hydraulic fracturing while generating mineral commodities as an economic resource must be economically viable and minimally intrusive to oil and gas operations.

## **1.2 Objectives:**

Broadly, the purpose of this thesis is to evaluate potential to ascertain mineral commodities found in produced waters of the contiguous United States. This thesis attempts to fulfill this purpose through the following list of objectives:

1. Summarize current U.S. operations that extract mineral commodities from produced waters or sedimentary basinal brines including both processing technologies and list generated compounds. Identify potential mineral commodities of interest and the geochemical relationships in the produced waters.
2. Generate a series of national maps for the purpose of identification and correlation between potential mineral commodity sources. For each mineral commodity, the maps for both the spatial distribution of commodity concentrations and economic value (based on current commodity values) are provided.
3. Present a comprehensive analysis of the data products used to highlight commodities and localities of: A) greatest economic potential for resource extraction; and B) elements that are of greatest potential for further exploration (i.e., prioritization of data needs).
4. Generate a series of statistical graphs and tables for the purpose of basic data analysis, computation of summary statistics, and examination of correlation between potential mineral commodity sources.

## **Chapter 2. Background**

Produced waters from hydrocarbon reservoirs are a mixtures of waters from various sources. Flowback water is the waste water that is returned immediately to the surface after hydraulic fracturing and generally is composed of fracturing fluid. Basinal brines, also commonly referred to as formation waters, are the water which co-exists naturally with the hydrocarbons and is present in the reservoirs prior to drilling and extraction. Produced waters are generally released after the wells have been in production for weeks or months, as the water source transitions away from the injected water. Thus produced waters are the typically saline water generated from hydrocarbon and geothermal reservoirs, which include both basinal brines and flowback water. This thesis will use this definition of produced waters.

The geochemistry of subsurface basinal brines is influenced by both extrinsic (e.g., climate, paleoseawater circulation and/or fluid flow) and intrinsic properties (e.g., complex fault systems, reservoir lithology, and mineralogy). Total dissolved solid (TDS) concentrations in produced waters vary from that of drinking water to several times the salinity of seawater (Alley et al., 2011; Clark and Veil, 2009; Kharaka and Hanor, 2007; Wilson et al., 1993). Produced waters with exceptionally high salinities have the propensity to contain mineral resource potential. Moreover, virtually every naturally-occurring element is found in produced waters (Collins, 1975; Kharaka and Hanor, 2007).

## **2.2 Geochemistry of Basinal Brines**

The salt concentration in modern, bulk seawater is 35 g/L, but in formation brines TDS can exceed 400 g/L (Figure 1.1). The primary sources of salinity in the most concentrated formation waters is remnant evaporated seawater or the dissolution of evaporative salts, such as halite (Boggs, 2006). However, mineral dissolution, breakdown and release of compounds from organic matter, and expulsion of elements during clay diagenesis are other reactions that can increase salinity in formation brines.

### **2.2.1 Subsurface basinal brine origins and evolution**

This section discusses various geologic and environment settings that produce and control brine chemistry. This section will be followed up with a discussion on salinity controls and localized salinity sources. Understanding geologic origins of brines leads to an enriched understanding of produced waters and how it is possible to potentially develop them as a natural resource for mineral extraction instead of waste material.

A major control on the geochemical composition in brines is the structure of the basin in which they reside and the environment at time of their formation. Basin settings influence lithology, deposition, and residence time for local waters. The basinal hydrogeology and how paleoseawater or meteoric waters moves and interacts within the basin can influence geochemical reactions. Sedimentary basins are broadly classified based on tectonic setting and characterized by stratigraphic intervals during the time of deposition (Krauskopf and Bird, 1995). Extensional basins, established in divergent settings, may include passive margin proto-oceanic rift troughs (new oceanic basin floor flanked by continental margins) (Vischer, 1999). Basin fills during extensional processes typically support progradational-retrogradational cycles: upward fining sequences of deep-water conglomerate-sandstone shales. During specific conditions, evaporation

of geographically trapped water leads to thick deposits of halite (NaCl) and other evaporative salts, as well as the potential for evaporated seawater to invade into permeable strata. Other depositional settings may include organic rich lacustrine deposits or intrusive volcanic suites of basalt or dikes (Krauskopf and Bird, 1995). Compressional basins, found in convergent settings, exist in a variety of environments such as remnant ocean or forearc basins. Some compressional basin characteristics include volcanic suites, oceanic floors and subduction complexes. Intracratonic basins overlie failed or fossil rifts and frequently exhibit a transgressive-regressive sedimentary cyclic sequence (e.g., Williston and Michigan Basins). The water-rock reactions in these types of basin are similar to those found in compressional basins. The biggest differences between the basins are the stability of the platform within the basin, the fault structures and the location of the structures within the basin. Also the residence time for brines to interact with the sediments and structure of the basin is variable. Through circulation and interaction with igneous, sedimentary or metamorphic rocks, water mineralization is generated through corresponding water-rock reactions and influences reservoir geochemistry.

### **2.2.2 Characterization of Brines**

Formation waters in most sedimentary basins are some variation that combines a mixture of meteoric water that dissolved evaporative salts minerals and/or evaporated paleoseawater. Beyond the basic origin of meteoric versus paleoseawater, formation waters go through a series of water-rock reaction, which further control their composition. Depending on the environment within the basin will depend on the geochemical reactions.

Seawater evaporation often results in the precipitation of salts containing calcium, magnesium, sodium, potassium, carbonate, and sulfate bearing evaporite minerals depending on the degree of evaporation and the composition of the starting seawater. This section discusses more

common general conditions followed by localized conditions that are more specific to a region. The evaporative sequence of minerals, with increasing evaporation, generally consists of calcite ( $\text{CaCO}_3$ )  $\rightarrow$  gypsum ( $\text{CaSO}_4 \cdot 2\text{H}_2\text{O}$ )  $\rightarrow$  halite ( $\text{NaCl}$ )  $\rightarrow$  sylvite ( $\text{KCl}$ )  $\rightarrow$  epsomite ( $\text{MgSO}_4 \cdot 7\text{H}_2\text{O}$ ) (Kharaka and Hanor, 2014). Other less abundant minerals, such as polyhalite ( $\text{K}_2\text{Ca}_2\text{Mg}(\text{SO}_4)_4 \cdot 2\text{H}_2\text{O}$ ), also form. If preserved, the relative abundance of minerals in the evaporative sequence can be an indicator for the brine origin. The mineral sequences also provide insight into water circulation and climatic conditions. Information on mineral concentrations also aid in characterizing the composition of the starting seawaters. Seawater during the Cambrian - Devonian periods and Jurassic - Cretaceous periods was enriched with  $\text{Ca}^{2+}$  and depleted in  $\text{SO}_4^{2-}$ , relative to modern seawater (Lowenstein et. al., 2003). The climate was arid during these intervals and ocean circulation was restricted in most marine basins.

Residual brines of seawater from these periods are calcium chloride ( $\text{CaCl}_2$ ) brines, which are characterized by:

$$2m_{\text{Ca}^{2+}} > 2m_{\text{SO}_4^{2-}} + m_{\text{HCO}_3} + 2m_{\text{CO}_3^{2-}},$$

(Hardie, 1983). In the Precambrian, Permian, Triassic and Quaternary periods basinal brines had elevated concentrations of  $\text{SO}_4^{2-}$ . During these periods, the climate was cooler and the ocean circulation patterns were not so restricted. This environment supported conditions for the seawater to decrease in  $\text{Ca}^{2+}$ , but increase in  $\text{Mg}^{2+}$  and  $\text{SO}_4^{2-}$  concentrations resulting in  $\text{MgSO}_4$  oceans, also referred to as aragonite seas (Lowenstein et al., 2003). Aragonite seas are also enriched in  $\text{Na}^{2+}$  residual fluids from these seawaters are dominated by Na and Cl.

### **2.2.3 Localized sources of salinity:**

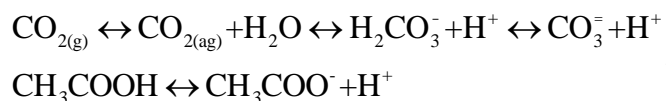
Outside of dissolution of evaporite minerals and residual evaporated paleoseawater, formation waters chemistry is often controlled by localized sources and are specific to that area or region. For instance, deposition of atmospheric aerosols is one solute source to the saline brines in the Murray basin, Australia. In this case, atmospheric deposition of salts derived from nearby evaporating seawater has extended geological timescales to create a significant salt input (Jones et al., 1994). Other examples for localized salinity are the North Slope of Alaska and McMurdo Sound in Antarctica where cryogenics processes were involved. In these regions, both 1) evaporation and burial of Paleozoic seawater and; 2) the freezing of Pleistocene seawater during continental glaciation are suggested salinity sources (Frank et al., 2010). During a long-term freezing conditions, such as continental glaciation, seawater becomes frozen and preserved as glacial ice. The process of freezing or evaporation of seawater geochemically separates the brines from the seawater. The concentrated brines may sink deeper into the basin, possibly slightly thawing out and infiltrating the sediments and ultimately being released back into open seawater, or concentrating the local brines after a warming period. During evaporation of thawing seawater, mirabilite is precipitated through the removal of the sulfate ions, rather than halite or gypsum precipitating from seawater (Herut, et al., 1990). The cyclic pattern of freezing and thawing during glaciation conditions alternates the environment for the potential to increase salinities through solute precipitation and dissolution.

Hydrothermal activities near volcanic systems or magmatic regions provide an additional localized source for solutes. The phase separation under both subcritical and supercritical conditions can impact local groundwater chemistry (Kharaka and Hanor, 2014). At pressure lower than the critical point of water, phase separation can produce low salinity vapor and high salinity

residual waters (Coumou, 2009). Supercritical conditions are reflective of magmatic systems (Fournier et al., 1974). At supercritical conditions, most minerals have lower solubilities so brines are more likely to become supersaturated and form minerals (Odu et al., 2015). During convection of supercritical fluids in the seafloor saline fluids from depth can mix with seawaters near the sea floor interface, creating large concentration gradients.

#### 2.2.4 pH and Alkalinity

The pH of brine waters in the petroleum field is noteworthy, but not critical in the evaluation of basinal brines. The pH of brine has a relatively small impact on salinity and but is directly linked to inorganic carbon and organic acids in produced waters. Generally, pH values decrease as the chlorinity increases in formation waters (Krauskopf and Bird, 1995). Anions of organic acids play a larger role in pH values for certain reservoirs, where they can be found in concentrations >1,000 mg/L. Dominant pH reactions involving CO<sub>2</sub> and carboxylic acids (example shown: acetic acid and acetate) systems include:



Alkalinity is the quantitative measure of pH buffering capacity in an aqueous solution. Basinal brines with high alkalinity concentrations are often associated with limestones, dolomites, other depositional carbonates, and or at reservoir temperatures where carboxylic acid anions are produced from organic matter at 80–120 °C. Waters produced from granites and sandstones result in low alkalinity with poor pH buffering abilities (Hem, 1989). Changes in alkalinity affect the crystal structure of the mineral.

### **2.2.5 Basin Lithology**

The differences in lithology can imprint distinctive geochemical signatures on associated brines. The lithological facies often include both marine (e.g., shale, carbonate and limestone) and nonmarine (e.g., granite, feldspar and sandstones) characteristics. Water-rock interaction is an essential component to basinal brine geochemistry through diagenetic evolution (Bray and Hanor, 1988). The following sections will briefly discuss carbonate and silicate influences and how they contribute to brine salinity.

#### **2.2.5.1 Carbonate Lithologies**

In general, carbonates are soluble in acidic conditions but exhibit relatively low solubility. Because of their pH dependence, their solubility is impacted by dissolved CO<sub>2</sub>. The replacement of one carbonate mineral by another mineral is common in metamorphic and sedimentary rocks, especially in hydrothermal veins. In particular, dolomitization, the conversion of calcite to dolomite, has been linked to depletion of Mg and Ca enrichment in produced waters in many basins. The variation of carbonate solubilities is complex, understanding basic conditions of the carbonate system help evaluate the brines and under what conditions they occurred in. Carbonate mineralization is temperature and pressure dependent.

#### **2.2.5.2. Silicate Lithologies**

Silicates are the most abundant minerals in the earth's crust. For this reason, they have the most potential to connect with basinal brines. They are found in every setting: subduction zones, continental collisions and subvolcanic terrains. In general, solubility of silicate minerals increases as with temperature and/or pressure.

Weathering and incongruent dissolution of aluminosilicate minerals is an important source of minor and trace elements in formation waters. For instance, albitization of plagioclase feldspars

is a noted source for Ca and similar elements which can substitute for Ca (e.g., Sr), and illite to smectite conversion produces Fe, Na, and Ca, while raising pH. The dissolution of clays minerals is another source of solutes in formation waters. The most predominant clay mineral is kaolinite ( $\text{KAlSi}_3\text{O}_8$ ) and forms during diagenesis and metamorphism crystallization of certain magmas (Krauskopf et al., 1995). The solubility of silicon such as those in clays (illite, smectite, serpentine) decreases with ambient temperature and pressure.

## **Chapter 3.0 Disposal Costs**

Historically, both commodity extraction from and reuse of produced waters began as early as the 1960's (Collins, 1970). In recent years, the oil and gas industry has been making great strides with water and commodity reuse options. The influence for improving water handling methods is motivated by saving money and revenue potential in recycling their own produced water for reuse in other drilling operations. An additional motivator is water scarcity; some hydrocarbon-bearing areas (e.g., California and west Texas) are or have been in recent draught conditions. When an oil and gas company or water management company can turn waste water into potable water, or at least reuse it, the combined communities gain both intrinsic and extrinsic returns. The current trend is increased produced water recycling and taking one step further, producing mineral commodities, has potential to reap larger societal benefits.

For a commodity to be considered for economic value or potential, it needs to be able to meet economic demand, maintain ample supply and be greater or equal to disposal costs. Determining disposal costs is complex, there is a variety of options and are often depicted by location and regulations. For example, the primary disposal method in the Appalachian Basin is offsite commercial trucking to injection wells or water treatment plants; the distance between the source well and the disposal site can exceed a 100 miles (Guerra et. al., 2011), Thus disposal costs in the Appalachian Basin can be more expensive than those in the Permian Basin, where onsite injection is at times available. There is divisibility in what defines disposal costs and is highly regulated for each location, even within each state.

The complexity of determining individual water management costs extends beyond localities and regulations. End product use (if there is a reuse option), salt water injection availability, freight transportation requirements, and inclement weather are a few additional factors

which influence disposal costs. Individual or grouped efforts derive the total disposal cost outcome. If a company is using an in-house operation, the cost to drill and maintain their own salt water disposal well can range with an upfront cost of \$2 million to \$7 million dollars, again depending on location and disposal method access (Veil, 2015). Water scarcity and technology also controls waste water disposal. Many municipalities encourage to recycling of produced water. In some cases, technology is used to desalinate produced water to different levels of potability, depending on the intended applications. Fees for offsite commercial disposal with disposal or treatments fees range from \$0.015 per barrel disposing at local municipalities to \$26.25 per barrel for land application at (netl.doe.gov, March 4, 2016). Water management costs, including disposal and treatment costs, range from \$0.07-\$1.60 per barrel and treatment costs ranging from \$0.20 to \$8.50 per barrel (Stackpole, 2013, Veil, 2015, Kobelski, 2003, Boysen et al., 2002, and Veil 1997). Quantifying disposal costs is difficult, generalizations are broad and an onsite analysis should be completed to make an informed decision during any exploration development.

Disposal costs include wide ranges in dollars per barrel prices depending on handling methods, burial, discharge, land application treatment and injection. To characterize the varying complexities and constraints in water management, states or portions of states, examined as part of this study, were separated into 6 groups based on similarities in geology, availability of disposal options, and so on. States, rather than geologic basins, were used because regulatory frameworks can greatly impact pricing, and because all available data are reported on a state-by-state basis. The disposal costs assigned for each group are not exact figures unless otherwise noted, but rather generalizations to allow for context of values of the various mineral commodities. These generalized values are based from multiple sources (Stackpole, 2013, Veil, 2015, Kobelski, 2003, Boysen et al., 2002, and Veil 1997). We define Group 1 as the Gulf Coast Region, also commonly

referred to as the Mississippi Embayment. The group includes the basins underlying Gulf Coastal Plain of East Texas, Louisiana, Mississippi, Alabama, and Arkansas. Based on available information, disposal costs in these areas range from \$0.35 to \$4.00 per barrel. Group 2 includes the Rocky Mountain Region, including Colorado, New Mexico, Utah, and Wyoming. Based on available information disposal costs for this group range from \$0.04 to \$5.05 per barrel. Group 3 is the central Midwest including Kansas, Oklahoma and western Texas. Based on available information disposal costs in these areas, disposal costs range from \$0.30 to \$4.00 per barrel, although there are no reported data for Kansas. Group 4 covers the Missouri Plateau and Black Hills regions, which include North Dakota, Montana and South Dakota. Based on available information from North Dakota, disposal costs in these areas range from \$0.35 to \$1.75 per barrel. Unfortunately, no data exist for Montana or South Dakota. Group 5 is Northeast and northern Appalachian Basin including Ohio, Pennsylvania, Michigan, Illinois, Kentucky, and West Virginia. Based on available information, disposal costs in these areas disposal costs range from \$0.25 to \$4.20 per barrel. Pennsylvania is the primary location for the Marcellus Shale gas production and disposal costs are particularly high due to a lack of appropriately classed disposal wells. There is some availability for onsite recycling in the Marcellus shale instead of cost for hauling waste water to Ohio. Disposal costs in Ohio are less expensive for in state operations; costs for out of state operators trucking produced waters into Ohio have increased substantially (Rassenfoss, 2011; Stackhole, 2013). Group 6 is defined as California. Estimated disposal costs here range from \$0.01 to \$0.09 per barrel. These costs are estimates for injection but do not include additional costs mandated by the states for each operator. For instance, some states, such as California and Pennsylvania, require chemical analysis and, in some cases, pre-treatment. Some of the chemical analysis tests can exceed \$250 per load. More complete disposal costs for

California are lacking and is considered as a major gap in the analysis. For easy reference a table has been created with minimum and maximum ranges for dedicated regions.

Table 1: Estimated produced water costs, by state, for six regions.

Group 1			Group 2			Group 3		
Gulf Coast Region			Rocky Mountain Region			Central Midwest		
AR	\$0.40	\$0.75	CO	\$0.04	\$2.80	KS	No data	No data
AL	\$0.35	\$0.50	NM	\$0.025	\$2.23	OK	\$0.30	\$0.65
LA	\$0.50	\$10.00	UT	\$0.50	\$0.75	TX	\$0.40	\$4.00
MS	\$0.37	\$0.60	WY	\$0.01	\$5.05			
TX	\$0.40	\$4.00						
Group 4			Group 5			Group 6		
Black Hills Region			Northeast Region			Western Region		
ND	\$0.35	\$1.75	OH	\$0.20	\$1.50	CA	\$0.01	\$0.09
MT	No Data		IL	No Data	No Data			
SD	No Data		MI	\$0.50	\$1.75			
			PA	\$0.25	\$4.20			
			KY	\$1.00	\$1.00			
			WV	\$0.25	\$1.00			

Table 1: Estimated produced water costs, by state, for the six regions described in the text. Data taken from Stackpole, 2013, Veil, 2015, Kobelski, 2003, Boysen et al., 2002, and Veil 1997.

The values presented are a general guideline when discussing the potential in mineral commodity exploration or development. Each instance must be considered individually and in completeness from exploration, development, disposal costs and commodity extraction. If a commodity is valued at \$4.00 per barrel and disposal costs are estimated at \$0.35 per barrel in one region and \$6.00 per barrel in another, the potential for revenue becomes heavily dependent upon these variations. Another potentially significant factoring cost is that to extract the commodities, which is outside the scope of this thesis.

## Chapter 4.0 Methods

Data sets containing geochemical information for produced waters are available from multiple sources. However, for the purpose of this thesis, the dataset is restricted to the USGS produced waters geochemical database, version 2.2 (Blondes et al., 2016), as it the largest and most comprehensive database of its kind. All data were processed and analyzed using R version 3.1.0. As a pre-processing step, quality assurance/quality control protocols were applied to identify statistical outliers that potentially represented erroneous results. All data for which charge balance error exceeded 10% were omitted, TDS was restricted to sample containing >10,000 mg/L, and only samples from depths of 500 feet or greater were included. The latter criteria avoided inclusion of shallow playa systems, which are fundamentally distinct. To ensure consistency, all data were converted to mg/l and all censored values (i.e., those reported below the detection limits) were replaced with missing values.

Basic summary statistics were calculated for each commodity identified in the produced waters database. Univariate analysis was conducted through creation of exploratory data analysis (combination of histogram, density trace, univariate scatterplots, and boxplots) and empirical cumulative density function plots. Because most constituents exhibit log-normal behavior, these plots were made in log 10 scale. In addition, conventional and robust estimates of the first three statistical moments (central tendency, spread, and symmetry) were calculated for each mineral commodity and summarized in a table. Kendall Tau correlation was applied to examine for monotonic co-association of elements. All negative ( $\tau < -0.1$ ) and all strong positive ( $\tau > 0.6$ ) correlations were noted for each commodity.

Maps of elemental concentrations for each of the mineral commodity in the produced database were generated. As the focus for this work is on only the highest value, they were

statistically visually separated for demonstration purposes. For a given constituent, small black triangles were used to identify locations of concentration where data exist but were below the 75<sup>th</sup> percentile, while color ramped symbols were applied to data locations where concentrations at equal to or greater than the 25<sup>th</sup> percentile, with the color ramp corresponding to their individual concentrations. This allows for the upper 25th percentile to be easily identifiable.

Based on the analysis of the concentration data and estimated mineral commodity values taken from the 2015 USGS Minerals Yearbook: Volume I.—Metals and Minerals (USGS, 2015), economic maps, in dollars per barrel, for each identified commodity were generated. For instance, if the original commodity value was provided in \$/kg of material, the concentration was converted to \$/barrel (bbl) using:

Concentration of elements in water (mg/L) \*commodity value (\$/kg) \*10<sup>-6</sup>(kg/mg) \* 159 (L/bbl) = (\$/bbl). The resulting maps show spatial variability in economic potential for each mineral commodity. These economic maps also serve to identify data gaps and suggest areas of future mineral exploration.

All mineral commodities, as defined by the USGS National Mineral Information Center, are categorized by their data gaps and data needs that correlate with potential for development or exploration. In addition, data coverage and scarcity is examined to evaluate potential for future mineral exploration. For example, cesium is a valuable commodity even at fairly low concentrations, but relatively data are present in the database. As such, cesium would be considered a mineral commodity worthy of additional geochemical exploration for produced waters.

The U.S. Geological Survey publishes metal prices annually and Minerals Yearbooks. For this investigation the 2015 Minerals Yearbook: Volume I.—Metals and Minerals was used to ascertain commodity values. The economic values are subject to current data resources that are available and can be adjusted in the future when markets shift or to customize to a specific area of interest. The economics and/or values applied are conservative estimates and are not considered as an exact figure, unless otherwise noted. Based on the statistical analysis, the identified mineral commodities listed by the USGS National Mineral Information Center are categorized by data gaps and needs that correlate with potential for development (i.e., extraction) or exploration (i.e., new data collection). In addition, data coverage and scarcity is examined to evaluate potential for future mineral exploration.

A literature review was used to aggregate information on mineral commodity extraction via existing domestic commercial operations from produced waters or sedimentary basinal brines. The review details both processing technologies and those compounds extracted. Both current and historical sources are examined (Angino, 1970; Clark and Veil, 2009b; Collins, 1970; Krukowski, 2008; Veil, 2015). In addition to extraction methods, economic history for mineral commodities are also evaluated (U.S. Geological Survey, 2014, 2012). These are mentioned in the section for each individual mineral commodity, as available, in Section 4.

For a commodity to be considered for economic value or potential, it must meet or exceed disposal cost. If the value of a commodity cannot exceed disposal costs, then the cost to produce it (even assuming no cost for extraction) would lead to a net loss in revenue. Table 1 (in Section 2.9) provides estimated ranges for disposal costs via salt water injection for many states, as categories by the six disposal groups. There are large disparities between available data in regards to disposal costs. Despite these uncertainties, comparison of mineral commodity values versus

estimated disposal costs help provide context for the approximate best-case scenario for its net worth.

In addition to mineral commodity evaluation, a brief discussion is included in the thesis that relates to some common extraction methods. This includes a review of existing technology used to extract iodine, bromine and salts. Desalination plants concentrate efforts on brackish and seawaters salinity concentrations which have lower salinities than basinal brines and produced waters in general. Desalination is being implemented in some areas on a smaller scale compared to traditional water utility plants, as the technology continues to improve and costs are reduced for brine treatment. To offset costs of water treatment methods, byproducts such as sodium chloride and magnesium chloride are being extracted.

## **Chapter 5.0 Mineral Commodities**

The 2015 version of United States Geologic Survey Minerals contains information on 85 commodities. Of these, 25 have potential to be extracted from produced waters (Appendix A). Most mineral commodities identified in produced waters would require further conversion, as availability is limited to elements (e.g., potassium is considered a commodity in its potash as  $[K_2O]$ ), with the exception of a few mineral commodities such as iodine, bromine and lithium.

Each commodity chapter in this report, begins with a summarized commodity section directly sourced from the 2015 Mineral Yearbook, which includes information for the periods of 2010- 2014 (U.S. Geological Survey, 2015). A more detailed report on products, commodities, annual values (production and pricing) can be found in the Minerals Yearbook and it is the primary source, unless otherwise noted, for all commodity descriptions. Following the commodity summary and information on current production from produced waters, each chapter includes statistical analysis summarizing data coverage and identifying any possible anomalies. Also includes is a section of a set of maps, the first map identifies the spatial distribution of the concentration of the associated element included in the produced water data base. This map also assists with identifying any data gap coverage that should be included for exploration purposes. The second map is an economic map (in \$/bbl) identified for the commodity. This map serves to identify areas for possible commodity development In addition to the economic maps, a linear-scale Tukey boxplot highlights the upper range in economic worth for each commodity. All chapters include a summarized section discussing the potential for economic exploration and development and in some cases technology which has been used to extract this commodity from produced waters or basin brines.

The commodity summary chapters are a guide for future produced water development and exploration. They outline areas of potential, opportunity and possible improvement to water management. The economic values are subject to change and commodity availability is subjected to technology improvements for extraction purposes. In some instances, one commodity may be more valuable than any other, but when combined can increase revenue margins and may present a valuable marketable commodity at no additional costs, such as the case with rubidium and cesium. Rubidium has a higher value than cesium but the removal technology is the same for both suggesting that for the price to extract rubidium, one could also remove cesium.

## **5.1 Barium**

### **Barium (Ba)**

#### **5.1.1 Commodity:**

Barium is a component of the mineral commodity barite ( $\text{BaSO}_4$ ). The majority of barite sold in the United States is to oil and gas operators as a weighting agent in drilling muds because of its non-magnetic characteristics and high density ( $4.5 \text{ g/cm}^3$ ). Barite is also used in x-ray equipment and fillers for paints. Most barite is currently obtained from mining of ore deposits. However, there are several U.S. locations with high Ba concentration in produced waters. The average the estimated value for barite in 2015 was \$125 per metric ton. Assuming a no-cost conversion of barium to barite (which is somewhat reasonable given the exceptionally low solubility of the mineral), barite values (as barium) were calculated.

#### **5.1.2 Geochemical Statistics:**

Barium concentrations were examined using two types of plots (Figure 2): a combination of a histogram, density trace, boxplot, and one-dimensional scatterplot (left side) and Empirical Cumulative Distribution Function (ECDF)-plot (right side) (Reimann et al., 2008). Interpretation of the EDCF-plot (Figure 2) shows variance that indicates multiple small sub populations with breaks at 0.15 mg/L and 2.0 mg/L. Overall, it follows a multi-modal distribution.

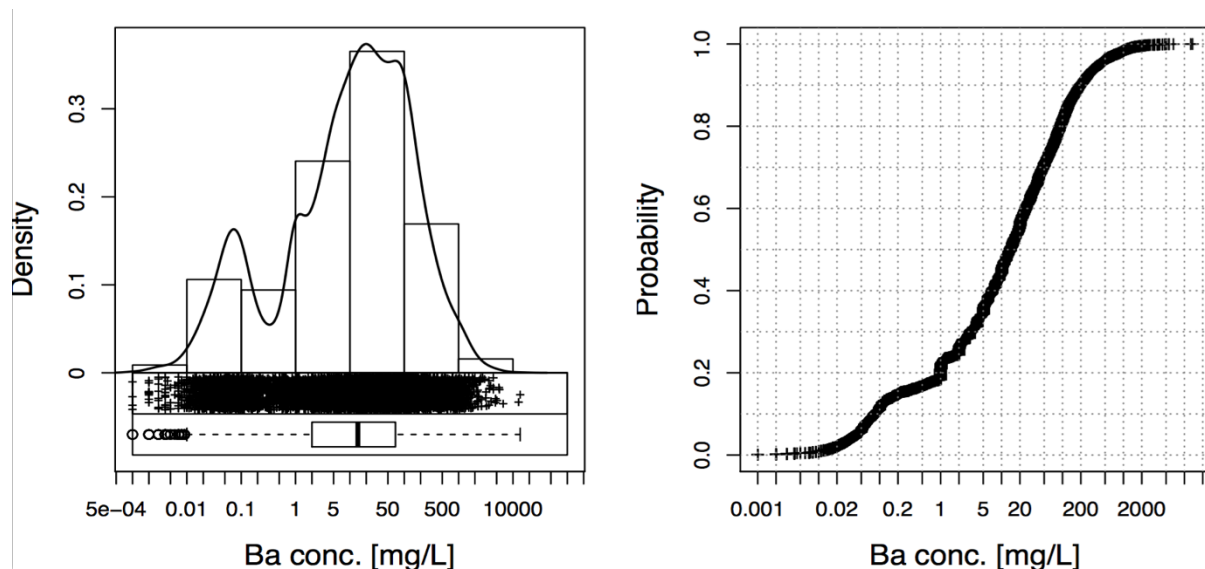


Figure 2: National EDA-plot in log scale, barium concentrations are bi-modal with small sub-populations at 0.15 and 2.0 mg/L

### 5.1.3 Summary Statistics:

Table 2. Univariate data analysis for barium.

	MIN	Q_0.05	Q1	MEDIAN	MEAN-log	MEAN	Q3	Q_0.95	MAX	SD	MAD	pσ	CV %	CVR %
Ba	0	0.042	2	14	8.53	93.89	69	401.2	13600	343.5	20.61	49.67	365.8	147.2

Calculations were compiled to include: minimum (MIN), 5<sup>th</sup> percentile (Q\_0.05), 25<sup>th</sup> percentile (Q1), median, geometric mean (MEAN\_log), mean, 75<sup>th</sup> percentile (Q3), 95<sup>th</sup> percentile (Q\_0.95), maximum (MAX), standard deviation (SD), pseudosigma (pσ), coefficient of variation (CV), and robust coefficient of variation (CVR).

### 5.1.4 Kendall Tau:

Barium does not positively correlate well with any other elements at  $\tau > 0.6$ . However, it does show some moderate correlation with Be ( $\tau = 0.58$ ), Co ( $\tau = 0.58$ ), and Li ( $\tau = 0.55$ ). Constituents negatively correlated with barium are SO<sub>4</sub> ( $\tau = -0.24$ ) and HCO<sub>3</sub> ( $\tau = -0.13$ ). The inverse correlations with SO<sub>4</sub> and HCO<sub>3</sub> are likely driven by the solubility of barite and witherite (BaCO<sub>3</sub>), suggesting these minerals are important in controlling the abundance of Ba in produced waters.

## 5.1.5 Maps:

### 5.1.5.1 Spatial Data

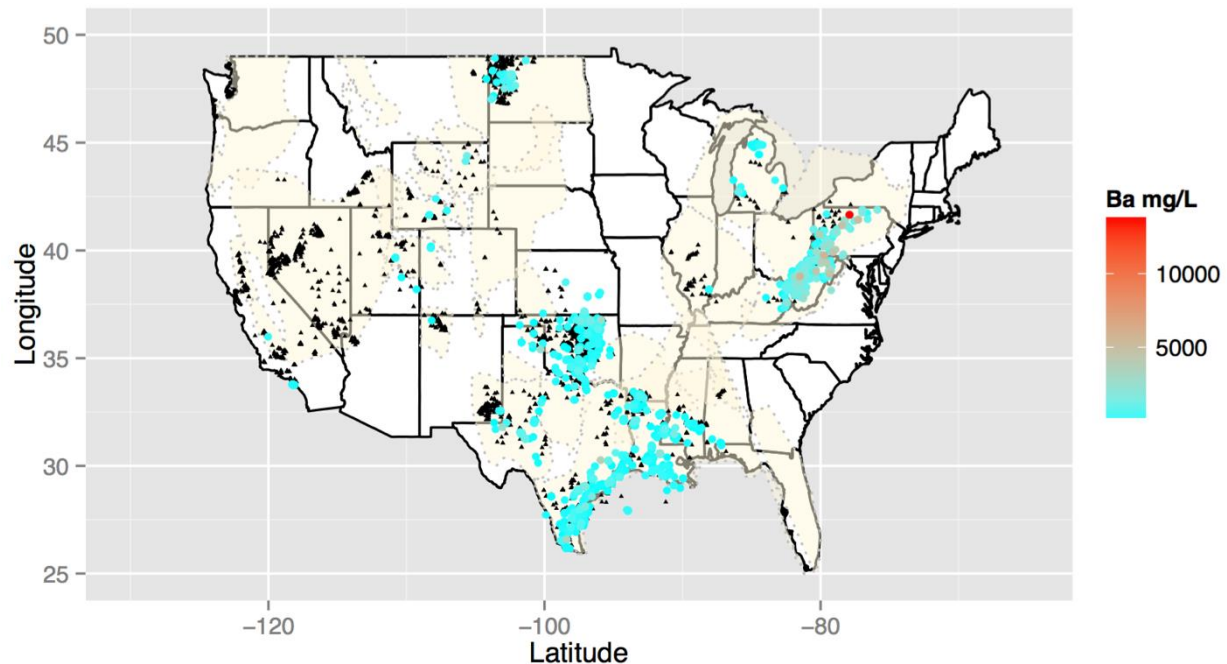


Figure 3: National spatial concentration map for barium. Black triangles identify locations where Ba concentration data exist but are below the 75th percentile. Color ramped symbols applied to the sites where concentrations exceed the 75th percentile.

The highest barium concentrations found in produced water samples are from the Marcellus Shale in the northern Appalachian Basin (Figure 3). Recent investigators have shown the local water-rock interactions, including leaching of Ba from the shale itself, the primary source of this anomaly (Stewart et al., 2015). Otherwise, barium concentration in produced waters are generally low, due to the low solubility of barite.

### 5.1.5.2 Estimated Economic Values for Barium

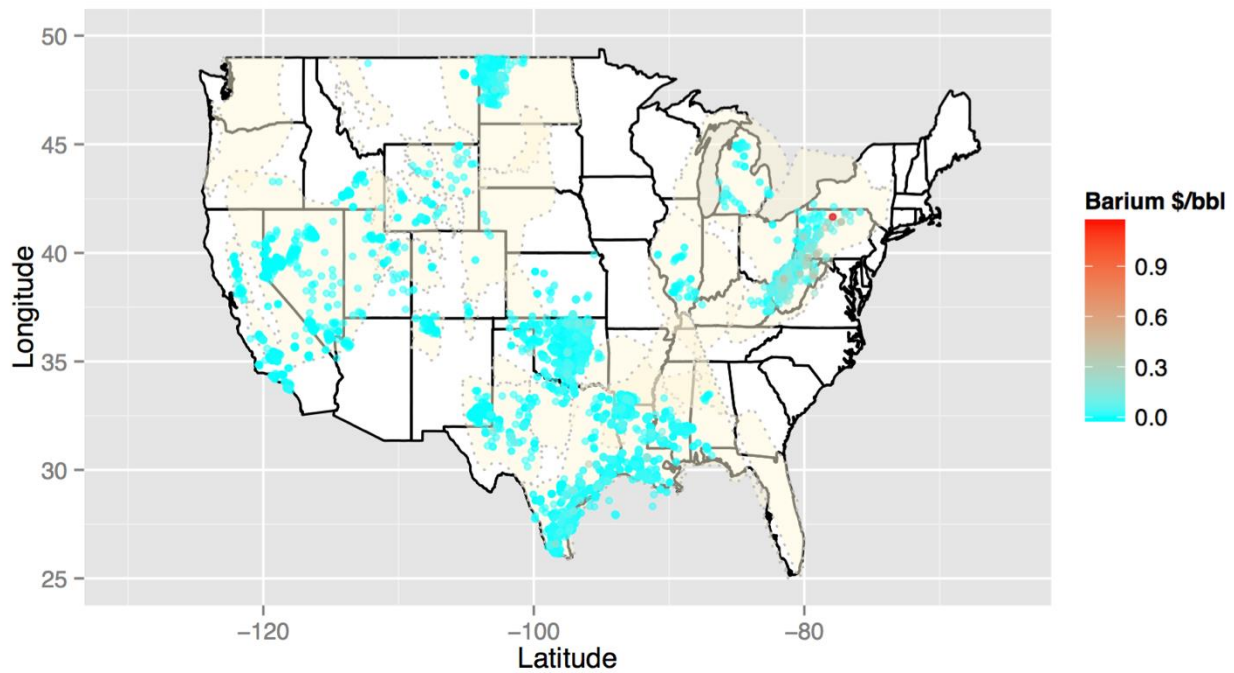


Figure 4: Economic concentration map identifying highest areas of interest: The Appalachian Basin

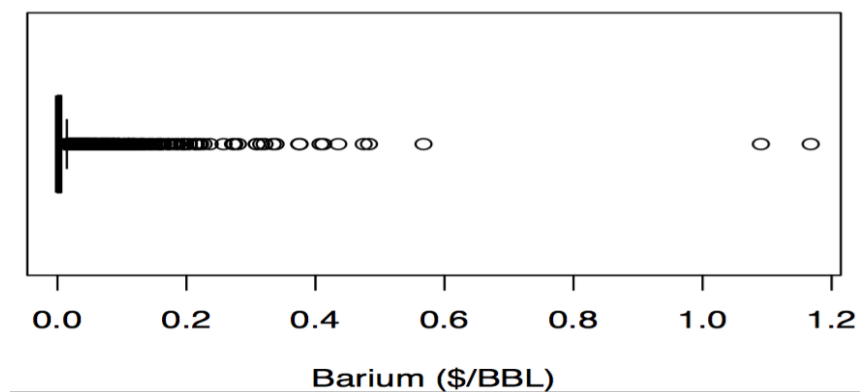


Figure 5: Tukey boxplot of economic values for barium in produced waters.

The estimated economic map (Figure 4) for barium applies the value provided by the USGS Minerals Yearbook in a \$/bbl based on concentration data from the spatial analysis maps. Barite commodity product is valued at \$125 metric ton ( $5.40 \times 10^{-7}$  per milligram per liter). Barium has an estimated value range from 0.10 to 0.6 \$/bbl with a few anomalous values exceeding \$1.00/bbl.

In the Northeast region, estimated disposal costs range from roughly \$0.20 to \$4.20 a barrel. Given estimated commodity values, the potential for commodity development for barium. In addition to anomalously high values that exceed \$1.00 the average is still moderate when compared to the disposal costs and has potential for further exploration and possible development.

#### **5.1.6 Summary:**

Barium is traditionally mined from ore deposits as barite, but has some potential to be generated from produced waters. National data coverage for barium in produced waters is reasonable, suggesting only moderate need for further exploration especially for Marcellus Shale where values are high but data are sparse. Potential for extraction of barium is minimal, as it does not exceed disposal costs for most regions outside of the Appalachian Basin. An extrinsic value for barium is in other products that can be removed from brines, such as magnesium carbonates and or calcium carbonates. Barium is often removed from solution during water treatment desalination plants. Barium causes scaling problems for both desalination water treatment plants and oil and gas field operations. In water treatment facilities, during descaling process additional barium carbonate is added until it is composed of precipitates of barium carbonate, magnesium carbonate and calcium. The precipitates are then treated to separate soluble from insoluble sulfates, thus resulting in barite (US Patent, 1970). Modifications to this method can be made to high saline waters in the Appalachian Basin.

## **5.2 Boron**

### **Boron (B)**

#### **5.2.1 Commodity:**

U.S commercial boron production is withheld due to proprietary information, but the value of boron was ascertained as the average value for exported boron at \$630 dollars per metric ton in 2015. Boron products include but are not limited to borax, boric acid ( $\text{B(OH)}_3$ ) and sodium borates. These compounds are used in the creation of glass, abrasives, cleaning products and in the production of semiconductors. Elemental boron is a metalloid and has limited commercial applications, thus boron-bearing compounds are most sought after (Crangle, 2013). Refining of brines does produce commercial grade boric acid and sodium borates (USGS, 2013). At present some boron compounds can be recovered from produced waters using methods such as reverse osmosis membranes, selective boron ion exchange resins, or dosing with chemical additives (Lenntech, 2016). Boron removal processes come with a variety of factors to consider prior to removal, i.e. temperature, pH, capital costs, and TDS limits (Rodarte and Smith, 2014; U.S. Geological Survey, 2015).

#### **5.2.2 Geochemical Statistics:**

Boron concentrations were examined using two types of plots (Figure 6): a combination of a histogram, density trace, boxplot, and one-dimensional scatterplot (left side) and Empirical Cumulative Distribution Function (ECDF)-plot (right side) (Reimann et al., 2008). The histogram and density trace plots suggest that B exhibits a bimodal distribution with a break at around 1 mg/L, with another subpopulation above 250 mg/L.

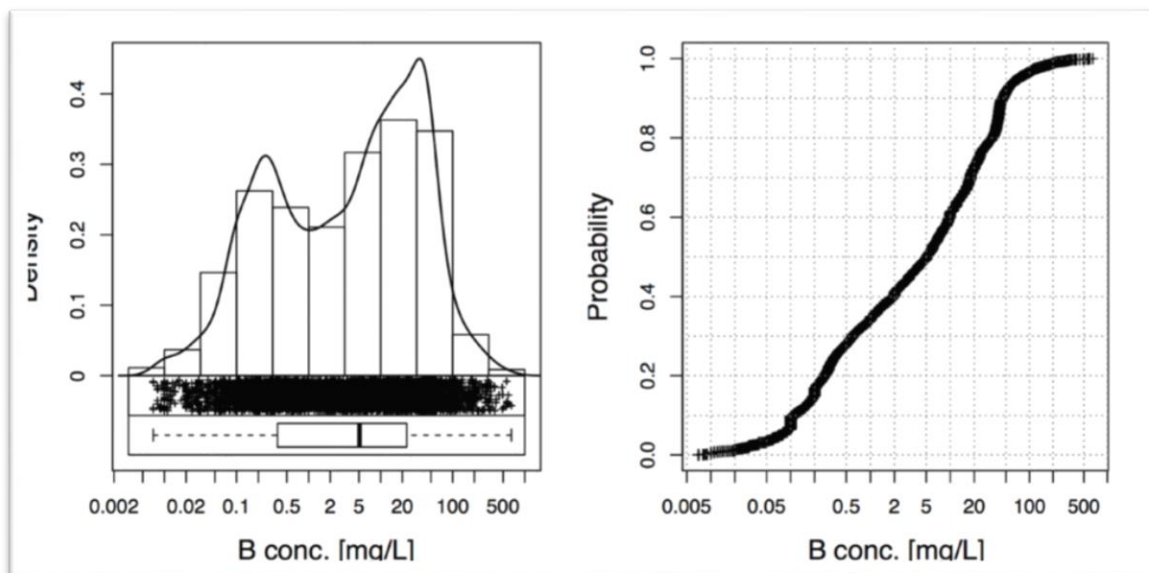


Figure 6: National EDA-plot in log scale, boron concentrations that is slightly right skewed with multiple populations with breaks at 1 mg/L and 250 mg/L. The EDCF plot on the right presents a sigmodal distribution curve.

### 5.2.3 Summary Statistics:

Table 3. Univariate data analysis for boron.

	MIN	Q_0.05	Q1	MEDIAN	MEAN -log	MEAN	Q3	Q_0.95	MAX	SD	MAD	pσ	CV %	CVR %
<b>B</b>	0.007	0.075	0.37	5.1	3.157	19.83	23	72	650	43.48	7.366	16.78	219.3	144.4

Calculations were compiled to include: minimum (MIN), 5<sup>th</sup> percentile (Q\_0.05), 25<sup>th</sup> percentile (Q1), median, geometric mean (MEAN\_log), mean, 75<sup>th</sup> percentile (Q3), 95<sup>th</sup> percentile (Q\_0.95), maximum (MAX), standard deviation (SD), pseudosigma (pσ), coefficient of variation (CV), and robust coefficient of variation (CVR).

### 5.2.4 Kendall Tau:

Boron does not positively correlate with any other elements at  $\tau > 0.6$ . However, it does show some moderate correlation with As ( $\tau = 0.58$ ), Mo ( $\tau = 0.58$ ), Se ( $\tau = 0.54$ ), Na ( $\tau = 0.53$ ), and Br ( $\tau = 0.53$ ). No elements were negatively correlated with boron at  $\tau < -0.1$ . Boron's association with Na and Br in produced waters indicates one of its sources is ancient seawater. Another potential boron source is leaching from clays (Kharaka, 2007).

## 5.2.5 Maps:

### 5.2.5.1 Spatial Data

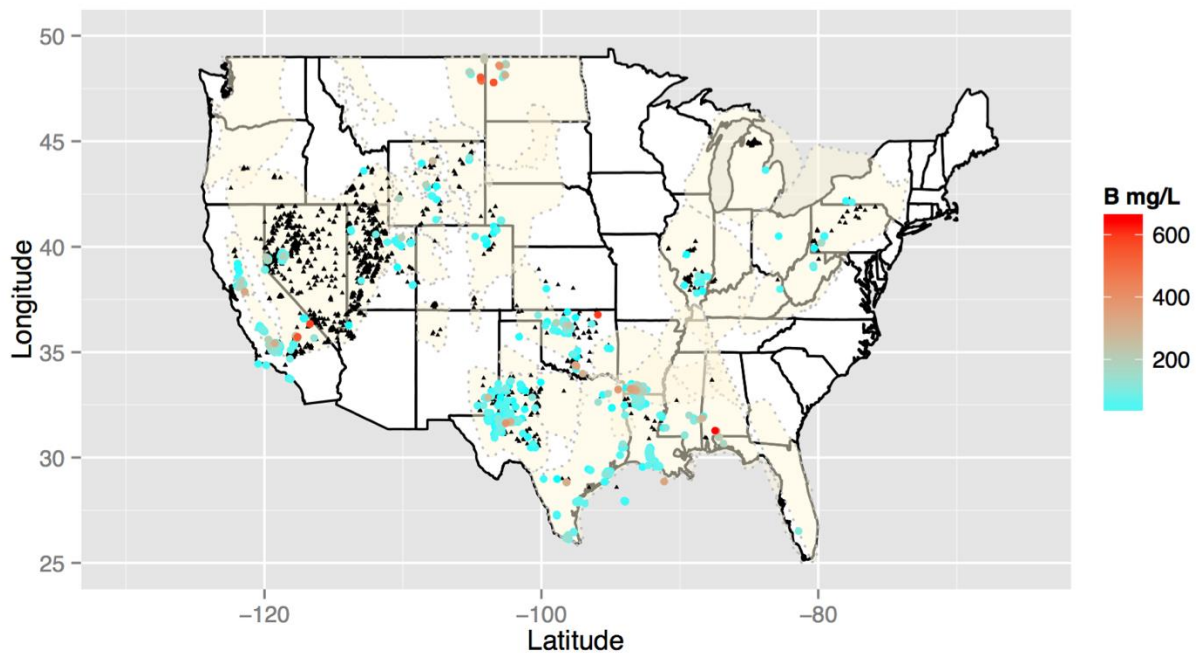


Figure 7: National spatial concentration map for boron. Black triangles identify locations where B concentration data exist but are below the 75th percentile. Color ramped symbols applied to the sites where concentrations exceed the 75th percentile.

The highest boron concentrations are located in the Smackover Formation in southern Arkansas, the Williston Basin, the Anadarko Basin and eastern portions of the Gulf Coast Basin. These plays are dominated by illite/smectite clays and/or contain marine-derived organic deposits. Prior to clays being buried, they are subjected to erosion and weathering, ultimately releasing boron into shallow portions of some sedimentary basins. In addition, produced waters from these regions are characterized as evaporated paleoseawater, which contains elevated levels of boron (Lowenstein et al., 2005).

### 5.2.5.2 Estimated Economic Values for Boron

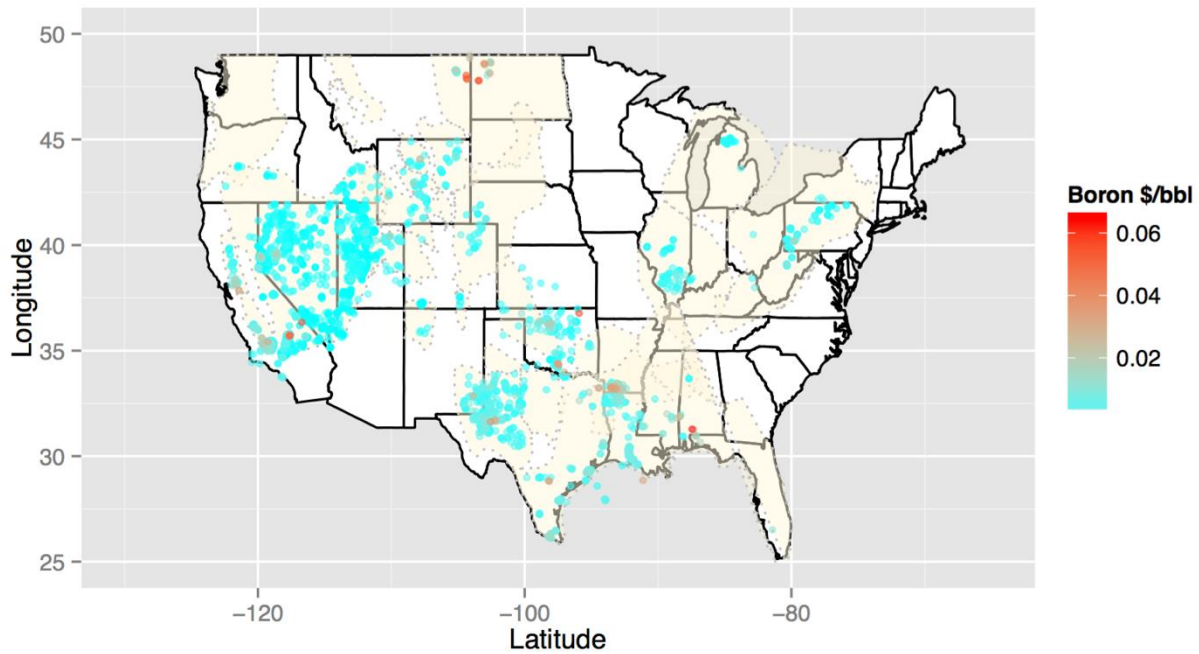


Figure 8: Economic concentration map identifying highest areas of value: The Smackover Formation, Williston Basin, Woodward Basin, Permian Basin and the Gulf Coast.

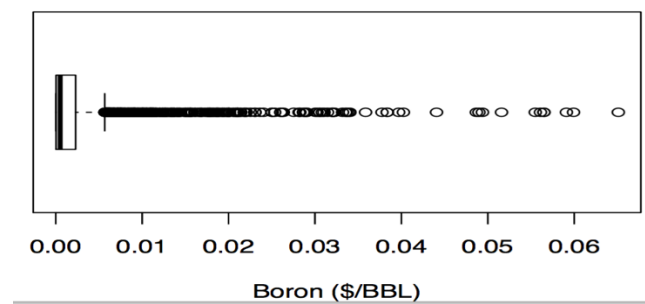


Figure 9: Tukey boxplot of economic values for boron in produced waters.

Using an export price of \$630 per metric ton ( $6.30\text{E-}07$  per milligram per liter) for boron, estimated value on a per barrel basis does not exceeds \$0.10. This is less than disposal costs in portions of Group 1, 3, and 4 suggesting there is some potential for economic extraction (cf. Table

1). Data coverage for boron is variable but at least moderate information is available for most basins, suggesting that the potential for future exploration is limited. However, boron can affect the ability to reuse produced waters, particularly gel-based fracturing fluids, so its removal may have more of an extrinsic value. When boron removal is combined with desalination treatment processes, the volume of boron produced as a byproduct during water treatment might generate enough boron to offset or even cover the cost of disposal (see Section 8). Thus, the greatest potential for boron is co-removal to allow for the use of water in other applications, rather than as a sole product.

#### **5.2.6 Summary:**

In general, at present there is little economic incentive to remove boron from produced waters or to ramp up exploration work. However, boron compounds can be problematic to oil and gas operations that utilize a gel fracturing fluid; it can prematurely offset the cross-linker by increasing the viscosity of the fracturing fluid at the surface (Rodarte and Smith, 2014). Most often boron is removed on-site, but can be separated from solution for minimal revenue. During the analysis of the case study (Section 8), it was determined if boron removal processes for the purposes of extraction were attached to a water treatment method, boron compound concentrations could reach a breakeven point. The data coverage in the database is sufficient to support the analysis. Boron can be produced as a commodity from produced waters, its general abundance might allow for production to exceed market demand, driving values lower.

## **5.3 Bromine**

### **Bromine (Br)**

#### **5.3.1 Commodity:**

Bromine is present in elevated concentrations in some brines and has historically been produced from high salinity waters (Warren, 2000). At present, it is generated from brines from the Smackover formation in Arkansas (Collins, 1970; Warren, 2000). Bromine is used in a variety of products including flame retardants, dyes, pharmaceuticals and insect repellants. In oilfield operations, bromide is used in drilling fluids, well completions, and packer applications. Due to proprietary information the product value has been withheld from the Minerals Yearbooks. However, through trade publications, it has been reported values average \$3500-\$3900 per metric ton, showing a 20% increase from the previous year (2014) (U.S. Geological Survey, 2015).

#### **5.3.2 Geochemical Statistics:**

Bromine concentrations were examined using two types of plots (Figure 10) that include a combination of a histogram, density trace, boxplot, and one-dimensional scatterplot (left side) and Empirical Cumulative Distribution Function (ECDF)-plot (right side) (Reimann et al., 2008). Interpretation of the EDA-plot (Fig. 8) suggests that Br concentrations exhibit a bimodal distribution with a break at around 5 mg/L. However, EDCF plot suggests that additional sub populations might exist with breaks near 2000 mg/l and 5200 mg/l.

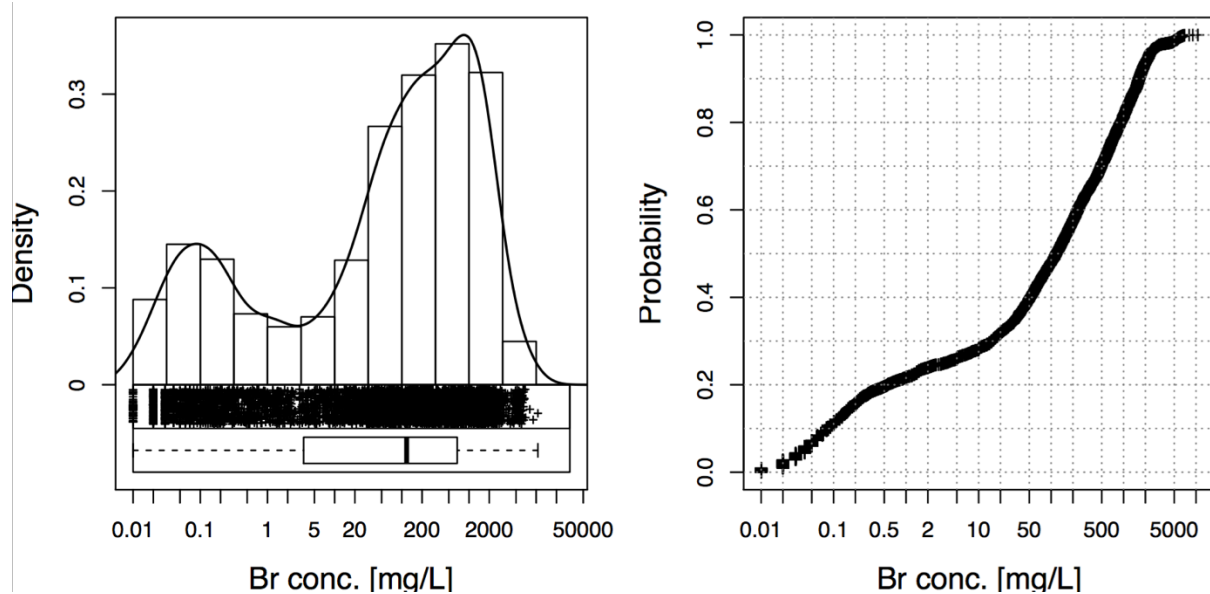


Figure 10: National EDA-plot in log scale, which includes a combination of a histogram, density trace, boxplot, and one-dimensional scatterplot (left side) and Empirical Cumulative Distribution Function (ECDF)-plot (right side). Bromine concentrations have a bimodal distribution and the EDCF plot has a sigmoidal distribution curve.

### 5.3.3 Summary Statistics:

Table 4. Univariate data analysis for bromine.

	MIN	Q_0.05	Q1	MEDIAN	MEAN-log	MEAN	Q3	Q_0.95	MAX	SD	MAD	$p\sigma$	CV %	CVR %
Br	0.01	0.04	3.45	117.9	37.77	538.5	667	2220	10600	966.9	174.7	491.9	179.5	148.2

Calculations were compiled to include: minimum (MIN), 5<sup>th</sup> percentile (Q\_0.05), 25<sup>th</sup> percentile (Q1), median, geometric mean (MEAN\_log), mean, 75<sup>th</sup> percentile (Q3), 95<sup>th</sup> percentile (Q\_0.95), maximum (MAX), standard deviation (SD), pseudosigma ( $p\sigma$ ), coefficient of variation (CV), and robust coefficient of variation (CVR).

### 5.3.4 Kendall Tau correlation:

In descending order, elements positively correlated ( $\tau > 0.6$ ) with Br include: Ca ( $\tau = 0.77$ ), Sr ( $\tau = 0.75$ ), Cl ( $\tau = 0.74$ ), Na ( $\tau = 0.66$ ), Mg ( $\tau = 0.65$ ), K ( $\tau = 0.64$ ), Pb ( $\tau = 0.64$ ), Co ( $\tau = 0.63$ ),

Mn ( $\tau=0.63$ ), and Be ( $\tau=0.61$ ). Lithium positively correlates at ( $\tau=0.59$ ). Constituents negatively correlated with Br are: Hg ( $\tau = -0.22$ ), S ( $\tau = -0.22$ ),  $\text{HCO}_3$  ( $\tau = -0.21$ ), and Si ( $\tau = -0.2$ ). Among these positive correlations the closest relationships are calcium, strontium, chloride, sodium, and magnesium and which are associated with basinal brines derived from paleo-evaporated seawater, suggesting this is one source of high Br concentrations (Kharaka and Hanor, 2014).

### 5.3.5 Maps:

#### 5.3.5.1 Spatial Distribution:

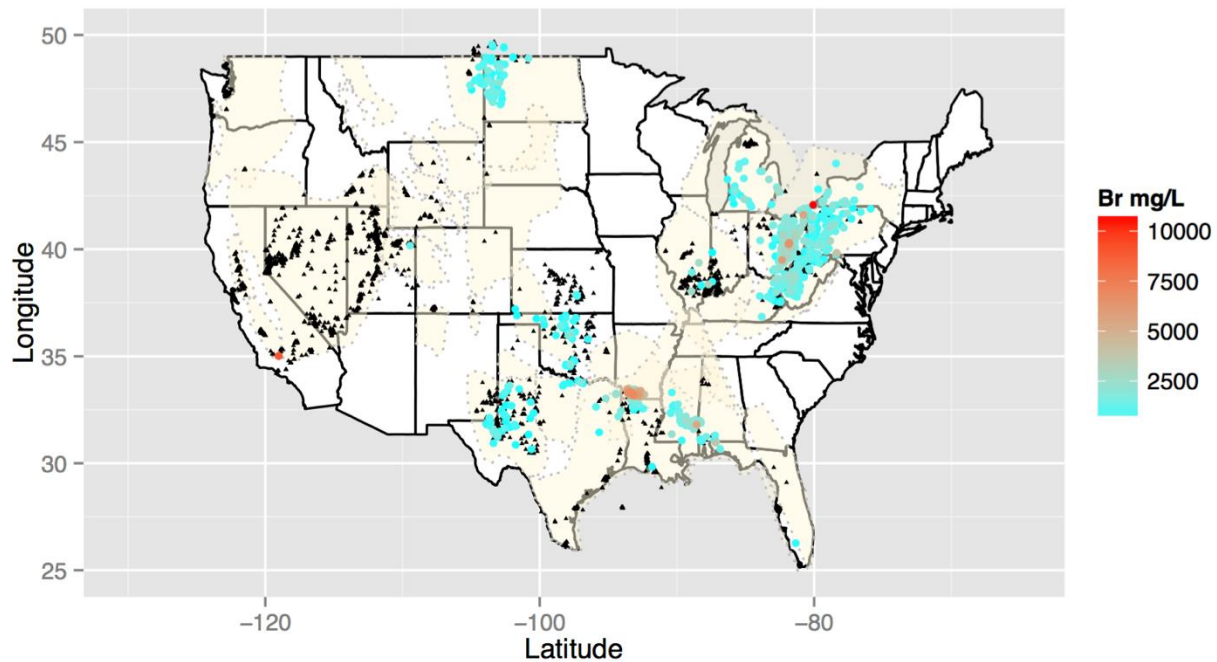


Figure 11: National spatial concentration map for bromine. Black triangles identify locations where Br concentration data exist but are below the 75th percentile. Color ramped symbols applied to the sites where concentrations exceed the 75th percentile.

Results indicate that the highest Br concentrations are found in produced waters from the Smackover Formation, Gulf Coast Basin and the western half of the Appalachian Basin (Budd 1991), and tend to be areas with the highest TDS concentrations (Figure 1). All three identified locations are characterized by ancient paleoevaporated seawater (Lowenstein et al., 2005). The map shows data coverage for bromine concentrations is rather extensive and moderately complete for a few primary locations. Coverage is limited in other areas. Data gaps that could be included, when available, would be regional locations, such as southern Texas, Colorado and Wyoming. The exploration potential for bromine is relatively moderate.

### 5.3.5.2 Estimated Economic Values:

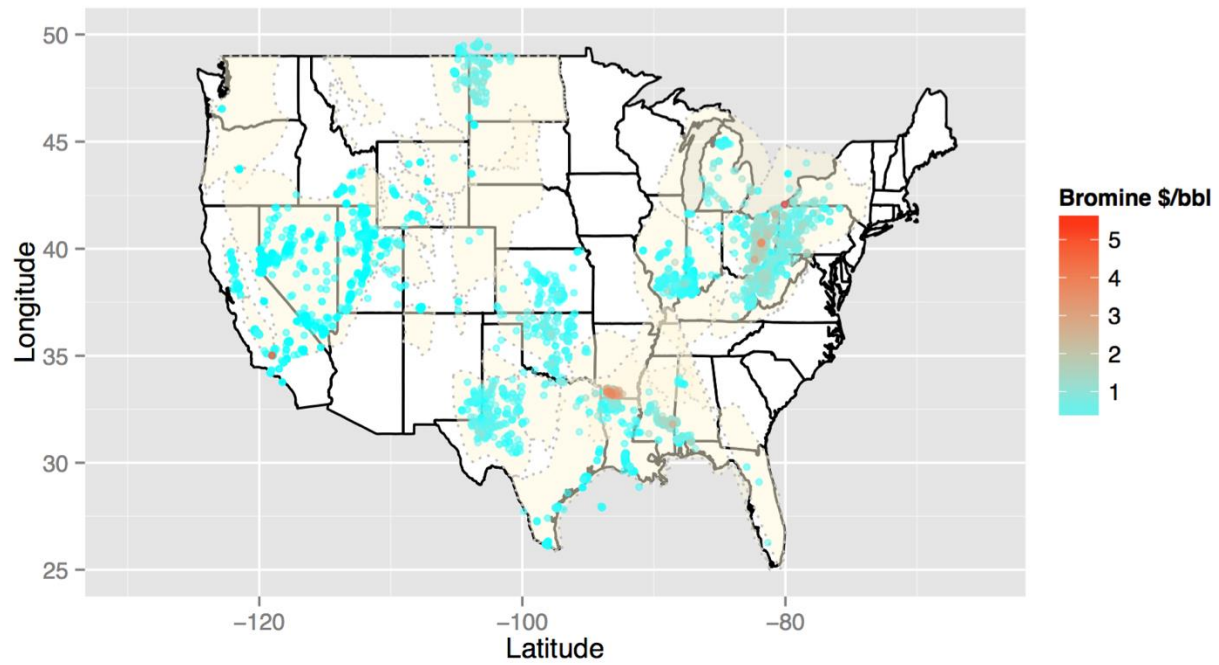


Figure 12: Economic concentration map identifying highest areas of interest: The Gulf Coast Basin, Smackover Formation and the Appalachian Basin.

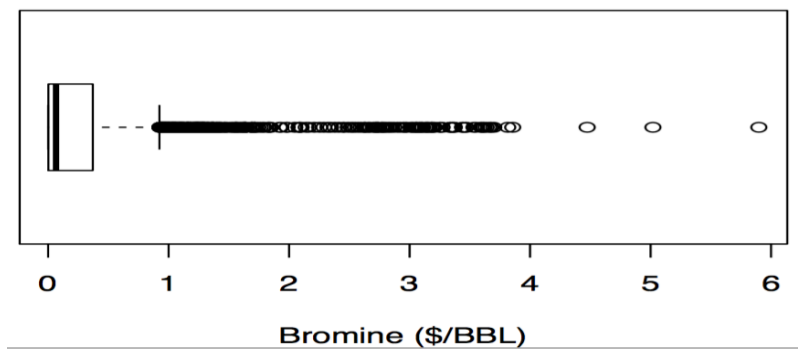


Figure 13: Tukey boxplot of economic values for bromine in produced waters.

Bromide commodities are valued at \$3500 per metric ton (\$3.50E-06 per milligram). Applied to the concentration results shown in (Figure 11), several areas show gross values in excess of \$1/bbl. However, disposal costs impact the potential profit. Analysis suggests that further development for bromine extraction is good, especially in the Smackover Formation and Gulf Coast basin, where values approach and exceed \$5/bbl and are in the Group 1 category, having the least expensive disposal costs. Conversely, western regions of the Appalachian Basin, the Michigan Basin, and Williston Basin have high potential value but the higher disposal costs for Group 4 and Group 5 states reduces potential for economic profit and local detailed analysis would be required. This is because Br in the identified locations will vary in profit potential with disposal costs. In the Smackover Formation, a multimillion dollar year business has thrived since the 1960's extracting bromide from the basinal brines (Warren, 2000). The potential for expansion in other basins is identified by here by the economic potential maps.

#### **5.3.6 Summary:**

The exploration and further development for bromine commodity products extends beyond the known commodity extraction operations in the Smackover Formation. Given the range of values and data coverage, potential for further exploration is moderate with some regional gaps. The commodity values, concentrations, and disposal costs, greatest potential for development exists in other basins such as the Williston, Illinois and Permian Basins, where disposal costs are moderately low. When considering development in the western Appalachian Basin, Michigan Basin, or Illinois Basin more economic analysis needs to be applied. Disposal costs are higher for these areas, but does not mean profits are limited for bromine extraction. Research needs to include local manufacturing plants that use bromine products, this may subset disposal expenses, thus making these locations much more profitable. There is consistency for high Br concentrations both

locally and regionally in identified places with high salinity concentrations. One significant challenge in the extraction of Br, is its separation from chloride. Bromine is also associated with other constituents that have profit potential, such as lithium, rubidium, cesium, and iodine (cf. Figure 1, Figure 51, Figure 23, and Figure 43), therefore may be more economical to extract elements as a group.

## **5.4 Cadmium**

### **Cadmium (Cd)**

#### **5.4.1 Commodity:**

Cadmium primary production is from byproduct zinc ore production. Due to proprietary information, the sale values have been withheld from the Minerals Yearbooks. Cadmium is used in nickel battery production, alloys and anticorrosive coatings. In 2013, average price was \$0.90 per pound according to the Platts Metals New York Dealer price, per the Mineral Yearbook report (U.S. Geological Survey, 2015). Cadmium concentrations are relatively low, but it is present in produced waters.

#### **5.4.2 Geochemical Statistics:**

Cadmium concentrations were examined using two types of plots (Figure 14): that include a combination of a histogram, density trace, boxplot, and one-dimensional scatterplot (left side) and Empirical Cumulative Distribution Function (ECDF)-plot (right side) (Reimann et al., 2008). Interpretation of the EDCF-plot (Figure 11) has a tri-modal distribution and shows a variance indicated by sub populations with breaks near 0.0005 mg/L and 0.01 mg/L. The density plots, histograms, boxplots and scatterplot suggest that Cd concentration is multi-modal, even on a log-scale.

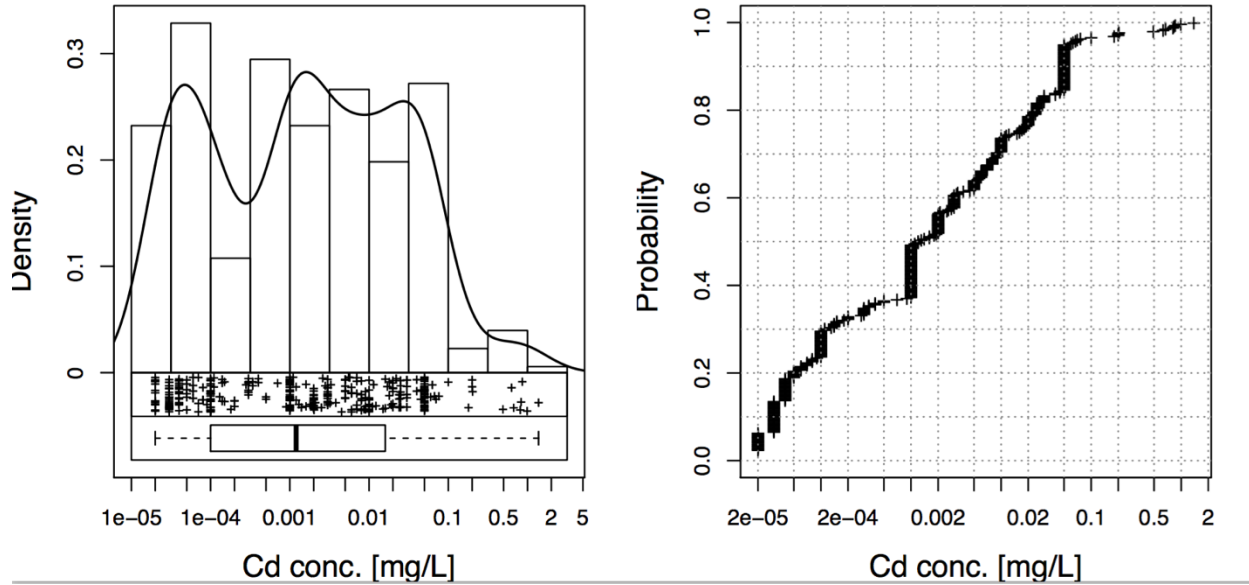


Figure 14: National EDA-plot in log scale, which includes a combination of a histogram, density trace, boxplot, and one-dimensional scatterplot (left side) and Empirical Cumulative Distribution Function (ECDF)-plot (right side). Cadmium concentrations shows a multi-modal distribution.

### 5.4.3 Summary Statistics:

Table 5. Univariate data analysis for cadmium.

	MIN	Q_0.05	Q1	MEDIAN	MEAN-log	MEAN	Q3	Q_0.95	MAX	SD	MAD	pσ	CV %	CVR %
Cd	0.00	0.00002	1.00E-04	0.0012	0.001514	0.03103	0.016	0.05	1.38	0.1293	0.001735	0.01179	416.7	144.6

Calculations were compiled to include: minimum (MIN), 5<sup>th</sup> percentile (Q\_0.05), 25<sup>th</sup> percentile (Q1), median, geometric mean (MEAN\_log), mean, 75<sup>th</sup> percentile (Q3), 95<sup>th</sup> percentile (Q\_0.95), maximum (MAX), standard deviation (SD), pseudosigma (pσ), coefficient of variation (CV), and robust coefficient of variation (CVR).

### 5.4.4 Kendall Tau correlation:

In descending order, elements positively correlated ( $\tau > 0.6$ ) with Cd include: Se ( $\tau = 0.63$ ), Cu ( $\tau = 0.63$ ), Cr ( $\tau = 0.62$ ), Pb ( $\tau = 0.62$ ), and Co ( $\tau = 0.61$ ). Constituents negatively correlated with Cd are: Si ( $\tau = -0.46$ ), I ( $\tau = -0.16$ ), and Ti ( $\tau = -0.12$ ). Among these positive correlations the closest relationships are selenium, copper, chromium, lead and cobalt. This grouping of elements is commonly found in sulfide metal ore deposits.

## 5.4.5 Maps:

### 5.4.5.1 Spatial Distribution:

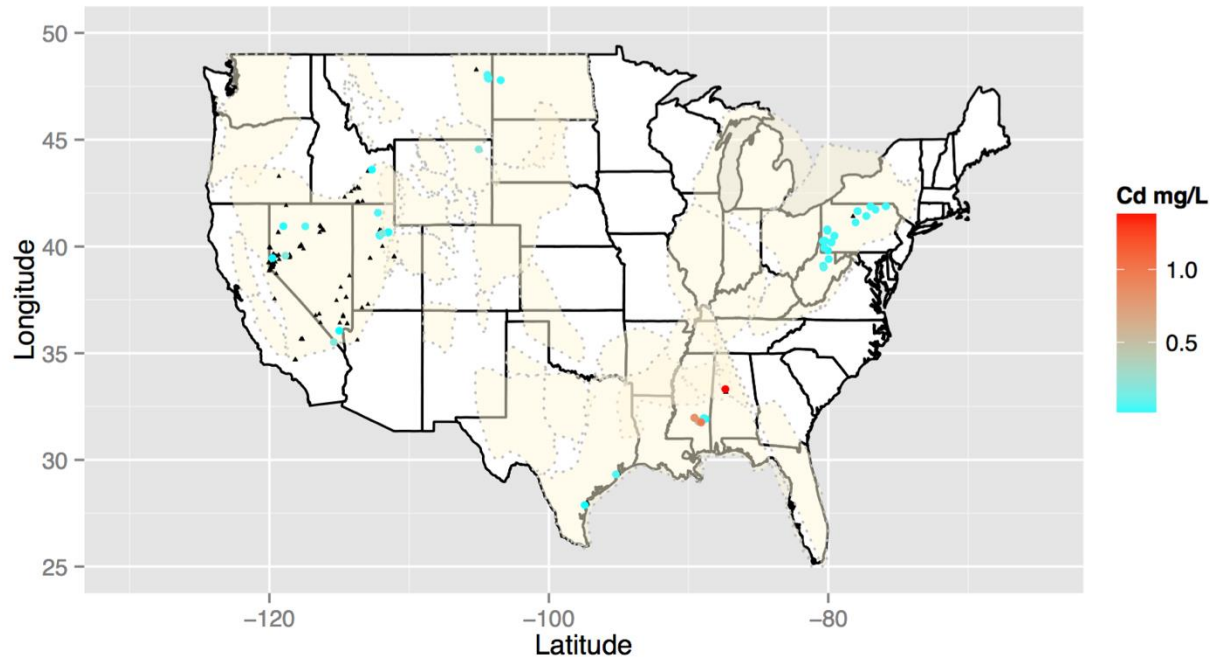


Figure 15: National spatial concentration map for cadmium. Black triangles identify locations where Cd concentration data exist but are below the 75th percentile. Color ramped symbols applied to the sites where concentrations exceed the 75th percentile.

Spatial distribution for Cd is extremely limited and data gaps are widespread. Cadmium is a minor or trace element in Mississippi Valley Type (MVT) mineral deposits that are abundant in proximity to the Black Warrior Basin and the Mississippi Embayment. Mississippi Valley Type ore deposits consist of sulfide minerals (zinc-lead ores) and are associated with large carbonate deposits (Leach, 2001). Depositional environments for MVT deposits vary from basement sediments, weathering and carbonate aquifers (Leach et al., 2010).

### 5.4.5.2 Estimated Economic Values:

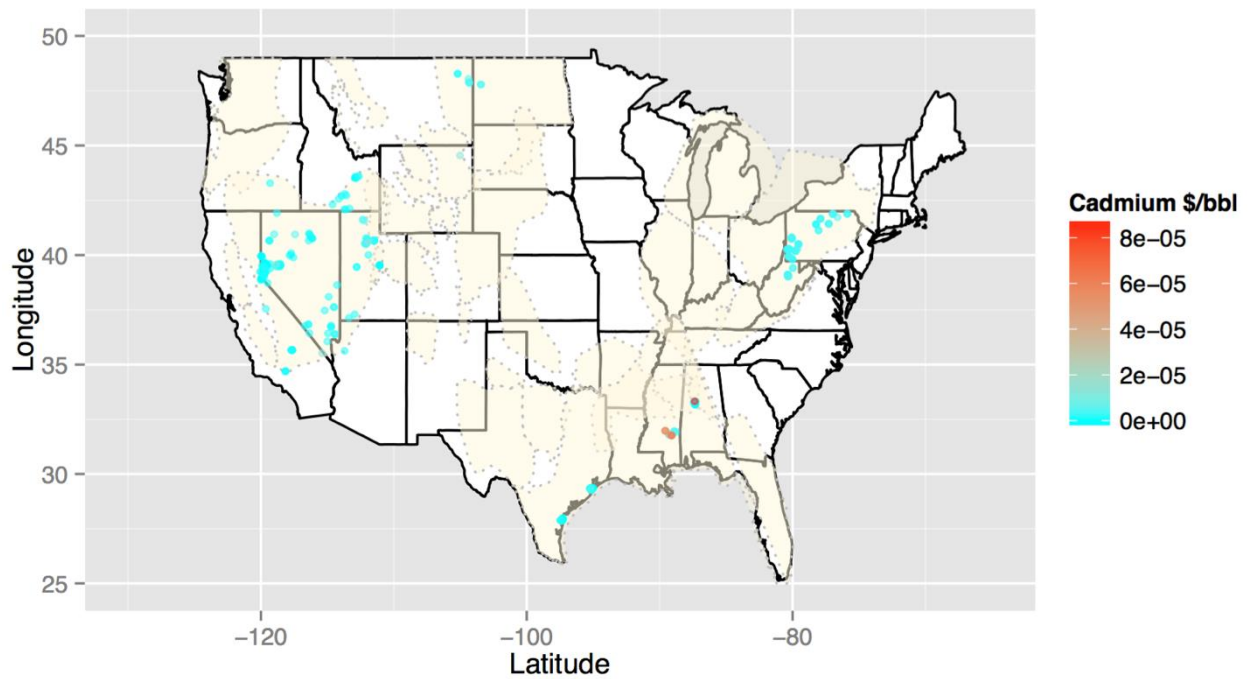


Figure 16: Economic concentration map identifying highest areas of interest; The Western Region, the Gulf Coast Basin (Black Warrior Basin) and Northeastern Region (the Appalachian Basin).

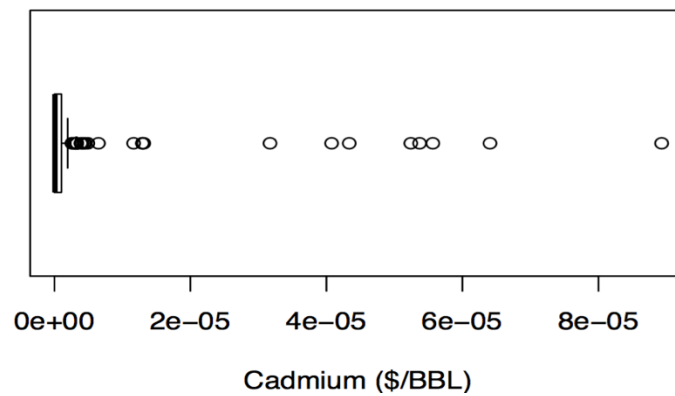


Figure 17: Tukey boxplot of economic values for boron in produced waters.

Cadmium potential for development is negligible in produced waters with estimated values <\$0.01/bbl for all data. Thus, the value for Cd is primarily limited to co-recovery. Despite large data gaps, results suggest there is minimal potential for exploration or development of cadmium commodities from produced waters.

#### **5.4.6 Summary:**

Given available data, both exploration and development for extraction of cadmium from produced waters has little to no potential. There is limited potential for extraction if it is combined with other elements co-associated with MVT ore deposits but does not currently appear profitable as a lone product. The spatial coverage of the data is restricted to select areas, so more data are needed to better understand cadmiums distributions, but the current economic values do not support further work. There are other known MVT deposits which could contain elevated levels of cadmium, but the produced waters database lacks cadmium data from these areas.

## **5.5 Calcium**

### **Calcium (Ca)**

#### **5.5.1 Commodity:**

The principal mineral commodities for calcium, according to the Minerals Yearbook, are lime and gypsum. It was estimated in 2014 that 19 million tons of gypsum were produced for manufacturing. Products vary from drywall to additives for metal leaching in gold and silver mining. Derivative chemical products of calcium consist of calcium carbonate, calcium chloride, calcium oxides, calcium hydroxides, and dolomitic hydrates. Usages for calcium range from agriculture applications to the pharmaceutical industry. In oilfield drilling operations, calcium carbonate (lime) is applied as an alkalinity buffer. Lime prices in 2012 range from \$2.30-\$3.70 per metric ton and for dolomitic hydrate \$7.90 per metric ton for a cumulative average for lime and dolomitic hydrate price is \$5.80 per metric ton (U.S. Geological Survey, 2015).

#### **5.5.2 Geochemical Statistics:**

Calcium concentrations were examined using two types of plots (Figure 18) that include a combination of a histogram, density trace, boxplot, and one-dimensional scatterplot (left side) and Empirical Cumulative Distribution Function (ECDF)-plot (right side) (Reimann et al., 2008). Interpretation of the EDCF-plot (Figure 5) has a progressive distribution and shows a multi-modal distribution with variances indicated by sub populations with breaks near 150 mg/L, 1500 mg/L, 7500 mg/L and 25000 mg/L. The density plots, histograms, boxplots and scatterplot suggest that Ca concentrations are heavily left skewed on a log-scale.

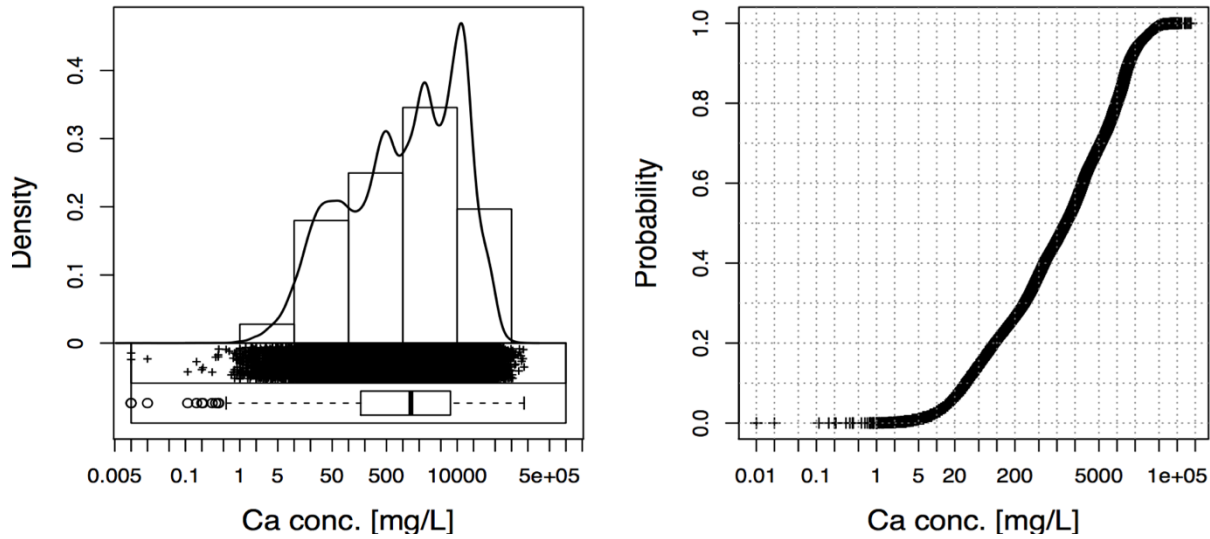


Figure 18: National EDA-plot in log scale, which includes a combination of a histogram, density trace, boxplot, and one-dimensional scatterplot (left side) and Empirical Cumulative Distribution Function (ECDF)-plot (right side). Calcium concentrations graph shows a multiple distribution.

### 5.5.3 Summary Statistics:

Table 6. Univariate data analysis for calcium.

	MIN	Q_0.05	Q1	MEDIAN	MEAN- log	MEAN	Q3	Q_0.95	MAX	SD	MAD	$p\sigma$	CV %	CVR %
Ca	0.00	16	168	1405	982.5	5580	7530	23660	170600	9476	2035	5457	169.8	144.9

Calculations were compiled to include: minimum (MIN), 5<sup>th</sup> percentile (Q\_0.05), 25<sup>th</sup> percentile (Q1), median, geometric mean (MEAN\_log), mean, 75<sup>th</sup> percentile (Q3), 95<sup>th</sup> percentile (Q\_0.95), maximum (MAX), standard deviation (SD), pseudosigma ( $p\sigma$ ), coefficient of variation (CV), and robust coefficient of variation (CVR).

### 5.5.4 Kendall Tau correlation:

In descending order, elements positively correlated ( $\tau > 0.6$ ) with Ca include: Br ( $\tau = 0.77$ ), Mg ( $\tau = 0.76$ ), Sr ( $\tau = 0.73$ ), Cl ( $\tau = 0.71$ ), Na ( $\tau = 0.65$ ), and K ( $\tau = 0.61$ ). Constituents negatively correlated with Ca are: HCO<sub>3</sub> ( $\tau = -0.47$ ), S ( $\tau = -0.31$ ), Hg ( $\tau = -0.16$ ) and B ( $\tau = -0.15$ ). Among these positive correlations the closest relationships are bromide, magnesium, strontium, chloride, sodium, and potassium which are associated with basinal brines derived from paleoevaporated seawater, suggesting this is a source of high Ca concentrations in produced waters (Kharaka and Hanor, 2014).

## 5.5.5 Maps:

### 5.5.5.1 Spatial Distribution:

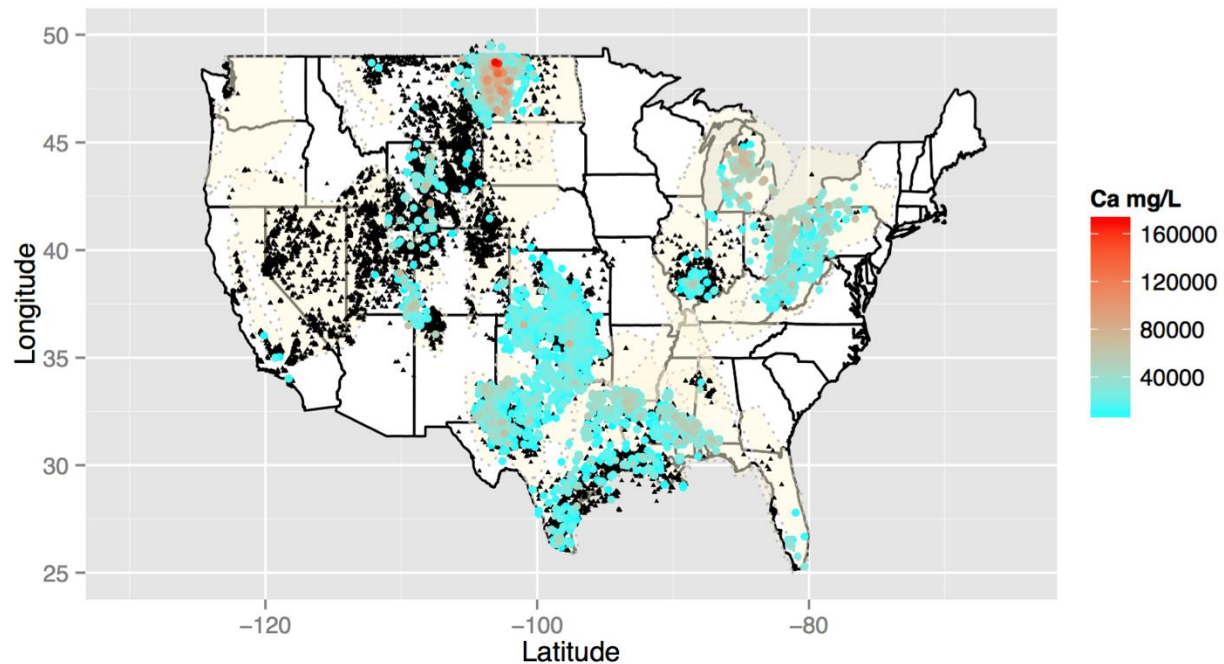


Figure 19: National spatial concentration map for calcium. Black triangles identify locations where Ca concentration data exist but are below the 75th percentile. Color ramped symbols applied to the sites where concentrations exceed the 75th percentile.

The spatial distribution of calcium correlates with the TDS map (Figure 1) with the highest concentration for Ca in the Williston Basin and other basins with high TDS waters (Appalachian, Michigan, Illinois, eastern Gulf Coast and Permian Basin basins). The spatial coverage for Ca is fairly well defined. However, there are some data gaps that could be completed or reported, such as California, Missouri and Tennessee. The elevated calcium concentrations in Figure 19 come from basins containing by ancient paleo-evaporated seawater (Lowenstein et al., 2005). The exploration potential for calcium is relatively low as the spatial coverage is well defined. In the Northeast Region it is a common practice during winter months to produce  $\text{CaCl}_2$  and/or  $\text{NaCl}$  salts for road deicing. In the Central Midwest, and Rocky Mountain regions developing salts for deicing and road dust control are potential uses for calcium salts.

### 5.5.5.2 Estimated Economic Values:

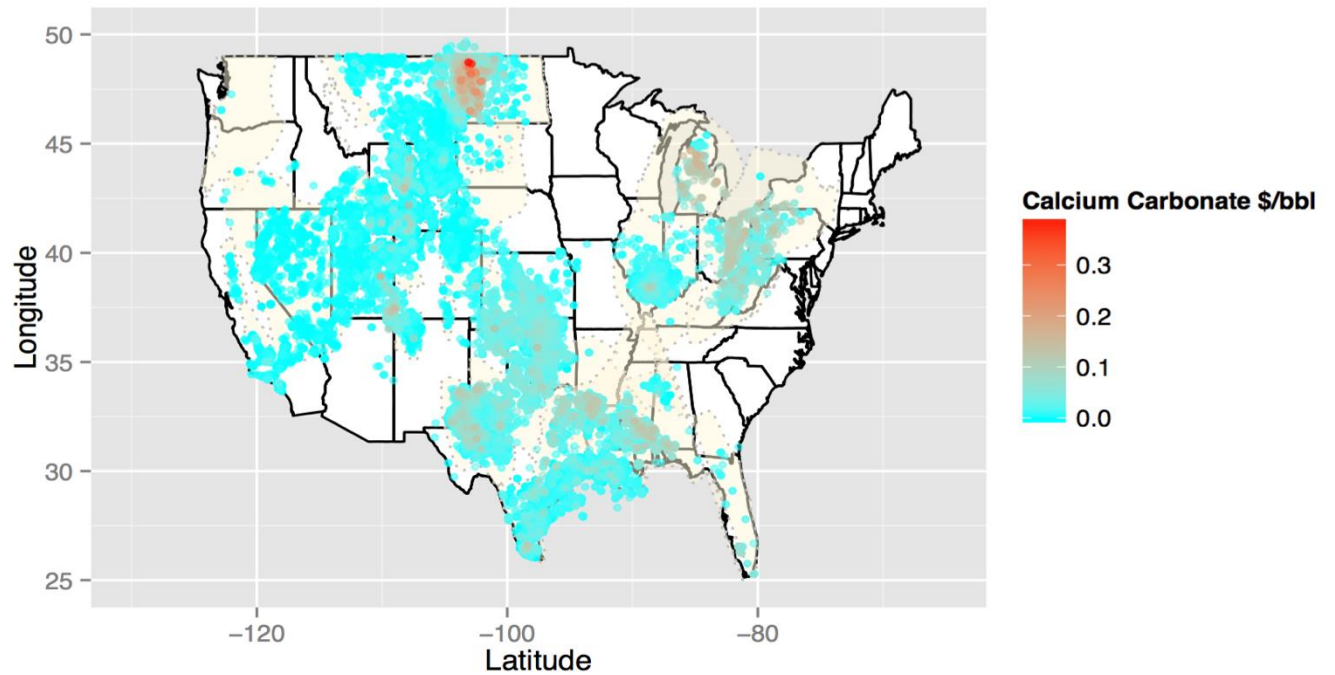


Figure 20: Economic concentration map for calcium identifying highest areas of interest; The Williston Basin, The Permian Basin, The Gulf Coast Basin, Smackover Formation and the Appalachian Basin.

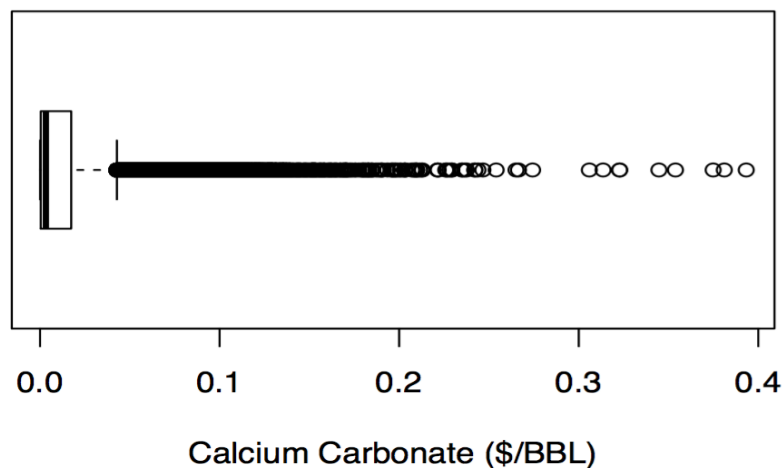


Figure 21: Tukey boxplot of economic values for calcium carbonate in produced waters.

Calcium carbonate commodities are valued at \$5.80 per metric ton (\$1.45E-08 per milligram). Applied to the concentration results several areas (Figures 20 and 21) show gross minimal values that meet or exceed disposal costs in most regions. In the Central Midwest (Group 3) and Ohio (Group 5) is the only area that the value meets disposal costs. Disposal costs vary and the variance in available technology keeps expenses low; the effect for potential profit is low to moderate. The potential for expansion in other basins is identified by both the spatial distribution and economic maps, however disposal costs are higher in these other regions. The Black Hills Region (Williston Basin) has the highest potential for development, based on the concentrations and disposal costs.

#### **5.5.6 Summary:**

Given the good data coverage for calcium, need for exploration is low, however product exploration for alternative calcium based products would be needed; the 2015 Mineral Commodity Yearbook only identifies lime as a commodity product. Calcium can be obtained all over the United States with little need for long term transport reducing product manufacturing or development costs. Further development for calcium commodity products extends beyond the known developments of salts in multiple basins. The commodity values, concentrations, and disposal costs, provide a limited potential for development in other basins. When considering development, supply and demand must be considered and may profit better if restricted to localized sources. Overall calcium is not a high valued commodity and logistics for transporting large amounts of salts, when it can be locally developed must be considered. Demand for Ca may seasonal as well, it can easily be produced in a large volume during the summer using evaporation ponds and sold during the winter months in the case of salt production. Calcium carbonate has other potential products and production volumes will depend on desired product. Calcium

concentrations are consistent both locally and regionally in identified regions with high salinity concentrations. Calcium is also associated with other constituents that have revenue potential, such as bromine, sodium, and magnesium (cf. Figure 1, Figure 11, Figure 87, Figure 57), therefore may be more economical to extract elements as a group.

## **5.6 Cesium**

### **Cesium (Cs)**

#### **5.6.1 Commodity:**

The principle source of cesium is pollucite, an ore mineral often associated with pegmatites. At present there is no domestic production of cesium. Some uses for cesium formate is during oil and gas field operations to control corrosion, fuel cells and polymer solar cells. Prices were ascertained from small markets at \$5.35 per gram (U.S. Geological Survey, 2015).

#### **5.6.2 Geochemical Statistics:**

Cesium concentrations were examined using two types of plots (Figure 22) that include a combination of a histogram, density trace, boxplot, and one-dimensional scatterplot (left side) and Empirical Cumulative Distribution Function (ECDF)-plot (right side) (Reimann et al., 2008). Interpretation of the EDCF-plot (Figure 22) has a progressive distribution and shows a variance indicated by sub populations with breaks near 1 mg/L and 10 mg/L. The density plots, histograms, boxplots and scatterplot suggest that Cs concentrations are mildly right skewed, even on a log-scale.

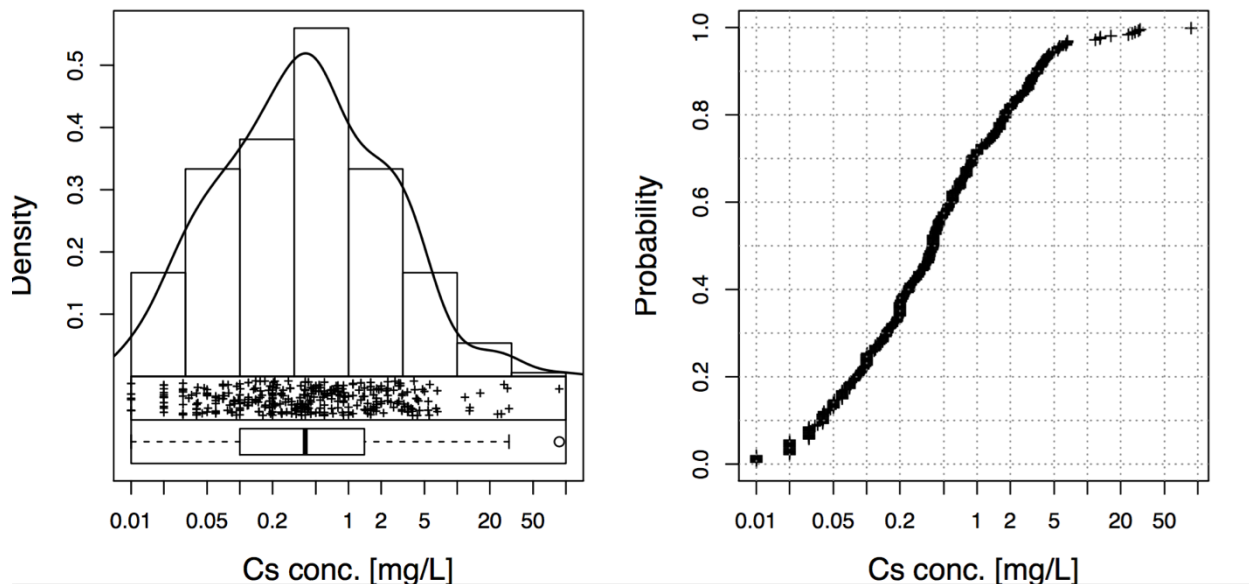


Figure 22: National EDA-plot in log scale, which includes a combination of a histogram, density trace, boxplot, and one-dimensional scatterplot (left side) and Empirical Cumulative Distribution Function (ECDF)-plot (right side). Cesium concentrations are skewed to the right.

### 5.6.3 Summary Statistics:

Table 7. Univariate data analysis for cesium.

	MIN	Q_0.05	Q1	MEDIAN	MEAN- log	MEAN	Q3	Q_0.95	MAX	SD	MAD	$p\sigma$	CV %	CVR %
Cs	0.00	0.02	0.1	0.4	0.3865	1.738	1.4	5.406	87	5.94	0.5041	0.9637	341.8	126

Calculations were compiled to include: minimum (MIN), 5<sup>th</sup> percentile (Q\_0.05), 25<sup>th</sup> percentile (Q1), median, geometric mean (MEAN\_log), mean, 75<sup>th</sup> percentile (Q3), 95<sup>th</sup> percentile (Q\_0.95), maximum (MAX), standard deviation (SD), pseudosigma ( $p\sigma$ ), coefficient of variation (CV), and robust coefficient of variation (CVR).

### 5.6.4 Kendall Tau correlation:

In descending order, elements positively correlated ( $\tau > 0.6$ ) with Cs include: Be ( $\tau = 1$ ), V ( $\tau = 0.8$ ), and As ( $\tau = 0.69$ ). Constituents negatively correlated with Cs are SO<sub>4</sub> ( $\tau = -0.19$ ), and Si ( $\tau = -0.11$ ). Extreme correlations of Cs with Be and U are controlled by the low numbers of samples where data for both sets of elements exist. Interestingly, Cs is often found naturally with Rb but they do not correlate strongly ( $\tau = 0.46$ ).

## 5.6.5 Maps:

### 5.6.5.1 Spatial Distribution:

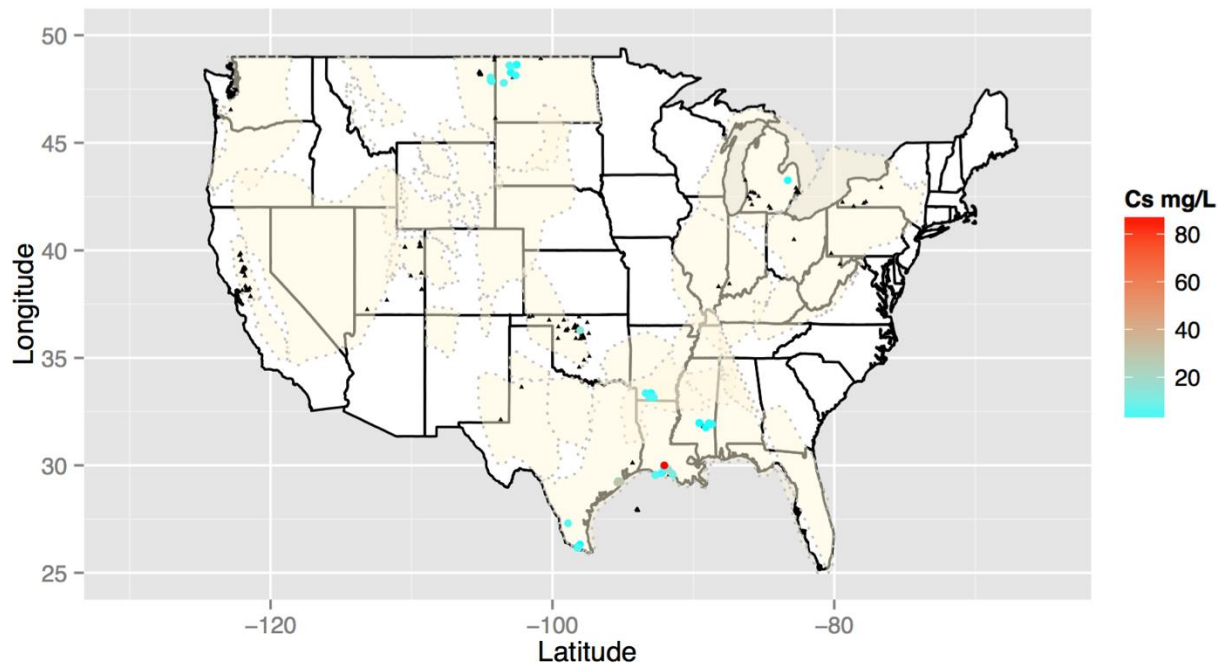


Figure 23: National spatial concentration map for cesium. Black triangles identify locations where Cs concentration data exist but are below the 75th percentile. Color ramped symbols applied to the sites where concentrations exceed the 75th percentile.

The spatial distribution of cesium is sparse nationally. The highest Cs concentrations occur along the eastern portion in the Gulf Coast Basin, near New Orleans. Elevated Cs concentrations along the Mississippi and Alabama border in an area with relatively high concentrations of base metal elements. The data coverage for Cs is poor, suggesting that if economic values exist, there may be potential for exploration.

### 5.6.5.2 Estimated Economic Values:

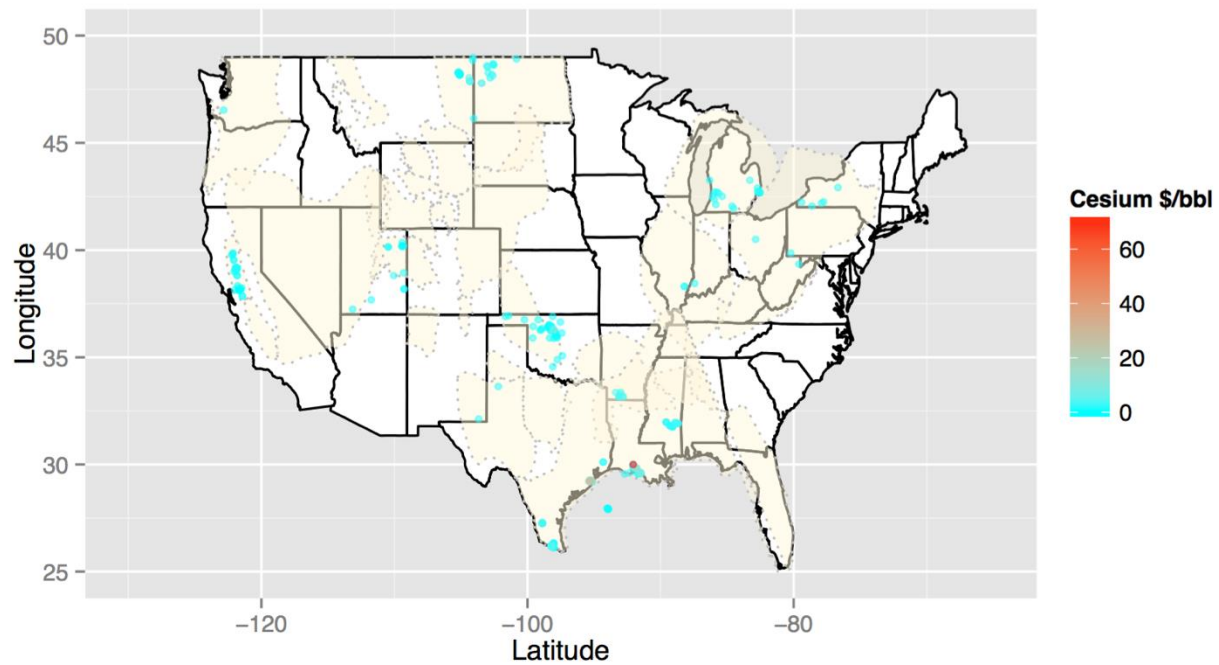


Figure 24: Economic concentration map for Cs identifying highest areas of interest: The Gulf Coast Basin.

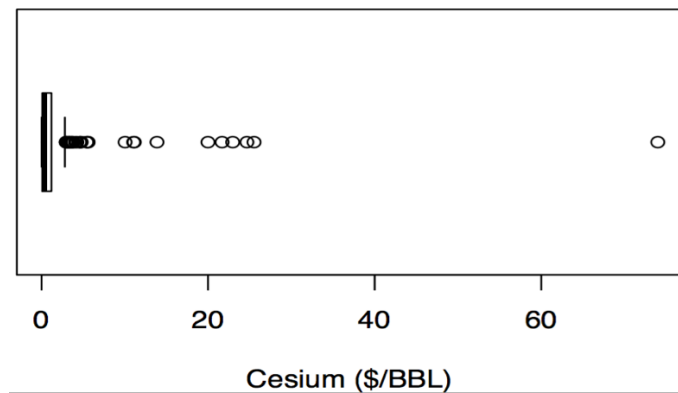


Figure 25: Tukey boxplot of economic values for cesium in produced waters.

Cesium commodities are valued at \$5.35 per gram (\$5.35E-03 per milligram per liter). Applied to the concentration results (Figures 24 and 25), areas are limited for potential development. There is an identified anomaly in the southern Gulf Coast Basin (near New Orleans,

Louisiana). Ignoring the anomaly, other samples have potential to be economic for both exploration and development for cesium commodity extraction (Figure 25). Assuming the anomaly is accurate, development possibilities increase. Cesium concentrations in many cases exceed \$10/bbl, thus making disposal costs negligible.

#### **5.6.6 Summary:**

The development of cesium as commodity from produced waters is likely a profitable avenue. Cesium is traditionally removed from pegmatite ore deposits. The source of Cs in produced waters is from leaching from igneous or metamorphic rocks (Collins, 1975). The Gulf Coast Basin is primarily made up of carbonate and sedimentary deposits, any source of igneous or metamorphic minerals is likely transported from the Black Prairie Basin located at the foothills of the Appalachian Basin. In some instances, Cs is absorbed in clays and can be released into brines. The commodity values, concentrations, and disposal costs, prove potential for development. Given the lack of data, and the high potential value there is considerable potential for exploration of cesium in produced waters.

## **5.7 Chromium**

### **Chromium (Cr)**

#### **5.7.1 Commodity:**

Chromium is produced in two primary forms: chromite and ferrochromium. Chromite is produced from ore deposits and ferrochromium is recovered through the recycling of steels through smelting or slag. Chromium is used for corrosion prevention and for hardening enhancement of alloys. For the purpose of the study, the ferrochromium values are used as they have greater potential for separation than chromite ore from produced waters. Ferrochromium alloy is valued at \$2190 per metric ton on a chromium basis. As of 2012 update, price average for chromite ore is \$168 per metric ton. Chromium can be removed from aqueous solutions using polymer-enhanced ultrafiltration methods (Aroua et al., 2007) or ion-exchange method.

#### **5.7.2 Geochemical Statistics:**

Chromium concentrations were examined using two types of plots (Figure 26) that include a combination of a histogram, density trace, boxplot, and one-dimensional scatterplot (left side) and Empirical Cumulative Distribution Function (ECDF)-plot (right side) (Reimann et al., 2008). Interpretation of the EDCF-plot shows that Cr has a bimodal distribution and shows a variance indicated by sub populations with breaks near 0.02 mg/L. The density plots, histograms, boxplots and scatterplot suggest that upper Cr population is right skewed, even on a log-scale.

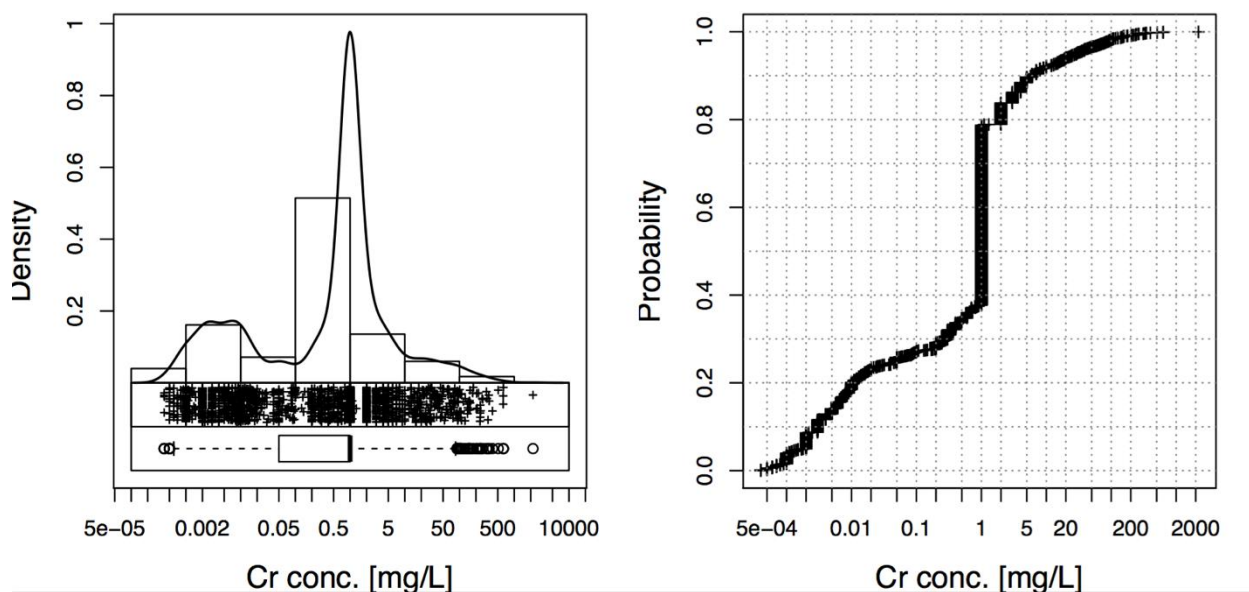


Figure 26: National EDA-plot in log scale, which includes a combination of a histogram, density trace, boxplot, and one-dimensional scatterplot (left side) and Empirical Cumulative Distribution Function (ECDF)-plot (right side). Chromium concentrations are right skewed and the graph shows a slight bi modal distribution.

### 5.7.3 Summary Statistics:

Table 8. Univariate data analysis for chromium.

	MIN	Q_0.05	Q1	MEDIAN	MEAN_log	MEAN	Q3	Q_0.95	MAX	SD	MAD	$p\sigma$	CV %	CVR %
<b>Cr</b>	4.00E-04	0.002	0.05	1	0.3448	8.277	1	29	2204	57.68	1.186	0.7042	696.8	118.6

Calculations were compiled to include: minimum (MIN), 5<sup>th</sup> percentile (Q\_0.05), 25<sup>th</sup> percentile (Q1), median, geometric mean (MEAN\_log), mean, 75<sup>th</sup> percentile (Q3), 95<sup>th</sup> percentile (Q\_0.95), maximum (MAX), standard deviation (SD), pseudosigma ( $p\sigma$ ), coefficient of variation (CV), and robust coefficient of variation (CVR).

### 5.7.4 Kendall Tau correlation:

The positively correlated elements at ( $\tau > 0.6$ ) with chromium include Cd ( $\tau = 0.62$ ) and Pb ( $\tau = 0.6$ ). In descending order, elements positively correlated ( $\tau > 0.5$ ) with Cr include: Ce ( $\tau = 0.56$ ), Ni ( $\tau = 0.56$ ), Co ( $\tau = 0.53$ ), Ba ( $\tau = 0.52$ ), Be ( $\tau = 0.52$ ), Cu ( $\tau = 0.52$ ), Ni ( $\tau = 0.52$ ) and Se ( $\tau = 0.51$ ). Constituents negatively correlated with Cr are: Th ( $\tau = -0.47$ ) and Hg ( $\tau = -0.14$ ).

## 5.7.5 Maps:

### 5.7.5.1 Spatial Distribution:

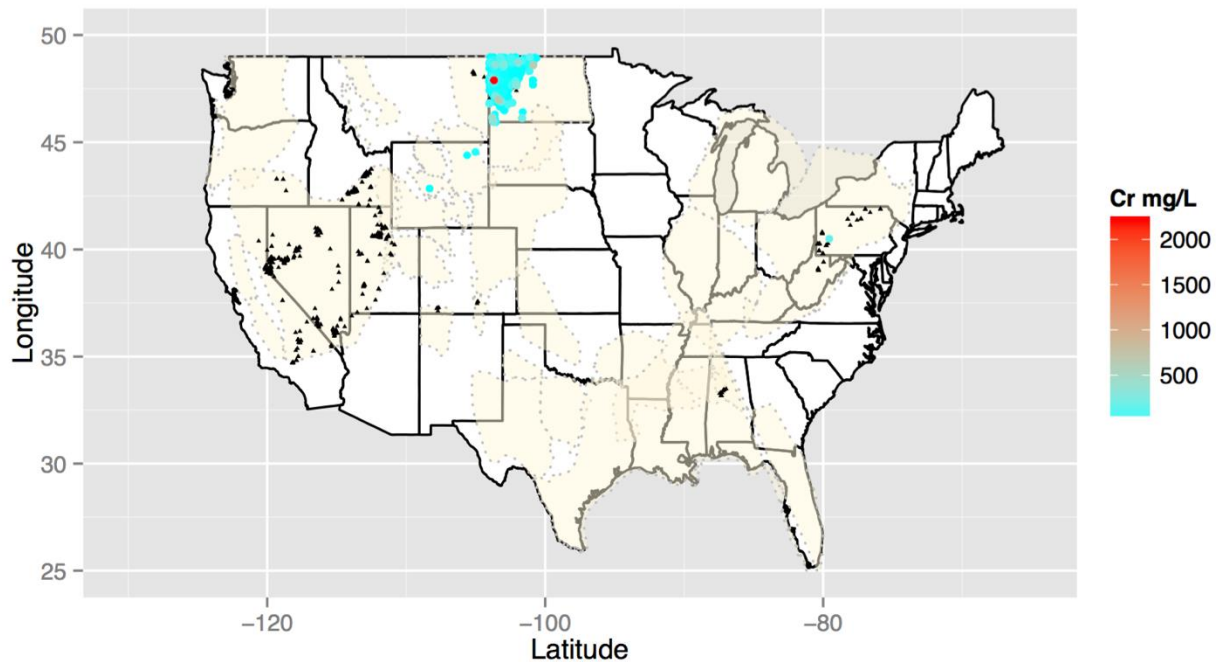


Figure 27: National spatial concentration map for chromium. Black triangles identify locations where Cr concentration data exist but are below the 75th percentile. Color ramped symbols applied to the sites where concentrations exceed the 75th percentile.

The spatial density of chromium data is highest in the North Dakota portion of the Williston Basin and there are large data gaps across much of the U.S. (Figure 27). In the Williston Basin, Cr concentrations may be a result of leaching from Cr-bearing basalts by basinal brines. Chromium can be removed from produced waters with the use of polymers. If Cr is found to be profitable, there is significant potential to fill in abundant data gaps.

### 5.7.5.2 Estimated Economic Values:

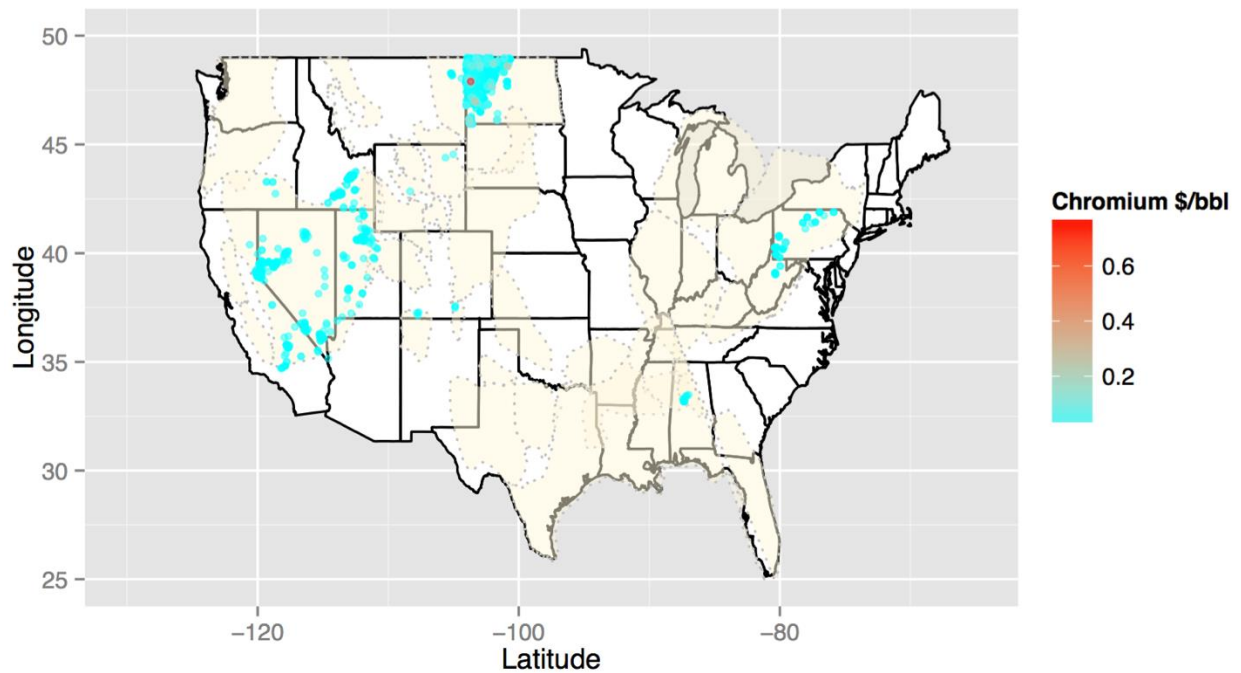


Figure 28: Economic concentration map identifying highest areas of interest: The Williston Basin.

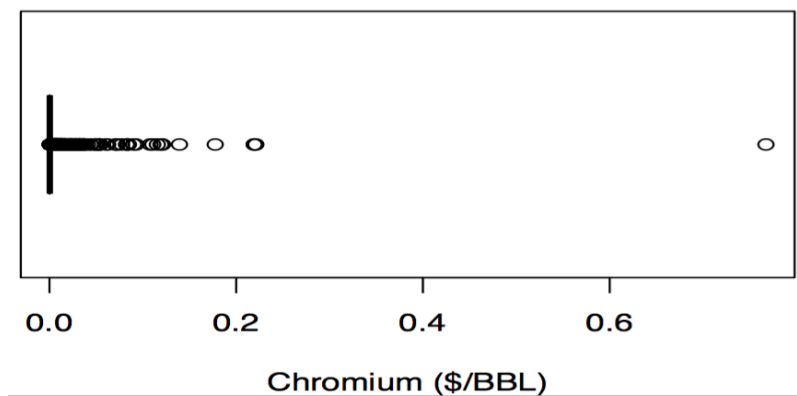


Figure 29: Tukey boxplot of economic values for chromium in produced waters.

Chromium commodities are valued by the USGS as ferrochromium at \$2190 per metric ton ( $9.91\text{E-}04$  per milligram per liter). Disposal costs for the Black Hills Region (Group 4) range from \$0.35 to \$1.75 per barrel. When analyzing the available data (commodity price, disposal

expenses and pricing for polymers for extraction), in most cases removing Cr for commercial production does not appear profitable for commodity removal (Figures 28 and 29). However, one possible exception is in the Williston Basin, where removal may be profitable as the region (Group 4) has moderate disposal costs.

#### **5.7.6 Summary:**

The development in produced waters for chromite or ferrochromium is restricted at this time. Data coverage is poor, suggesting room for exploration, but low economic values tend to favor limited return for the effort. The technology costs and methodology expenses need to be reduced before further exploration potential increases.

## **5.8 Cobalt**

### **Cobalt (Co)**

#### **5.8.1 Commodity:**

Cobalt products have diverse commercial application, from rechargeable battery electrodes to resistant alloys such as diamond tools and corrosion resistant steels. Other uses are for manufacturing catalysts, humidity indicators and recording media. Cobalt prices in 2014 averaged \$14.40 per pound.

#### **5.8.2 Geochemical Statistics:**

Cobalt concentrations were examined using two types of plots (Figure 30) that include a combination of a histogram, density trace, boxplot, and one-dimensional scatterplot (left side) and Empirical Cumulative Distribution Function (ECDF)-plot (right side) (Reimann et al., 2008). Interpretation of the EDA-plot (Figure 21) suggests a bimodal distribution and shows a variance indicated by sub populations with breaks near 0.05 mg/L and possibly 5 mg/L. The density trace plot also suggest that Co concentrations are right skewed, even on a log-scale.

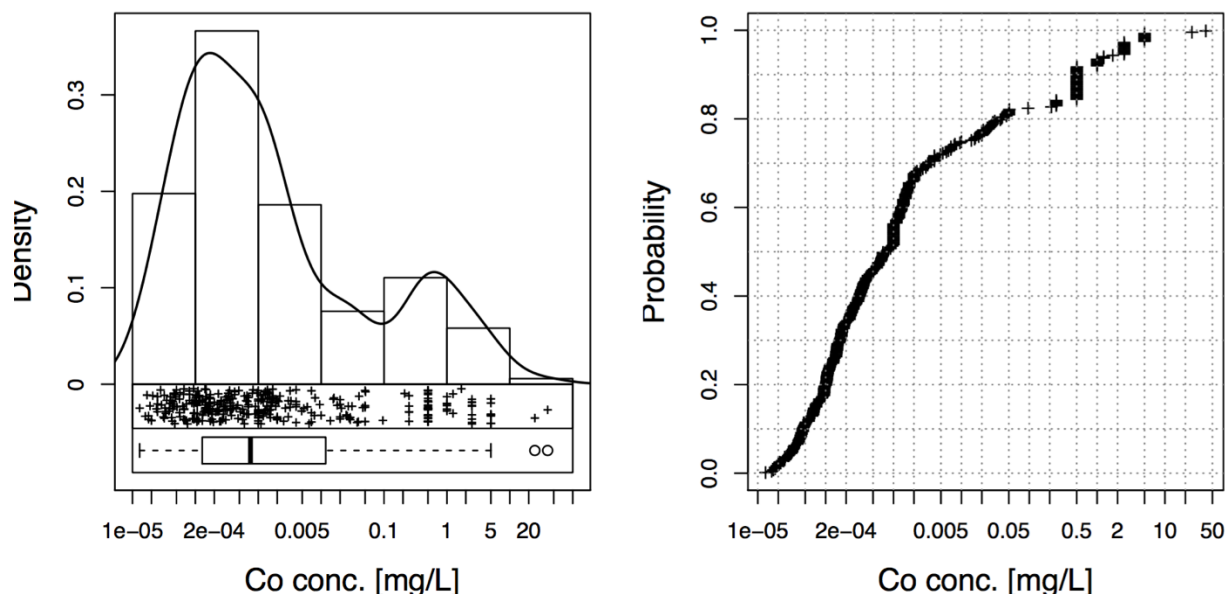


Figure 30: National EDA-plot in log scale, which includes a combination of a histogram, density trace, boxplot, and one-dimensional scatterplot (left side) and Empirical Cumulative Distribution Function (ECDF)-plot (right side). Cobalt concentrations are bimodal with a right skewed tail.

### 5.8.3 Summary Statistics:

Table 9. Univariate data analysis for cobalt.

	MIN	Q_0.05	Q1	MEDIAN	MEAN_log	MEAN	Q3	Q_0.95	MAX	SD	MAD	$p\sigma$	CV %	CVR %
Co	1.30E-05	3.22E-05	1.29E-04	7.53E-04	1.76E-03	0.4383	0.011	2.5	40	2.654	1.03E-03	8.06E-03	605.5	137.2

Calculations were compiled to include: minimum (MIN), 5<sup>th</sup> percentile (Q\_0.05), 25<sup>th</sup> percentile (Q1), median, geometric mean (MEAN\_log), mean, 75<sup>th</sup> percentile (Q3), 95<sup>th</sup> percentile (Q\_0.95), maximum (MAX), standard deviation (SD), pseudosigma ( $p\sigma$ ), coefficient of variation (CV), and robust coefficient of variation (CVR).

### 5.8.4 Kendall Tau correlation:

In descending order, elements positively correlated ( $\tau > 0.6$ ) with Co include: Ni ( $c = 0.7$ ), Pb ( $\tau = 0.65$ ), Sr ( $\tau = 0.64$ ), Br ( $\tau = 0.63$ ), Mn ( $\tau = 0.61$ ), and Cd ( $\tau = 0.61$ ). The only constituent negatively correlated with Co is I ( $\tau = -0.19$ ). Co-association of Co with Ni and other base metals is well documented in geochemical settings.

## 5.8.5 Maps:

### 5.8.5.1 Spatial Distribution:

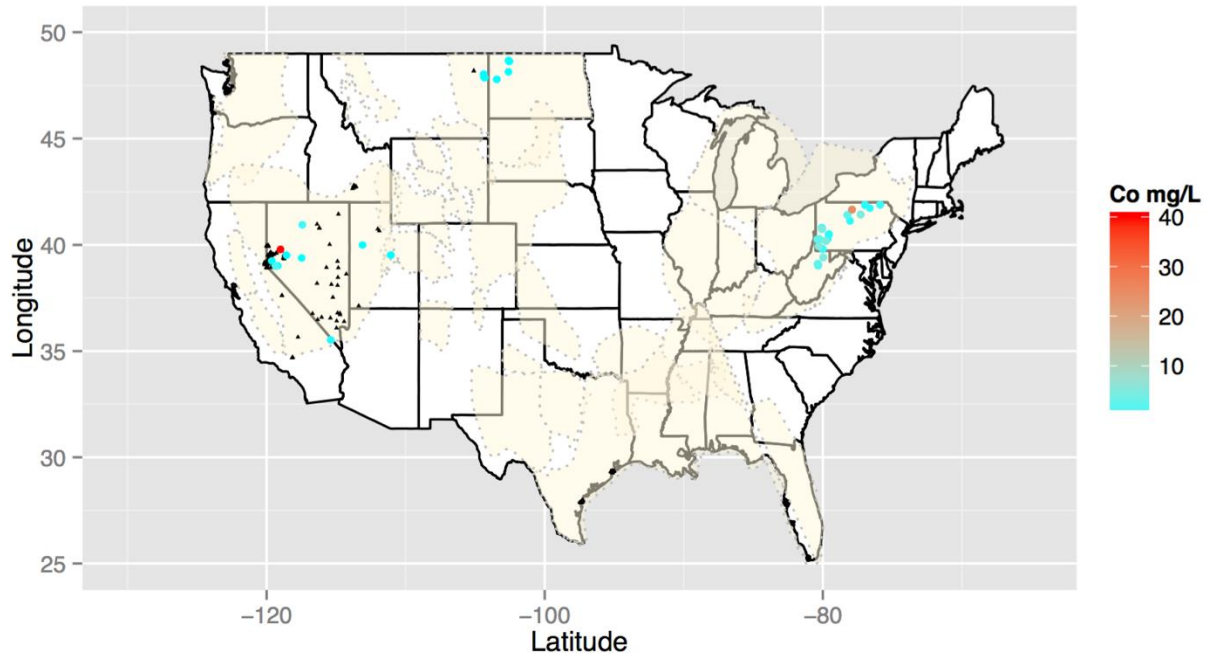


Figure 31: National spatial concentration map for cobalt. Black triangles identify locations where Co concentration data exist but are below the 75th percentile. Color ramped symbols applied to the sites where concentrations exceed the 75th percentile.

The spatial distribution for Co is sparse (Figure 31); the highest concentrations were observed in samples from the Great Basin followed by the Williston Basin and northern area of the Appalachian Basin. There are large data gaps for Co, thus given relatively high commodity values there is potential for exploration in produced waters. Cobalt in produced waters may result from a result from source rock leaching by basinal waters.

### 5.8.5.2 Estimated Economic Values:

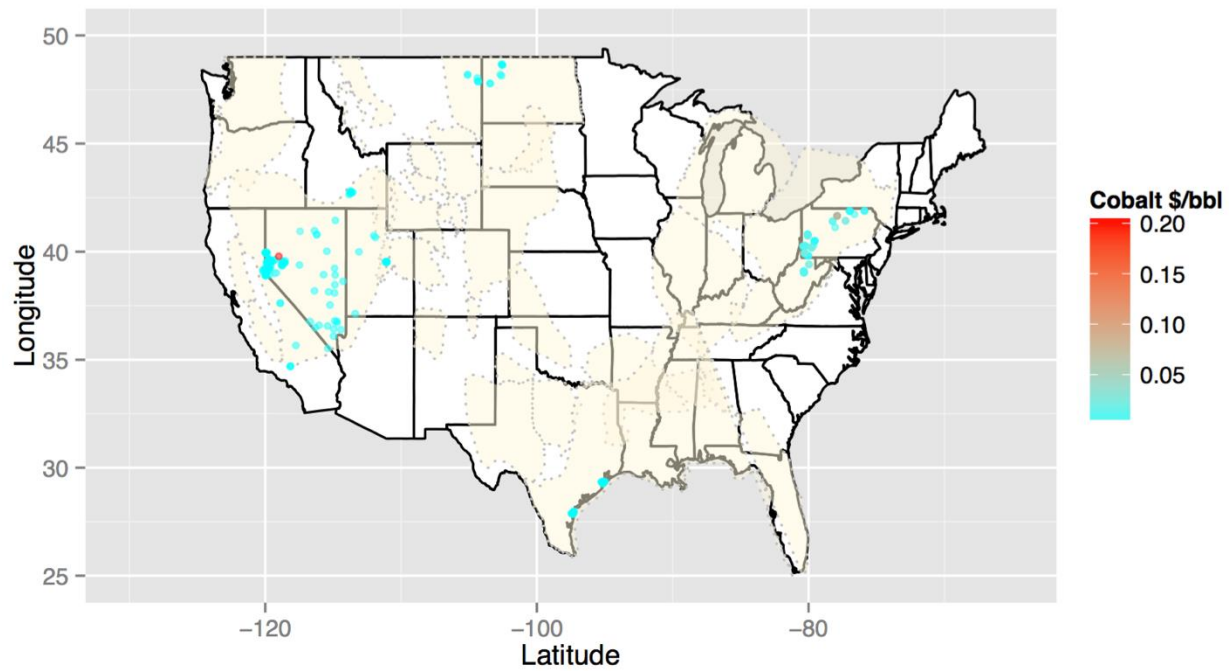


Figure 32: Economic map for Co identifying highest areas of interest: California, Nevada and upper Appalachian Basin.

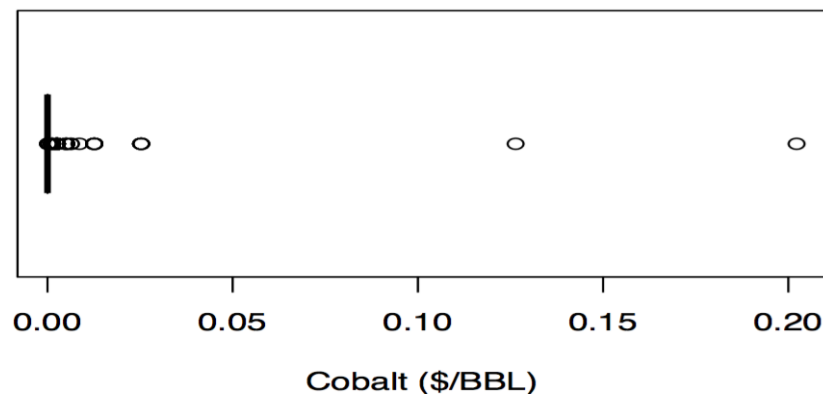


Figure 33: Tukey boxplot of economic values for cobalt in produced waters.

Cobalt commodities are valued by the USGS at \$14.40 per pound ( $3.18 \times 10^{-5}$  per milligram per liter). Outside of a single outlier in Nevada and another outlier in Pennsylvania

(Figure 32 and 33), produced waters contain commodity values well below disposal costs. Disposal costs are the limiting factor for cobalt extraction. Even with limited spatial data, the development potential for cobalt is relatively low.

#### **5.8.6 Summary:**

The potential exploration for Co and Co extraction from produced waters is minimal at this time. There is a future for exploration should discovery of concentrations considerably higher than the existing maximum of 40 mg/L be found. There are several known methods to remove cobalt from water: magnetic removal, ion exchange and chemical reduction, to mention a few. Therefore, there is potential to remove the commodity, but the current value based on the current extent of concentration data limit the development potential.

## **5.9 Copper**

### **Copper (Cu)**

#### **5.9.1 Commodity:**

Copper products are used in various industries, particularly manufacturing. Copper is traditionally mined in open pit ore deposits; the most economical method for collection is through secondary recovery in leaching. In a few select locations copper concentrations have been recognized in the produced waters database. As of May 2015, copper price average was \$2.95 per pound. Copper is successfully being precipitated from brine waters using activated carbons prepared from pomegranate peel (Lenntech.com) and (U.S. Geological Survey, 2015).

#### **5.9.2 Geochemical Statistics:**

Copper concentrations were examined using two types of plots (Figure 34) that include a combination of a histogram, density trace, boxplot, and one-dimensional scatterplot (left side) and Empirical Cumulative Distribution Function (ECDF)-plot (right side) (Reimann et al., 2008). Interpretation of the EDCF-plot (Figure 34) shows a variance indicated by sub populations with breaks near 0.002 mg/L, 0.01 mg/L, 0.2 mg/L and 1 mg/L. The density plots, histograms, boxplots and scatterplot suggest that Cu concentration are multi-modal and right skewed, on a log-scale.

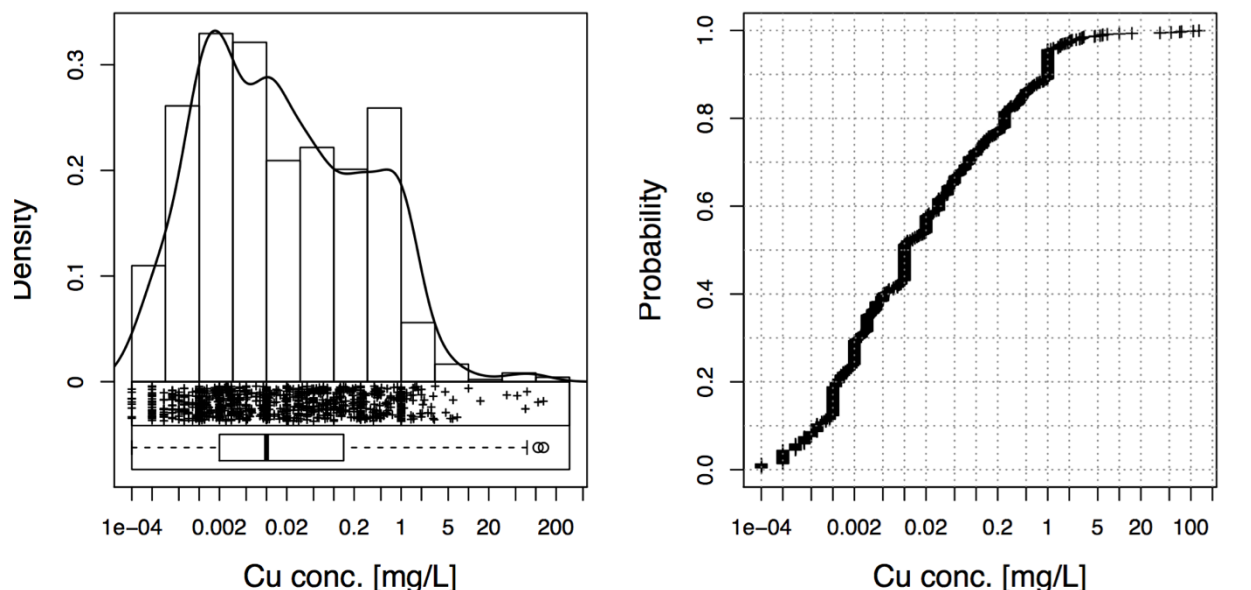


Figure 34: National EDA-plot in log scale, which includes a combination of a histogram, density trace, boxplot, and one-dimensional scatterplot (left side) and Empirical Cumulative Distribution Function (ECDF)-plot (right side). Copper concentrations are right skewed.

### 5.9.3 Summary Statistics:

Table 10. Univariate data analysis for copper.

	MIN	Q_0.05	Q1	MEDIAN	MEAN_log	MEAN	Q3	Q_0.95	MAX	SD	MAD	pσ	CV %	CVR %
<b>Cu</b>	0	3.00E-04	0.002	0.01	0.01683	0.7359	0.14	1	130	6.689	0.01453	0.1023	908.9	145.3

Calculations were compiled to include: minimum (MIN), 5<sup>th</sup> percentile (Q\_0.05), 25<sup>th</sup> percentile (Q1), median, geometric mean (MEAN\_log), mean, 75<sup>th</sup> percentile (Q3), 95<sup>th</sup> percentile (Q\_0.95), maximum (MAX), standard deviation (SD), pseudosigma (pσ), coefficient of variation (CV), and robust coefficient of variation (CVR).

### 5.9.4 Kendall Tau correlation:

In descending order, elements positively correlated ( $\tau > 0.6$ ) with Cu include: Be ( $\tau = 0.67$ ), Se ( $\tau = 0.63$ ), and Cd ( $\tau = 0.63$ ). Constituents negatively correlated with Co is:  $\text{BO}_3$  ( $\tau = -0.67$ ) and Si ( $\tau = -0.47$ ).

## 5.9.5 Maps:

### 5.9.5.1 Spatial Distribution:

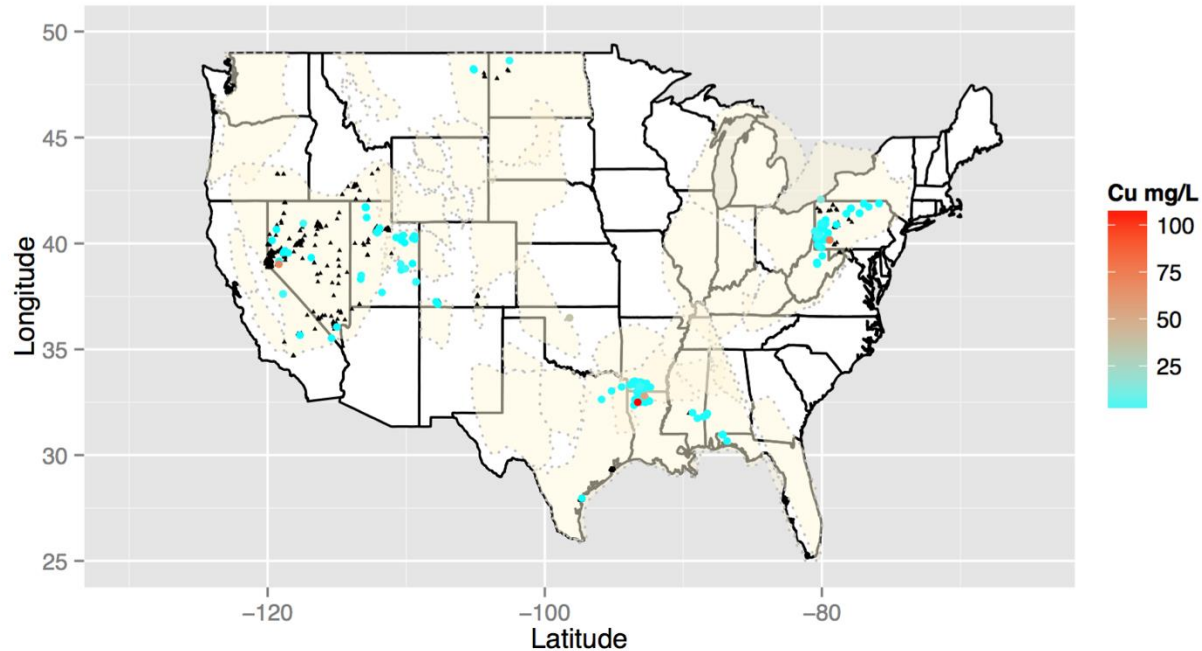


Figure 35: National spatial concentration map for copper. Black triangles identify locations where Cu concentration data exist but are below the 75th percentile. Color ramped symbols applied to the sites where concentrations exceed the 75th percentile.

The spatial distribution for copper is sparse, the highest concentration is in the Smackover Formation in the Gulf Coast Region (Figure 35). The Northeast and Black Hills Regions have moderate concentration values. There are large gaps for copper in the data. Disposal costs for Group 1 pose the greatest potential for development, Groups 5 and 6 can be more expensive and overall concentrations are not significant enough to warrant development from produced waters. There is potential with copper extraction if combined with other constituents known for these areas, such as bromine or magnesium depending the removal process as to not interfere with extraction of other elements of interest.

### 5.9.5.2 Estimated Economic Values:

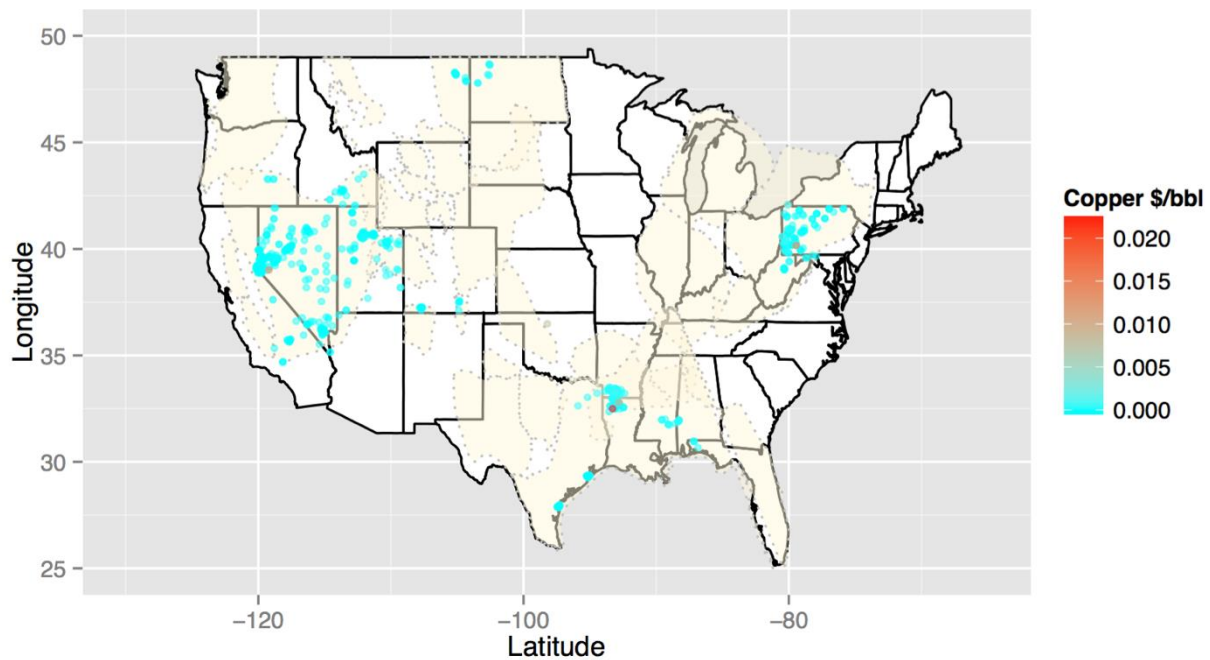


Figure 36: Economic map for copper identifying highest areas of interest: California, Nevada and the Smackover Formation.

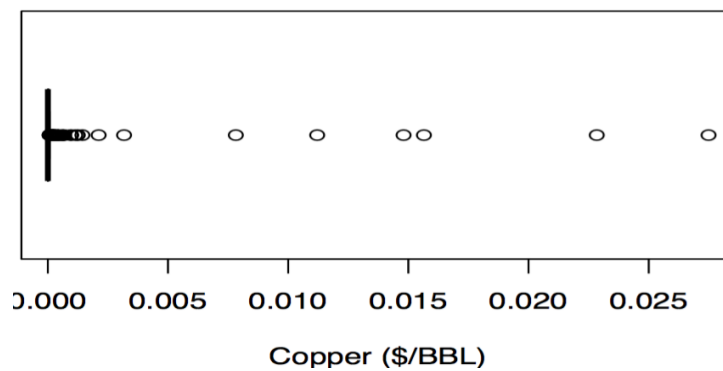


Figure 37: Tukey boxplot of economic values for copper in produced waters.

Copper commodities are valued by the USGS at \$2.95 per pound ( $1.33 \times 10^{-6}$  per milligram per liter). Overall, copper in produced waters does not have a high enough concentration or value

to promote extraction for profit (Figures 36 and 37). Disposal costs for Group 5 and Group 6 are considered among the highest and it is not recommended for removal from these regions. Group 1 has limited potential for commodity extraction if the technology costs can be reduced for removal. This is also subjective to the amount of available data within the database. Should copper be the target commodity more exploration is encouraged. It should also be noted that in Nevada, Utah and southern Pennsylvania, known copper deposits exist and have been actively mined for decades. In these areas enriched in produced waters may be due to leaching from ore deposits. In the Gulf Coast Basin, the source of copper is more than likely a result from leaching and has been transported from another location.

#### **5.9.6 Summary:**

Copper has minimal potential for development at this time. There is little need for exploration as only at concentrations 2-3 orders of magnitude higher than the highest data point would it be valued above the range of disposal costs. There are several known methods to remove copper from water (e.g., ion exchange and chemical reduction). Therefore, methods exist to remove the commodity, however, the value and known available concentrations limit the development potential.

## **5.10 Fluorspar**

### **Fluorspar (CaF<sub>2</sub>)**

#### **5.10.1 Commodity:**

The USGS commodity Summary Report does not include fluorine as a mineral commodity. However, the commodity list does include calcium fluorspar (CaF<sub>2</sub>), a byproduct of petroleum alkylation and hydrofluoric acid (HF) production. Thus, this section will consider fluorspar as produced from fluoride in produced waters. Fluorspar is used in metallurgic and ceramic processes, enamels, and welding. Hydrofluoric acid itself is used in processing applications to make aluminum and uranium products. The price value as of 2014 ranged from \$310-\$350 per ton (U.S. Geological Survey, 2015).

#### **5.10.2 Geochemical Statistics:**

Fluorine concentrations were examined using two types of plots (Figure 38) that include a combination of a histogram, density trace, boxplot, and one-dimensional scatterplot (left side) and Empirical Cumulative Distribution Function (ECDF)-plot (right side) (Reimann et al., 2008). Interpretation of the EDCF-plot shows a variance indicated by sub populations with breaks near 0.01 mg/L, 0.5 mg/L, 2 mg/L and 5 mg/L. The density plots, histograms, boxplots and scatterplot suggest that F concentrations are slightly right skewed, on a log-scale.

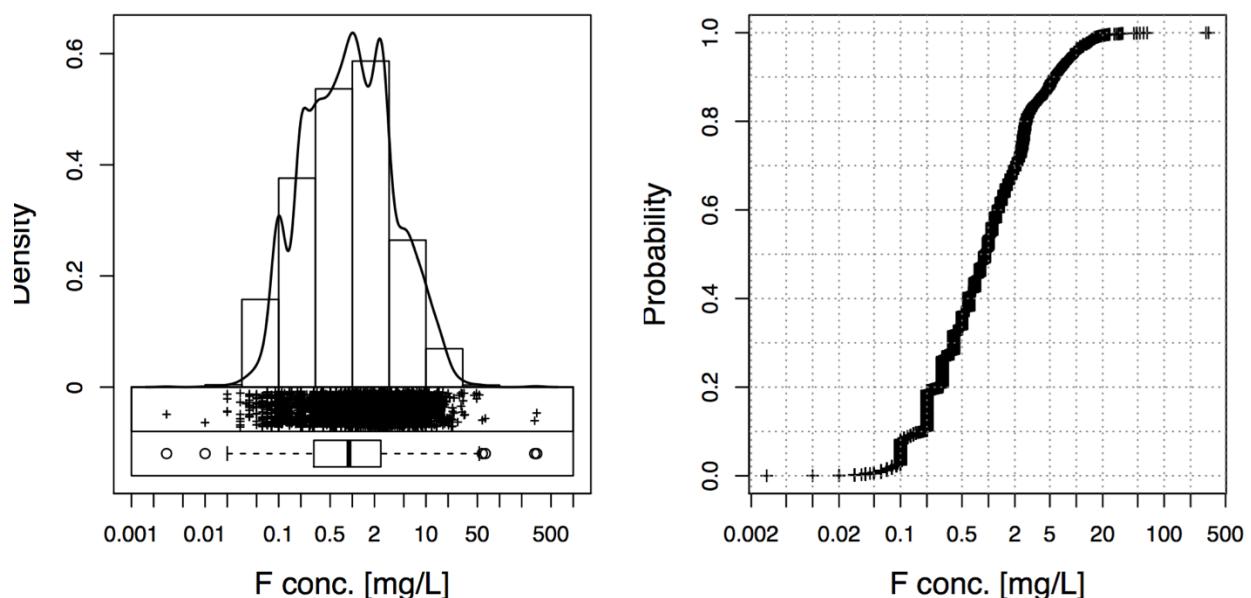


Figure 38: National EDA-plot in log scale, which includes a combination of a histogram, density trace, boxplot, and one-dimensional scatterplot (left side) and Empirical Cumulative Distribution Function (ECDF)-plot (right side). Fluorine concentrations are right skewed.

### 5.10.3 Summary Statistics:

Table 11. Univariate data analysis for fluorine.

	MIN	Q_0.05	Q1	MEDIAN	MEAN_log	MEAN	Q3	Q_0.95	MAX	SD	MAD	pσ	CV %	CVR %
<b>F</b>	0.003	0.1	0.3	0.9	0.9024	2.303	2.44	9.1	320	7.067	1.038	1.586	306.9	115.3

Calculations were compiled to include: minimum (MIN), 5<sup>th</sup> percentile (Q\_0.05), 25<sup>th</sup> percentile (Q1), median, geometric mean (MEAN\_log), mean, 75<sup>th</sup> percentile (Q3), 95<sup>th</sup> percentile (Q\_0.95), maximum (MAX), standard deviation (SD), pseudosigma (pσ), coefficient of variation (CV), and robust coefficient of variation (CVR).

### 5.10.4 Kendall Tau correlation:

Fluorine does not correlate positively or negatively with any elements considered in the Produced Waters Database ( $-0.1 > \tau > 0.6$ ).

## 5.10.5 Maps:

### 5.10.5.1 Spatial Distribution:

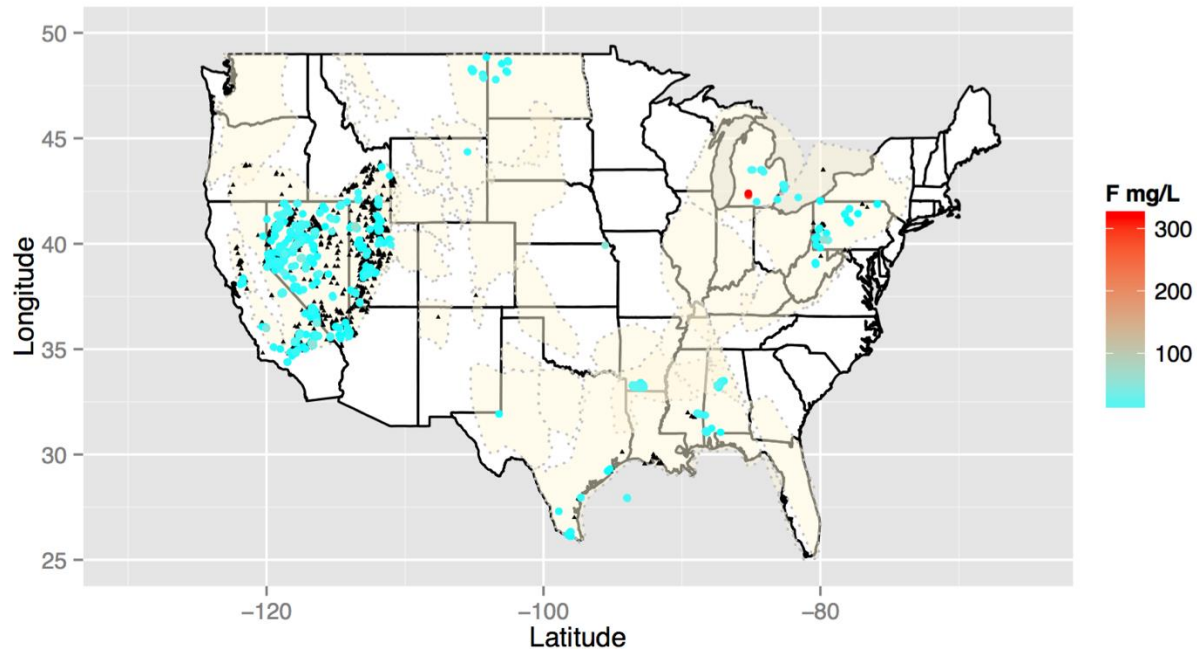


Figure 39: National spatial concentration map for fluoride. Black triangles identify locations where F concentration data exist but are below the 75th percentile. Color ramped symbols applied to the sites where concentrations exceed the 75th percentile.

The spatial distribution for fluorine is sparse with the highest concentration in the Michigan Basin and some enrichment in Nevada and California (Figure 39). High fluoride is indicative of F-bearing minerals from hydrothermal veins (Tropper and Manning, 2007). There is need for more complete the data to better assess its concentration across more basins. Exploration and development potential is limited for brine extraction but not unreasonable. Fluorine enrichment is found in Group 5 and Group 6 states, regions that traditionally maintain higher disposal costs.

### 5.10.5.2 Estimated Economic Values:

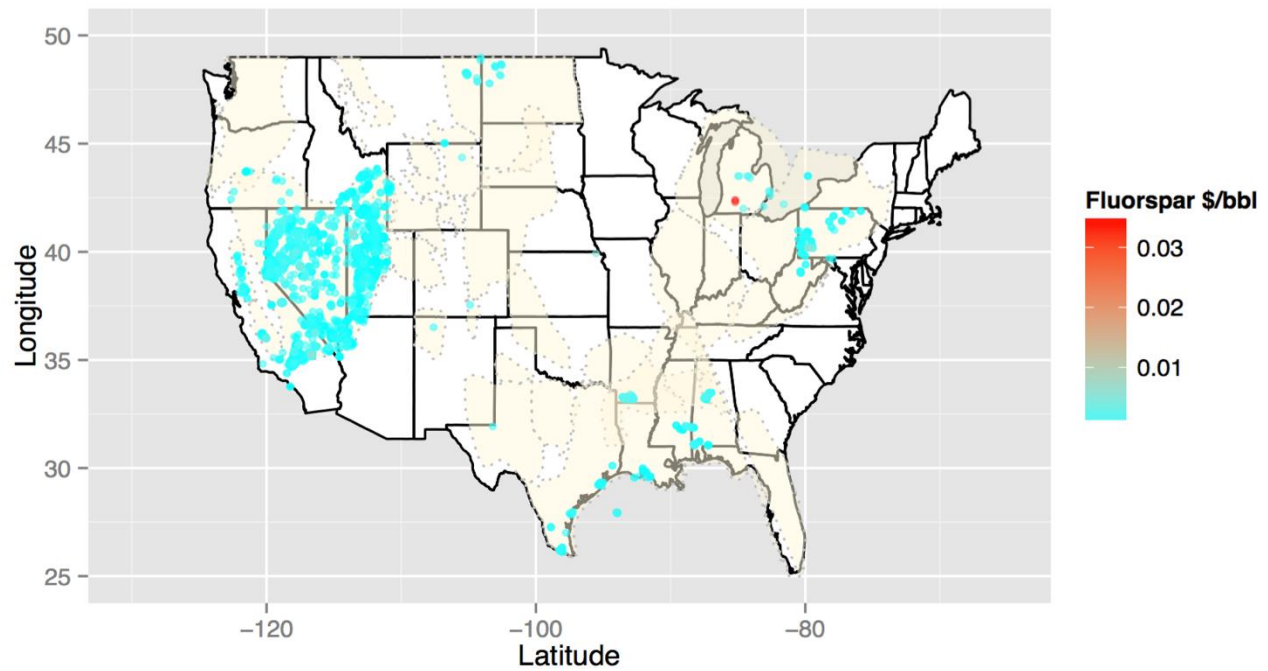


Figure 40: Economic map for fluorine identifying highest areas of interest: The Michigan Basin

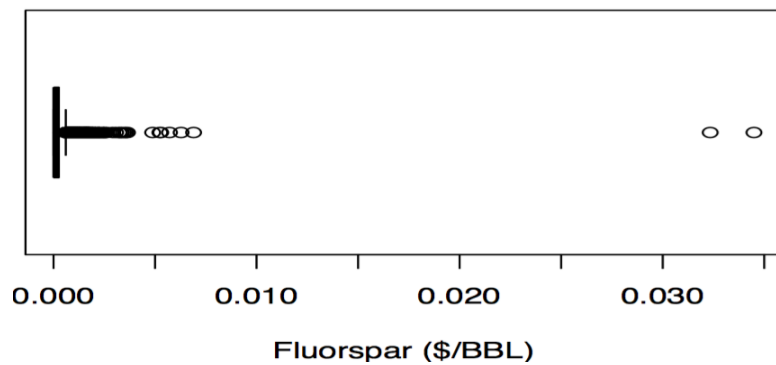


Figure 41: Tukey boxplot of economic values for fluorspar in produced waters.

The USGS Commodity Minerals Yearbook does not include values for fluorine; the value for fluorspar was applied to the fluoride concentrations (assuming stoichiometric conversion) to a

determined economic values. The spatial distribution concentration findings in identified regions correlates with igneous and metamorphic settings with the exception of the Michigan Basin. The Michigan Basin brines have relatively high concentrated brines. Research in dissolved fluorite concluded the elevated fluorine concentrations are consistent within brines (Tropper and Manning, 2007).

#### **5.10.6 Summary:**

There is minimal potential for development of fluorine in produced waters at this time. There is little need for exploration as only at concentrations 2-3 orders of magnitude higher than the highest data point would it be valued above the range of disposal costs. Spatial association between F anomalies in produced waters and F-rich mineral deposits suggests F in produced waters may have potential for identifying other fluoride mineral resources. For examples, hydrothermal fluorine minerals can be indicators for rare earth elements. Rare earth elements are considered highly valuable and sought after in mining explorations, the map may provide a visual for possible sources.

## **5.11 Iodine**

### **Iodine (I)**

#### **5.11.1 Commodity:**

Iodine is produced domestically in the United States from brines in the Anadarko Basin near Woodward, Oklahoma, and in the Smackover Formation in Arkansas. Iodine is used for medical production, photographic uses, biocides, food additives, and inks. Due to proprietary information, pricing is inferred and the current value for iodine is \$39.00/kg. This is an average in 2014 and includes cost, insurance and freight values (U.S. Geological Survey, 2015).

#### **5.11.2 Geochemical Statistics:**

Iodine concentrations were examined using two types of plots (Figure 42) that include a combination of a histogram, density trace, boxplot, and one-dimensional scatterplot (left side) and Empirical Cumulative Distribution Function (ECDF)-plot (right side) (Reimann et al., 2008). Interpretation of the EDCF-plot shows a slight variance indicated by sub populations with breaks near 1 mg/l and 10 mg/l. The density plots, histograms, boxplots and scatterplot suggest that I concentrations are left skewed on a log scale.

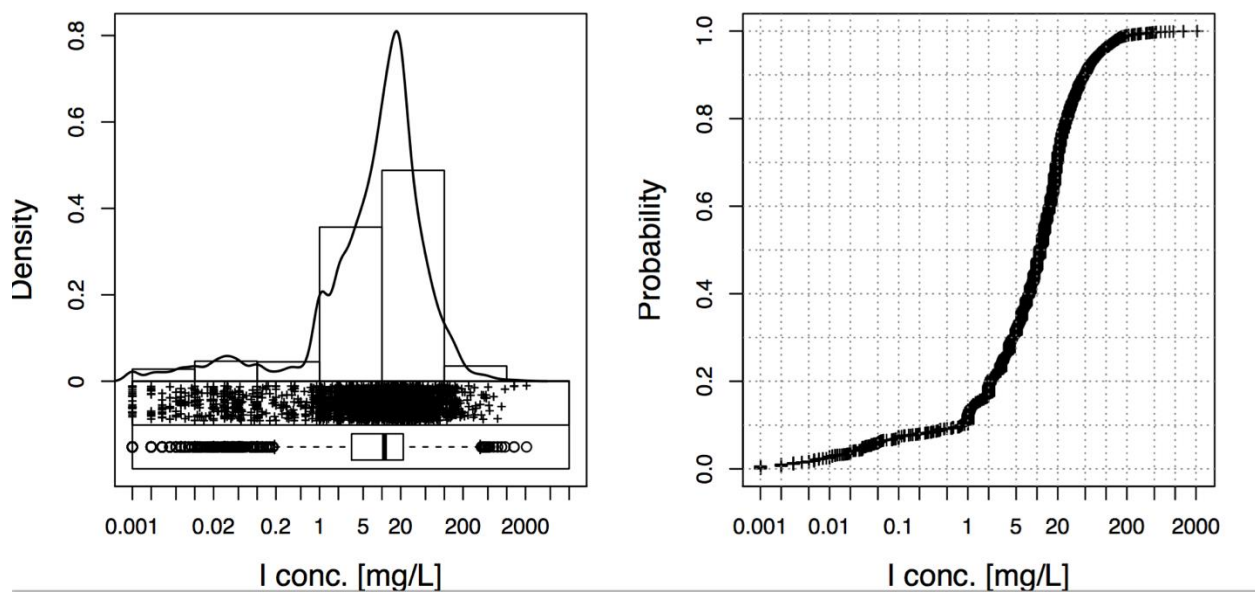


Figure 42: National EDA-plot in log scale, which includes a combination of a histogram, density trace, boxplot, and one-dimensional scatterplot (left side) and Empirical Cumulative Distribution Function (ECDF)-plot (right side). Iodine concentrations are skewed to the left and the graph shows a bimodal distribution.

### 5.11.3 Summary Statistics:

Table 12. Univariate data analysis for iodine.

	MIN	Q_0.05	Q1	MEDIAN	MEAN_log	MEAN	Q3	Q_0.95	MAX	SD	MAD	$p\sigma$	CV %	CVR %
I	0	0.0321	3.26	11	6.568	23.86	22	80	2080	67.58	13.14	13.89	283.3	119.4

Calculations were compiled to include: minimum (MIN), 5<sup>th</sup> percentile (Q\_0.05), 25<sup>th</sup> percentile (Q1), median, geometric mean (MEAN\_log), mean, 75<sup>th</sup> percentile (Q3), 95<sup>th</sup> percentile (Q\_0.95), maximum (MAX), standard deviation (SD), pseudosigma ( $p\sigma$ ), coefficient of variation (CV), and robust coefficient of variation (CVR).

### 5.11.4 Kendall Tau correlation:

The element iodide positively correlates ( $\tau > 0.6$ ) with Se ( $\tau = 0.64$ ). Constituents negatively correlated with I are Be ( $\tau = -0.42$ ), Ni ( $\tau = -0.37$ ), Co ( $\tau = -0.19$ ), Cd ( $\tau = -0.16$ ), and As ( $\tau = -0.11$ ).

## 5.11.5 Maps:

### 5.11.5.1 Spatial Distribution:

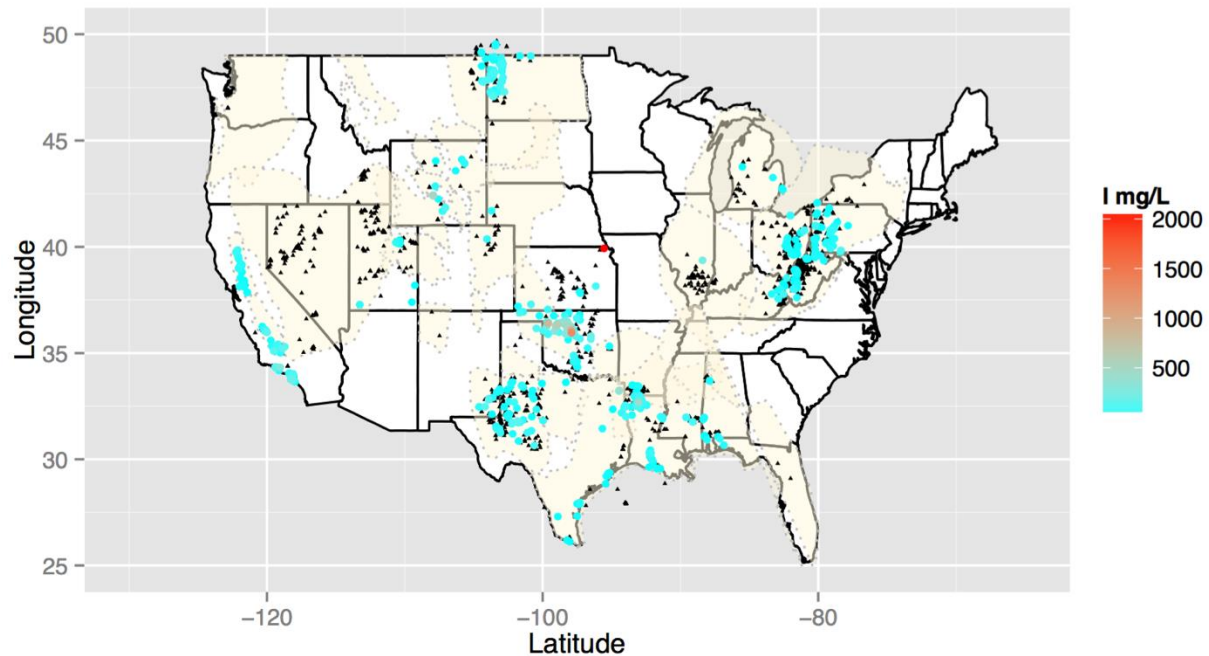


Figure 43: National spatial concentration map for iodine. Black triangles identify locations where iodine concentration data exist but are below the 75th percentile. Color ramped symbols applied to the sites where concentrations exceed the 75th percentile.

Results indicate the highest concentrations of iodine are found in the Anadarko Basin and moderately high concentrations in the Smackover Formation (Figure 43). Given high economic values, the existence of moderate to large data gaps suggests that exploration potential for iodine is relatively high. Due to the paucity of data, anomalies in other areas may exist but cannot be identified. Areas for possible future exploration include the Permian Basin, south Texas and southern Gulf Coastal Plain. There is an anomalously high concentration of I near Troy, Kansas. The map shows data coverage for iodine concentrations is moderate. The economics for being a Group 4 and Group 5 for disposal locations, reduces potential for economic profit and local

detailed analysis would be required. All identified locations are characterized by ancient paleoevaporated seawater; high levels of iodine are associated with organic-rich marine deposits.

#### 5.11.5.2 Estimated Economic Values:

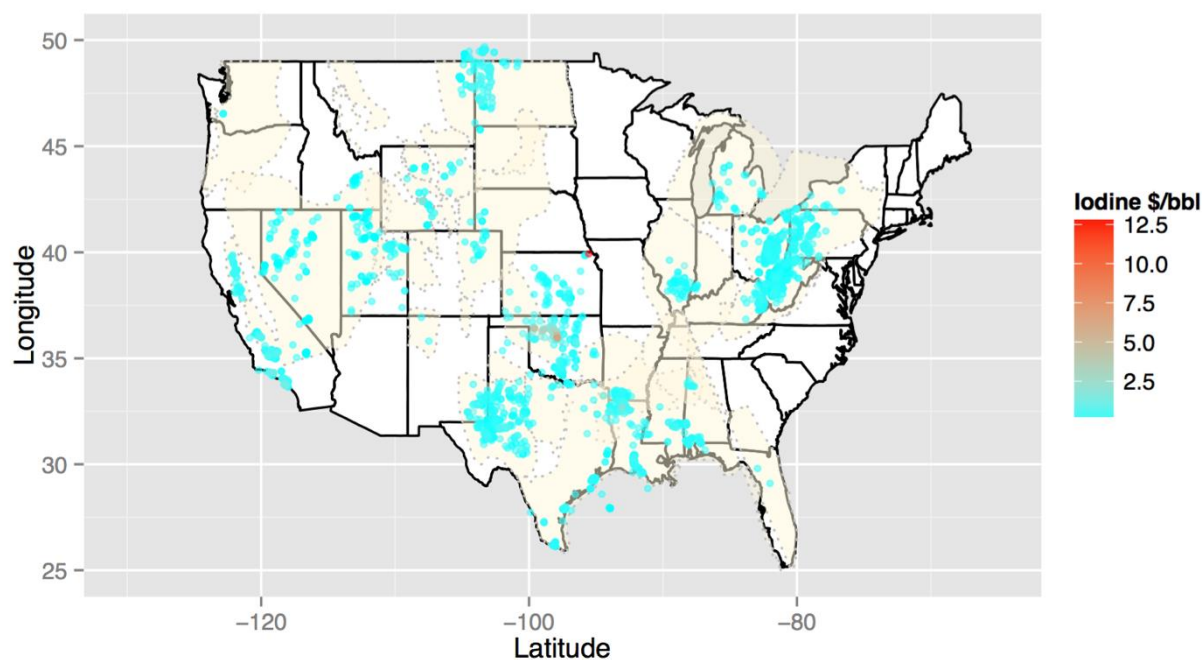


Figure 44: Economic map for iodine identifying highest areas of interest: The Anadarko Basin and the Gulf Coast Basin.

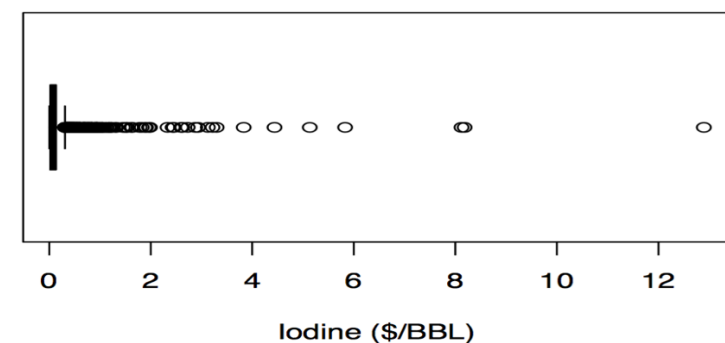


Figure 45: Tukey boxplot of economic values for iodine in produced waters.

Iodine commodities are valued at \$39.00 per kilogram (\$3.90E-05 per milligram). Applied to the concentration results shown in Figures 44 and 45, several areas show gross values in excess of \$1/bbl. The anomalously high concentration near Troy, Kansas, estimates iodine values near \$12.50/bbl. Currently, iodide is produced in the Anadarko Basin and the Smackover Formation from produced waters. The potential growth is high for iodine commodity extraction especially in Group 3, the least expensive region for disposal. Conversely, the Appalachian Basin is considered Group 5, a higher invested expenditure, with the concentration moderately high profit potential is still there. Group 6 has the least potential for development due to extensive regulations with produced waters and further analysis would be required. In the Anadarko basin a multimillion dollar year business has thrived since the 1960's extracting iodine from the basinal brines (Hammer and Levine, 2012). The potential for expansion in other basins is clearly identified by both the spatial distribution and economic potential maps.

#### **5.11.6 Summary:**

Data coverage for iodine is moderate and should be considered for future expansion. The development for iodine commodity products extends beyond the known developments in the Smackover Formation. The commodity values, concentrations, and disposal costs, greatest potential for development exists in other basins such as the Gulf Coast Basin and Permian Basin. When considering development in the western Appalachian Basin or Williston Basin more economic analysis needs to be applied. Disposal costs are higher for these areas, but does not mean profits are limited for iodine extraction. Iodine is also associated with other constituents in the Central Midwest and Gulf Coast Regions that have profit potential, such as bromine, lithium, and magnesium (cf. Figure 1, Figure 11, Figure 51, Figure 57), it may be more economical to extract elements as a group.

## **5.12 Lead**

### **Lead (Pb)**

#### **5.12.1 Commodity:**

The primary source for lead production is mining of mineral deposits. Lead can also be recovered through secondary refining processes. Lead is a corrosive metal that is used in a magnitude of products ranging from heavy construction materials to batteries. Lead is found in produced waters, with highest concentrations in the Gulf Coast and Black Warrior Basins. Lead can successfully be precipitated from brine waters using activated carbons prepared from pomegranate peel (Lenntech.com). The average price as of 2015 is \$1.07 per pound (U.S. Geological Survey, 2015).

#### **5.12.2 Geochemical Statistics:**

Lead concentrations were examined using two types of plots (Figure 46) that include a combination of a histogram, density trace, boxplot, and one-dimensional scatterplot (left side) and Empirical Cumulative Distribution Function (ECDF)-plot (right side) (Reimann et al., 2008). Interpretation of the EDCF-plot shows a bi-modal distribution with slight variances indicated by sub populations with a breaks near 5 mg/l. The density plots, histograms, boxplots and scatterplot suggest that Pb concentration are left skewed, even on a log-scale.

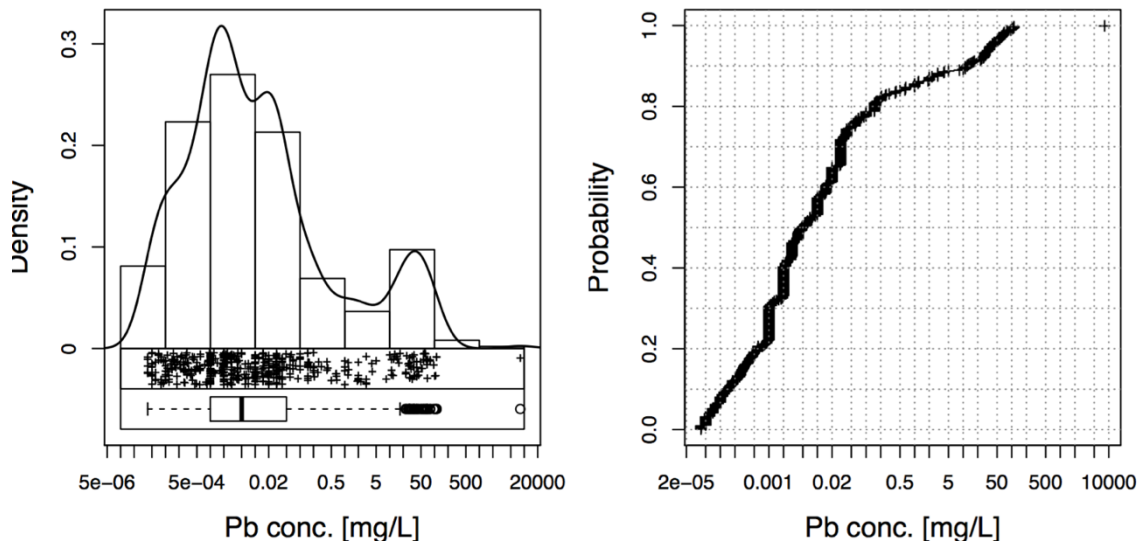


Figure 46: National EDA-plot in log scale, which includes a combination of a histogram, density trace, boxplot, and one-dimensional scatterplot (left side) and Empirical Cumulative Distribution Function (ECDF)-plot (right side). Lead concentrations are skewed to the left and the graph shows a bimodal distribution.

### 5.12.3 Summary Statistics:

Table 13. Univariate data analysis for lead.

	MIN	Q_0.05	Q1	MEDIAN	MEAN_log	MEAN	Q3	Q_0.95	MAX	SD	MAD	$p\sigma$	CV %	CVR %
<b>Pb</b>	4.00 E-05	7.00E-05	0.001	0.005	0.01192	21.4	0.05	37.6	8187	368.9	0.007339	0.03632	1724	146.8

Calculations were compiled to include: minimum (MIN), 5<sup>th</sup> percentile (Q\_0.05), 25<sup>th</sup> percentile (Q1), median, geometric mean (MEAN\_log), mean, 75<sup>th</sup> percentile (Q3), 95<sup>th</sup> percentile (Q\_0.95), maximum (MAX), standard deviation (SD), pseudosigma ( $p\sigma$ ), coefficient of variation (CV), and robust coefficient of variation (CVR).

### 5.12.4 Kendall Tau correlation:

In descending order, elements positively correlated ( $\tau > 0.6$ ) with Pb include: Be ( $\tau = 0.75$ ), Ti ( $\tau = 0.69$ ), Zn ( $\tau = 0.65$ ), Br ( $\tau = 0.64$ ), Ni ( $\tau = 0.65$ ), Co ( $\tau = 0.65$ ), Se ( $\tau = 0.63$ ), and Cd ( $\tau = 0.62$ ). The constituent negatively correlated with Pb is Si ( $\tau = -0.17$ ).

## 5.12.5 Maps:

### 5.12.5.1 Spatial Distribution:

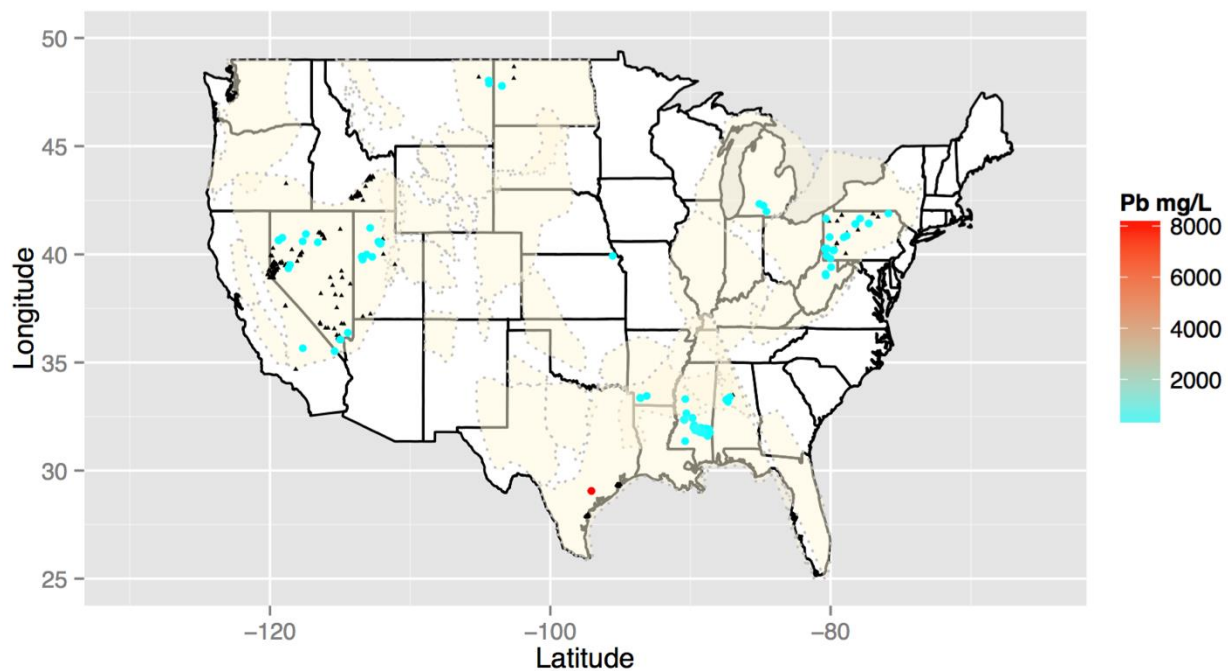


Figure 47: National spatial concentration map for lead. Black triangles identify locations where lead concentration data exist but are below the 75th percentile. Color ramped symbols applied to the sites where concentrations exceed the 75th percentile.

Results indicate the highest concentration for Pb in the Galveston/Corpus Christie, Texas area and appears to be an anomaly, being roughly 100 times higher than the next largest sample (Figure 47). The average range for the top 25% is closer to 50 mg/L. Spatial distribution for Pb is limited and large data gaps are present. Lead is a base metal associated with MVT mineral deposits and clastic-dominated lead-zinc ores that are hosted in shales, sandstones, siltstone or mixed clastic rocks (Leach et al., 2010). Environments for lead concentrations vary with basement sediments (Leach et al., 2010). Exploration potential for lead is high as the data coverage is low.

### 5.12.5.2 Estimated Economic Values:

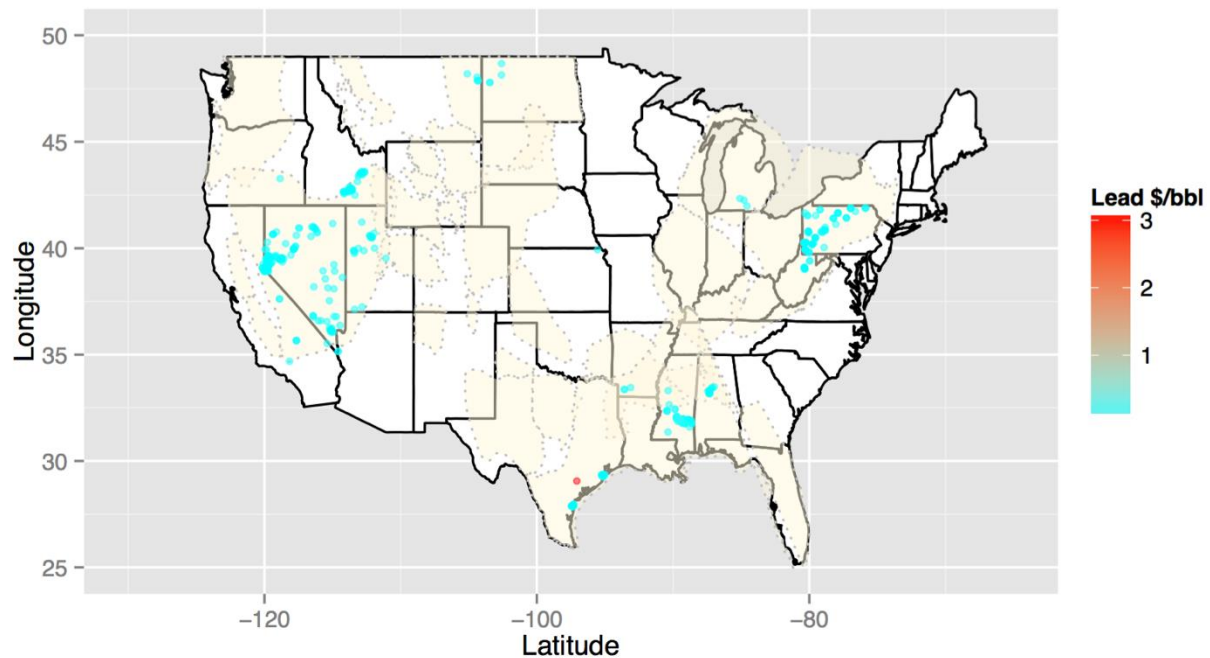


Figure 48: Economic map for lead identifying highest areas of interest: The Gulf Coast Basin, Smackover Formation and the Appalachian Basin.

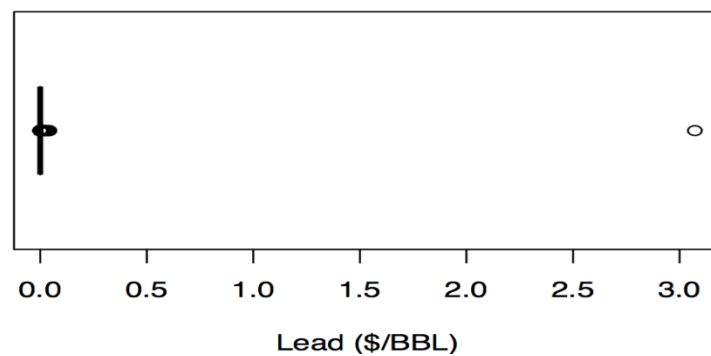


Figure 49: Tukey boxplot of economic values for lead in produced waters

Lead commodities are valued at \$1.07 per pound (\$2.36E-06 per milligram). Applied to the concentration results shown in Figure 47, gross values for lead in some areas (approximately \$.10 per barrel) exceed disposal costs (Figures 48, 49). Disposal costs are a variable that effects

the potential profit. There is an identified anomaly for elevated lead concentrations which generates a value of approximately \$3.00 per barrel, the concentration value has not been verified as accurate. The only potential for Pb is combining the commodity with other elements, such as beryllium, zinc, bromine, nickel, cobalt and cadmium.

#### **5.12.6 Summary:**

Development potential for lead extraction is limited to minimal. Co-existing production with other base metals could be considered. The commodity values, concentrations, and disposal costs, reduce potential for most regions, the Gulf Coast region has greatest potential for development, with low to moderate disposal costs. When considering development in the western Appalachians or Williston Basin more economic analysis needs to be applied. Disposal costs are higher for these areas, and other commodities that could be extracted with lead may not be as available. Substantial data gaps exists, but concentrations would have to be 1-2 orders of magnitude beyond the current range of data to be significantly more economic. As such there is to moderate potential for further exploration.

## **5.13 Lithium**

### **Lithium (Li)**

#### **5.13.1 Commodity:**

Lithium production comes from two sources: ore deposits and basinal brines. Lithium is produced in three forms: lithium carbonate, lithium chloride and lithium hydroxide; the former two are produced from brines. Lithium is used in the manufacturing of batteries, polymers, aluminum production and pharmaceuticals. The consumer applications of Li continue to grow with the demand for personal laptops, cellular devices and computer tablets. Due to proprietary information, Li price averages are subjective; the most recent data are from 2013. Lithium carbonate price averages are based on import values of \$5.64 per kilogram and lithium hydroxide values were \$7.43 per kilogram. In China, lithium carbonate-battery grade averages \$6,380 per metric ton. Lithium is found in produced waters at high concentrations in multiple locations (U.S. Geological Survey, 2015).

#### **5.13.2 Geochemical Statistics:**

Lithium concentrations were examined using two types of plots (Figure 50) that include a combination of a histogram, density trace, boxplot, and one-dimensional scatterplot (left side) and Empirical Cumulative Distribution Function (ECDF)-plot (right side) (Reimann et al., 2008). Interpretation of the EDCF-plot (Figure 50) has a bi-modal with a break near 0.1 mg/L. The density plots, histograms, boxplots and scatterplot suggest that the higher concentration population is right skewed.

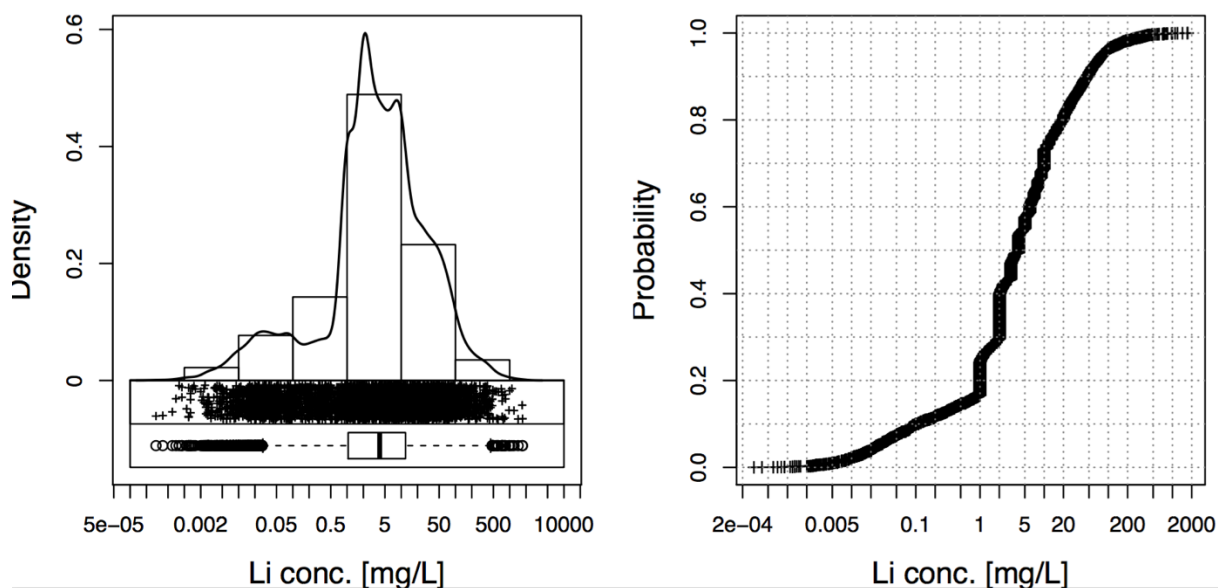


Figure 50: National EDA-plot in log scale, which includes a combination of a histogram, density trace, boxplot, and one-dimensional scatterplot (left side) and Empirical Cumulative Distribution Function (ECDF)-plot (right side). Lithium concentrations are left skewed and the graph shows a multiple distribution.

### 5.13.3 Summary Statistics:

Table 14. Univariate data analysis lithium.

	MIN	Q_0.05	Q1	MEDIAN	MEAN_log	MEAN	Q3	Q_0.95	MAX	SD	MAD	$p\sigma$	CV %	CVR %
Li	3.00E-04	0.025	1.05	4	3.175	20.52	12	80.3	1730	69.07	5.271	8.117	336.6	131.8

Calculations were compiled to include: minimum (MIN), 5<sup>th</sup> percentile (Q\_0.05), 25<sup>th</sup> percentile (Q1), median, geometric mean (MEAN\_log), mean, 75<sup>th</sup> percentile (Q3), 95<sup>th</sup> percentile (Q\_0.95), maximum (MAX), standard deviation (SD), pseudosigma ( $p\sigma$ ), coefficient of variation (CV), and robust coefficient of variation (CVR).

### 5.13.4 Kendall Tau correlation:

In descending order, elements positively correlated ( $\tau > 0.6$ ) with Li include Sr ( $\tau = 0.68$ ), K ( $\tau = 0.66$ ), Rb ( $\tau = 0.64$ ), Cl ( $\tau = 0.62$ ), and Na ( $\tau = 0.61$ ). Although slightly below the cutoff, Li is also positively correlated with Br ( $\tau = 0.59$ ). Constituents negatively correlated with Li and Hg ( $\tau = -0.12$ ),  $\text{HCO}_3$  ( $\tau = -0.12$ ), and Si ( $\tau = -0.15$ ). The positive correlations with the listed elements are of important for consideration of co-production or using other elements as path finders.

### 5.13.5 Maps:

#### 5.13.5.1 Spatial Distribution:

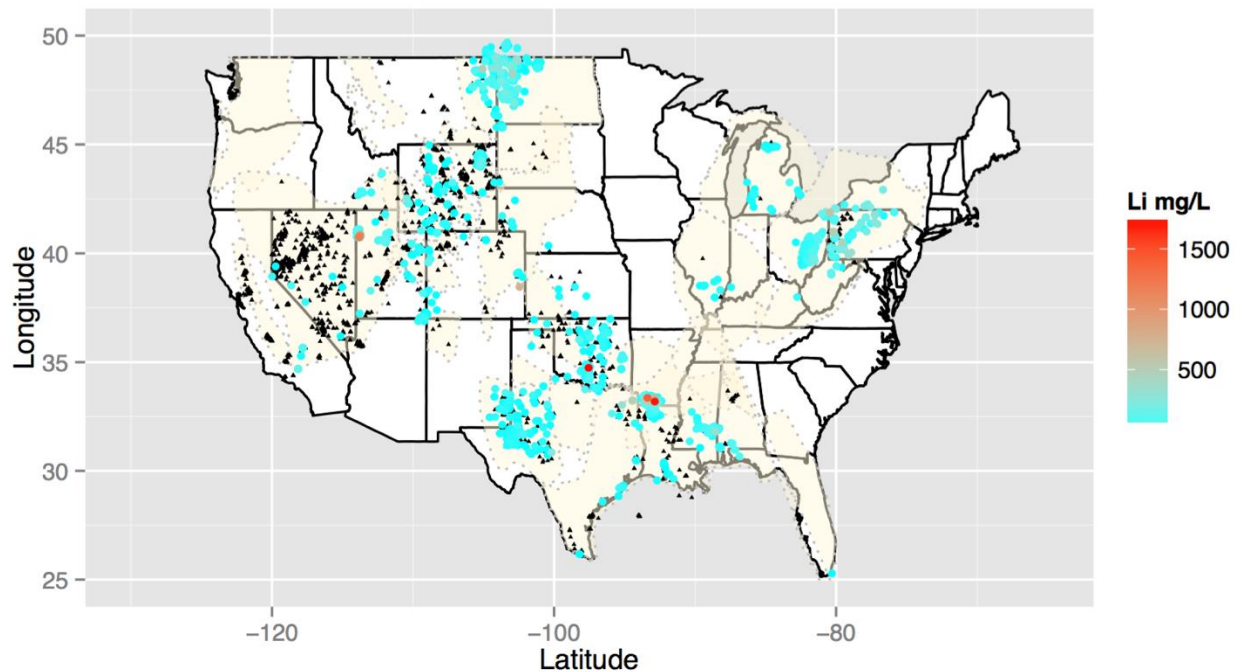


Figure 51: National spatial concentration map for lithium. Black triangles identify locations where Li concentration data exist but are below the 75th percentile. Color ramped symbols applied to the sites where concentrations exceed the 75th percentile.

The spatial distribution of lithium concentration data is fairly complete with minimal large scale data gaps, but with potential for more fine scale data (Figure 51). The highest Li concentrations are from the Smackover Formation in Arkansas and southern Oklahoma. Some data exceed 1500 mg/L. Group 1 and Group 3 maintain some of the lowest disposal costs thus increasing the potential for development. Particular regions with moderate disposal costs still present opportunity to generate profits if a detailed economic analysis is completed. Careful consideration must be applied as to not over stimulate products thus ultimately driving the product value down.

### 5.13.5.2 Estimated Economic Values:

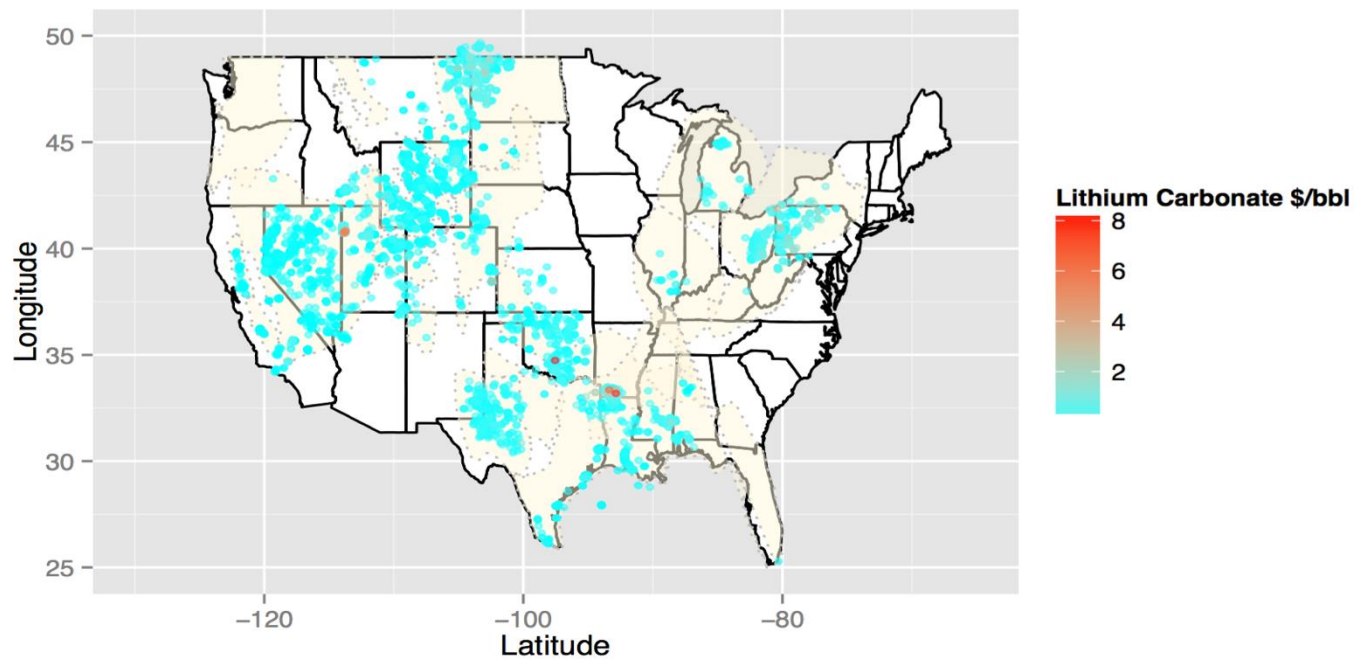


Figure 52: Economic map for lithium carbonate identifying highest areas of interest: the Gulf Coast Basin, areas where the Smackover is present, and the northern Appalachian Basin.

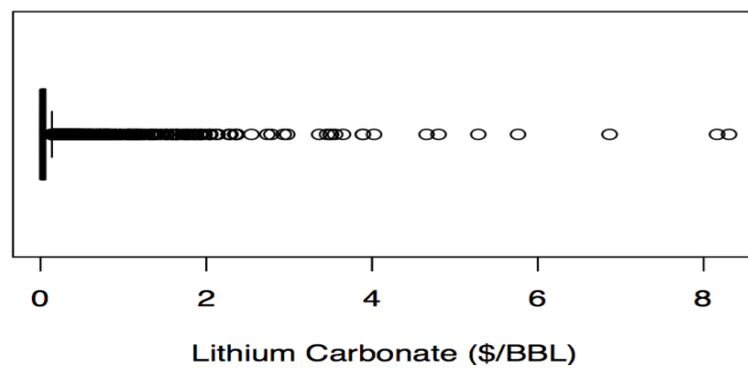


Figure 53: Tukey boxplot of economic values for lithium carbonate in produced waters

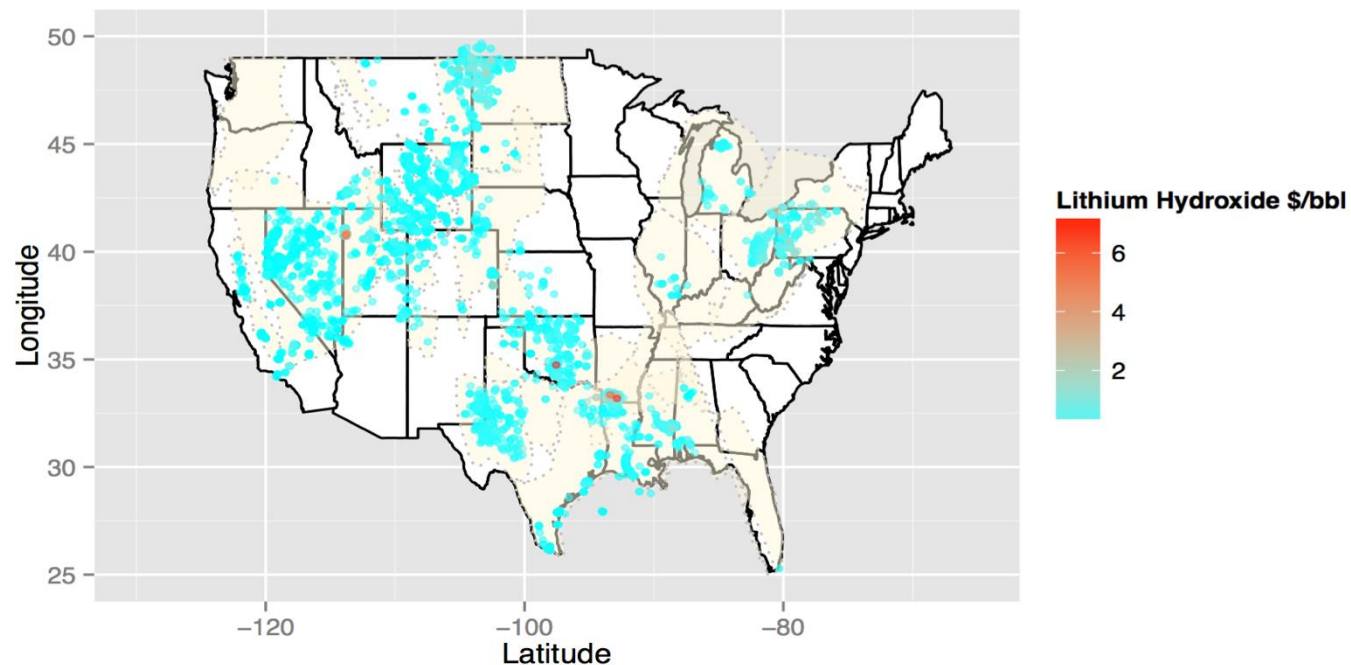


Figure 54: Economic map for lithium hydroxide identifying highest areas of interest: the Gulf Coast Basin, areas where the Smackover Formation is present, the Central Midwest Region, and the northern Appalachian Basin.

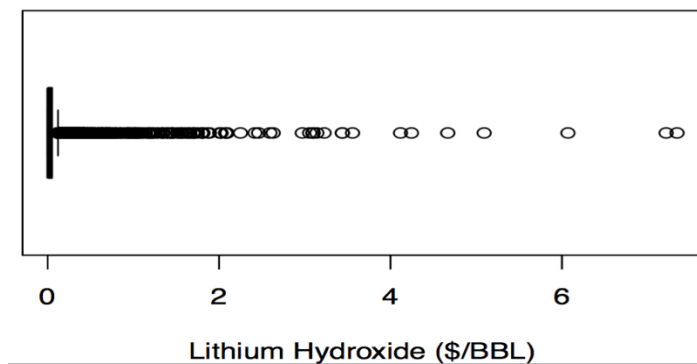


Figure 55: Tukey boxplot of economic values for lithium hydroxide in produced waters

Lithium commodities are divided into two commodities: lithium carbonate at \$5.64 per kilogram (\$3.02E-05 per milligram per liter) and lithium hydroxide at \$7.43 per kilogram. (\$2.56E-05 per milligram per liter). Economic results shown that potential for future development potential for lithium is high, regardless of form extracted. In locations such as the Northeast Region, where disposal costs are relatively high, Li might still be profitable, especially when combined with other valuable commodities. Lithium is currently extracted from basinal brines in the Smackover Formation. There is high potential for development in other basins.

#### **5.13.6 Summary:**

Lithium is currently produced from brines from the Smackover Formation and this analysis suggests that the potential to expand to other regions is high. Data exploration has moderate potential based on current concentration coverages. To increase revenue, lithium could be combined with other co-associated commodities such as bromine, rubidium, and potassium, as they are associated (see correlation discussion). Co-production can increase potential revenue and help offset disposal costs. Caution should be adhered to the market as to not increase supply so much that a stockpile increase exceeds demand and lowers the product commodity value. Domestically increasing production may also have greater benefit and limit the dependency on foreign imports.

## 5.14 Magnesium

### Magnesium (Mg)

#### 5.14.1 Commodity:

Magnesium and magnesium-bearing compounds are used multiple industries including environmental applications, pharmaceuticals, and agriculture. Magnesium sources include seawater, brines, and mineral deposits. According to Platts Metals Week, annual average price in 2013 was \$2.17 per pound. U.S production price averages are proprietary information (U.S. Geological Survey, 2015).

#### 5.14.2 Geochemical Statistics:

Magnesium concentrations were examined using two types of plots (Figure 56) that include a combination of a histogram, density trace, boxplot, and one-dimensional scatterplot (left side) and Empirical Cumulative Distribution Function (ECDF)-plot (right side) (Reimann et al., 2008). The EDCF-plot indicates that magnesium has a progressive distribution and shows a variance indicated by sub populations with breaks near 1 mg/L, 25 mg/L, and 100 mg/L. The density plots, histograms, boxplots and scatterplot suggest that Mg concentration are left skewed on a log-scale.

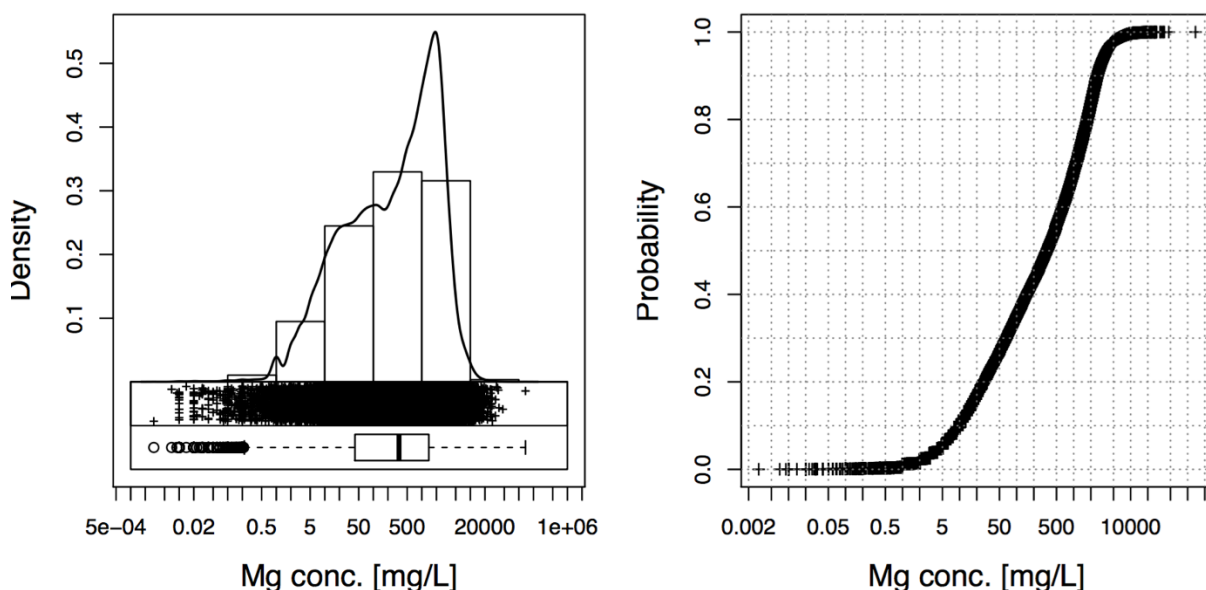


Figure 56: National EDA-plot in log scale, which includes a combination of a histogram, density trace, boxplot, and one-dimensional scatterplot (left side) and Empirical Cumulative Distribution Function (ECDF)-plot (right side). Magnesium concentrations are left skewed and the graph shows a multiple distribution.

### 5.14.3 Summary Statistics:

Table 15. Univariate data analysis magnesium

	MIN	Q_0.05	Q1	MEDIAN	MEAN-log	MEAN	Q3	Q_0.95	MAX	SD	MAD	pσ	CV %	CVR %
Mg	0	5	42	339	220.5	969.6	1394	3568	137100	1632	487.8	1002	168.3	143.9

Calculations were compiled to include: minimum (MIN), 5<sup>th</sup> percentile (Q\_0.05), 25<sup>th</sup> percentile (Q1), median, geometric mean (MEAN\_log), mean, 75<sup>th</sup> percentile (Q3), 95<sup>th</sup> percentile (Q\_0.95), maximum (MAX), standard deviation (SD), pseudosigma (pσ), coefficient of variation (CV), and robust coefficient of variation (CVR).

### 5.14.4 Kendall Tau correlation:

In descending order, elements positively correlated ( $\tau > 0.6$ ) with Mg include: Ca ( $\tau = 0.76$ ), Br ( $\tau = 0.65$ ), Cl ( $\tau = 0.65$ ), Sr ( $\tau = 0.62$ ), and Na ( $\tau = 0.61$ ). Additional elements are positively correlated at slightly lower levels ( $\tau > 0.5$ ): K ( $\tau = 0.57$ ), Co ( $\tau = 0.54$ ), Li ( $\tau = 0.53$ ), and Mn ( $\tau = 0.53$ ). Constituents negatively correlated with Mg are HCO<sub>3</sub> ( $\tau = -0.44$ ), BO<sub>3</sub> ( $\tau = -0.19$ ), Hg ( $\tau = -0.13$ ), and Si ( $\tau = -0.11$ ), and. The positive correlations with the listed elements are of important consideration for co-production or using other elements as path finders. Correlations at ( $\tau > 0.5$ ) were included to shows that Mg is co-associated with a variety of other constituents.

## 5.14.5 Maps:

### 5.14.5.1 Spatial Distribution:

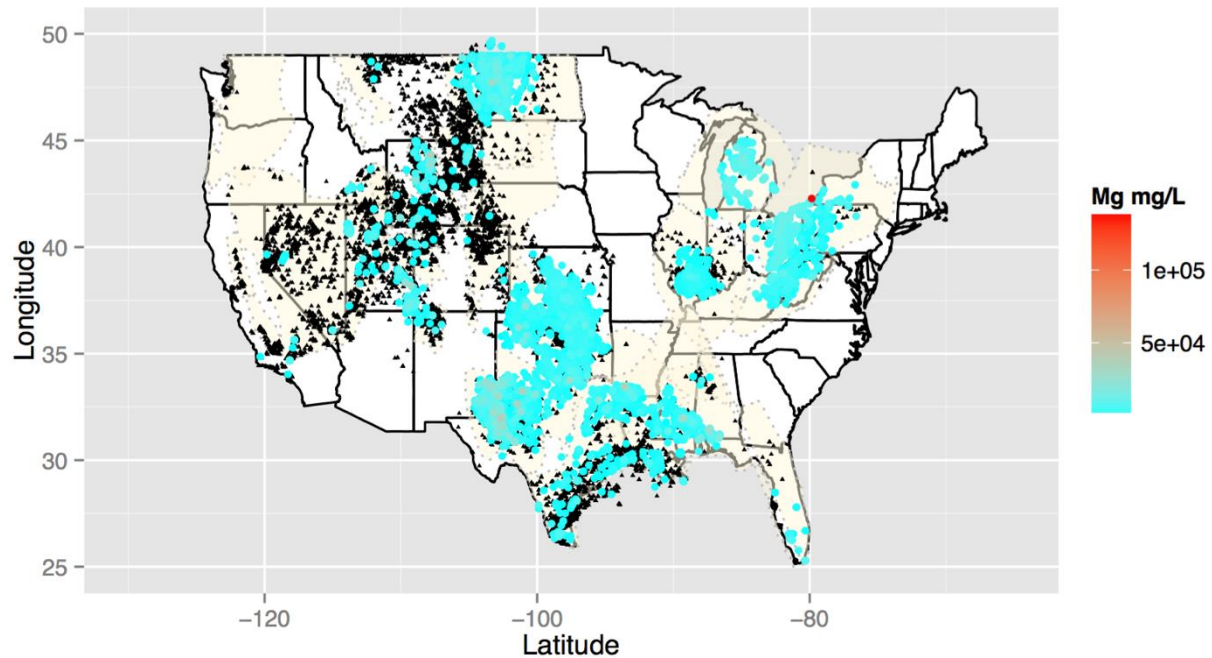


Figure 57: National spatial concentration map for magnesium. Black triangles identify locations where Mg concentration data exist but are below the 75th percentile. Color ramped symbols applied to the sites where concentrations exceed the 75th percentile.

The spatial distribution of magnesium data is well established with few data gaps (Figure 57). Areas with the highest Mg concentrations also exhibit high TDS (Figure 1), including the Williston Basin, the Permian Basin, the Gulf Coast Basin, the Appalachian Basin, and the Palo Duro Basin. Magnesium concentrations in some samples exceed 100,000 mg/L. Group 1 and Group 3 areas maintain some of the lowest disposal costs, thus increasing the potential for development. Particular regions with moderate disposal costs still present opportunity to generate profit if a detailed economic analysis supports extraction. Careful consideration must be applied as to not over stimulate products, thus ultimately driving the product value down.

#### 5.14.5.2 Estimated Economic Values:

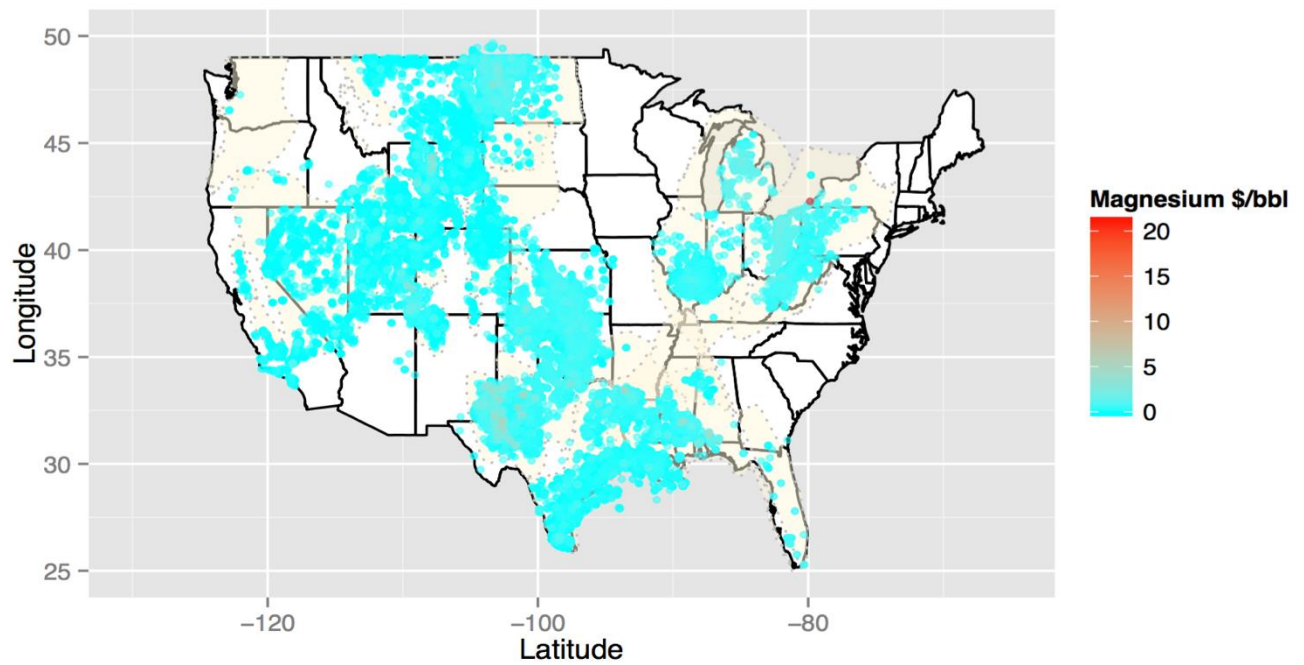


Figure 58: Economic map for magnesium identifying highest areas of interest: the northern Appalachian Basin, Gulf Coast Region, Permian Basin, and the Williston Basin.

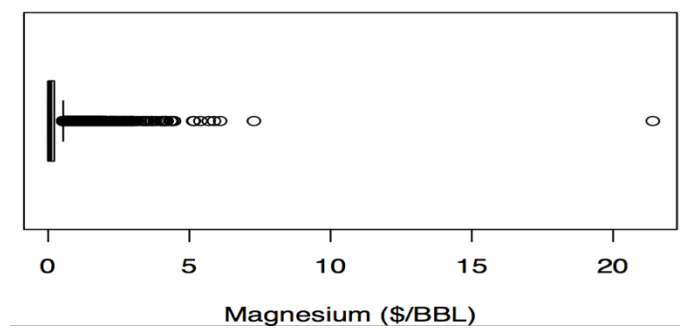


Figure 59: Tukey boxplot of economic values for magnesium in produced waters.

Magnesium hydroxide, the primary mineral commodity produced from Mg, is valued at \$2.17 per pound (\$9.82E-07 per milligram per liter). Applied to the concentration results shown in Figure 57, extensive areas exhibit potential for development. Continuous improvements to extraction methodologies and technology could drive Mg production from produced waters. Magnesium is currently extracted during desalination as salt products (MgCl<sub>2</sub>). Magnesium chloride can be precipitated out during evaporation, as a byproduct, and could be considered as an additional commodity that is not identified as a commodity in the USGS Minerals Commodity Yearbook. The potential to expand is high. Overall, magnesium extraction has high potential in all regions, as the value in the upper few percent can exceed disposal costs.

#### **5.14.6 Summary:**

Given the high number and density of magnesium concentration data, the exploration potential is minimal. Development in produced waters for magnesium commodity products has a high potential in all considered regions. To increase revenue from the identified high concentrated regions, Mg can be combined with other commodities such as bromine, iodine, and lithium, or co-produced with NaCl. Many other constituents correlate well with Mg and thus, could be considered for removal if technology costs can be reduced and the other elements effectively separated from Mg. The profit potential increases with presumably constant disposal costs when combined with other elements of interest. Caution should be adhered to the market as to not increase supply so much that a stockpile increase exceeds demand and lowers the product commodity value. Domestically increasing production may also have greater benefit and limit the dependency on foreign imports. Market supply and demand needs to be analyzed, if all regions begin production simultaneously there is potential to drop the price of the commodity.

## **5.15 Manganese**

### **Manganese (Mn)**

#### **5.15.1 Commodity:**

Domestic production for manganese ore deposits ceased during the 1970's. Manganese is mined from ore deposits and imported into the United States for manufacturing. Manganese is used for the production in fertilizers, animal feed, battery cells and some steel manufacturing. High concentrations of manganese in produced waters are known to exist. The average price for manganese ore in 2014 was \$4.30 per metric ton which includes factored costs of insurance and transportation (U.S. Geological Survey, 2015).

#### **5.15.2 Geochemical Statistics:**

Manganese concentrations were examined using two types of plots (Figure 60) that include a combination of a histogram, density trace, boxplot, and one-dimensional scatterplot (left side) and Empirical Cumulative Distribution Function (ECDF)-plot (right side) (Reimann et al., 2008). The ECDF-plot suggests a bimodal distribution and with breaks near 0.25 mg/L, 10 mg/L, and 150 mg/L. The density plots, histograms, boxplots and scatterplot support this conclusion.

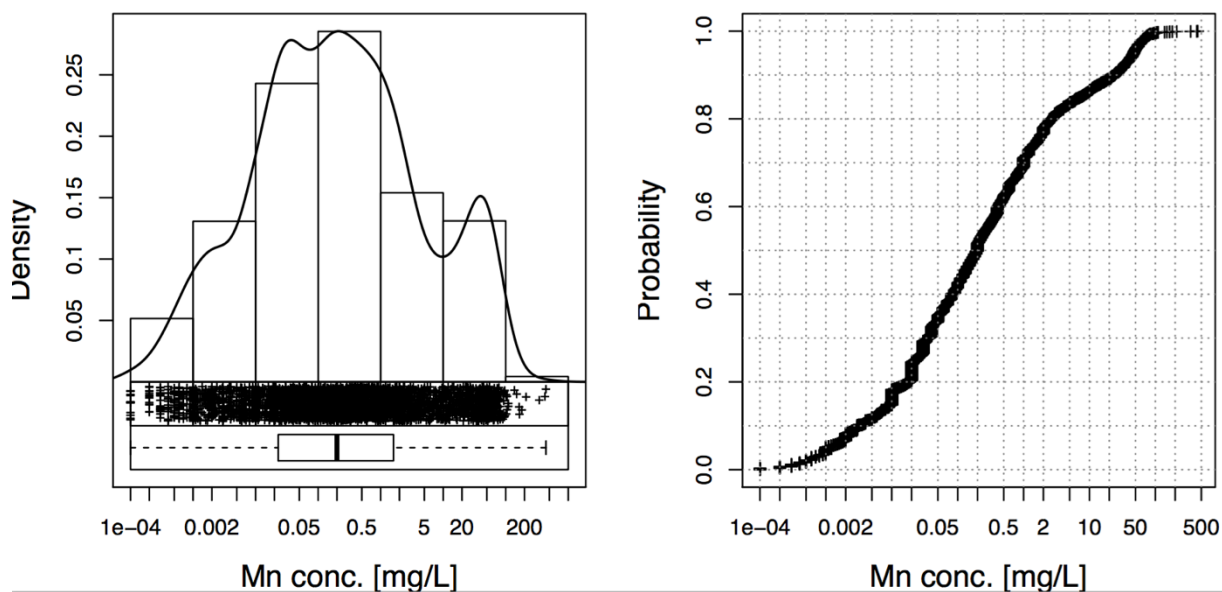


Figure 60: National EDA-plot in log scale, which includes a combination of a histogram, density trace, boxplot, and one-dimensional scatterplot (left side) and Empirical Cumulative Distribution Function (ECDF)-plot (right side). Manganese concentrations are slightly right and the graph shows a multiple distribution.

### 5.15.3 Summary Statistics:

Table 16. Univariate data analysis for manganese.

	MIN	Q_0.05	Q1	MEDIAN	MEAN_log	MEAN	Q3	Q_0.95	MAX	SD	MAD	pσ	CV %	CVR %
<b>Mn</b>	1.00E-04	0.001	0.023	0.2	0.2067	6.598	1.605	46.9	440.5	20.45	0.2933	1.173	310	146.6

Calculations were compiled to include: minimum (MIN), 5<sup>th</sup> percentile (Q\_0.05), 25<sup>th</sup> percentile (Q1), median, geometric mean (MEAN\_log), mean, 75<sup>th</sup> percentile (Q3), 95<sup>th</sup> percentile (Q\_0.95), maximum (MAX), standard deviation (SD), pseudosigma (pσ), coefficient of variation (CV), and robust coefficient of variation (CVR).

### 5.15.4 Kendall Tau correlation:

In descending order, elements positively correlated ( $\tau > 0.6$ ) with Mn include Sr ( $\tau = 0.64$ ), Br ( $\tau = 0.63$ ), and Co ( $\tau = 0.61$ ). In descending order, elements positively correlated ( $\tau > 0.5$ ) with Mn include Na ( $\tau = 0.59$ ), Li ( $\tau = 0.58$ ), Pb ( $\tau = 0.58$ ), Cl ( $\tau = 0.56$ ), Ca ( $\tau = 0.55$ ), Ba ( $\tau = 0.53$ ), Mg ( $\tau = 0.53$ ), Be ( $\tau = 0.51$ ), and K ( $\tau = 0.51$ ). Constituents negatively correlated with Mn are Hg ( $\tau = -0.22$ ), and S ( $\tau = -0.21$ ). Correlations at ( $\tau > 0.5$ ) were included to show other commonly associated with magnesium.

## 5.15.5 Maps:

### 5.15.5.1 Spatial Distribution:

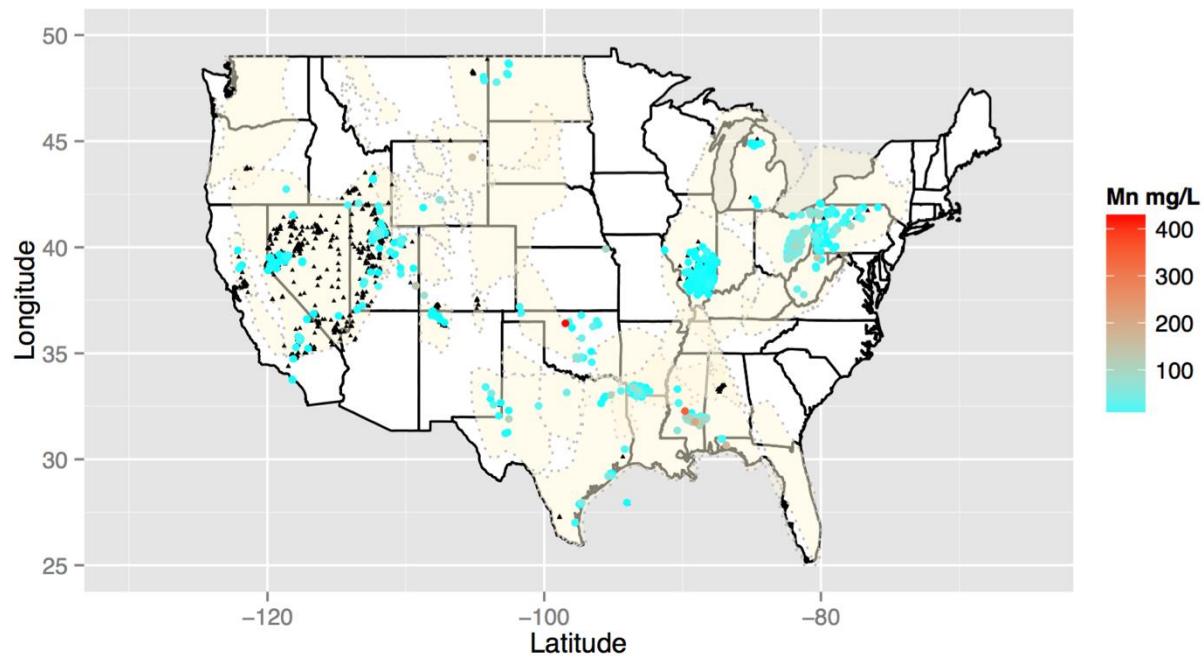


Figure 61: National spatial concentration map for manganese. Black triangles identify locations where Mn concentration data exist but are below the 75th percentile. Color ramped symbols applied to the sites where concentrations exceed the 75th percentile.

The spatial distribution of manganese data is moderately complete with some large data gaps (Figure 61). The highest Mn concentrations are found in the Gulf Coast Basin (consistent with MVTs), Central Midwest (Anadarko Basin), Northeastern Region (western Appalachian Basin) and Black Hills Region (Williston Basin). Sparse data in some regions suggests there may be room for exploration. Group 1 and Group 3 states maintain some of the lowest disposal costs thus increasing the potential for development, should it prove cost effective to remove Mn from produced waters in these areas. Particular regions with moderate disposal costs minimize all potential for development in Mn commodities.

### 5.15.5.2 Estimated Economic Values:

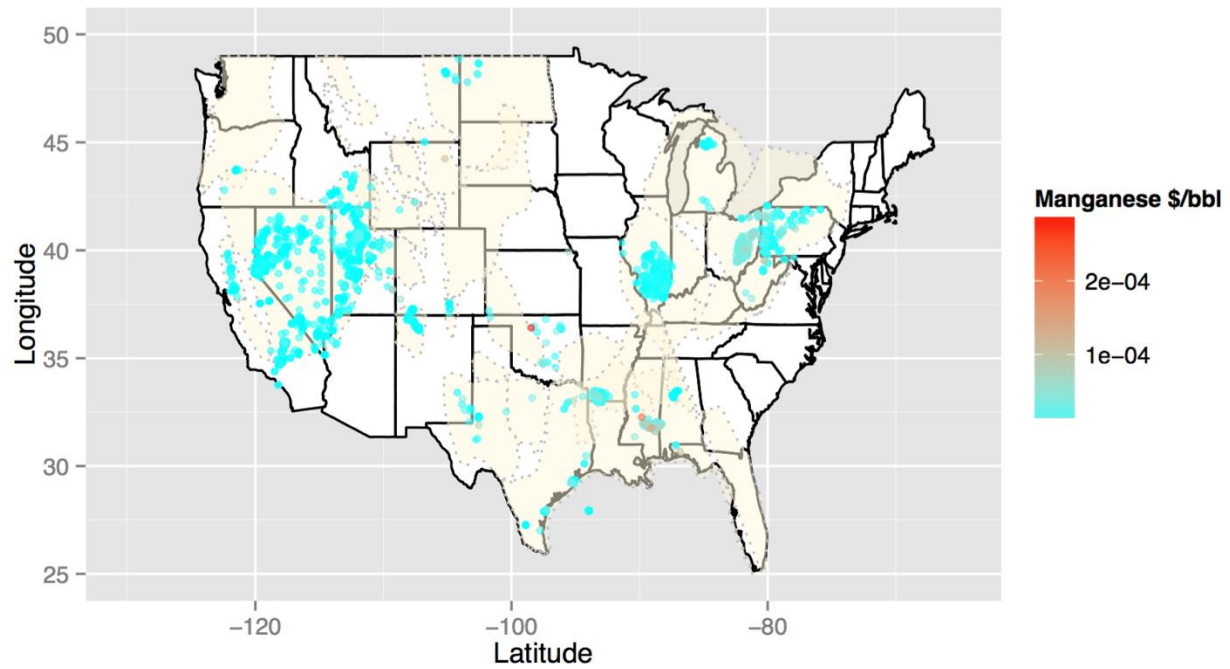


Figure 62: Economic map for Mn identifying highest areas of interest: the Anadarko Basin.

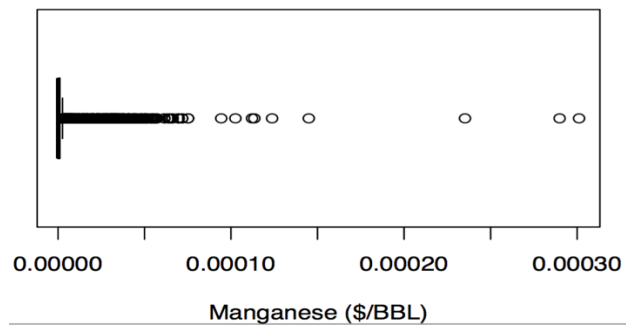


Figure 63: Tukey boxplot of economic values for manganese in produced waters

Manganese is the primarily mined from ore deposits and the commodity is valued at \$4.30 per metric ton (\$4.30E-09 per milligram per liter). Applied to the concentration results, there is little potential for development (Figures 62, 63). In the case where disposal costs exceed commodity value, the potential for economic success is eliminated. Manganese does correlate statistically with other commodities, such as bromine, that do have potential. If Manganese can be separated from solution while removing other commodities, it may become economic. Otherwise it is still less expensive and easier to continue with current sources.

#### **5.15.6 Summary:**

There is little potential for extraction of manganese from for all regions. To generate revenue, the best opportunity would be combining with other commodities such as bromine, iodine, and lithium. There is currently no known domestic production for manganese in the United States. Another known source for manganese is from deep sea dredging for manganese nodules, such off the coast of Japan. The only present potential for economic development of manganese in produced waters is if removal processes are inexpensive enough and operations expenses are low enough to offset the cost. There also would need to be a market with high enough demand to warrant such activities. Market supply and demand needs to be analyzed, especially in the area of foreign trades before any production can occur. While data gaps exist, the value of Mn in produced waters are so low that there appears to be little need.

## **5.16 Mercury**

### **Mercury (Hg)**

#### **5.16.1 Commodity:**

Mercury production as a mineral commodity ceased in 1992 and elemental mercury is banned from export out of the United States under the Mercury Export Ban Act of 2008. Mercury end products include barometers, thermostats, and medical devices. Mercury is also a secondary byproduct of equipment recycling and from previous metal (silver and gold) mining. The average import price for mercury is approximately \$1850 per 76-pound flask. There are some data in the produced waters database. The data are from areas are remote and concentrations are relatively low (U.S. Geological Survey, 2015).

#### **5.16.2 Geochemical Statistics:**

Mercury concentrations were examined using two types of plots (Figure 2): a combination of a histogram, density trace, boxplot, and one-dimensional scatterplot (left side) and Empirical Cumulative Distribution Function (ECDF)-plot (right side) (Reimann et al., 2008). Interpretation of the EDCF-plot (Figure 64) shows a variance indicated by sub populations with breaks near 0.0001 mg/L, 0.005 mg/L, and .001 mg/L. The density plots, histograms, boxplots and scatterplot suggest that Hg concentrations are right skewed, even on a log-scale.

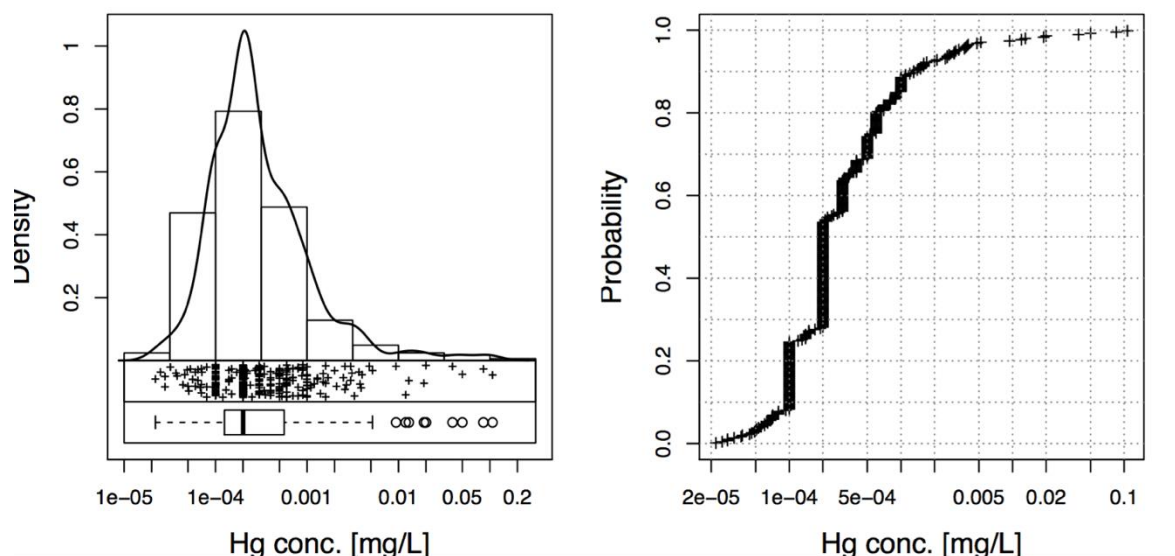


Figure 64: National EDA-plot in log scale, which includes a combination of a histogram, density trace, boxplot, and one-dimensional scatterplot (left side) and Empirical Cumulative Distribution Function (ECDF)-plot (right side). Fluorine concentrations are right skewed.

### 5.16.3 Summary Statistics:

Table 17. Univariate data analysis for mercury.

	MIN	Q_0.05	Q1	MEDIAN	MEAN_log	MEAN	Q3	Q_0.95	MAX	SD	MAD	pσ	CV %	CVR %
<b>Hg</b>	2.20E-05	6.40E-05	0.0001275	2.00E-04	0.0003018	0.001554	0.0005475	0.003065	0.107	0.008444	0.0001483	0.0003113	543.4	74.13

Calculations were compiled to include: minimum (MIN), 5<sup>th</sup> percentile (Q\_0.05), 25<sup>th</sup> percentile (Q1), median, geometric mean (MEAN\_log), mean, 75<sup>th</sup> percentile (Q3), 95<sup>th</sup> percentile (Q\_0.95), maximum (MAX), standard deviation (SD), pseudosigma (pσ), coefficient of variation (CV), and robust coefficient of variation (CVR).

### 5.16.4 Kendall Tau correlation:

Mercury does not positively correlate with any elements considered in the Produced Waters Database at  $\tau > 0.6$ . The constituents that negatively correlate with are Br ( $\tau = -0.22$ ), Mn ( $\tau = -0.22$ ), Sr ( $\tau = -0.19$ ), Ca ( $\tau = -0.16$ ), Na ( $\tau = -0.15$ ), Cr ( $\tau = -0.14$ ), Cl ( $\tau = -0.13$ ), Mg ( $\tau = -0.13$ ), and Li ( $\tau = -0.12$ ).

## 5.16.5 Maps:

### 5.16.5.1 Spatial Distribution:

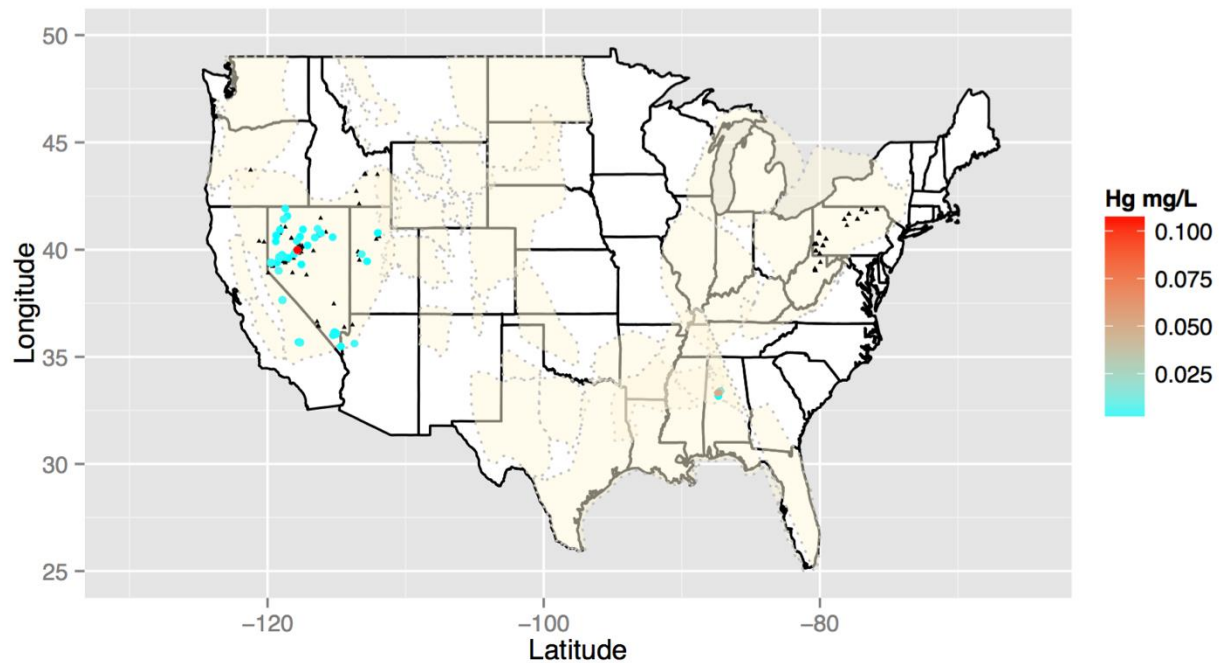


Figure 65: National spatial concentration map for mercury. Black triangles identify locations where Hg concentration data exist but are below the 75th percentile. Color ramped symbols applied to the sites where concentrations exceed the 75th percentile.

The spatial distribution for mercury is sparse, with the highest concentrations Nevada, California, and the Black Warrior Basin. There is need for further testing to complete the data distribution. Thus there is potential for future exploration. The mercury concentrations are located in states within Groups 3 and 6, regions that traditionally maintain higher disposal costs.

### 5.16.5.2 Estimated Economic Values:

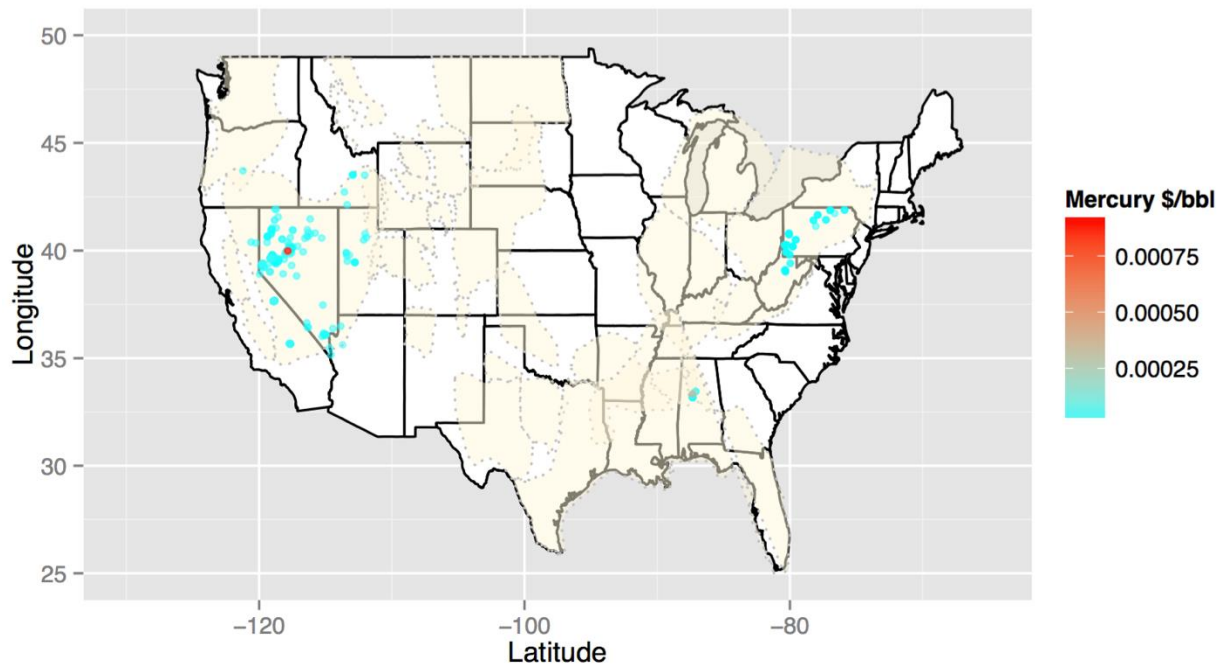


Figure 66: Economic map for mercury identifying highest areas of interest: Nevada.

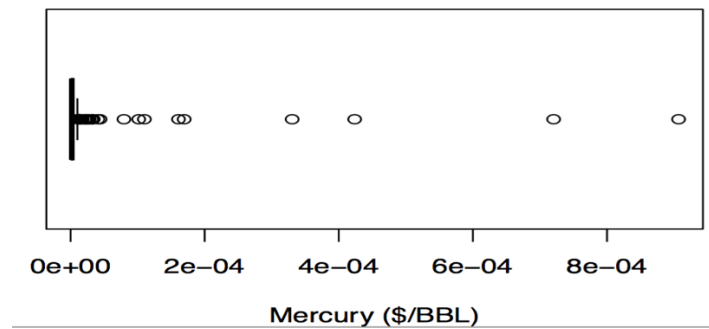


Figure 67: Tukey boxplot of economic values for mercury in produced waters.

The USGS Commodity Minerals Yearbook value for mercury is at \$1850 per flask (\$5.33E-05 per milligram per liter). Given observed concentrations, the value of Hg in produced waters is negligible. Mercury has no potential for development in the United States.

#### **5.16.6 Summary:**

Given its exceptional low value, there is no potential for extraction of mercury from produced waters. Although data gaps are large, the reported values are orders of magnitude needed for economically significant value. However, the spatial concentration data may be useful for ore deposit location identification for other potential elements or commodities. Mercury can be concentrated and removed from produced waters. Experimental tests have demonstrated that through ultrafiltration methods and polymers can concentrate Hg in the permeate for removal.

## **5.17 Molybdenum**

### **Molybdenum (Mo)**

#### **5.17.1 Commodity:**

Molybdenum comes from ore deposits, which are actively mined throughout the world. The United States has 13 molybdenum-producing mines, mainly in the west. Molybdenum is often co-associated with copper. Molybdenum is sought after for alloy production and can often be recycled. However, there is no known secondary separation processes for recovery or refining. The average price in 2014 for molybdenum is \$26.90 per kilogram.

#### **5.17.2 Geochemical Statistics:**

Molybdenum concentrations were examined using two types of plots (Figure 68) including a combination of a histogram, density trace, boxplot, and one-dimensional scatterplot (left side) and Empirical Cumulative Distribution Function (ECDF)-plot (right side) (Reimann et al., 2008). Interpretation of the EDCF-plot (Figure 68) shows variance that indicates sub populations with breaks at 0.05 mg/l and 0.25 mg/l. The density plots, histograms, boxplots and scatterplot suggest that Mo concentration are bimodal and right skewed, even on a log-scale.

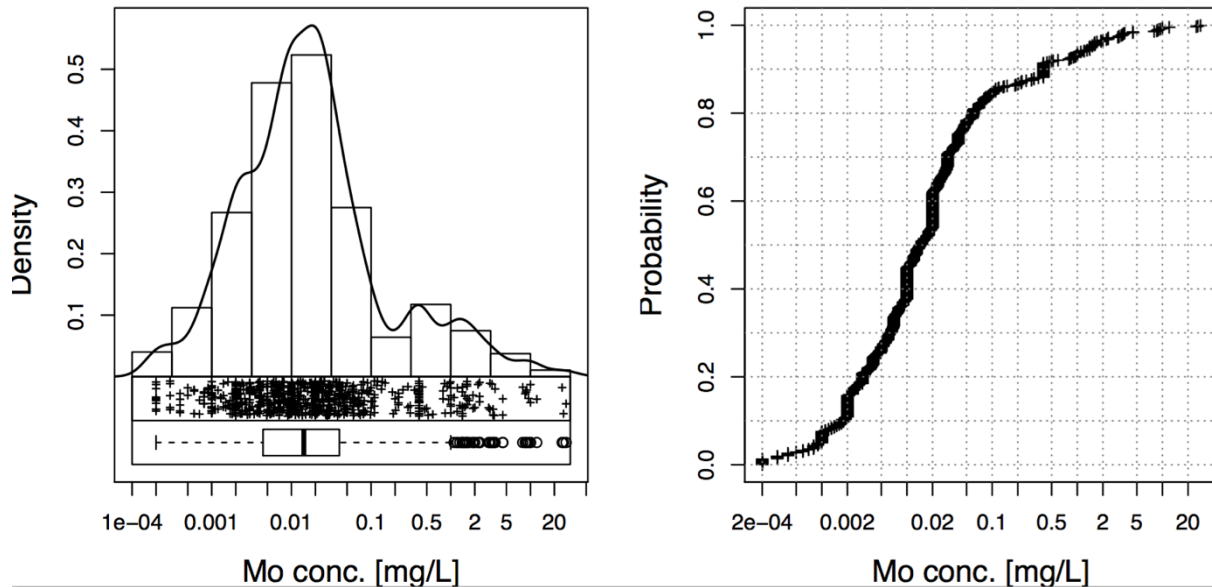


Figure 68: National EDA-plot in log scale, molybdenum concentrations that is left skewed with multiple populations at 0.25 mg/L and 50 mg/L

### 5.17.3 Summary Statistics:

Table 18. Univariate data analysis molybdenum.

	MIN	Q_0.05	Q1	MEDIAN	MEAN_log	MEAN	Q3	Q_0.95	MAX	SD	MAD	pσ	CV %	CVR %
Mo	2.00E-04	0.001	0.0044	0.0143	0.01759	0.3628	0.04	1.4	28	1.98	0.01809	0.02639	545.7	126.5

Calculations were compiled to include: minimum (MIN), 5<sup>th</sup> percentile (Q\_0.05), 25<sup>th</sup> percentile (Q1), median, geometric mean (MEAN\_log), mean, 75<sup>th</sup> percentile (Q3), 95<sup>th</sup> percentile (Q\_0.95), maximum (MAX), standard deviation (SD), pseudosigma (pσ), coefficient of variation (CV), and robust coefficient of variation (CVR).

### 5.17.4 Kendall Tau:

Molybdenum does not positively correlate well with other elements at ( $\tau > 0.6$ ), however at ( $\tau > 0.5$ ), it positively correlates (in descending order) with B ( $\tau = 0.58$ ), Na ( $\tau = 0.57$ ) and Pb ( $\tau = 0.54$ ). There are no constituents that negatively correlated with molybdenum.

## 5.17.5 Maps:

### 5.17.5.1 Spatial Data

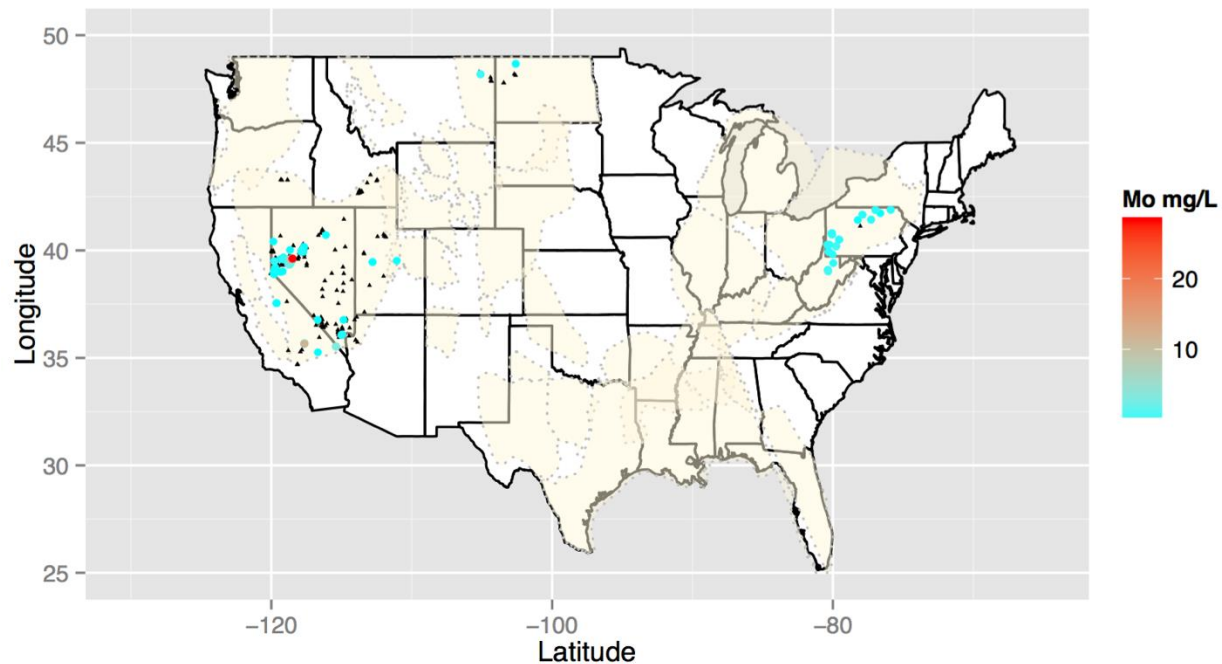


Figure 69: National spatial concentration map for molybdenum. Black triangles identify locations where Mo concentration data exist but are below the 75th percentile. Color ramped symbols applied to the sites where concentrations exceed the 75th percentile.

The spatial coverage for molybdenum is limited so there is potential for exploration. One possible source of elevated molybdenum concentrations is leaching for mineral deposits and hydrothermally altered rocks. A possible secondary source is from ancient seawater; Mo positively correlates with Na and B which are consistent with a seawater origin. It is also noteworthy that salinity of produced waters in Nevada, California and surrounding region (cf. Figure 1) are relatively low. In the produced waters database, there are concentrations greater than 20 mg/L, located in Nevada near copper, molybdenum and silver mineral deposit occurrences. There are moderate concentrations approximately 10 mg/L in the Northern Appalachian Basin also in an area of historic copper mining.

### 5.17.5.2 Estimated Economic Values for Molybdenum

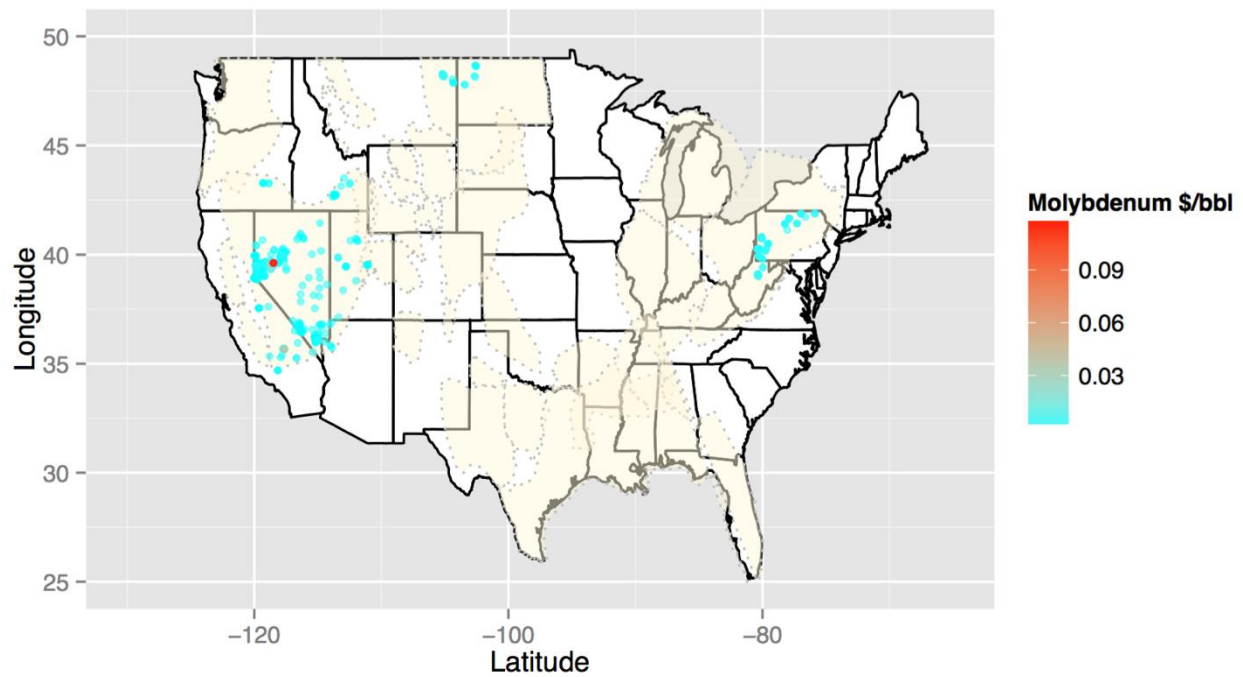


Figure 70: Economic map for molybdenum identifying highest area of interest: Nevada

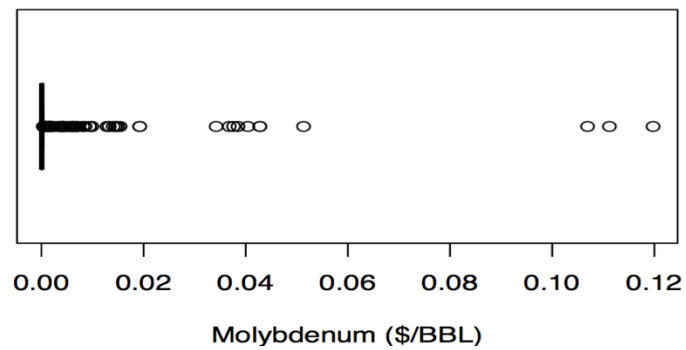


Figure 71: Tukey boxplot of economic values for molybdenum in produced waters.

The estimated economic map (Figure 70) for molybdenum applies the value provide by the USGS Minerals Yearbook in a \$/bbl based on concentration data from the spatial analysis maps.

Molybdenum commodities are valued at \$ 26.90 per kilogram from ore deposits (\$2.69E-05 per milligram per liter). Although molybdenum is available in produced waters, costly separation expenses and relatively low concentrations does not make molybdenum likely for economic production. The commodity does not meet or exceed disposal costs for either region for which data exist, therefore the development for Mo from produced waters is not likely to be economically viable.

#### **5.17.6 Summary:**

Exploration for spatial data is moderate as coverage is sparse, however the development extraction for molybdenum from brines is poor. Molybdenum extraction from traditional ore deposits appears more economic. The spatial data is limited to regions that have higher disposal costs than most regions, thus limiting profitability through extraction methods. Molybdenum can be recovered from secondary processing from ore deposits. Through the use of polymers, it may be applicable to produced waters, further analysis is required and beyond the scope of this thesis.

## **5.18 Nickel**

### **Nickel (Ni)**

#### **5.18.1 Commodity:**

Nickel is mined traditionally from ore deposits. Domestic production has only recently seen a comeback via the underground Eagle Mine in Michigan. Nickel is mined for alloy applications, steel manufacturing and products used in the petroleum industry. The price average for the United States has been withheld for proprietary information, however the London Metal Exchange has listed an average cash value of \$16,863 per metric ton (U.S. Geological Survey, 2015).

#### **5.18.2 Geochemical Statistics:**

Nickel concentrations were examined using two types of plots (Figure 72) that include a combination of a histogram, density trace, boxplot, and one-dimensional scatterplot (left side) and Empirical Cumulative Distribution Function (ECDF)-plot (right side) (Reimann et al., 2008). Interpretation of the EDCF-plot (Figure 72) shows a slight variance indicated by sub populations with breaks near 0.1 mg/L, and 1 mg/L. The density plots, histograms, boxplots and scatterplot suggest that Ni concentration are right skewed, even on a log-scale.

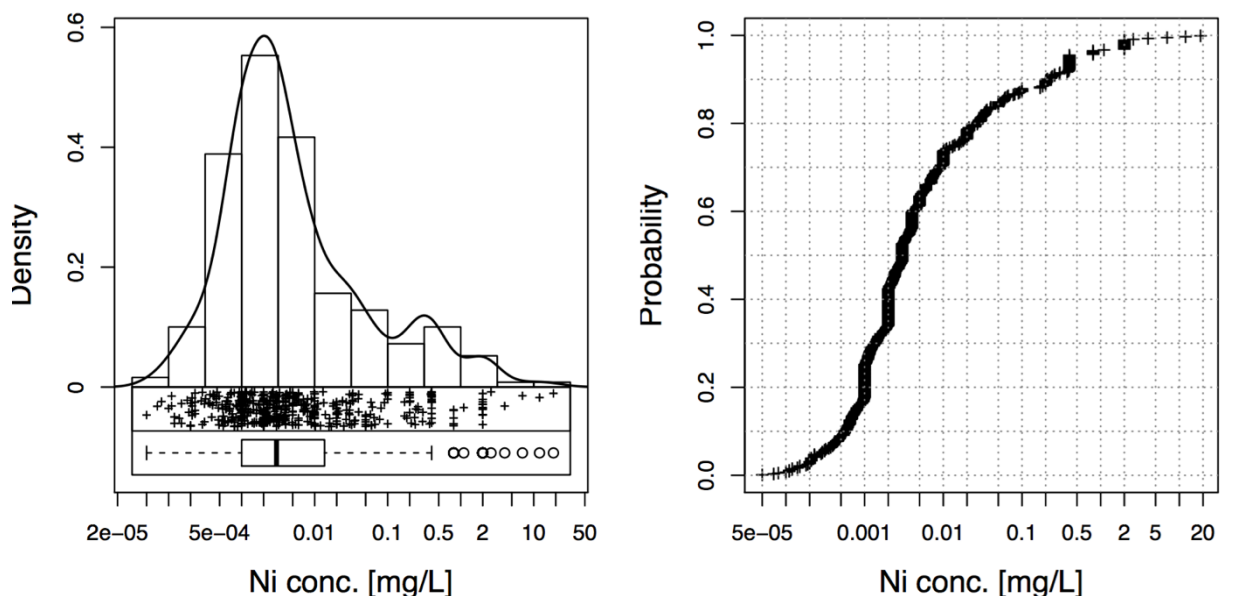


Figure 72: National EDA-plot in log scale, which includes a combination of a histogram, density trace, boxplot, and one-dimensional scatterplot (left side) and Empirical Cumulative Distribution Function (ECDF)-plot (right side). Nickel concentrations are skewed to the right and the graph shows a bimodal distribution.

### 5.18.3 Summary Statistics:

Table 19. Univariate data analysis for nickel.

	MIN	Q_0.05	Q1	MEDIAN	MEAN-log	MEAN	Q3	Q_0.95	MAX	SD	MAD	pσ	CV %	CVR %
Ni	5.00E-05	0.000289	0.001	0.003	0.00519	0.1741	0.01365	0.4	18.6	1.097	0.003366	0.009377	630	112.2

Calculations were compiled to include: minimum (MIN), 5<sup>th</sup> percentile (Q\_0.05), 25<sup>th</sup> percentile (Q1), median, geometric mean (MEAN\_log), mean, 75<sup>th</sup> percentile (Q3), 95<sup>th</sup> percentile (Q\_0.95), maximum (MAX), standard deviation (SD), pseudosigma (pσ), coefficient of variation (CV), and robust coefficient of variation (CVR).

### 5.18.4 Kendall Tau correlation:

In descending order, elements positively correlated ( $\tau > 0.6$ ) with Ni include Co ( $\tau = 0.7$ ), Pb ( $\tau = 0.65$ ), and Be ( $\tau = 0.61$ ). The only constituents negatively correlated with Ni are I ( $\tau = -0.37$ ) and Si ( $\tau = -0.11$ ).



## 5.18.5 Maps:

### 5.18.5.1 Spatial Distribution:

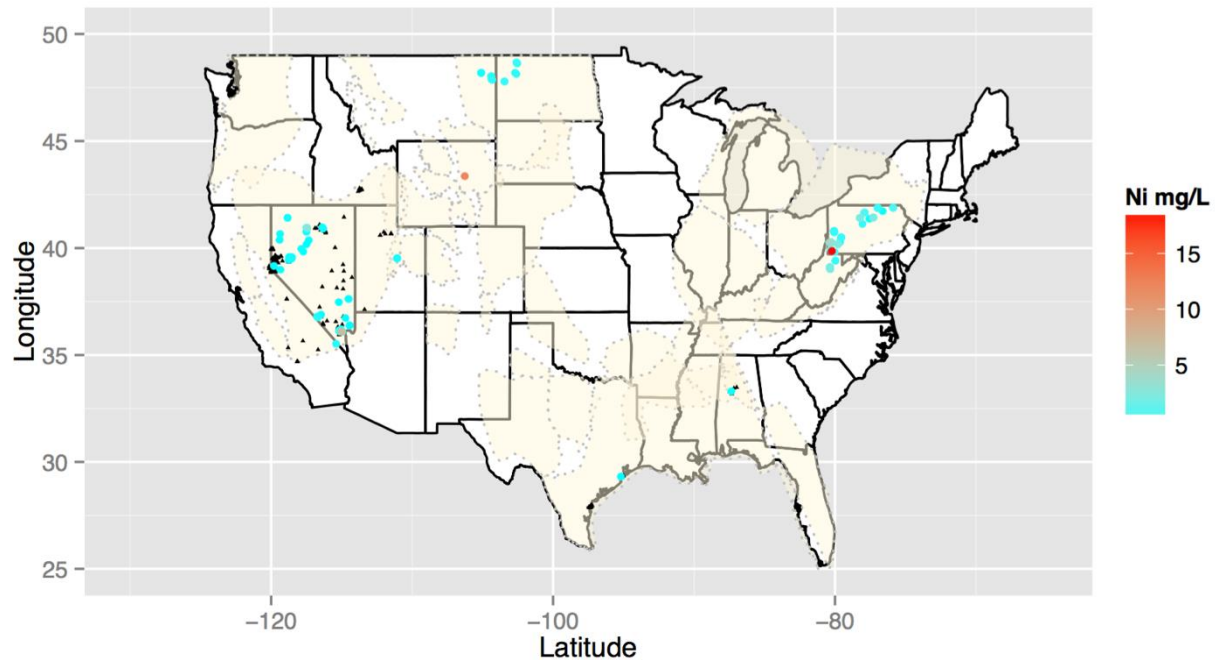


Figure 73: National spatial concentration map for nickel. Black triangles identify locations where Ni concentration data exist but are below the 75th percentile. Color ramped symbols applied to the sites where concentrations exceed the 75th percentile.

Results indicate the highest nickel concentration are found in the central Appalachian Basin, and an anomaly in Powder River Basin. Spatial distribution for nickel is limited, with large data gaps suggesting potential for further exploration. Nickel correlates with other elements found in sulfide minerals, such as lead and cobalt.

### 5.18.5.2 Estimated Economic Values:

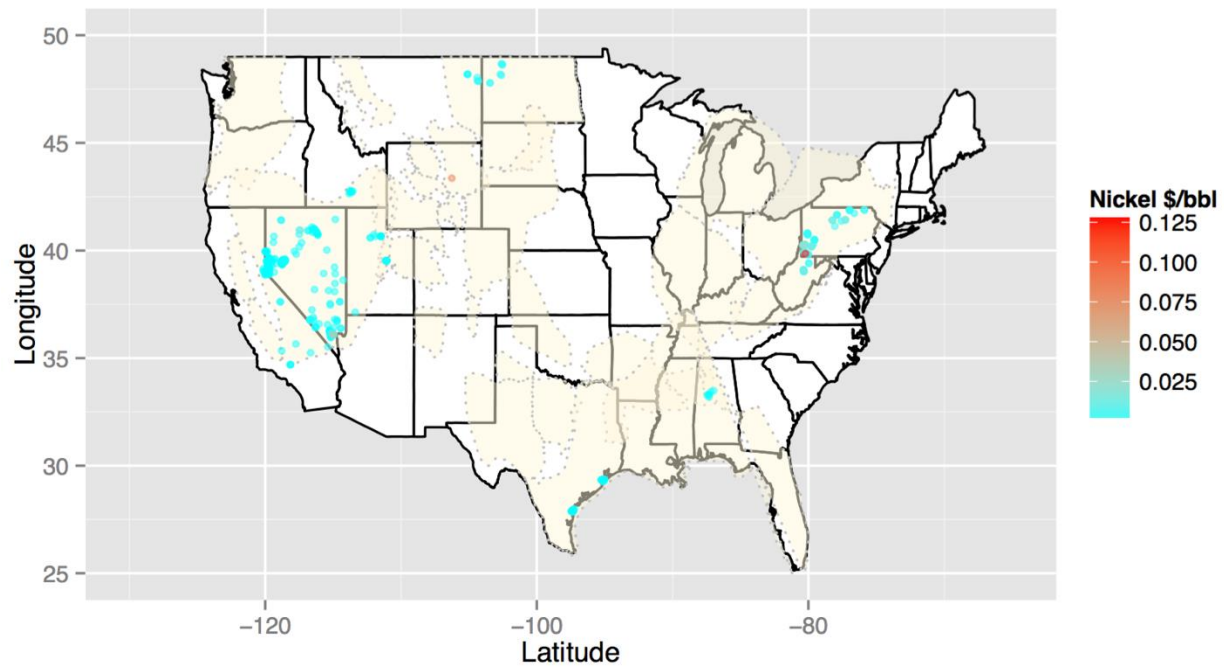


Figure 74: Economic map for nickel identifying highest areas of interest: northern Appalachian Basin.

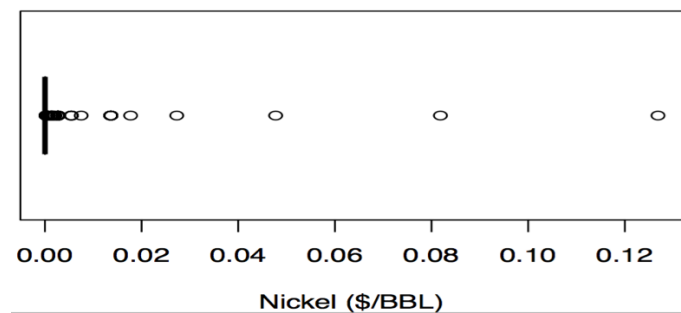


Figure 75: Tukey boxplot of economic values for nickel in produced waters.

Nickel is valued at \$16,863 per metric ton ( $4.29 \times 10^{-5}$  per milligram per liter). Applied to the concentration results shown in Figure 73, none of the areas gross values exceed disposal costs (Figure 74 and 75). Thus the greatest potential for nickel extraction is from co-production with other elements, such as beryllium, cobalt and lead.

**5.18.6 Summary:**

Potential for extraction of nickel from produced waters is limited but it could be co-produced with other commodities. Data coverage is poor and if found at concentrations at least 1 order of magnitude higher than the current range, economically significant quantities may be present. As such, there is moderate potential for further exploration.

## **5.19 Potash**

### **Potash ( $K_2O$ )**

#### **5.19.1 Commodity:**

The USGS Mineral Commodity Summary Report includes potash as a mineral commodity. Potash can be created from potassium (which is a constituent found in produced waters), Potash is largely produced from sylvite and langbeinite ores from underground mines and deep-well solution mining. Sylvite can also be crystalized from brines using solar evaporation or use of a flotation process to separate potassium chloride from byproduct sodium chloride. Potash is used primarily in the agriculture industry for crop and soil amendments. The price value for potash in 2014 is \$350 per metric ton (U.S. Geological Survey, 2015).

#### **5.19.2 Geochemical Statistics:**

Potassium concentrations were examined using two types of plots (Figure 76) that include a combination of a histogram, density trace, boxplot, and one-dimensional scatterplot (left side) and Empirical Cumulative Distribution Function (ECDF)-plot (right side) (Reimann et al., 2008). Interpretation of the EDCF-plot (Figure 76) shows a variance indicated by subpopulations with breaks near 10 mg/L, 1000 mg/L and 25000 mg/L. The density plots, histograms, boxplots and scatterplot suggest that potassium concentration data are multi-modal.

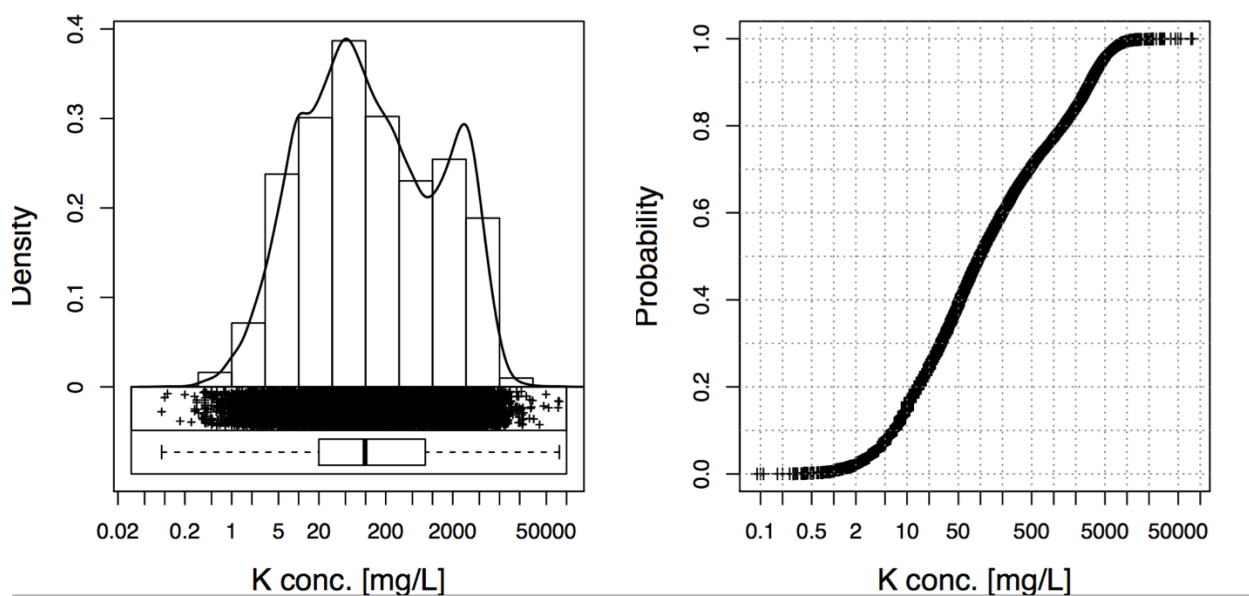


Figure 76: National EDA-plot in log scale, which includes a combination of a histogram, density trace, boxplot, and one-dimensional scatterplot (left side) and Empirical Cumulative Distribution Function (ECDF)-plot (right side). Potassium concentrations are right skewed.

### 5.19.3 Summary Statistics:

Table 20. Univariate data analysis for potassium.

	MIN	Q_0.05	Q1	MEDIAN	MEAN-log	MEAN	Q3	Q_0.95	MAX	SD	MAD	pσ	CV %	CVR %
<b>K</b>	0	3.6	20	98	119.4	922.4	780	4700	78200	2123	136.4	563.4	230.1	139.2

Calculations were compiled to include: minimum (MIN), 5<sup>th</sup> percentile (Q\_0.05), 25<sup>th</sup> percentile (Q1), median, geometric mean (MEAN\_log), mean, 75<sup>th</sup> percentile (Q3), 95<sup>th</sup> percentile (Q\_0.95), maximum (MAX), standard deviation (SD), pseudosigma (pσ), coefficient of variation (CV), and robust coefficient of variation (CVR).

### 5.19.4 Kendall Tau correlation:

In descending order, elements positively correlated ( $\tau > 0.6$ ) with K include Cl ( $\tau = 0.69$ ), Na ( $\tau = 0.67$ ), Li ( $\tau = 0.66$ ), Rb ( $\tau = 0.66$ ), Br ( $\tau = 0.64$ ), and Ca ( $\tau = 0.61$ ). Constituents negatively correlated with K are: S ( $\tau = -0.13$ ), and HCO<sub>3</sub> ( $\tau = -0.19$ ). It is noted that potassium is co-associated with other alkali metals (i.e., Li, Rb, and Na) and elements found in seawater (i.e., Cl, Br, and Ca).

## 5.19.5 Maps:

### 5.19.6.1 Spatial Distribution:

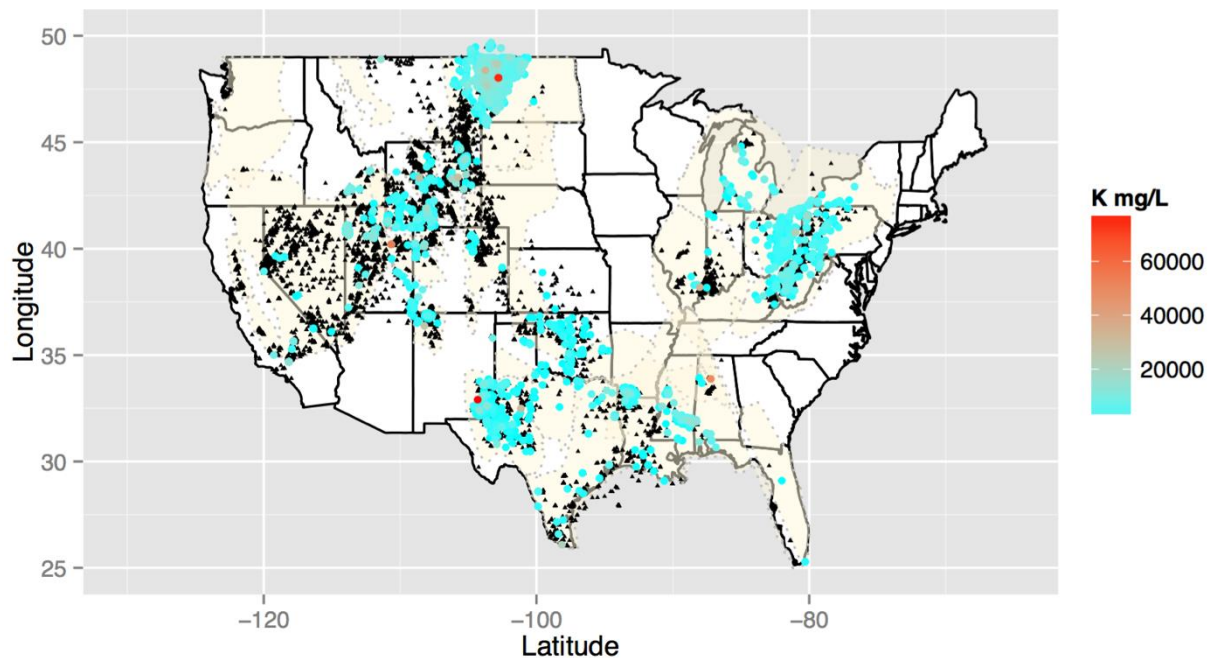


Figure 77: National spatial concentration map for potassium. Black triangles identify locations where K concentration data exist but are below the 75th percentile. Color ramped symbols applied to the sites where concentrations exceed the 75th percentile.

The coverage for potassium is good with few data gaps. The highest concentrations are found in the Black Hills Region (Williston Basin), Rocky Mountain Region (western Delaware Basin), and southern region of the Appalachian Basin (Black Warrior Basin). Moderate concentrations are found throughout the contiguous United States. Exploration for spatial data is low to moderate, exploration in extraction for other potassium based products that is not potash ash is high. Disposal costs will vary from each location (\$0.06-\$10.00) and must be studied in detail prior to any development.

### 5.19.5.2 Estimated Economic Values:

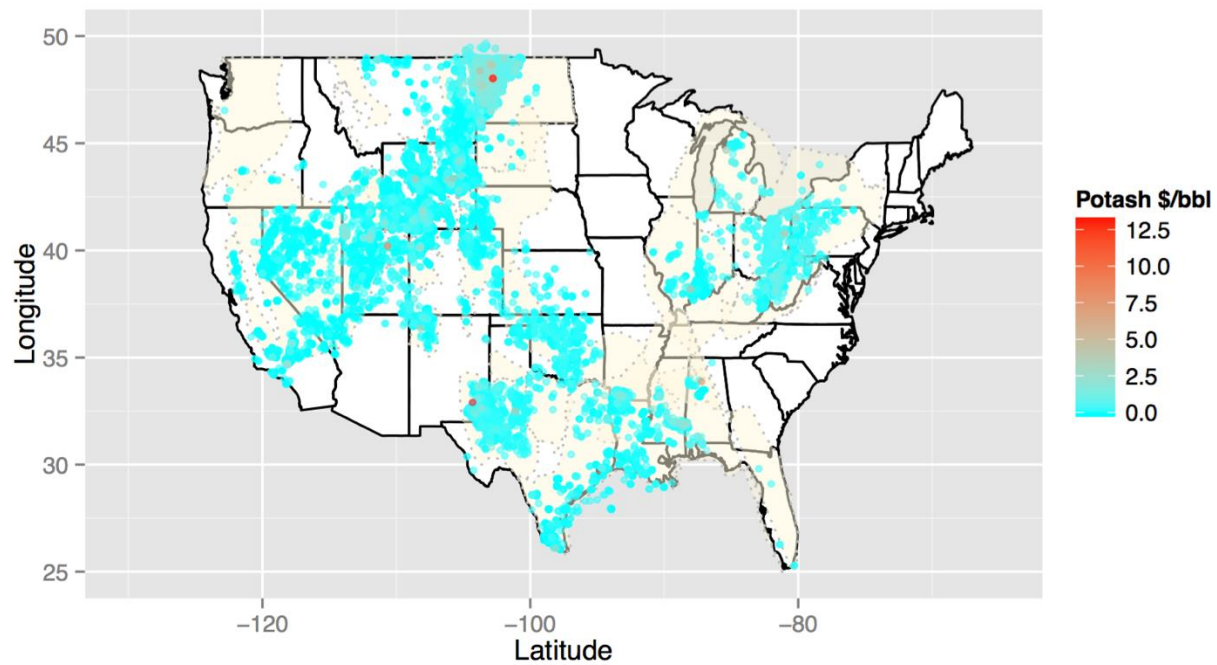


Figure 78: Economic map for potassium identifying highest areas of interest: The Williston and Permian basins.

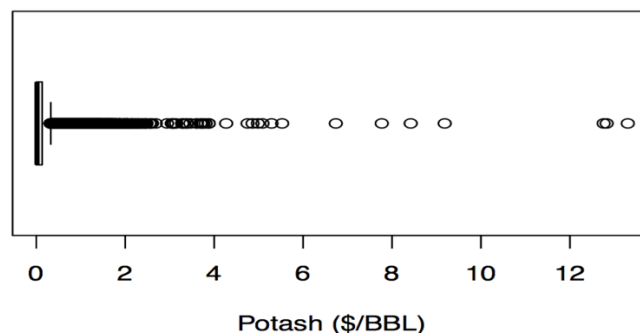


Figure 79: Tukey boxplot of economic values for potash in produced waters.

Potash is valued at \$350 per metric ton ( $1.07\text{E-}06$  per milligram per liter). Applied to the concentration results shown in Figure 77, there is potential for further development (Figures 78 and 79). Continuous improvements to methodology and technology could drive production from

produced waters for revenue as opposed to disposing. Potash is currently extracted during deep-well solution mining of evaporite minerals and potassium chloride can be precipitated out during evaporation of brines as a byproduct, and could be considered as an additional commodity that is not identified as a commodity in the USGS Minerals Commodity Yearbook. The potential to expand is high. Overall, producing potassium commodity products should be considered for potential in all regions as the value can exceed disposal costs.

#### **5.19.6 Summary:**

The extraction potential is moderate to high for development in produced waters for potash and other potassium based products. To increase revenue from the identified high concentrated regions, K could be combined with other commodities such as bromine, iodine, and lithium. Caution should be adhered to the market as to not increase supply so much that a stockpile increase exceeds demand and lowers the product commodity value. Market supply and demand needs to be analyzed, if all regions begin production simultaneously there is potential to drop the price of the commodity. As the data coverage is good, potential for further exploration is low.

## **5.20 Rubidium**

### **Rubidium (Rb)**

#### **5.20.1 Commodity:**

Rubidium is not actively mined in the United States. However, rubidium is associated with evaporite minerals and is concentrated in some brines. Rubidium is primarily imported for manufacturing to the United States. Rubidium-bearing products used in the biomedical field for treatments for thyroid cancer, electronics, specialty glass and fiber optics. Rubidium is not actively traded, but 2014 prices for 10-gram ampoules of rubidium formate hydrate and rubidium chloride were \$55.10 and \$209, respectively (U.S. Geological Survey, 2015).

#### **5.20.2 Geochemical Statistics:**

Rubidium concentrations were examined using two types of plots (Figure 80) that include a combination of a histogram, density trace, boxplot, and one-dimensional scatterplot (left side) and Empirical Cumulative Distribution Function (ECDF)-plot (right side) (Reimann et al., 2008). Interpretation of the ECDF-plot (Figure 80) shows a bimodal distribution. The variance indicated by sub populations with breaks near 3 mg/L. The density plots, histograms, boxplots and scatterplot suggest that Rb concentrations are slightly right skewed, on a log-scale.

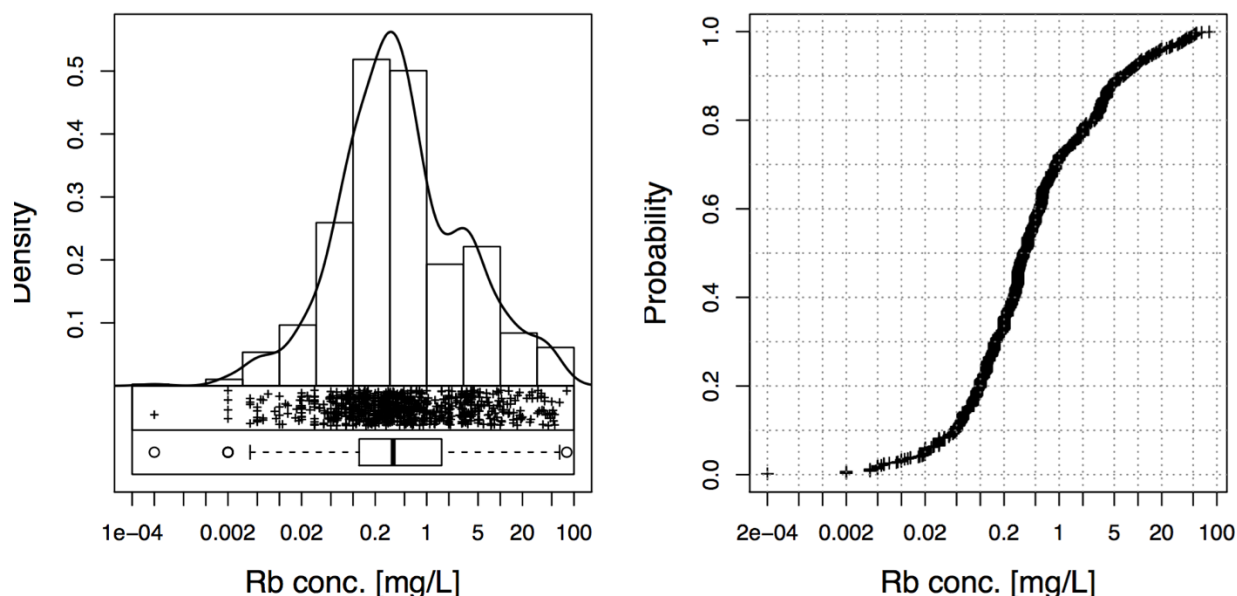


Figure 80: National EDA-plot in log scale, which includes a combination of a histogram, density trace, boxplot, and one-dimensional scatterplot (left side) and Empirical Cumulative Distribution Function (ECDF)-plot (right side). Rubidium concentrations are left skewed.

### 5.20.3 Summary Statistics:

Table 21. Univariate data analysis for rubidium.

	MIN	Q_0.05	Q1	MEDIAN	MEAN_log	MEAN	Q3	Q_0.95	MAX	SD	MAD	pσ	CV %	CVR %
<b>Rb</b>	0	0.02	0.121	0.3505	0.4399	3.03	1.6	15.65	80	8.539	0.4159	1.096	281.8	118.7

Calculations were compiled to include: minimum (MIN), 5<sup>th</sup> percentile (Q\_0.05), 25<sup>th</sup> percentile (Q1), median, geometric mean (MEAN\_log), mean, 75<sup>th</sup> percentile (Q3), 95<sup>th</sup> percentile (Q\_0.95), maximum (MAX), standard deviation (SD), pseudosigma (pσ), coefficient of variation (CV), and robust coefficient of variation (CVR).

### 5.20.4 Kendall Tau correlation:

In descending order, elements positively correlated ( $\tau > 0.6$ ) with Rb include K ( $\tau = 0.66$ ), Li ( $\tau = 0.64$ ), and Se ( $\tau = 0.64$ ). The only constituent that negatively correlates with Rb is HCO<sub>3</sub> ( $\tau = -0.2$ ).

## 5.20.5 Maps:

### 5.20.5.1 Spatial Distribution:

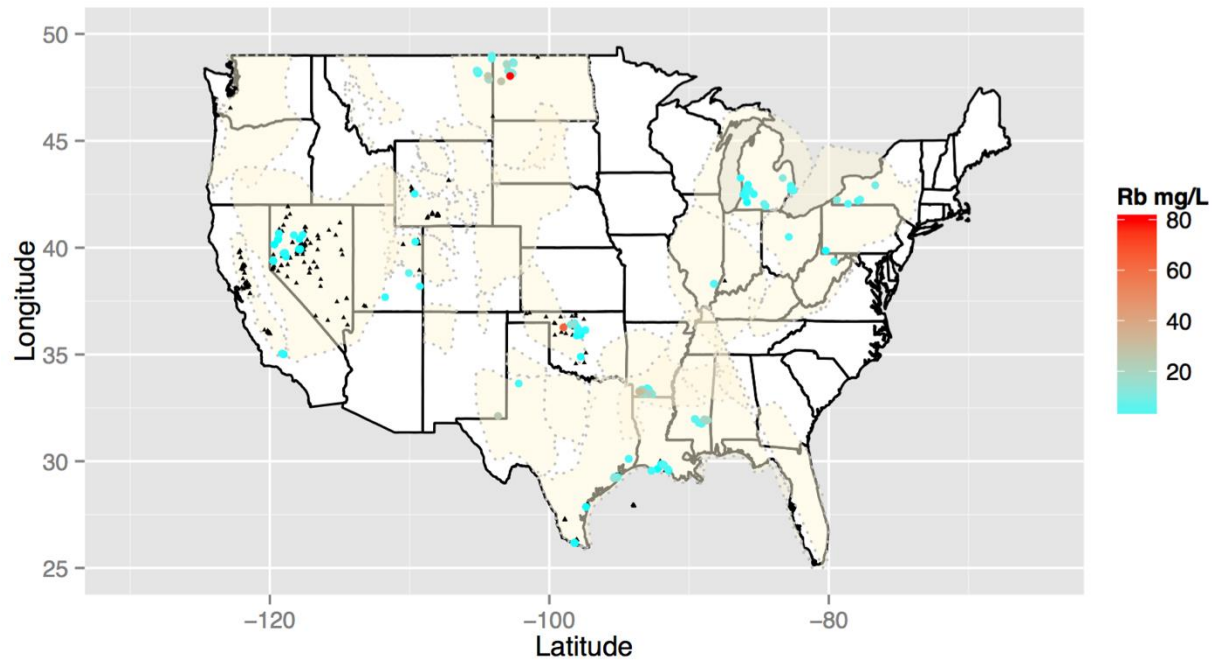


Figure 81: National spatial concentration map for rubidium. Black triangles identify locations where Rb concentration data exist but are below the 75th percentile. Color ramped symbols applied to the sites where concentrations exceed the 75th percentile.

The coverage for rubidium is sparse, with sizeable data gaps resulting in high potential for data exploration. The highest concentrations are found in the Williston and Anadarko Basins. The disposal costs for both areas are moderate and may impact profit potential.

### 5.20.5.2 Estimated Economic Values:

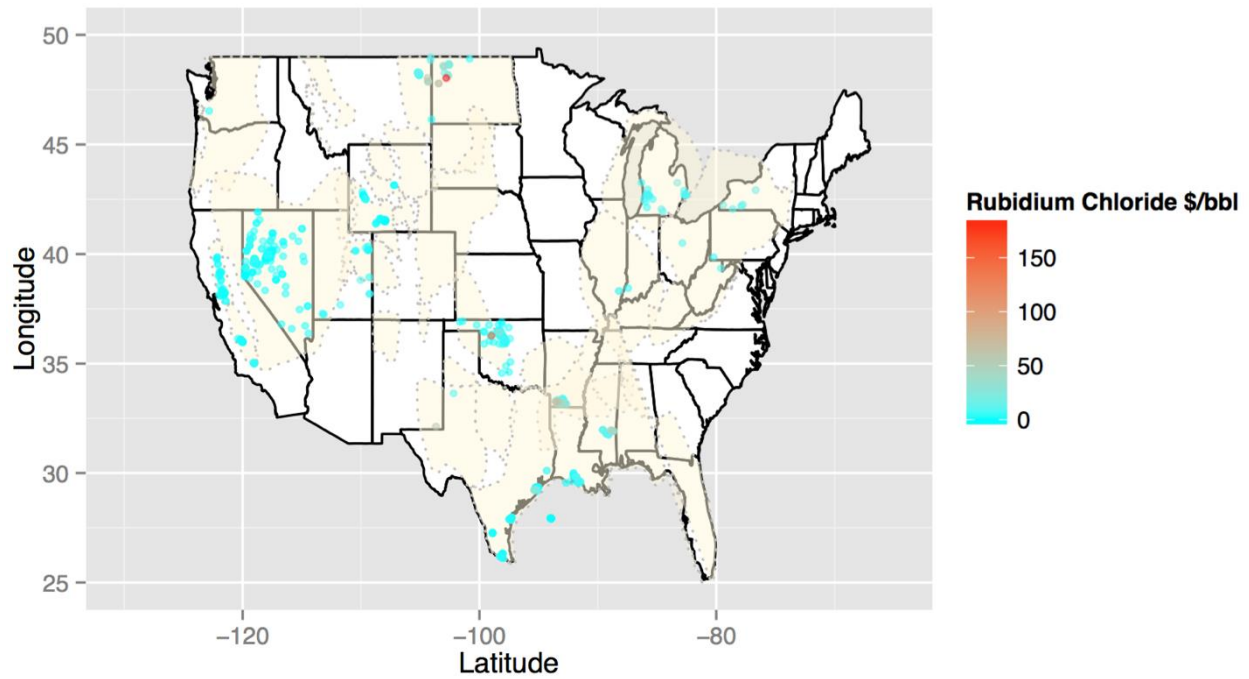


Figure 82: Economic map for rubidium chloride identifying areas of highest interest: The Anadarko Basin, the Gulf Coast Basin and the Western Region.

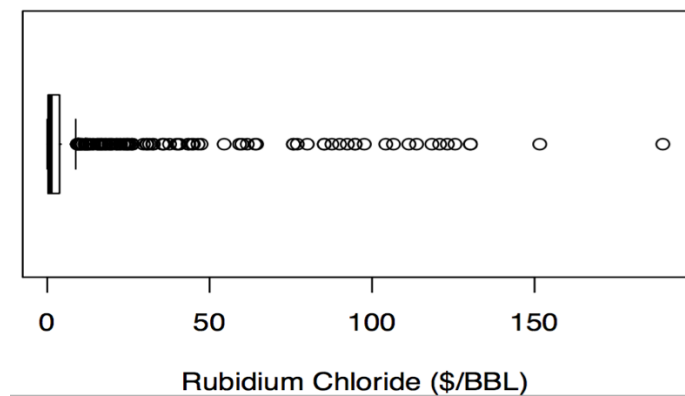


Figure 83: Tukey boxplot of economic values for rubidium chloride in produced waters.

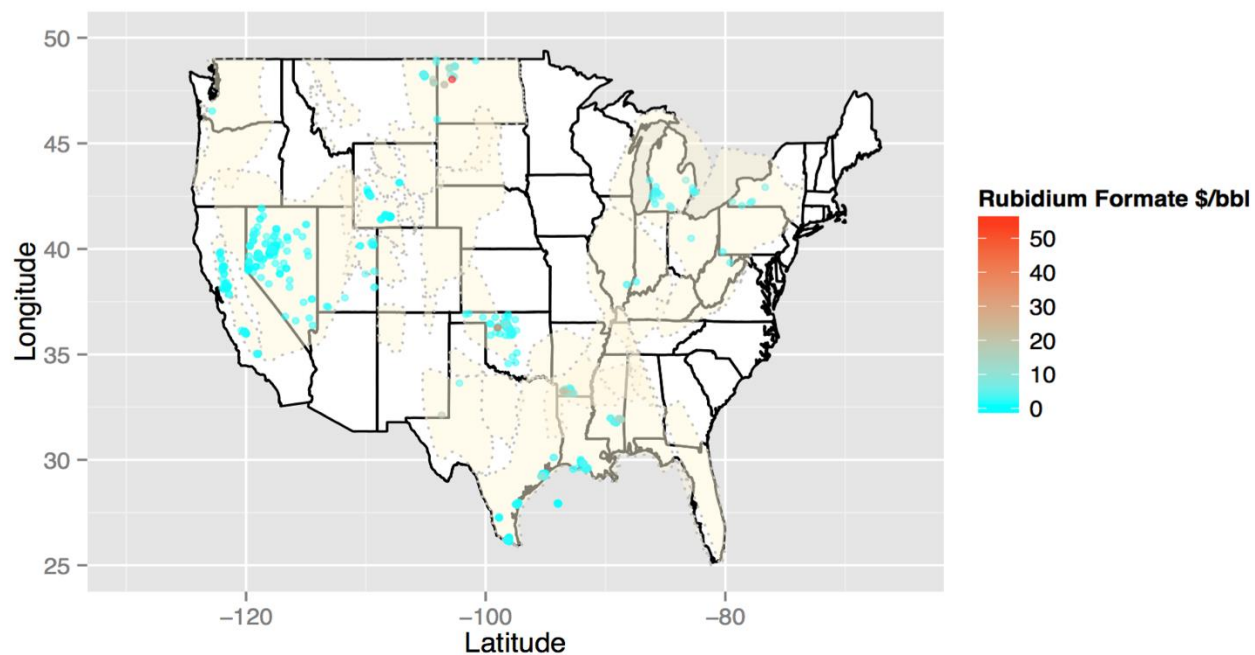


Figure 84: Economic for rubidium formate identifying areas of highest interest: the Anadarko Basin, the Gulf Coast Basin and the Western Region.

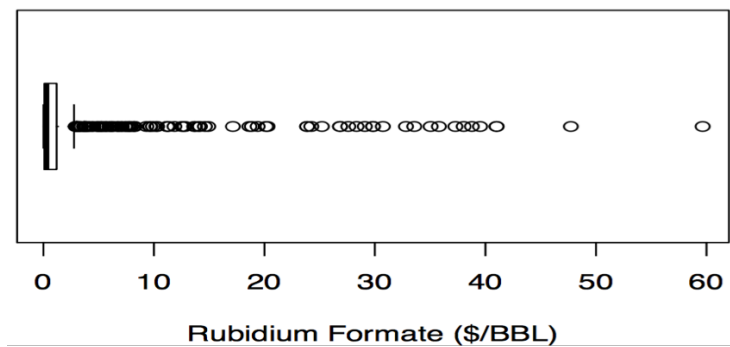


Figure 85: Tukey boxplot of economic values for rubidium formate in produced waters.

Rubidium is an identified commodity but is not actively traded on the open market. Rubidium has two marketable products, rubidium formate and rubidium chloride. Pricing in 2014 for 10-gram ampoules for rubidium formate was \$55.10 (\$4.60E-03 per milligram per liter) and rubidium chloride was \$209 (\$1.49E-02 per milligram per liter). Rubidium has high potential for development in commodity extraction. When values are applied to the concentration results shown in Figure 81, even considering a moderate value of \$10.00/bbl for both rubidium formate or rubidium chloride, the profit potential exceeds disposal costs (Figures 82-85).

#### **5.20.6 Summary:**

Upper economic values for rubidium in produced waters are quite high, suggesting a high potential for extraction. Moreover, incomplete data coverage with large gaps suggests potential for exploration is also high. To increase revenue from the identified high concentrated regions, Rb should be combined with other commodities such as cesium (Figure 24) and/or lithium (Figure 51). To be successful in the market with Rb there needs to be a change in commodity acquisitions; currently Rb is only imported in the United States and could be developed in country.

## **5.21 Salt**

### **Salt (NaCl)**

#### **5.21.1 Commodity:**

Sodium is used here as a proxy for salt (halite), as sodium is typically the limiting constituent in producing salt from produced waters. Products which require salt are numerous. Specific applications include building and construction materials, medicinal purposes, de-icing road treatments and water desalination. To take a conservative approach, economic values will be assumed using the lowest quality salt at \$8.49 per metric ton. High purity salt can sell for significantly high values.

#### **5.21.2 Geochemical Statistics:**

Sodium concentrations were examined using two types of plots (Figure 86) that include a combination of a histogram, density trace, boxplot, and one-dimensional scatterplot (left side) and Empirical Cumulative Distribution Function (ECDF)-plot (right side) (Reimann et al., 2008). Interpretation of the EDCF-plot (Figure 86) has a progressive distribution and shows a variance indicated by subpopulations with breaks near 1000 mg/L and 9000 mg/L. The density plots, histograms, boxplots and scatterplot suggest that Na concentration are heavily left skewed, on a log-scale.

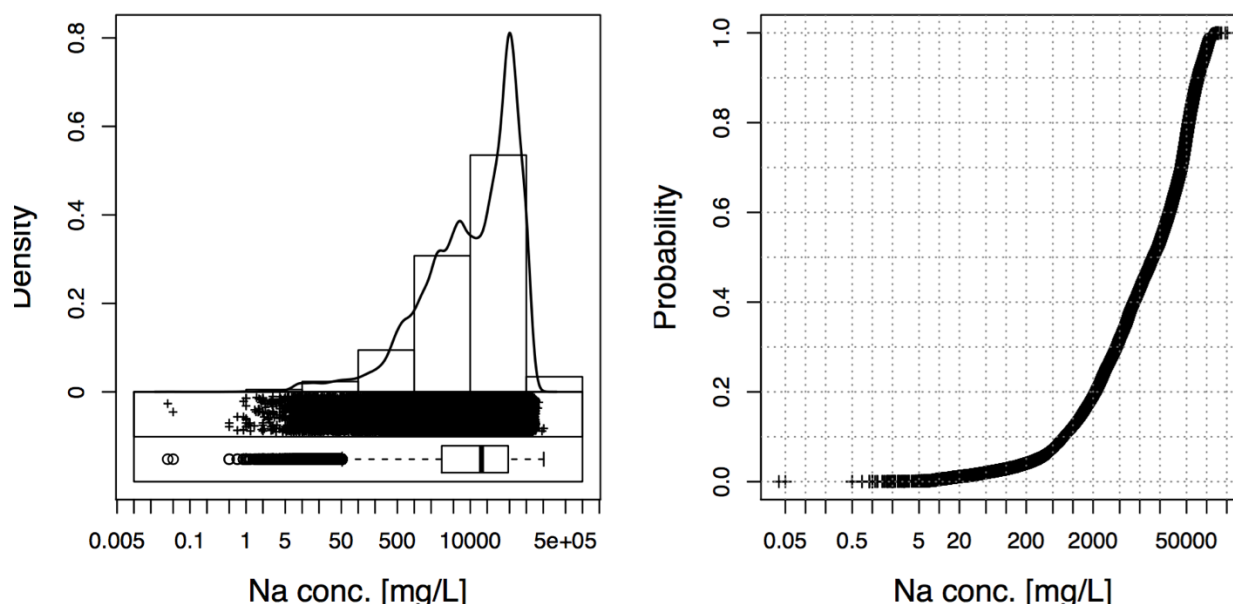


Figure 86: National EDA-plot in log scale, which includes a combination of a histogram, density trace, boxplot, and one-dimensional scatterplot (left side) and Empirical Cumulative Distribution Function-plot (right side). Sodium concentrations are left skewed and the graph shows a multiple distribution.

### 5.21.3 Summary Statistics:

Table 22. Univariate data analysis for sodium.

	MIN	Q_0.05	Q1	MEDIAN	MEAN -log	MEAN	Q3	Q_0.95	MAX	SD	MAD	pσ	CV %	CVR %
Na	0.04	292	3096	15810	10000	28360	47470	93200	204300	30360	21950	32900	107.1	138.8

Calculations were compiled to include: minimum (MIN), 5<sup>th</sup> percentile (Q\_0.05), 25<sup>th</sup> percentile (Q1), median, geometric mean (MEAN\_log), mean, 75<sup>th</sup> percentile (Q3), 95<sup>th</sup> percentile (Q\_0.95), maximum (MAX), standard deviation (SD), pseudosigma (pσ), coefficient of variation (CV), and robust coefficient of variation (CVR).

### 5.21.4 Kendall Tau correlation:

In descending order, elements positively correlated ( $\tau > 0.6$ ) with Na include Cl ( $\tau = 0.9$ ), K ( $\tau = 0.67$ ), Br ( $\tau = 0.66$ ), Ca ( $\tau = 0.65$ ), Sr ( $\tau = 0.63$ ), Li ( $\tau = 0.61$ ), and Mg ( $\tau = 0.61$ ). Constituents negatively correlated with Na are: is: HCO<sub>3</sub> ( $\tau = -0.35$ ), Hg ( $\tau = -0.15$ ), S ( $\tau = -0.23$ ), and Si ( $\tau = -0.12$ ).

## 5.21.5 Maps:

### 5.21.5.1 Spatial Distribution:

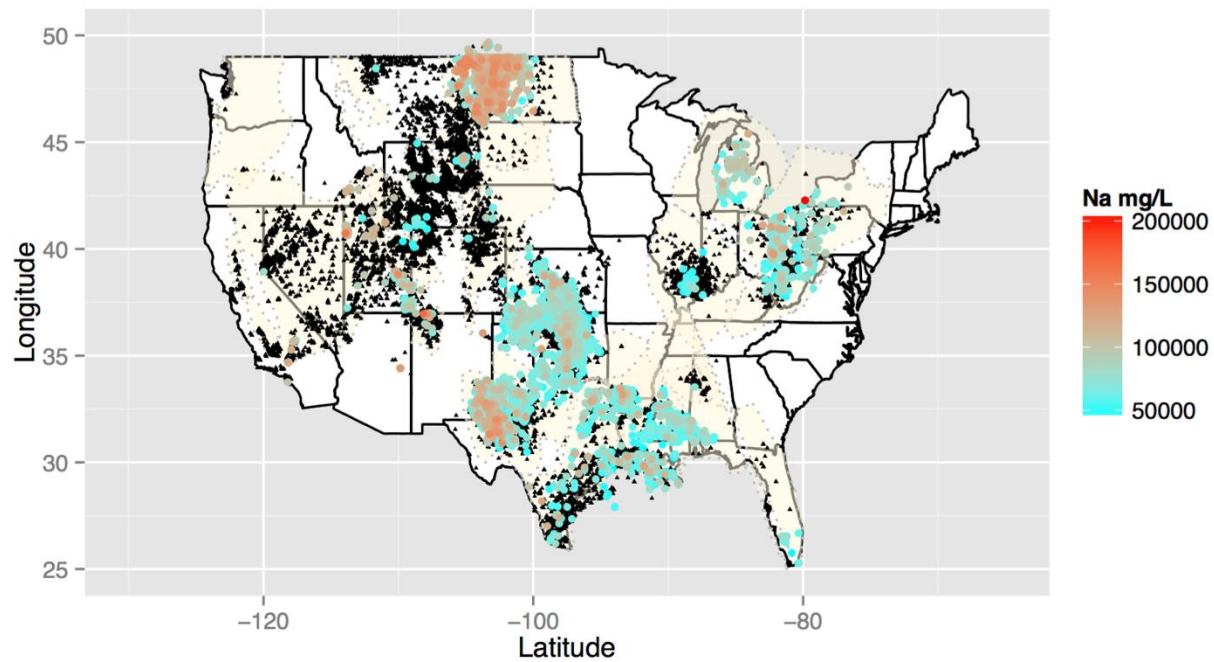


Figure 87: National spatial concentration map for sodium. Black triangles identify locations where Na concentration data exist but are below the 75th percentile. Color ramped symbols applied to the sites where concentrations exceed the 75th percentile.

The coverage for sodium concentration is very good, with minimal data gaps. Sodium concentrations are proportional to TDS concentrations (Figure 1). In some basins, Na concentration levels exceed 200 g/L. With such high concentrations, the potential for extraction is interminable. Particular regions with higher disposal costs still present opportunity to generate profit if a detailed economic analysis is completed to correlate compare product demand against available supply. Careful consideration must be applied as to not over stimulate products thus ultimately driving the product value down.

### 5.21.5.2 Estimated Economic Values:

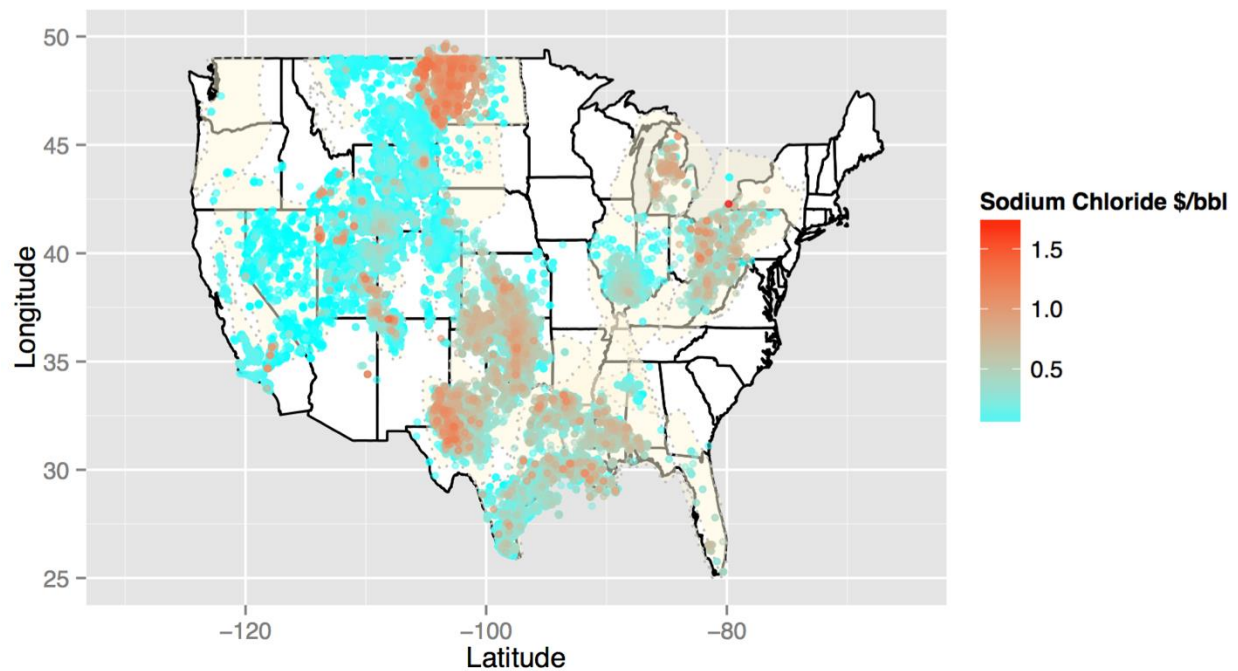


Figure 88: Economic map for salt identifying highest areas of interest: Permian, Anadarko, Williston, Appalachian, Michigan and Gulf Coast basins.

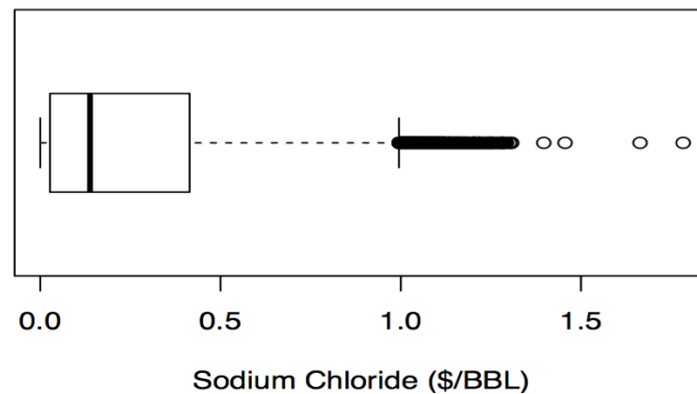


Figure 89: Tukey boxplot of economic values for sodium chloride in produced waters.

Sodium chloride is valued at \$8.49 per metric ton ( $5.49 \times 10^{-8}$  per milligram of Na per liter).

Applied to the concentration results shown in Figure 88, areas are nearly boundless for potential

development (Figures 88 and 89). Continuous improvements in salt production from produced waters are being made suggesting brines as a viable source.

#### **5.21.6 Summary:**

There is little potential for data exploration of sodium as the current coverage is extensive with few data gaps. Extraction of salt from produced waters is potentially a profitable venue, especially when combined with the extraction of other commodities such as bromine, magnesium and lithium. When salt is combined with other commodities, the revenue potential increases with little addition disposal cost. Caution should be adhered when looking to increase salt production from other regions and impacts of seasonal demand may be important for regions like the Central Midwest. The commodity is of moderate value, however long distance shipping costs could dampen potential profit. Market supply and demand needs to be analyzed, if all regions begin producing salt simultaneously there is potential to drop the price of the commodity.

## 5.22 Soda Ash

### Soda Ash ( $\text{Na}_2\text{CO}_3$ )

#### 5.22.1 Commodity:

Soda ash or sodium carbonate is produced in the United States, primarily through solution mining in Wyoming. The sum of carbonate plus bicarbonate (on a carbonate basis), referred to here as gross carbonate ( $\text{gCO}_3$ ) is used as a proxy for soda ash, as  $\text{gCO}_3$  is typically the limiting constituent in producing soda ash from produced waters. Soda ash is used in glass, soaps, detergents and fertilizer manufacturing. Current pricing for soda ash as of 2014 was \$290 per short ton. The demand and consumption rates are expected to continue (U.S. Geological Survey, 2015).

#### 5.22.2 Geochemical Statistics:

Sodium concentrations were examined using two types of plots (Figure 90) that include a combination of a histogram, density trace, boxplot, and one-dimensional scatterplot (left side) and Empirical Cumulative Distribution Function (ECDF)-plot (right side) (Reimann et al., 2008). The EDCF-plot (Figure 90) shows a near normal distribution. The density plots, histograms, boxplots and scatterplot suggest that  $\text{gCO}_3$  concentration are slightly left skewed, on a log-scale.

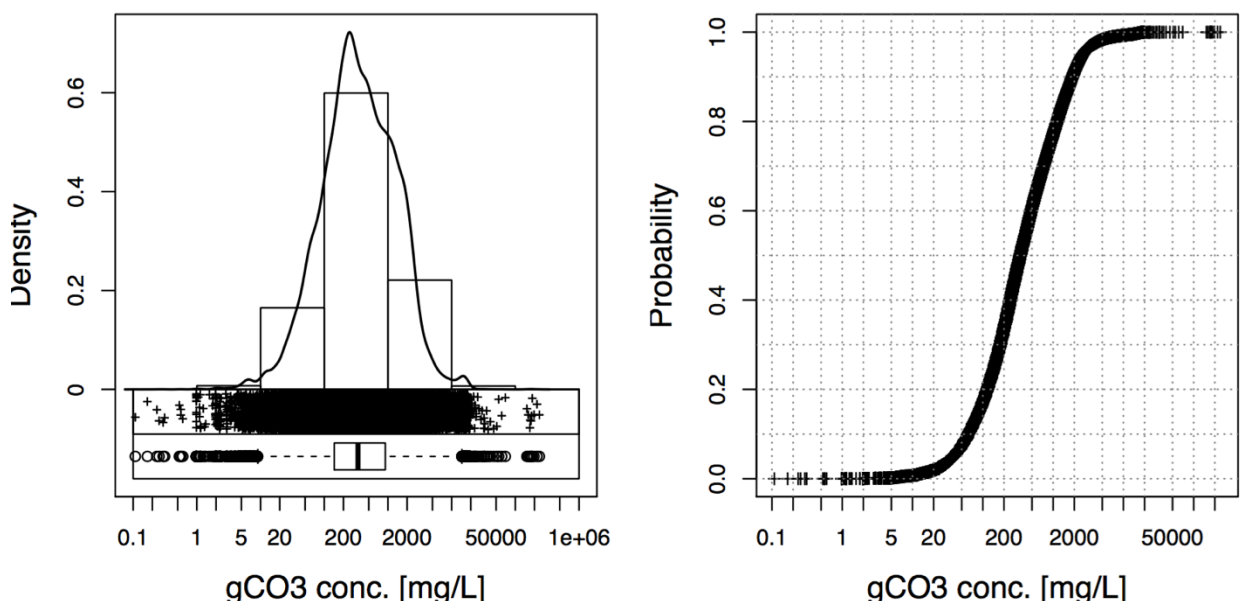


Figure 90: National EDA-plot in log scale, which includes a combination of a histogram, density trace, boxplot, and one-dimensional scatterplot (left side) and Empirical Cumulative Distribution Function (ECDF)-plot (right side). Sodium concentrations are left skewed.

### 5.22.3 Summary Statistics:

Table 23. Univariate data analysis for gross carbonate.

	MIN	Q_0.05	Q1	MEDIAN	MEAN -log	MEAN	Q3	Q_0.95	MAX	SD	MAD	pσ	CV %	CVR %
gCO <sub>3</sub>	0.1082	37.78	143.6	339.3	344.7	832.1	909.8	2639	238600	2604	373.2	568	313	110

Calculations were compiled to include: minimum (MIN), 5<sup>th</sup> percentile (Q\_0.05), 25<sup>th</sup> percentile (Q1), median, geometric mean (MEAN\_log), mean, 75<sup>th</sup> percentile (Q3), 95<sup>th</sup> percentile (Q\_0.95), maximum (MAX), standard deviation (SD), pseudosigma (pσ), coefficient of variation (CV), and robust coefficient of variation (CVR).

### 5.22.4 Kendall Tau correlation:

The gross carbonate values do not positively correlate with other elements at or near ( $\tau > 0.6$ ). Constituents negatively correlated with gCO<sub>3</sub> are: Br ( $\tau = -0.47$ ), Mg ( $\tau = -0.44$ ), Na ( $\tau = -0.35$ ), Cl ( $\tau = -0.38$ ), Sr ( $\tau = -0.31$ ), Be ( $\tau = -0.28$ ), Rb ( $\tau = -0.21$ ), K ( $\tau = -0.19$ ), Ba ( $\tau = -0.13$ ), Li ( $\tau = -0.12$ ), Mn ( $\tau = -0.09$ ), Cs ( $\tau = -0.02$ ), and Hg ( $\tau = -0.02$ ).

## 5.22.5 Maps:

### 5.22.5.1 Spatial Distribution:

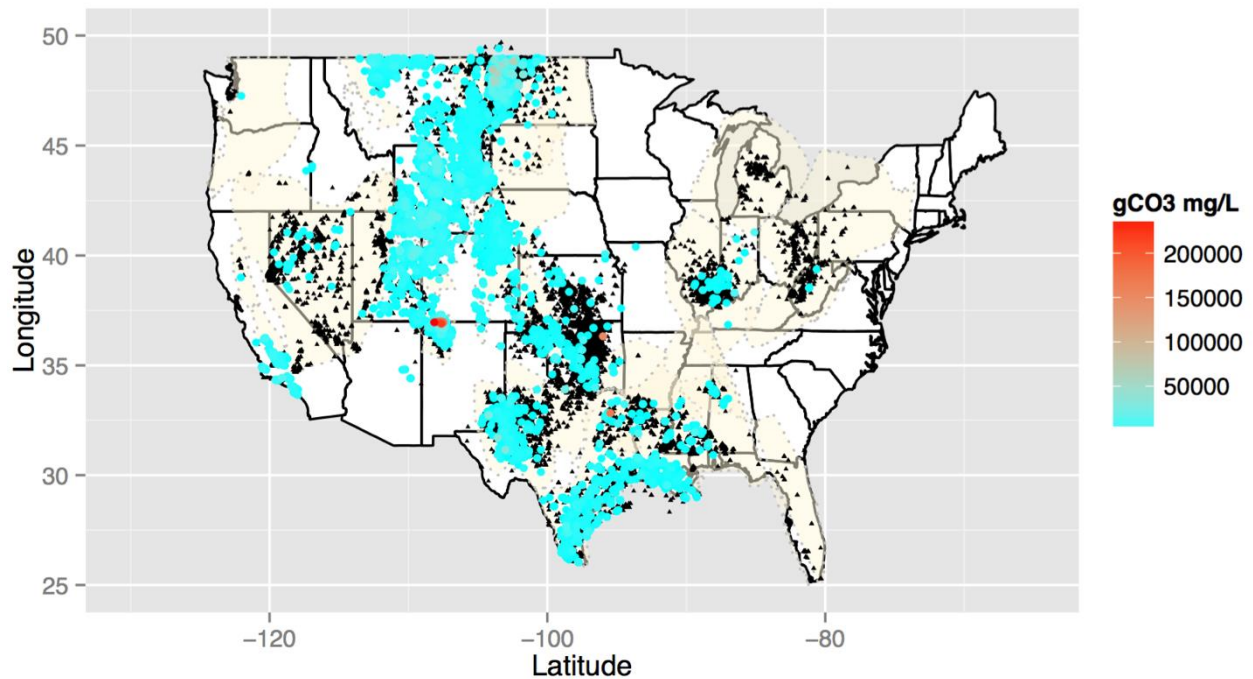


Figure 91: National spatial concentration map for total available carbonate. Black triangles identify locations where Na concentration data exist but are below the 75th percentile. Color ramped symbols applied to the sites where concentrations exceed the 75th percentile.

The data coverage for gCO<sub>3</sub> concentration in produced waters is good (Figure 91). For this reason, potential for exploration is relatively low. Concentrations exceeding 50,000 mg/L can be located in many basins. The highest concentrations are found in the Williston Basin, parts of the central Midwest and the Gulf Coast Basin. Disposal costs range from \$.20 to \$10.00 per barrel per liter throughout the identified regions.

### 5.22.5.2 Estimated Economic Values:

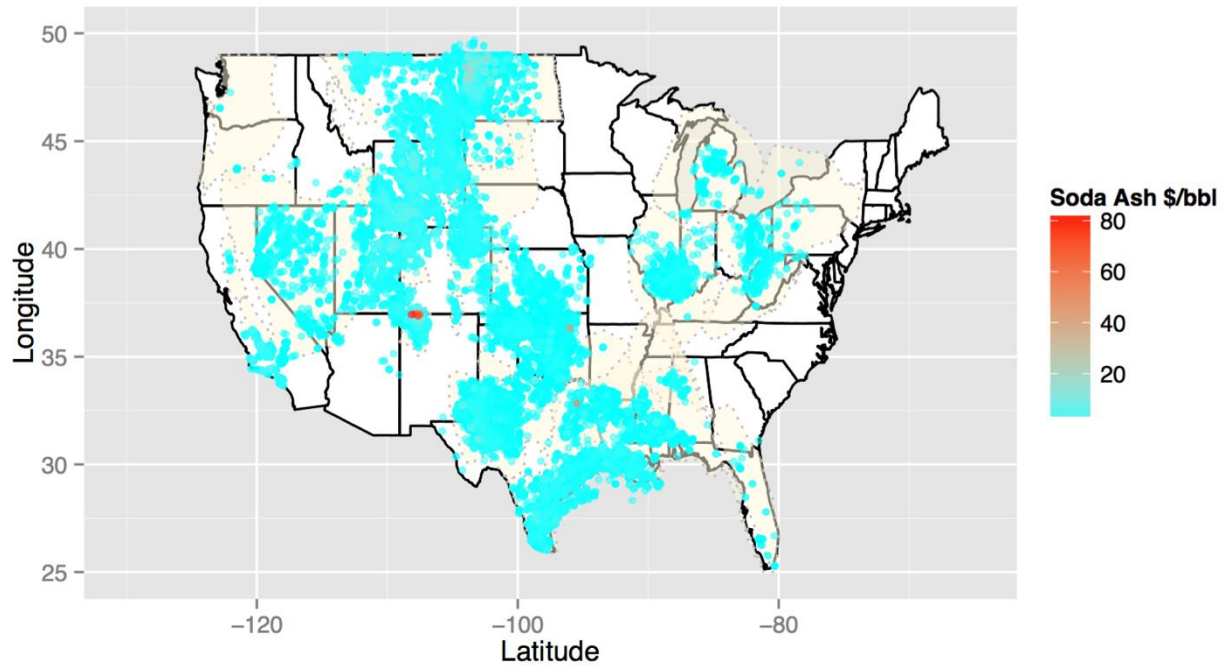


Figure 92: Economic map for soda ash identifying highest areas of interest: Anadarko Basin, Appalachian Basin, Gulf Coast Basin, Permian Basin, San Juan Basin and Williston Basin.

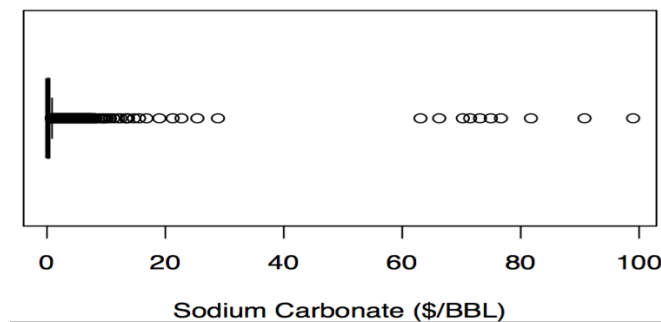


Figure 93: Tukey boxplot of economic values for sodium carbonate in produced waters.

Sodium carbonate is an identified commodity that is actively produced through solution mining. Soda Ash products have a wide range of end uses, with an expected continuation of growth and the potential value in produced water, may be used as an additional source. Pricing in 2014

for a short ton of sodium carbonate was \$290 (\$7.39E-07 per milligram per liter). Results suggest there is moderate potential for further development and in many regions; soda ash values exceed local disposal costs (Figures 92 and 93). There is also a possibility in capturing CO<sub>2</sub> and converting it to soda ash from CO<sub>2</sub> flooding projects. Overall, producing sodium carbonate commodity products should be considered for potential. Development potential is moderate; a comparative analysis needs to be completed to determine if solution mining is still more economical than recovery from brines

#### **5.22.6 Summary:**

The development potential in produced waters for soda ash has moderate potential for expansion. Despite the relatively high net worth, the nearly pervasive data coverage suggests there is little potential for exploration. Soda ash production may be included with production for other sodium based products to reduce overall production costs, but may not be necessary as many regions can exceed \$10/bbl. Other constituents that correlate well with Na, might allow for co-extraction to increase revenues. Caution should be adhered to the market as to not increase supply so much that a stockpile increase exceeds demand and lowers the product commodity value. Market supply and demand needs to be analyzed, if all regions begin production simultaneously there is potential to drop the price of the commodity.

## 5.23 Strontium

### Strontium (Sr):

#### 5.23.1 Commodity:

Strontium is primarily imported; production in the United States ceased in 2006. Some end uses for strontium compounds are magnets, alloys and drilling fluids for oil and gas production. Strontium is currently priced at import value of \$50.00 per metric ton and is expected to increase (U.S. Geological Survey, 2015).

#### 5.23.2 Geochemical Statistics:

Strontium concentrations were examined using two types of plots (Figure 94) that include a combination of a histogram, density trace, boxplot, and one-dimensional scatterplot (left side) and Empirical Cumulative Distribution Function (ECDF)-plot (right side) (Reimann et al., 2008). Interpretation of the density trace plot shows a possibly bimodal distribution. The variance indicated by sub populations with breaks near 1 mg/L and 100 mg/L. The ECDF plot demonstrates a slight left tail. The density plots, histograms, boxplots and scatterplot suggest that Sr concentration are slightly left skewed, on a log-scale.

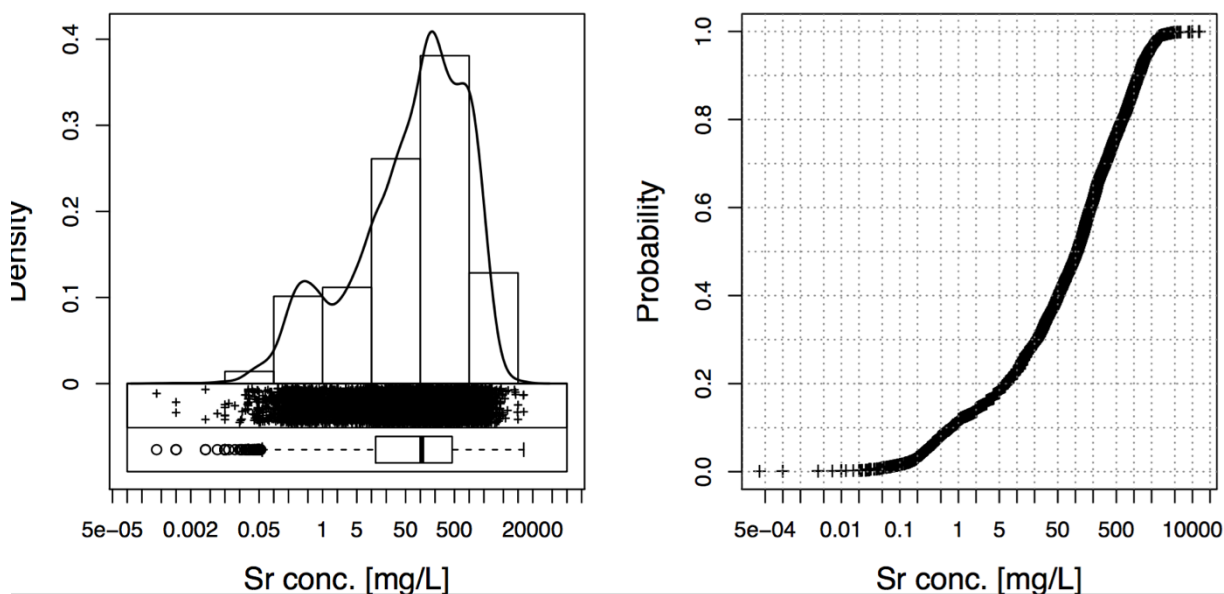


Figure 94: National EDA-plot in log scale, which includes a combination of a histogram, density trace, boxplot, and one-dimensional scatterplot (left side) and Empirical Cumulative Distribution Function (ECDF)-plot (right side). Strontium concentrations are left skewed.

### 5.23.3 Summary Statistics:

Table 24. Univariate data analysis for strontium.

	MIN	Q_0.05	Q1	MEDIAN	MEAN-log	MEAN	Q3	Q_0.95	MAX	SD	MAD	pσ	CV %	CVR %
<b>Sr</b>	0	0.29	12.16	107	58.24	391	448.9	1730	13100	726.3	156.4	323.8	185.7	146.2

Calculations were compiled to include: minimum (MIN), 5<sup>th</sup> percentile (Q\_0.05), 25<sup>th</sup> percentile (Q1), median, geometric mean (MEAN\_log), mean, 75<sup>th</sup> percentile (Q3), 95<sup>th</sup> percentile (Q\_0.95), maximum (MAX), standard deviation (SD), pseudosigma (pσ), coefficient of variation (CV), and robust coefficient of variation (CVR).

### 5.23.4 Kendall Tau correlation:

In descending order, elements positively correlated ( $\tau > 0.6$ ) with Sr include Cl ( $\tau = 0.69$ ), Mn ( $\tau = 0.64$ ), Br ( $\tau = 0.75$ ), Ca ( $\tau = 0.73$ ), Mg ( $\tau = 0.62$ ), Li ( $\tau = 0.68$ ), Na ( $\tau = 0.63$ ) and Co ( $\tau = 0.64$ ). The only constituents that negatively correlate with Sr are HCO<sub>3</sub> ( $\tau = -0.31$ ), Hg ( $\tau = -0.19$ ), S ( $\tau = -0.23$ ), and Si ( $\tau = -0.12$ ). The inverse correlation between Sr and HCO<sub>3</sub> and Sr and SO<sub>4</sub>, are likely due to controls on strontium concentrations due to the low solubility of strontianite (SrCO<sub>3</sub>) and celestite (SrSO<sub>4</sub>).

## 5.23.5 Maps:

### 5.23.5.1 Spatial Distribution:

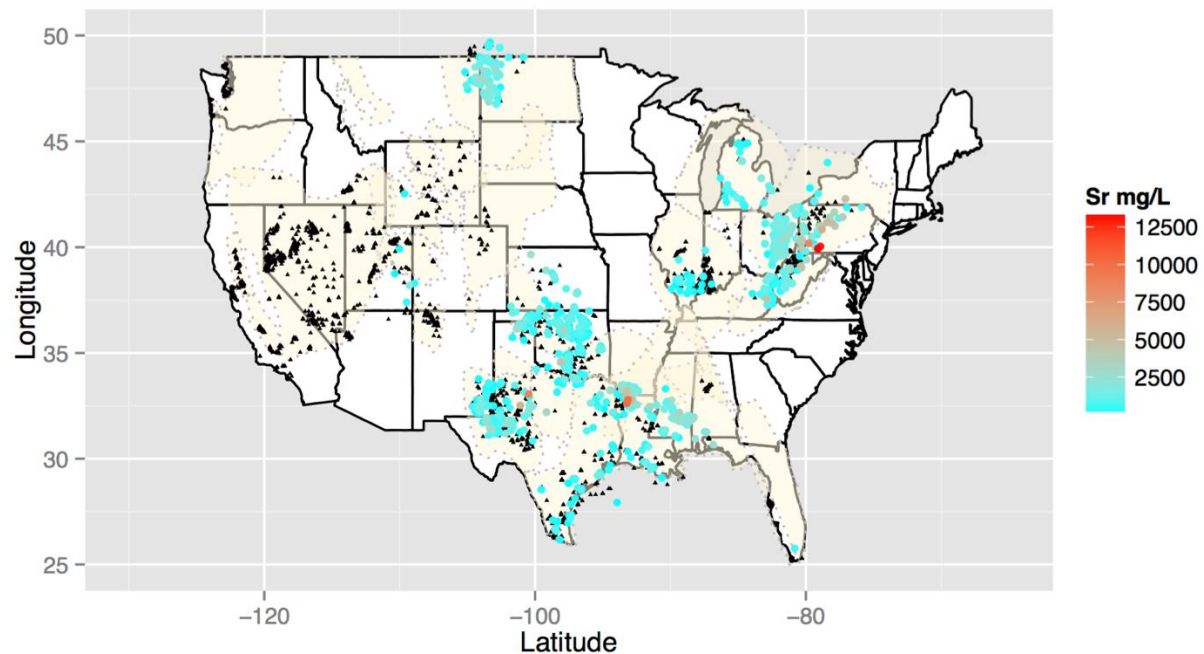


Figure 95: National spatial concentration map for strontium. Black triangles identify locations where Sr concentration data exist but are below the 75th percentile. Color ramped symbols applied to the sites where concentrations exceed the 75th percentile.

The data coverage for strontium is moderate but variable throughout the U.S. (Figure 95). Strontium concentrations can exceed 10,000 mg/L in some areas. The highest strontium concentrations occur in the northern Appalachian Basin and the Smackover Formation in Arkansas. Exploration potential for strontium is relatively low given data coverage, although there are data gaps in portions of the western half of the United States.

### 5.23.5.2 Estimated Economic Values:

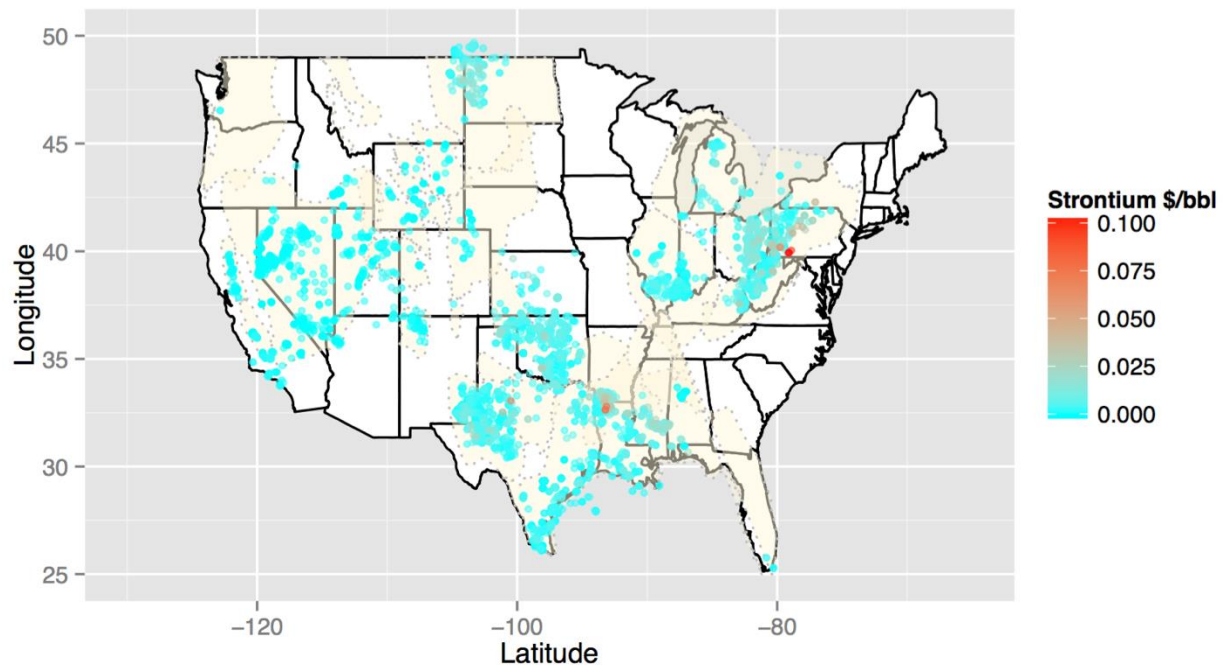


Figure 96: Economic concentration map for strontium identifying highest areas of interest: The Central Midwest Region and Northeast Region.

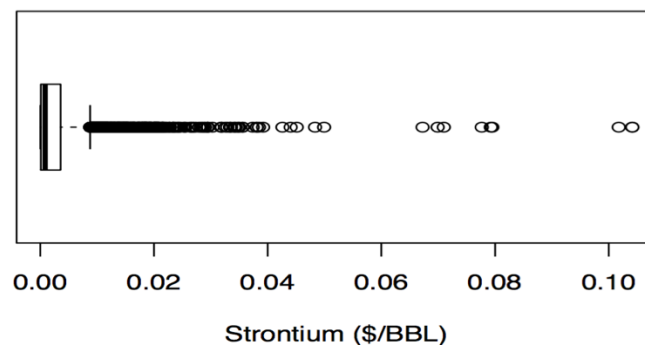


Figure 97: Tukey boxplot of economic values for strontium in produced waters.

Strontium is imported for alloy and magnet uses in manufactured goods. Pricing in 2014 was \$50.00 per metric ton (\$5.00E-08 per milligram per liter). The least expensive disposal price exceeds the highest values available for Sr, ultimately nulling profit potential for development, at this time. Including co-extraction, there is still little potential to meet the minimum disposal costs for most regions. There is insignificant potential to develop Sr extraction from produced waters.

#### **5.23.6 Summary:**

Potential for both extraction and exploration for strontium is low. The demand for Sr does not appear to increase in market forecasts (USGS, 2015). The value and concentration levels do not support the minimum requirements of exceeding disposal costs, to be considered for further development. The data coverage is fair and could be more complete but sufficient enough to complete the analysis.

## **5.24 Sulfur**

### **Sulfur (S):**

#### **5.24.1 Commodity:**

Sulfur commodities, such as elemental sulfur and sulfuric acid, are both imported and exported. Sulfur is mostly mined and recovered through secondary processes at petroleum refineries and natural gas production. Recovery technology and methods are continuously improving and production is expected to increase. Prices vary from import to export products and prices are expected to increase in 2015. As most sulfur in produced water occurs as sulfate, this section will consider solely the conversion of sulfate to sulfur as the mineral commodity.

#### **5.24.2 Geochemical Statistics:**

Sulfur concentrations were examined using two types of plots (Figure 98) that include a combination of a histogram, density trace, boxplot, and one-dimensional scatterplot (left side) and Empirical Cumulative Distribution Function (ECDF)-plot (right side) (Reimann et al., 2008). Interpretation of the ECDF-plot (Figure 98) shows a possible bi modal distribution. The variance indicated by sub populations with breaks near 1 mg/L and 1000 mg/L. The density trace plot demonstrates a slight sigmodal distribution curve. The density plots, histograms, boxplots and scatterplot suggest that  $\text{SO}_4$  concentration are slightly right skewed, on a log-scale.

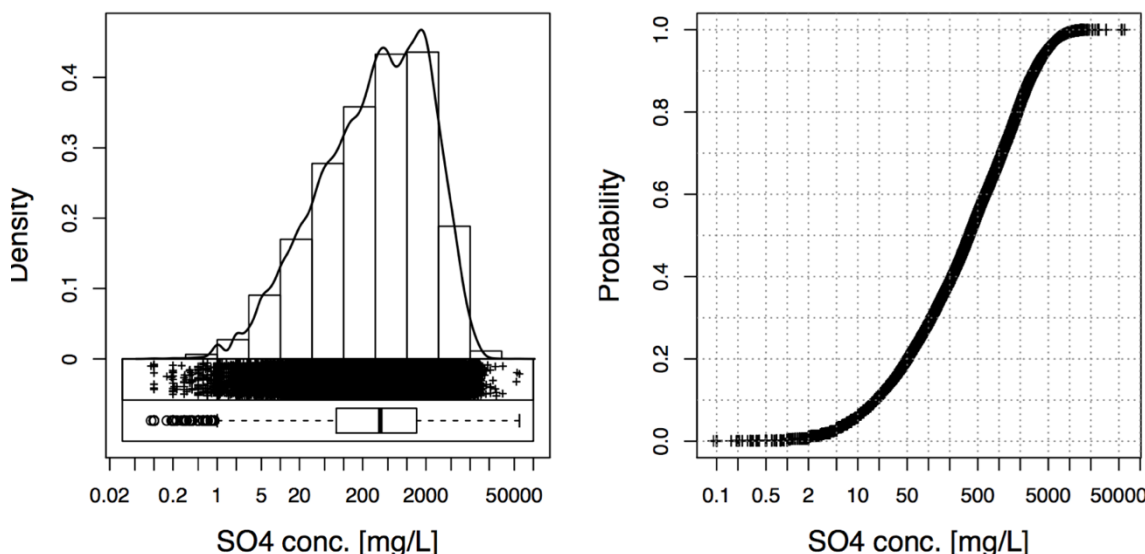


Figure 98: National EDA-plot in log scale, which includes a combination of a histogram, density trace, boxplot, and one-dimensional scatterplot (left side) and Empirical Cumulative Distribution Function (ECDF)-plot (right side). Sulfur concentrations are right skewed.

### 5.24.3 Summary Statistics:

Table 25. Univariate data analysis for sulfate.

	MIN	Q_0.05	Q1	MEDIAN	MEAN -log	MEAN	Q3	Q_0.95	MAX	SD	MAD	pσ	CV %	CVR %
SO <sub>4</sub>	0	8	76.5	378.4	296.2	1123	1426	4751	60000	1821	525.5	1000	162.1	138.9

Calculations were compiled to include: minimum (MIN), 5<sup>th</sup> percentile (Q\_0.05), 25<sup>th</sup> percentile (Q1), median, geometric mean (MEAN\_log), mean, 75<sup>th</sup> percentile (Q3), 95<sup>th</sup> percentile (Q\_0.95), maximum (MAX), standard deviation (SD), pseudosigma (pσ), coefficient of variation (CV), and robust coefficient of variation (CVR).

### 5.24.4 Kendall Tau correlation:

Sulfate does not positively correlate with any elements at or near ( $\tau > 0.6$ ). The constituents that negatively correlate with SO<sub>4</sub> is: Be ( $\tau = -0.3$ ), BO<sub>3</sub> ( $\tau = -0.26$ ), Ba ( $\tau = -0.24$ ), and Cs ( $\tau = -0.19$ ).

## 5.24.5 Maps:

### 5.24.5.1 Spatial Distribution:

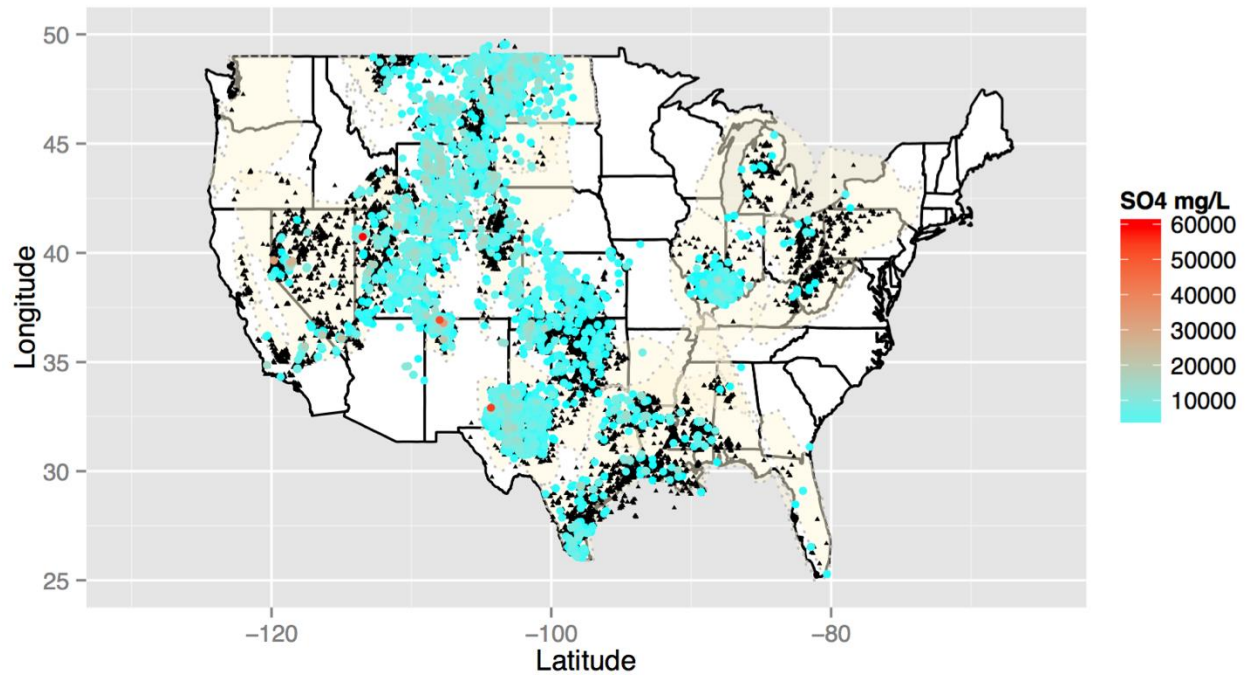


Figure 99: National spatial concentration map for sulfur. Black triangles identify locations where sulfate concentration data exist but are below the 75th percentile. Color ramped symbols applied to the sites where concentrations exceed the 75th percentile.

The spatial distribution for sulfate is moderate, the highest concentration is in the Permian Basin and the Black Hills Region. Exploration for spatial data is relatively low and fairly established. The sulfate concentration map can be considered to identify sulfur concentrations.

### 5.24.5.2 Estimated Economic Values:

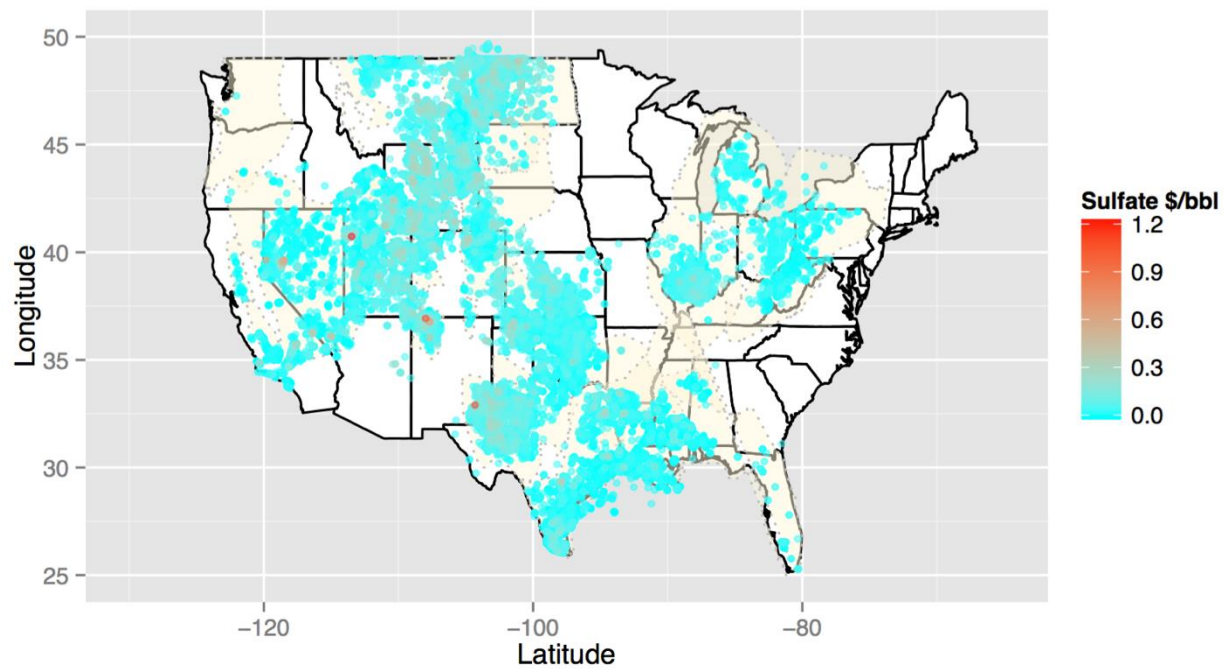


Figure 100: Economic concentration map identifying highest areas of interest; The Permian Basin and the Black Hills Region.

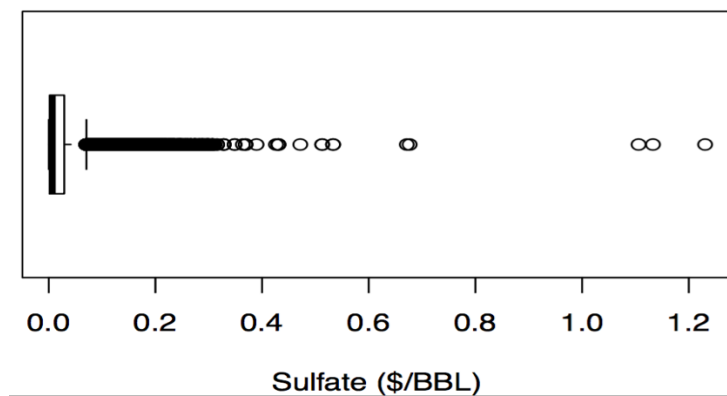


Figure 101: Tukey boxplot of economic values for sulfate in produced waters.

Sulfur is an identified commodity that mostly imported for alloy and magnet uses in manufactured goods. Pricing in 2014 was \$129.00 per metric ton (\$1.29E-07 per milligram per

liter). To consider sulfur for development, the potential in the Permian Basin is low to moderate and for the Black Hill Regions is low to not at all. There is little potential to develop S extraction from produced waters.

#### **5.24.6 Summary:**

Sulfur exploration, extraction and development potential for is low. The value and concentration levels do not support the minimum requirements of exceeding disposal costs, to be considered for further development. The data coverage is poor and could be more complete but sufficient enough to complete the analysis.

## **5.25 Zinc**

### **Zinc (Zn):**

#### **5.25.1 Commodity:**

Zinc is primarily mined from traditional ore deposits in the United States. Zinc is also recovered from secondary smelter processes. Zinc is used for various metal alloy based products for galvanizing, brass and bronze based alloys. Crude Zinc oxide is also recovered from electric arc furnace dust.

#### **5.25.2 Geochemical Statistics:**

Zinc concentrations were examined using two types of plots (Figure 102) that include a combination of a histogram, density trace, boxplot, and one-dimensional scatterplot (left side) and Empirical Cumulative Distribution Function (ECDF)-plot (right side) (Reimann et al., 2008). Interpretation of the density trace shows a bimodal distribution. The variance indicated by sub populations with breaks near 0.05 mg/L and 3 mg/L. The density plots, histograms, boxplots and scatterplot suggest that Zinc concentrations have a bimodal distribution with a slight right skew.

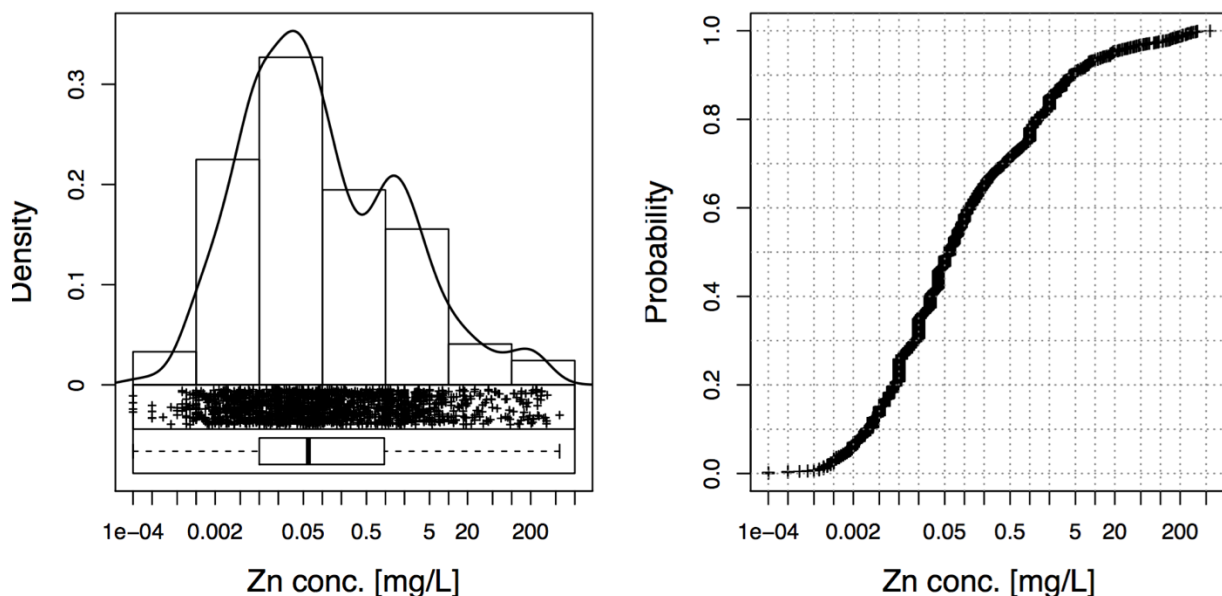


Figure 102: National EDA-plot in log scale, which includes a combination of a histogram, density trace, boxplot, and one-dimensional scatterplot (left side) and Empirical Cumulative Distribution Function (ECDF)-plot (right side). Zinc concentrations have a bimodal distribution with a slight right skew.

### 5.25.3 Summary Statistics:

Table 26. Univariate data analysis for zinc.

	MIN	Q_0.05	Q1	MEDIA N	MEAN- log	MEAN	Q3	Q_0.95	MAX	SD	MAD	pσ	CV %	CVR %
<b>Zn</b>	1.00E-04	0.0017	0.01	0.06	0.09668	7.271	0.951	18.04	575	37.26	0.08436	0.6976	512.5	140.6

Calculations were compiled to include: minimum (MIN), 5<sup>th</sup> percentile (Q\_0.05), 25<sup>th</sup> percentile (Q1), median, geometric mean (MEAN\_log), mean, 75<sup>th</sup> percentile (Q3), 95<sup>th</sup> percentile (Q\_0.95), maximum (MAX), standard deviation (SD), pseudosigma (pσ), coefficient of variation (CV), and robust coefficient of variation (CVR).

### 5.25.4 Kendall Tau correlation:

The only element positively correlated ( $\tau > 0.6$ ) with Zn is Pb ( $\tau = 0.65$ ). Zinc and lead have similar chemical characteristics and are commonly co-associated geochemically.

## 5.25.5 Maps:

### 5.25.5.1 Spatial Distribution:

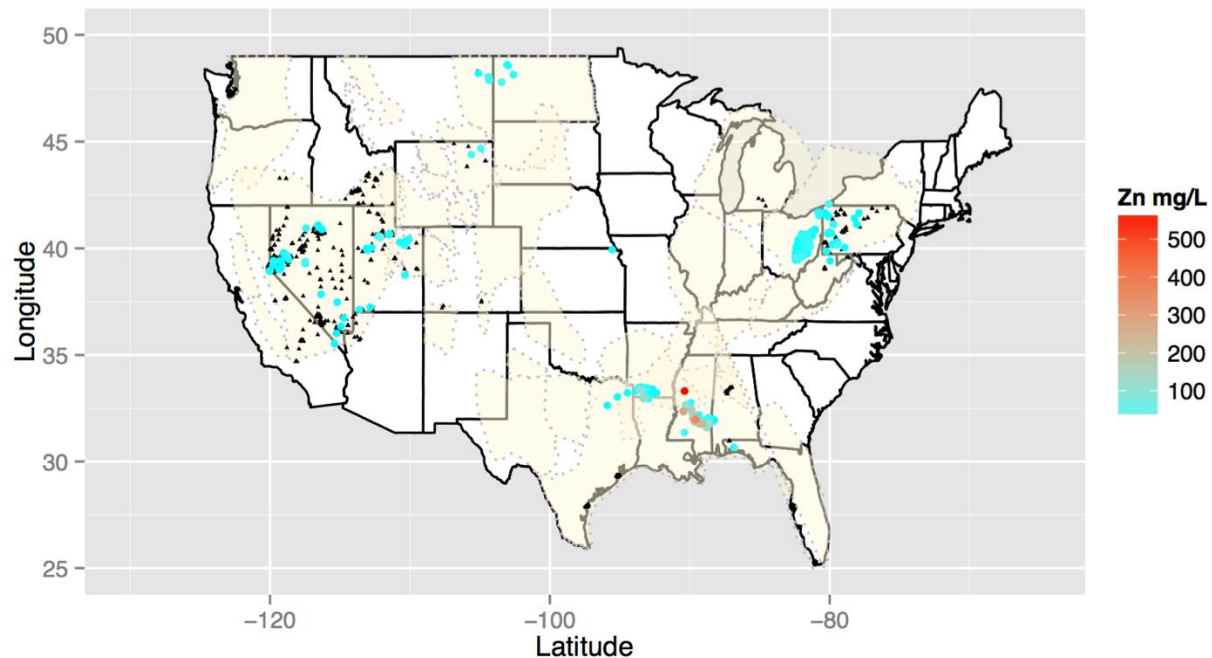


Figure 103: National spatial concentration map for zinc. Black triangles identify locations where Zn concentration data exist but are below the 75th percentile. Color ramped symbols applied to the sites where concentrations exceed the 75th percentile.

The spatial distribution for zinc is limited and data gaps are wide spread. The highest zinc concentrations occur in the Mississippi Interior Salt Basin. This is in proximity to known sulfide ore deposits (zinc-lead ores) and may be a local source of zinc. Brines with high iron content may be indicative to leaching from host lithology (<http://pubs.usgs.gov/sir/2010/5070/a/pdf/SIR10-5070A.pdf>). The sulfur concentrations are located in regions that traditionally maintain mid-range to high disposal costs. There is need for further exploration to better characterize zinc concentrations in many basins. Development potential is limited for brine extraction. The development potential is high if extraction is considered with other commodity elements.

### 5.25.5.2 Estimated Economic Values:

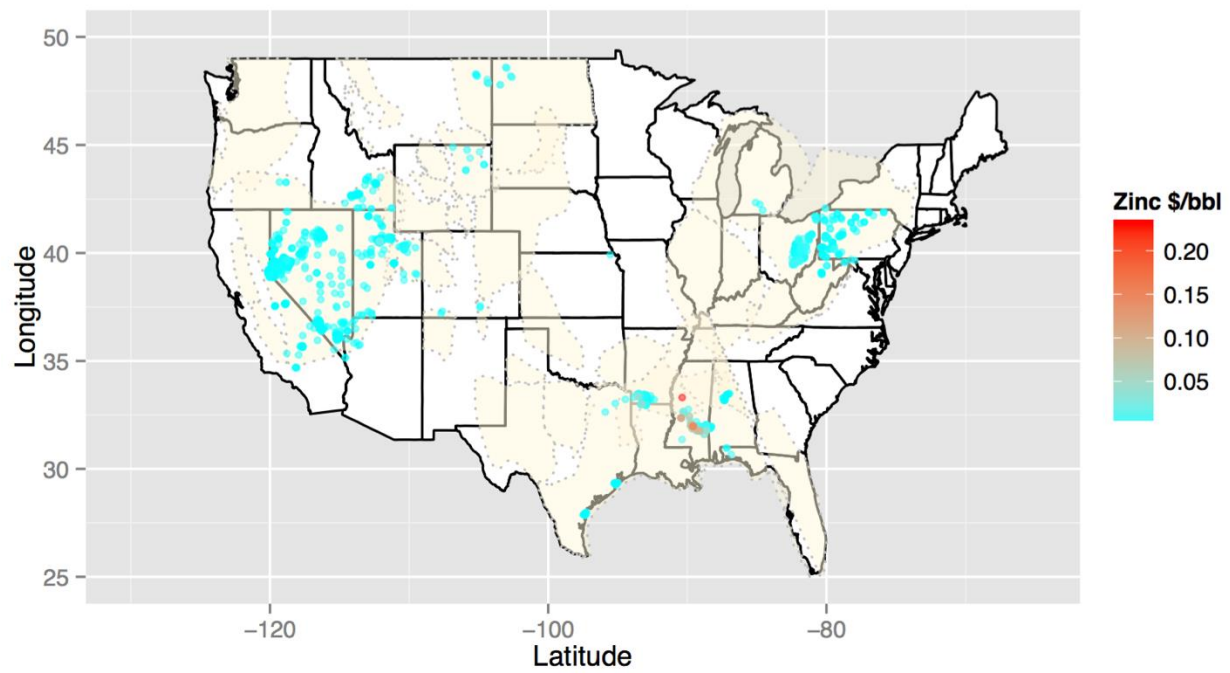


Figure 104: Economic map for zinc identifying highest areas of interest: The Gulf Coast Region.

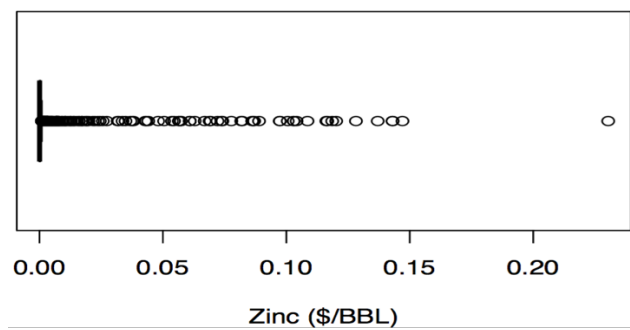


Figure 105: Tukey boxplot of economic values for zinc in produced waters.

Zinc is a metal element associated with MVT mineral deposits. Zinc commodities are valued at \$1.14 per pound (\$2.52E-06 per milligram). Applied to the concentration results shown in Figure 103, gross values (ranges from \$0.05-\$0.20 per barrel) in most areas are below most disposal costs (Figures 104 and 105). The greater potential for zinc is co-extraction with other commodities, such as beryllium, lead, bromine, nickel, cobalt and cadmium. However, the potential for extraction of zinc or other base metals is relatively low because of their low value, so it may be more cost effective to continue with traditional mining methods from ore deposits.

#### **5.25.6 Summary:**

The value of zinc in produced waters does not exceed disposal costs, thus has low potential for development. The data coverage is poor and if concentrations one order of magnitude higher than the current upper range exist, zinc may have some economic value. For this reason, there is moderate potential for extraction. The commodity values, concentrations, and disposal costs, reduce potential for most regions, although the Gulf Coast region has greatest potential for development.

## **Chapter 6. Grouped Commodities**

This section examines the potential economic value from co-extraction of commodities. Co-extraction has potential to increase economic value of produced waters, given that the disposal costs are assumed constant regardless of the number of commodities removed. In this case, the groups of commodities include alkali metals (Li, Na, K, Cs, Rb), alkaline earth elements (Mg, Ca, Sr, Ba), transition metals (Co, Cr, Cd, Cu, Hg, Pb, Mn, Mo, Ni, Zn) and halogens (Br, Cl, F, I). Maps showing summed mineral commodity value for each group were completed in the same fashion as those for the individual elements. These groups were chosen because of geochemical similarities between the elements within each group (thus similar methods for removal) and because, in most cases, the elements are highly correlated. In addition to the grouped maps, a Tukey boxplot of the gross grouped commodity values was created.

## 6.1 Alkali Metals

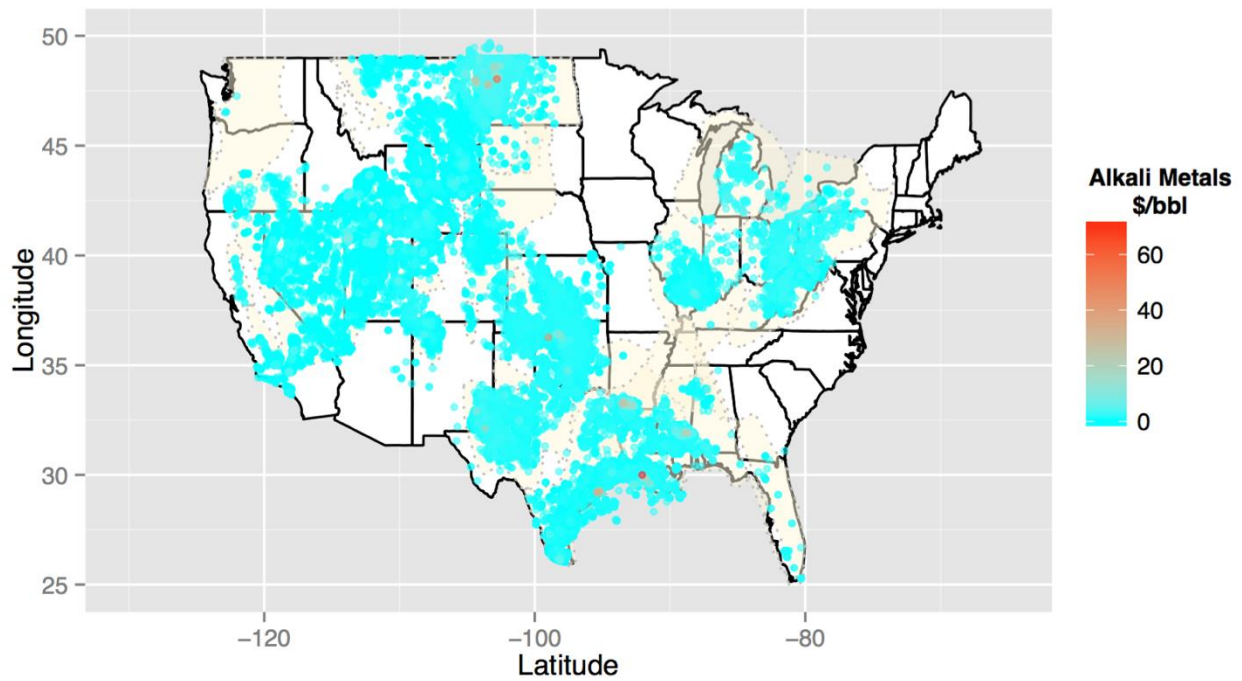


Figure 106: Grouped economic value map for alkali metals, identifying areas of interest; The Gulf Coast Basin, Smackover Formation and the Williston Basin.

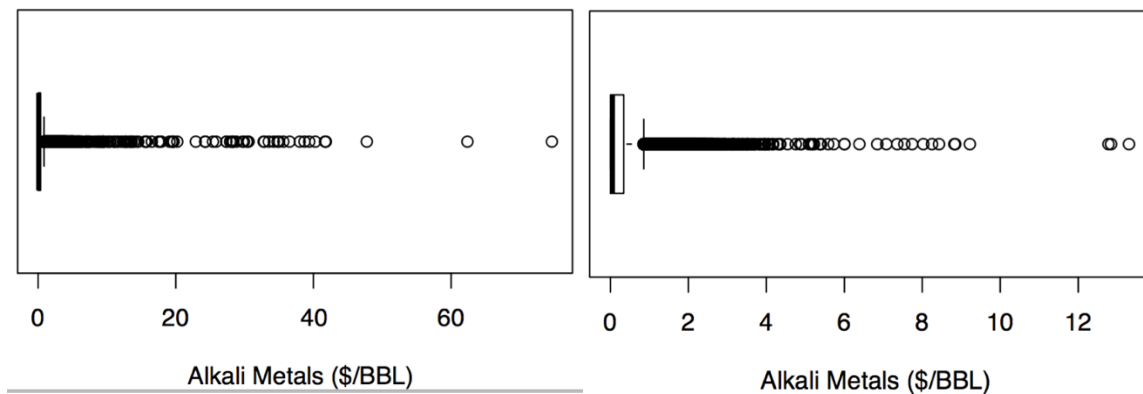


Figure 107: Tukey boxplot of economic values for alkali metals in produced waters. Left: All alkali metals. Right: Alkali metals excluding Rb and Cs.

**Summary:**

Alkali metals examined here include cesium, potassium, lithium carbonate, sodium and rubidium formate. Alkali metals are associated in nature and are water soluble, making them readily available for extraction and separation. In Figure 106, all alkali metals have been grouped together. Points where, their revenue potential exceeds disposal costs exist in all regions. There are two economic box plots presented. Figure 107 is the complete sum of all combined potential commodities available for extraction in produced waters. The box plot on the right is the sum of all potentially available alkali metal commodities except for rubidium and cesium. Due to the paucity of the data and their high value, they are separated from the calculations to provide a more conservative approach. Cesium, rubidium and lithium products have the highest potential for long term development and require the most spatial data exploration. In some cases, these three elements still exceed disposal costs in all regions excluding the outliers. In Figure 107 on the right, the mid-range economic concentrations can be profitable at \$20.00/bbl. The spatial coverage for the alkali metals is fairly complete, with the exception of cesium and rubidium. These two elements have by far the largest value of the alkali metals, indicating these are elements which need further exploration. The extraction potential for these combined elements is high. Economically, salt and potash have low potential and these products are mostly beneficial for regional or local application. Alkali metals can also be combined with halogens and alkaline earth metals to potentially increase revenue as many these elements (bromine, iodine and magnesium) are well correlated. Elemental sodium and potassium may be considered for other non-recognized USGS commodities, such as potassium chloride, baking soda, and/or caustic sodas.

## 6.2 Alkaline Earth Metals

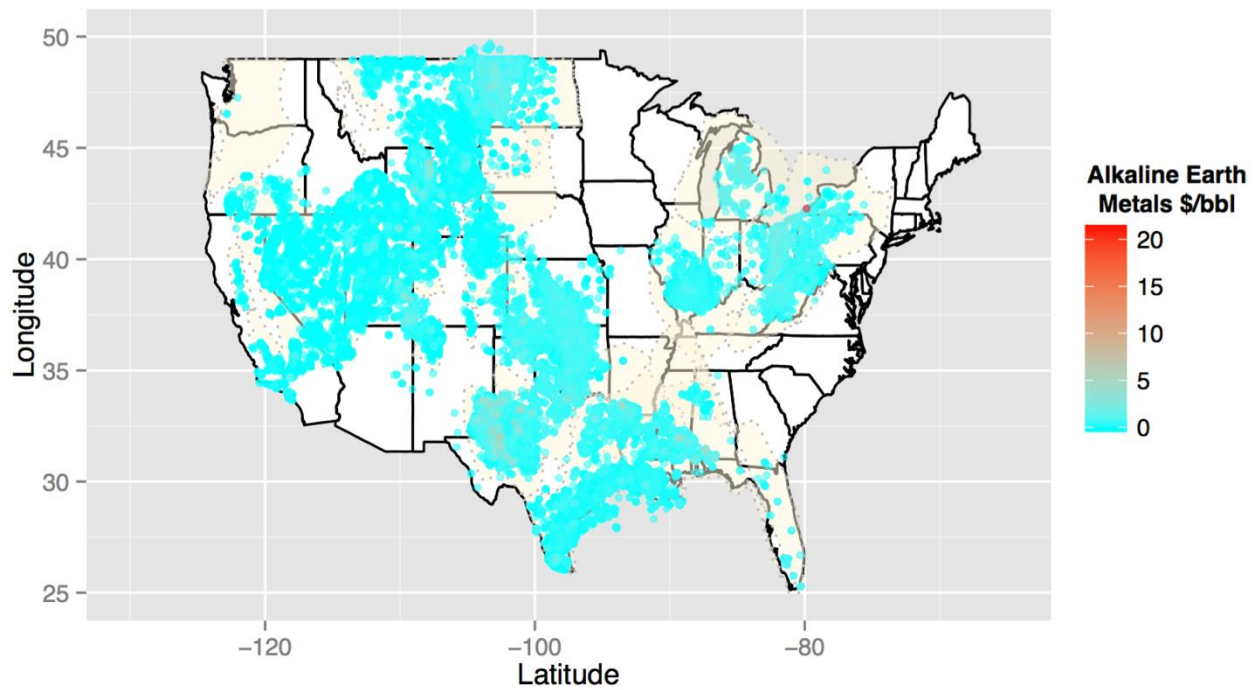


Figure 108: Grouped economic value map for alkaline earth metals, identifying areas of interest: the Gulf Coast, Permian and Appalachian Basins.

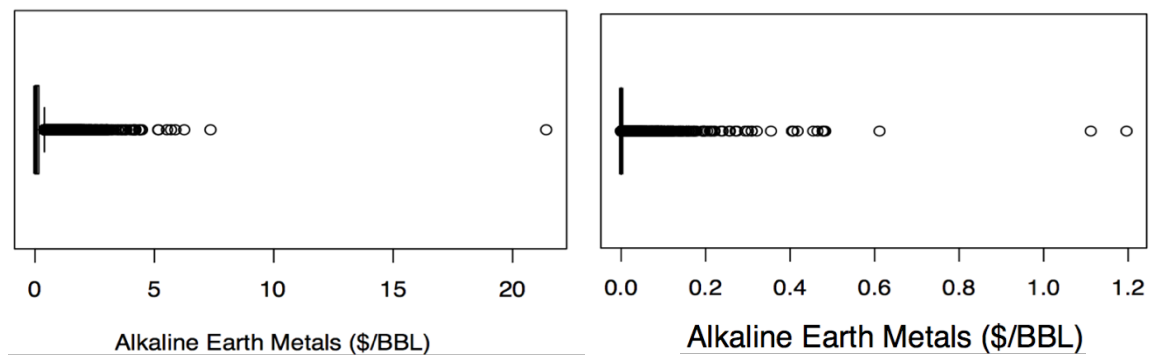


Figure 109: Tukey boxplot of economic values for alkaline earth metals in produced waters. Left: All alkali earth metals. Right: Barium and Strontium only.

**Summary:**

Alkaline earth metals examined here include barium, calcium, magnesium and strontium. Alkaline earth metals are often found together and magnesium and calcium are among the most abundant elements in natural waters. In Figure 108, all alkaline earth metals have been grouped together to show the gross mineral commodities value. Combined, the revenue potential meets or exceeds disposal costs for most regions. There are two economic box plots presented. Figure 109 is the combined potential commodities for all of the alkaline earth metals examined here. The box plot on the right shows the sum just barium and strontium. Economically, soda ash and magnesium provide immense revenue opportunities; these products may benefit greater from regional or local operations. Barium and strontium have the low-medium potential for extraction, but could benefit from further exploration. In Figure 109 (right), the mid-range economic concentrations of \$0.40/bbl, exceeding disposal costs in some locations. The Permian Basin and the Gulf Coast Basin have the highest economic values paired with the lowest disposal costs. The Appalachian Basin has the highest concentrations but is among the highest for disposal. The extraction of alkaline earth elements appears economic primarily from co-extraction, given the relatively similar value of the various constituents. These alkaline earth metals can also be combined with halogens and alkali metals to potentially increase revenue, as many these elements (sodium, bromine and potassium) are well correlated.

### 6.3 Transition Metals

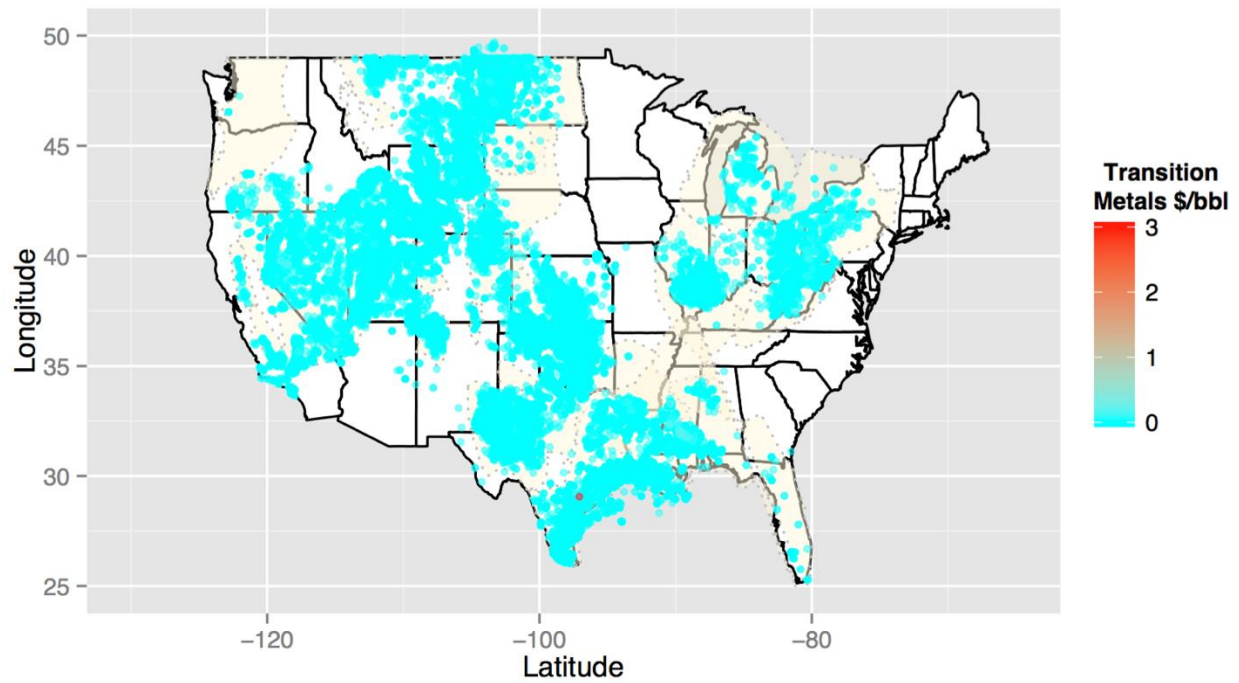


Figure 110: Grouped economic value map for transition metals, identifying areas of interest: The Gulf Coast Basin.

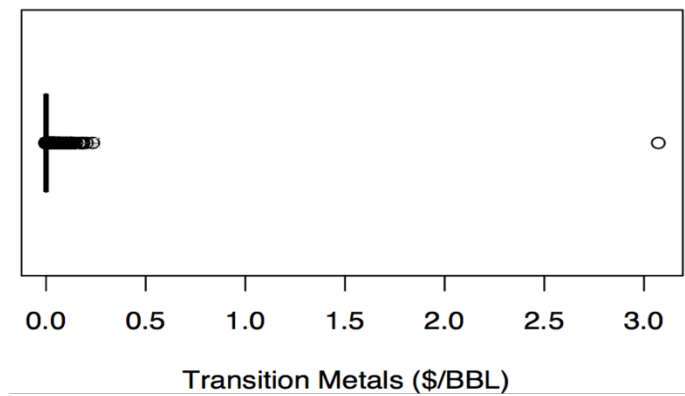


Figure 111: Tukey Boxplot of economic values for transition metals in produced waters.

**Summary:**

Transition metals examined here include cobalt, chromium, cadmium, copper, lead, manganese, mercury, molybdenum, nickel, and zinc. Transition metals are metallic elements, making them characteristically efficient heat and electrical conductors, allowing for their use in alloy products, catalysts and building materials. When combined, the profit potential of the transition metals is still low and valued less than disposal costs for most regions (Figures 110, 111). Transition metals are quarried through traditional mining practices and this is still most likely the most profitable method for extraction. In Figure 111, mid-range economic concentrations do not exceed \$0.25/bbl, substantially less than disposal costs in most areas. The outlier at \$3.00/bbl is lead concentration that has not been confirmed as a reliable value (more than two orders of magnitude higher than the next highest sample) and is not considered for economic development. The spatial data for the transition metals is relatively incomplete and if economically valuable elements are found, there is in need of further exploration. The extraction potential of these elements is poor.

## 6.4 Halogens

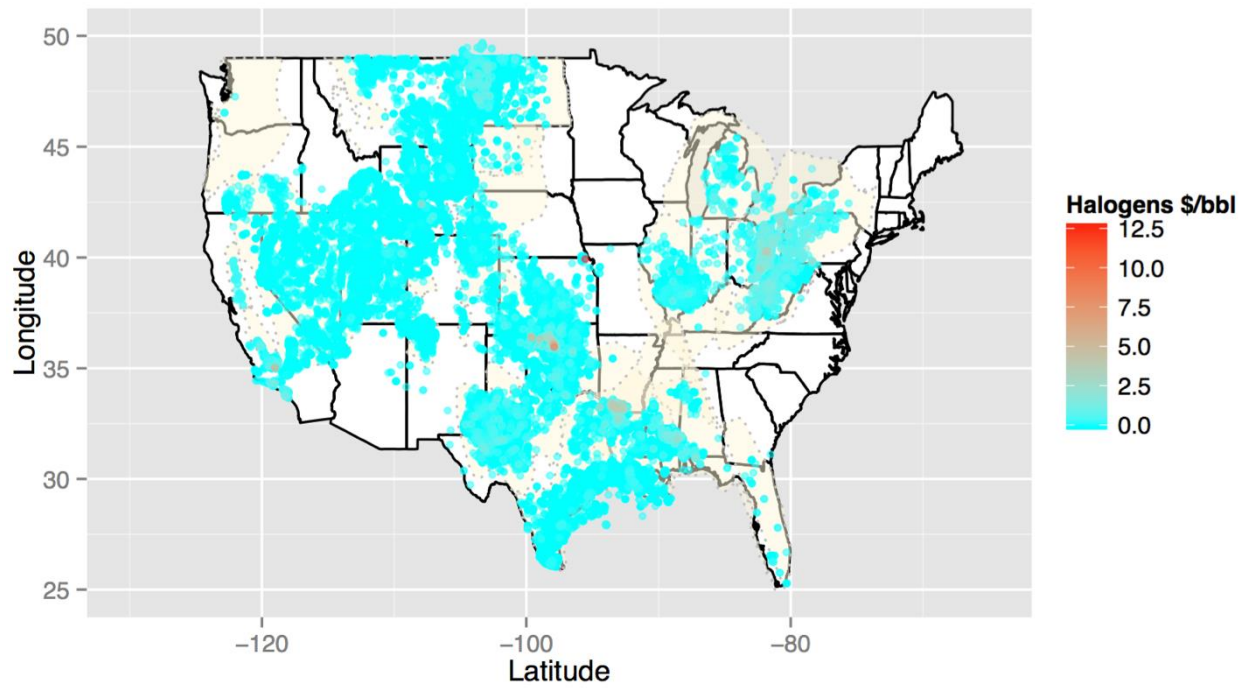


Figure 112: Grouped economic value map for halogens, identifying areas of interest: the Anadarko Basin, Smackover Formation and the Appalachian Basin.

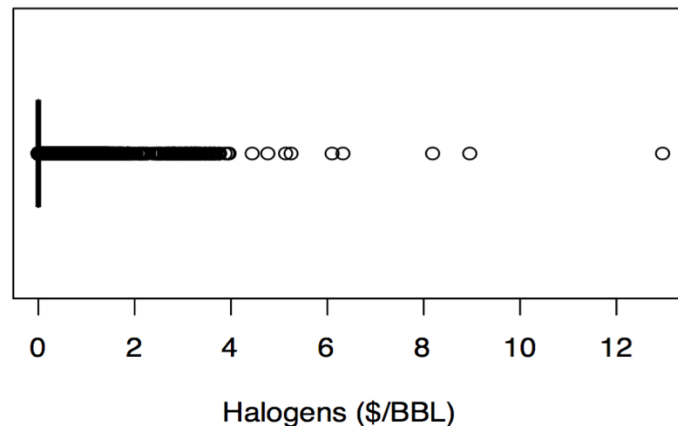


Figure 113: Tukey boxplot of economic values for halogens in produced waters.

**Summary:**

Halogens examined here include bromine, chloride, fluorine, and iodine. In Figures 112 and 113, all halogens have been grouped together. Combined, the revenue potential meets or exceeds disposal costs for most regions the mid-range economic concentrations can be near \$2.00/bbl, or greater, depending on location. The Smackover Formation and the Anadarko Basin have the highest potential with the lowest disposal costs while the Appalachian Basin also contains samples with high concentrations of halogens but is also an area of high disposal costs. The spatial data for the halogens is moderately complete, although iodine and bromine could benefit from further exploration. Individually, many of the halogens have extraction potential, but as shown here can be combined together for higher potential value. These halogens can also be combined with alkali metals and alkaline earth metals to potentially increase revenue as many elements (sodium, lithium and potassium) are well correlated.

## **Chapter 7. Permian Basin Case Study**

The principle application of mineral commodity extraction and whether there is potential has been applied to the Permian Basin to demonstrate viability and practicality of using produced waters as an additional commodity resource. The applied analysis is not to be considered as an exact determination and would require expert engineering knowledge to be applied during a pilot study. The Permian Basin is modeled because of its access to a fresh water supply, subsurface injections wells and is comparatively the least expensive for waste water disposal. The low cost for produced water injection in the Permian Basin could increase revenues, should there be profit potential in the Permian Basin, similar methods could be applied to areas where water management is more expensive to reduce costs and diversify a company's portfolio.

## 7.1 Permian Basin background

The Permian Basin consists of two major sub-basins, the Delaware Basin to the west and the Midland Basin to the east, separated by the Central Basin Platform. The formation waters in the Permian Basin consist of both paleo evaporated seawater, meteoric waters and, mixtures thereof. The marine origins and rock lithology contribute to the higher concentrations of bromine, iodine, lithium, magnesium, and potassium in the basinal brines. These elements in the Permian Basin, are found in relative abundance and high concentrations thus, making them targets for exploration and development. A complete univariate statistical summary of the all available elements can be found in Table 26.

Table 27. Univariate data analysis for all available constituents.

	MIN	Q_0.05	Q1	MEDIAN	MEAN-log	MEAN	Q3	Q_0.95	MAX	SD	MAD	Pseudosigma	CV %	CVR %
<b>TDS</b>	61	7942	40040	83140	67860	105100	153900	269100	506900	83810	80820	84420	79.77	97.21
<b>B</b>	0.41	3.615	8.392	17	16.17	25.7	33	72.99	396.3	34.5	16.12	18.24	134.2	94.84
<b>Ba</b>	0.0339	0.0507	0.1025	0.5375	0.9743	34.46	5.11	208.3	2478	141.8	0.7188	3.712	411.6	133.7
<b>Br</b>	0.9	5.25	79.12	222.9	149.5	290.1	420.3	828.6	1519	277.1	225.2	252.9	95.54	101
<b>HCO3</b>	0	0	0	176.8	310.5	354	480	1369	13930	547.6	262.2	355.8	154.7	148.3
<b>gCO3</b>	0.9834	49.47	162.7	310	308.9	520.3	667.4	1586	33000	836	286.9	374.1	160.7	92.55
<b>Ca</b>	1.01	288	1460	2975	2850	5482	7250	17550	66380	6492	3213	4292	118.4	108
<b>Cl</b>	8	2940	26100	52200	39310	63590	95000	155000	245400	48270	48830	51070	75.9	93.54
<b>I</b>	1	1.05	3.222	7.82	7.935	16.77	19.97	52.75	320.3	27.72	8.54	12.42	165.3	109.2
<b>K</b>	0.62	39.1	187.4	408	350.8	775.4	724.8	2426	78200	2629	360.3	398.4	339.1	88.3
<b>Li</b>	1	2	4.95	9.5	8.863	15.56	16.88	35.91	493	37.91	8.021	8.844	243.6	84.43
<b>Mg</b>	0.2003	100	458	1008	881.9	1691	1969	5762	37620	2410	955.1	1120	142.5	94.76
<b>Mn</b>	0.1	0.1225	0.28	0.47	0.9238	6.75	2.35	39.05	101.6	17.99	0.3929	1.534	266.5	83.59
<b>Na</b>	20	2120	14140	27610	21650	32970	47710	80280	146800	24770	24110	24890	75.12	87.33
<b>SO4</b>	1	93.8	609.3	1441	1103	1920	2700	5340	55230	1907	1424	1550	99.31	98.87
<b>Sr</b>	0.03	10.04	26.23	65.5	72.43	213.4	199.2	988.3	8794	469	77.27	128.2	219.8	118

Table 26. Calculations were compiled to include: minimum (MIN), 5<sup>th</sup> percentile (Q\_0.05), 25<sup>th</sup> percentile (Q1), median, geometric mean (MEAN\_log), mean, 75<sup>th</sup> percentile (Q3), 95<sup>th</sup> percentile (Q\_0.95), maximum (MAX), standard deviation (SD), pseudosigma ( $\rho\sigma$ ), coefficient of variation (CV), and robust coefficient of variation (CVR). Statistical representation of the geochemistry of the Permian Basin. Number of samples analyzed (n=7206).

The USGS produced waters geochemical database, version 2.2 (Blondes et al., 2016), was used for the case study; the data was analyzed using R Statistical program version 3.1.0. The historic data is primarily obtained from conventional and unconventional reservoirs. Efforts show that the bulk geochemistry of produced waters from shale formations are similar to those for adjacent non-shale reservoirs (Engle and Rowan, 2014), thus results from conventional reservoirs

can be applied to non-conventional reservoirs. Through statistical outlier analysis, elements with the highest concentration and commodities identified by the USGS will be the focus for potential exploration and development; bromine, iodine, lithium, magnesium and potash.

The most cost effective manner industry wide is to dispose of produced waters using subsurface injection. Using methods outlined below, it can be demonstrated that beneficial use of produced waters can be an economically viable in many cases. Water is a critical component for oil and gas drilling operations, some drilling operators own their own water wells and pay for flow lines to the storage tanks or pits and, some water wells are leased from the landowner or rancher, in addition to the leases, there can be an addition cost of adding flow lines. Water must be purchased and there is the added cost to conditioning the water for reuse. The cost for brine water is approximately \$2.00/barrel for non-fracturing uses. The cost of receiving water varies on end product usage for example; company A pays \$.60/bbl, but also spends \$88 per hour for a truck, and one load may take three to four hours for 130 bbls of water. Company B spends \$2.75-\$3.00 (sometimes as much as \$5.00) per barrel; they are responsible for slickwater fracturing and require 5000-10,000 bbls of water. Disposal costs of produced waters in the Permian Basin range from \$0.30-\$4.00 per/bbl. In general, water usage is key component in oil and gas field operations and can be expensive for both source and disposal. To offset or eliminate the costs, if we can extract valuable mineral commodities that enrich these waters, margins can shift from cost to profit.

## **7.2 Bromine in the Permian Basin**

Production for bromine rich brines continues today and is currently extracted from deep wells out of the Smackover Formation located in Arkansas (Warren, 2000). The company profile states gross annual revenue of \$159 million from bromine extraction. Their extraction processes are from sedimentary basinal brines, accounting for one-third of world production (U.S. Geological Survey, 2014). According to Markets and Markets, a global market research firm, the demand for bromide is projected to increase by 9.0% by the year 2018 (Markets and Markets, 2014).

### 7.2.1 Geochemical Statistics:

Bromine concentrations were examined using two types of plots (Figure 114): that include a combination of a histogram, density trace, boxplot, and one-dimensional scatterplot (left side) and Empirical Cumulative Distribution Function (ECDF)-plot (right side) (Reimann et al., 2008). Interpretation of the EDA-plot (Figure 114) suggests that Br concentrations exhibit a bimodal distribution with a break at around 20 mg/L. However, EDCF plot suggests that additional sub populations might exist with breaks near 5 mg/l and 200 mg/l.

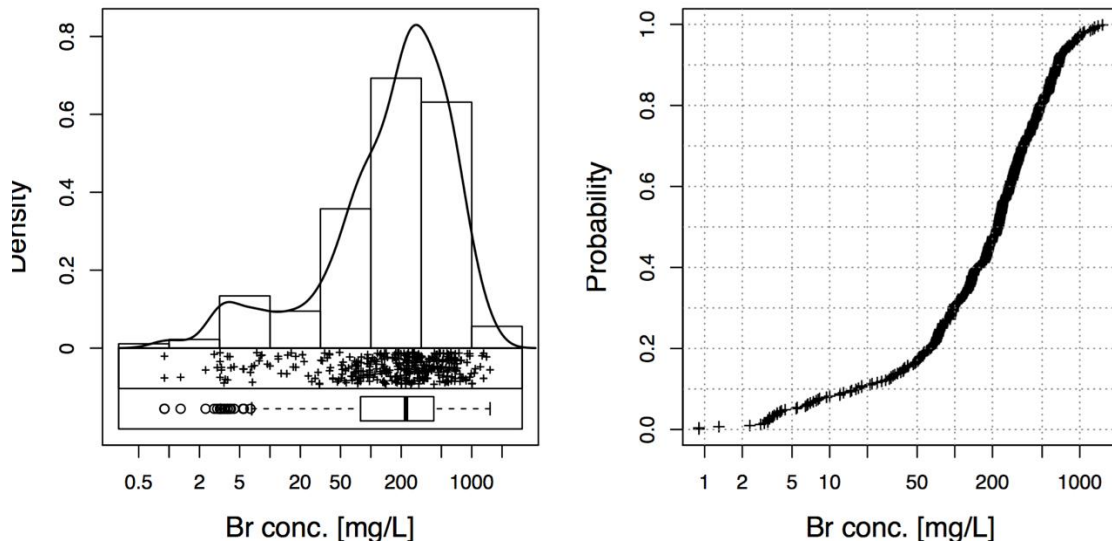


Figure 114: National EDA-plot in log scale, which includes a combination of a histogram, density trace, boxplot, and one-dimensional scatterplot (left side) and Empirical Cumulative Distribution Function (ECDF)-plot (right side). Bromine concentrations have a bimodal distribution and the EDCF plot has a sigmoidal distribution curve.

## 7.2.2 Maps:

### 7.2.2.1 Spatial Distribution:

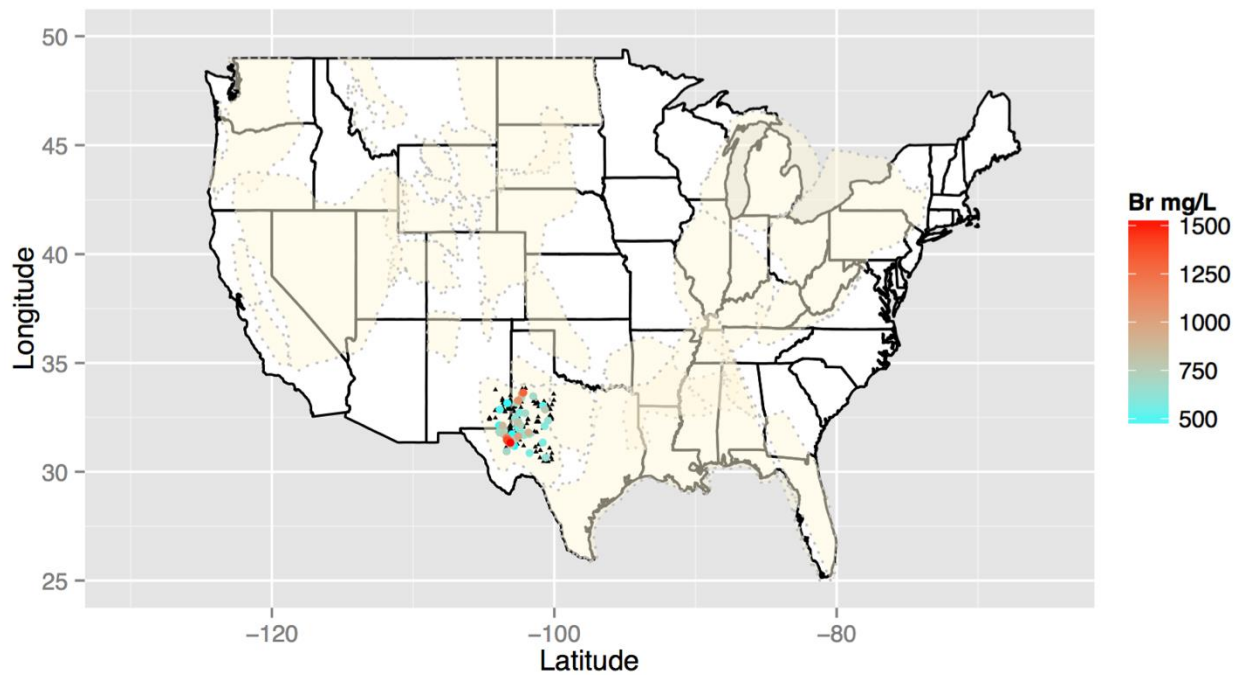


Figure 115: National spatial concentration map for bromine. Black triangles identify locations where Br concentration data exist but are below the 75th percentile. Color ramped symbols applied to the sites where concentrations exceed the 75th percentile.

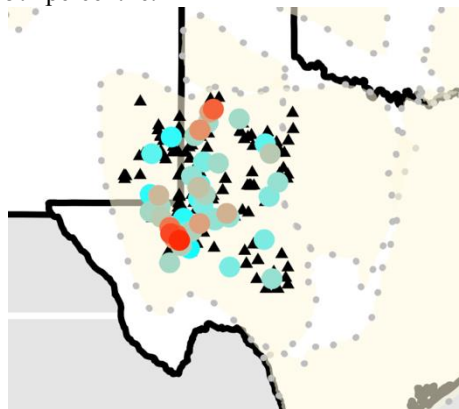


Figure 116: Magnified view of the Permian Basin spatial concentration map for bromine. Black triangles identify locations where Br concentration data exist but are below the 75th percentile. Color ramped symbols applied to the sites where concentrations exceed the 75th percentile.

Results indicate that the highest Br concentrations are found in produced waters from the Permian Basin, and tend to be areas with the highest TDS concentrations (Figure 1). The identified

locations are characterized by ancient paleoevaporated seawater and is consistent with restricted ocean circulation (Lowenstein et al., 2005). The map shows data coverage for bromine concentrations is rather extensive and moderately complete for a few primary locations.

#### 7.2.2.2 Estimated Economic Values:

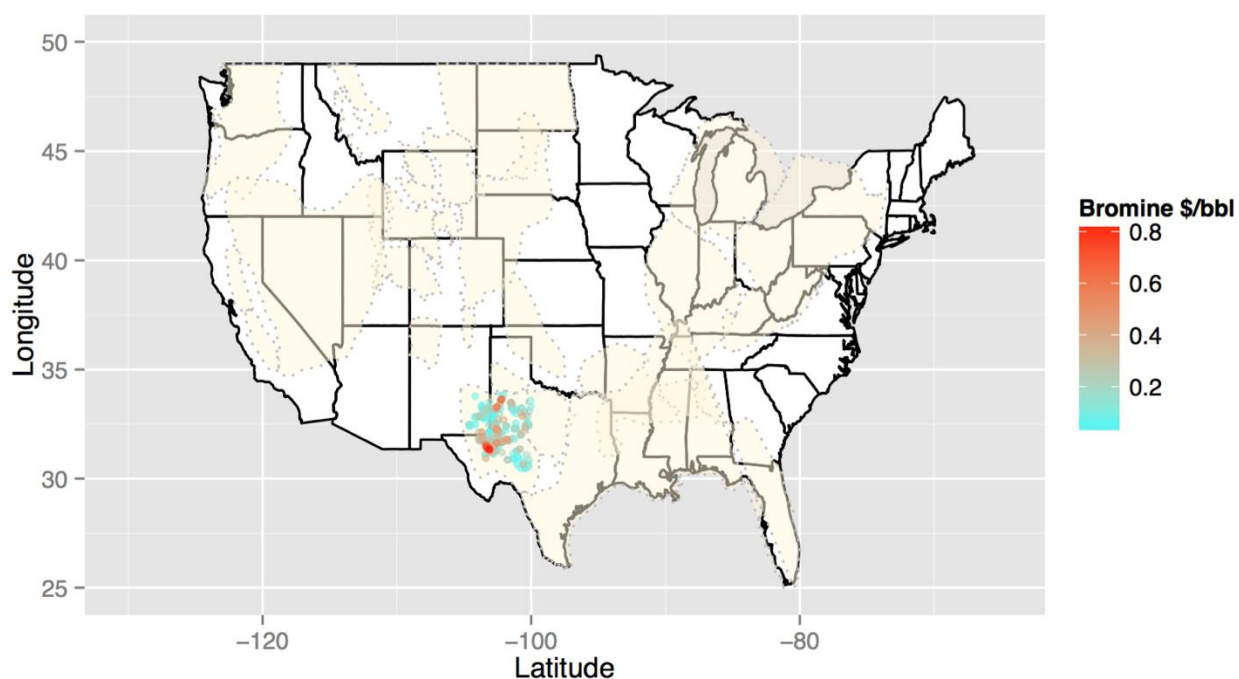


Figure 116: Economic concentration map identifying highest areas of interest.

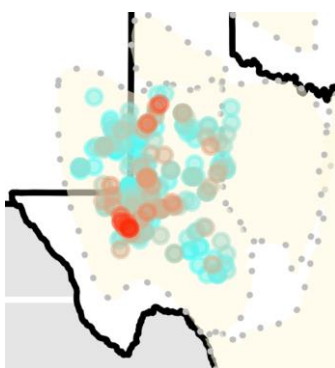


Figure 117: Magnified economic bromine Permian Basin concentration map identifying highest areas of interest.

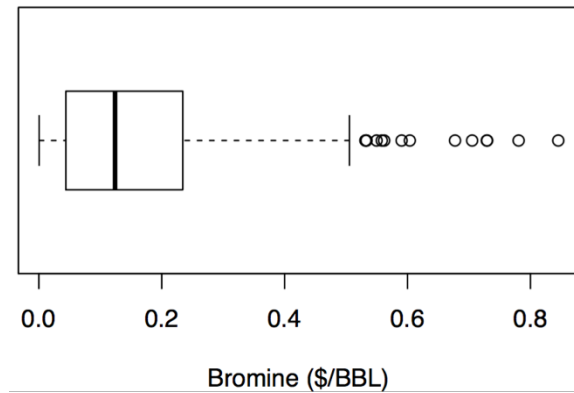


Figure 118: Tukey boxplot of economic values for identifying bromine in Permian Basin produced waters.

Bromide commodities are valued at \$3500 per metric ton ( $3.50\text{E-}06$  per milligram), showing gross values in excess of \$0.50/BBL. Analysis conclude that further development for bromine extraction is good. In the Smackover Formation, a multimillion dollar year business has thrived since the 1960's extracting bromide from the basinal brines (Warren, 2000). The potential for expansion in the Permian is identified by the economic potential maps.

### Summary:

Exploration, extraction and development for bromine commodity products extends beyond the known commodity extraction operations in the Smackover Formation. The commodity value, concentrations, and disposal costs, prove great potential for development. There is consistency for high Br concentrations with high salinity concentrations. One significant challenge in the extraction of Br, is its separation from chloride. Bromine is also associated with other constituents that have profit potential, such as lithium, rubidium, cesium, and iodine (cf. Figure 1, Figure 51, Figure 23, and Figure 43), therefor may be more economical to extract elements as a group.

### **7.3 Iodine in the Permian Basin**

The largest extraction operations of iodine is in the Anadarko Basin, Woodward, Oklahoma and accounts for 1% of domestic iodine production (Krukowski, 2008). Iodine production is primarily sourced from subsurface wells. The U.S imports 99% of its iodine from Chile and Japan (Johnson, 1994). Iodine has practical uses in pharmaceutical manufacturing (x-ray machines, over the counter medications, water purification) and in component manufacturing for electronics (Brownstein, 2009).

### 7.3.1 Geochemical Statistics:

Iodine concentrations were examined using two types of plots (Figure 119) that include a combination of a histogram, density trace, boxplot, and one-dimensional scatterplot (left side) and Empirical Cumulative Distribution Function (ECDF)-plot (right side) (Reimann et al., 2008). Interpretation of the ECDF-plot shows a multi-modal distribution indicated by sub populations with breaks near 2 mg/l, 10 mg/l and 100 mg/l. The density plots, histograms, boxplots and scatterplot suggest that I concentration are left skewed, even on a log-scale, possibility indicating.

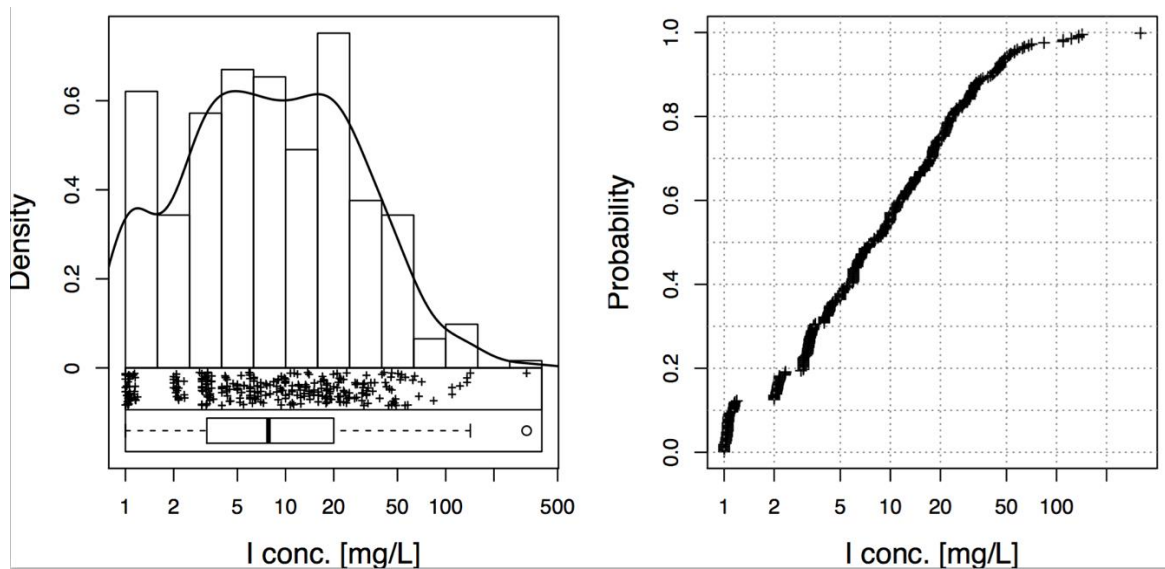


Figure 119: Permian Basin EDA-plot in log scale, which includes a combination of a histogram, density trace, boxplot, and one-dimensional scatterplot (left side) and Empirical Cumulative Distribution Function (ECDF)-plot (right side). Iodine concentrations have a multi-modal distribution.

## 7.3.2 Maps:

### 7.3.2.1 Spatial Distribution:

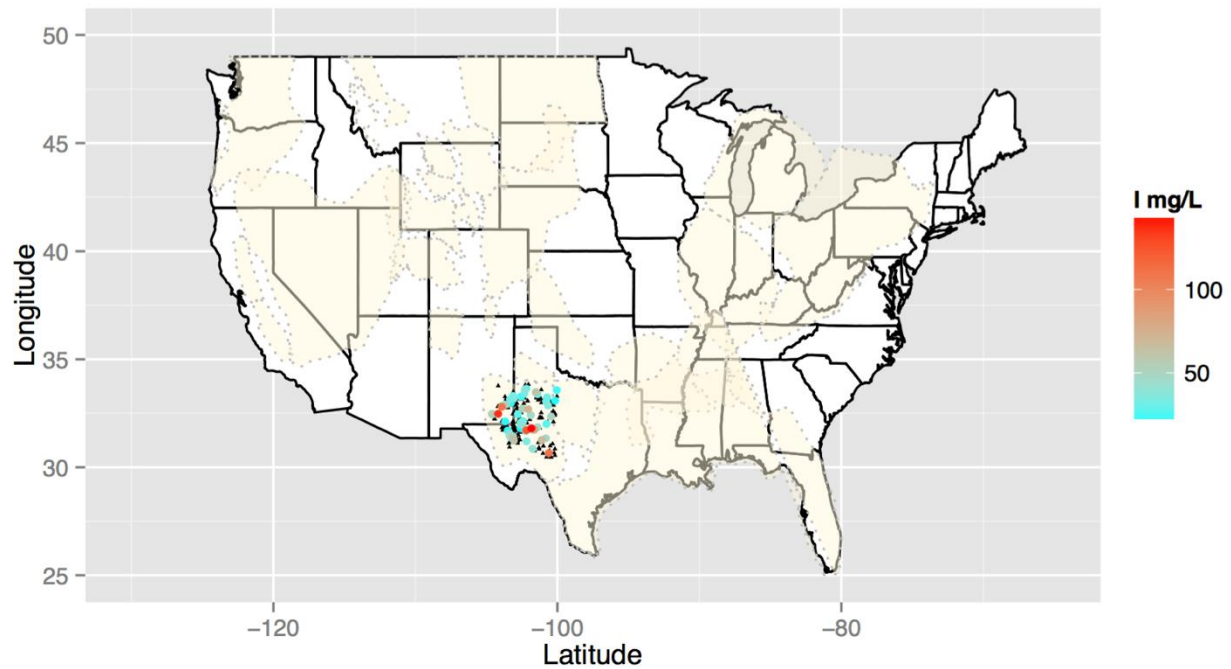


Figure 120: Permian Basin spatial concentration map for bromine. Black triangles identify locations where iodine concentration data exist but are below the 75th percentile. Color ramped symbols applied to the sites where concentrations exceed the 75th percentile.

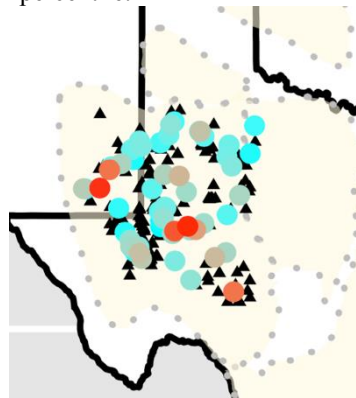


Figure 121: Magnified view of the Permian Basin spatial concentration map for iodine. Black triangles identify locations where Br concentration data exist but are below the 75th percentile. Color ramped symbols applied to the sites where concentrations exceed the 75th percentile.

Results indicate the highest concentrations of iodine found in the Permian Basin. The map shows data coverage for iodine concentrations is moderate. The exploration for spatial data

potential for iodine is relatively low. All identified locations are characterized by ancient paleoevaporated seawater; high levels of iodine are associated with organic-rich marine deposits.

#### 7.3.2.2 Estimated Economic Values:

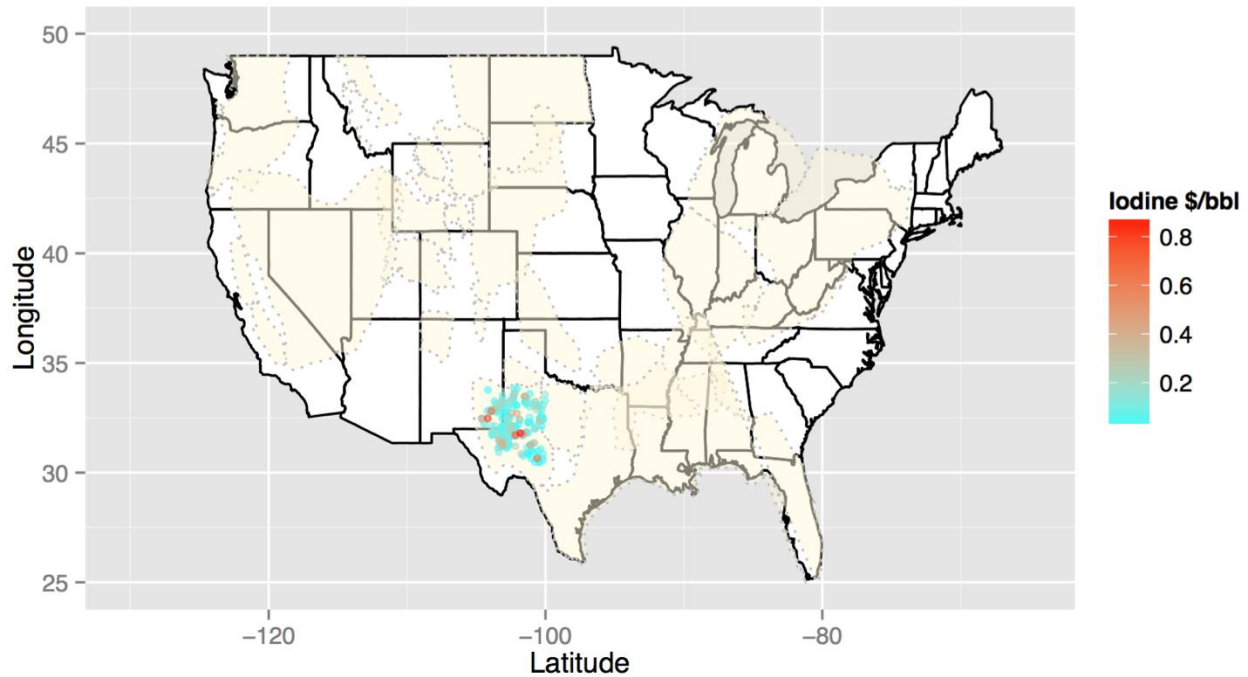


Figure 122: Permian Basin economic map for iodine identifying highest areas of interest.

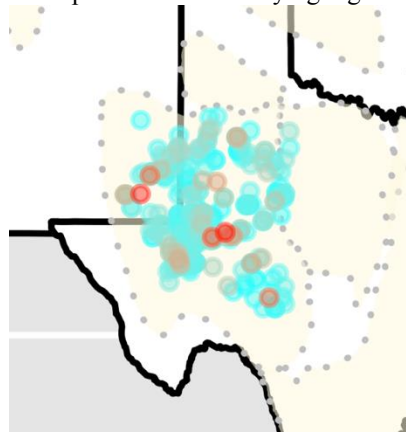


Figure 123: Magnified economic iodine Permian Basin concentration map identifying highest areas of interest.

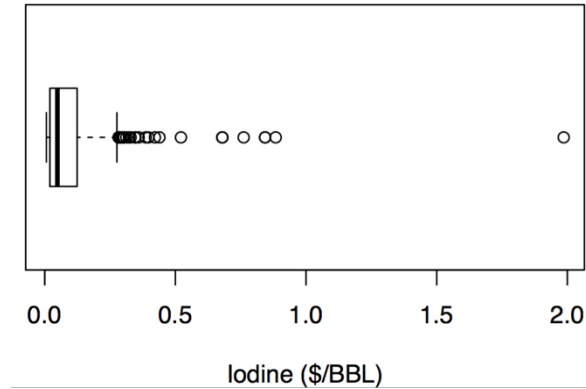


Figure 124: Tukey boxplot of economic values for identifying iodine in Permian Basin produced waters.

Iodine commodities are valued at \$39.00 per kilogram ( $3.90\text{E-}05$  per milligram). Applied to the concentration results shown in Figure 120 and 122, several areas show gross values in excess of \$0.50/bbl. Currently, iodide is produced in the Anadarko Basin and the Smackover Formation from produced waters. The development potential growth is high for iodine commodity extraction for the Permian Basin.

### 7.3.3 Summary:

Data exploration is moderately complete, the development for iodine commodity products extends into the Permian Basin. Iodine is also associated with other constituents in the Central Midwest and Gulf Coast Regions that have revenue potential, such as bromine, lithium, and magnesium (cf. Figure 1, Figure 11, Figure 51, Figure 57), it may be more economical to extract elements as a group.

#### **7.4 Lithium in the Permian Basin**

From 2003 to 2007 demand for lithium is growing by eight percent per year. Lithium commodities are divided into two commodities: lithium carbonate at \$5.64 per kilogram ( $\$3.02\text{E-}05$  per milligram per liter) and lithium hydroxide at \$7.43 per kilogram. ( $\$2.56\text{E-}05$  per milligram per liter). Due to proprietary information U.S lithium price averages are subjective and production data is withheld. Some uses for lithium are in manufacturing polymers, air purification, lithium batteries for hybrid automobiles along with glass and ceramics (Code of Federal Regulations, 2010).

#### 7.4.1 Geochemical Statistics:

Lithium that include a combination of a histogram, density trace, boxplot, and one-dimensional scatterplot (left side) and Empirical Cumulative Distribution Function (ECDF)-plot (right side) (Reimann et al., 2008). Interpretation of the EDCF-plot (Figure 125) has a slight bimodal distribution curve with a break near 1.5 mg/L and 5 mg/L. The density plots, histograms, boxplots and scatterplot suggest that the higher concentration population is right skewed.

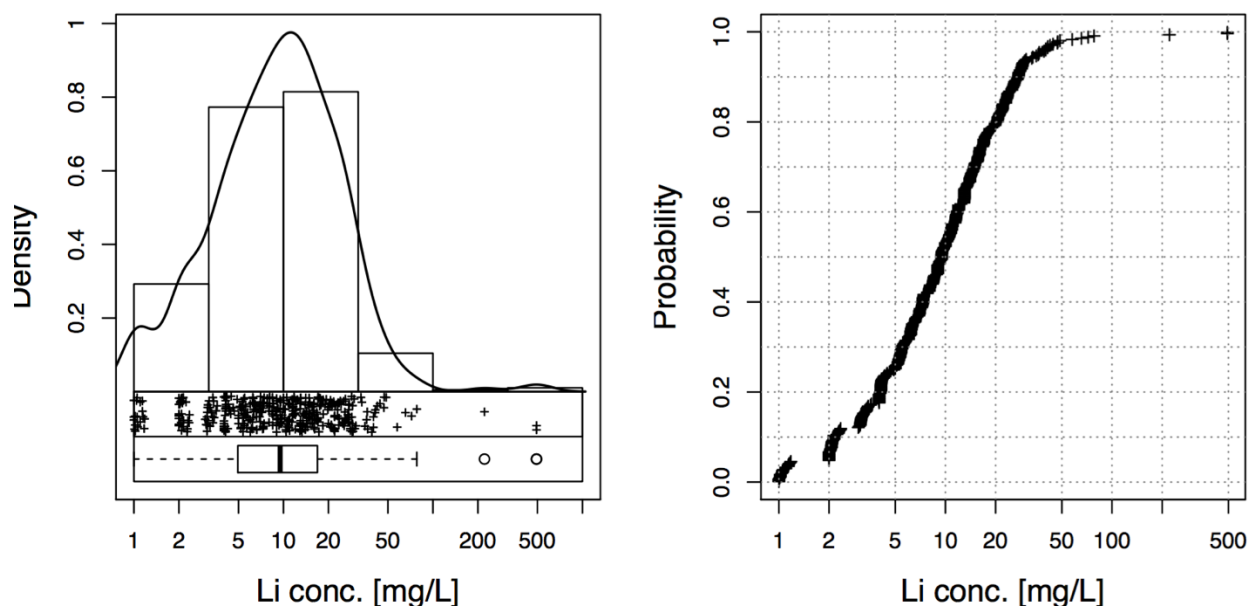


Figure 125: Permian Basin EDA-plot in log scale, which includes a combination of a histogram, density trace, boxplot, and one-dimensional scatterplot (left side) and Empirical Cumulative Distribution Function (ECDF)-plot (right side). Lithium concentrations are right skewed and the graph shows a multiple distribution.

## 7.4.2 Maps:

### 7.4.2.1 Spatial Distribution:

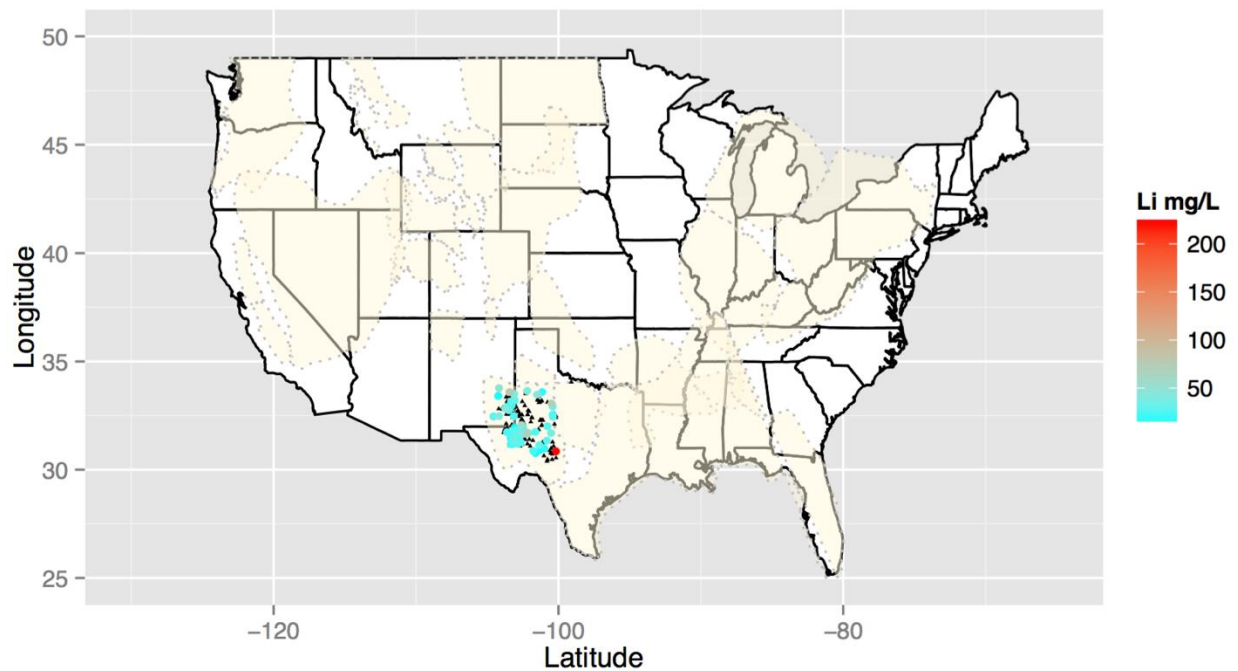


Figure 126: Permian Basin spatial concentration map for lithium. Black triangles identify locations where Li concentration data exist but are below the 75th percentile. Color ramped symbols applied to the sites where concentrations exceed the 75th percentile.

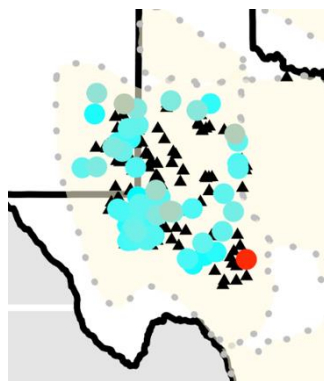


Figure 127: Magnified view of the Permian Basin spatial concentration map for lithium. Black triangles identify locations where Br concentration data exist but are below the 75th percentile. Color ramped symbols applied to the sites where concentrations exceed the 75th percentile.

The spatial distribution of lithium data is fairly moderate; the highest Li concentrations are located in the lower portion of the Permian Basin. The Permian Basin regions has moderate to

low disposal costs and therefore present opportunity for potential beneficial commodity production.

#### 7.4.2.2 Estimated Economic Values:

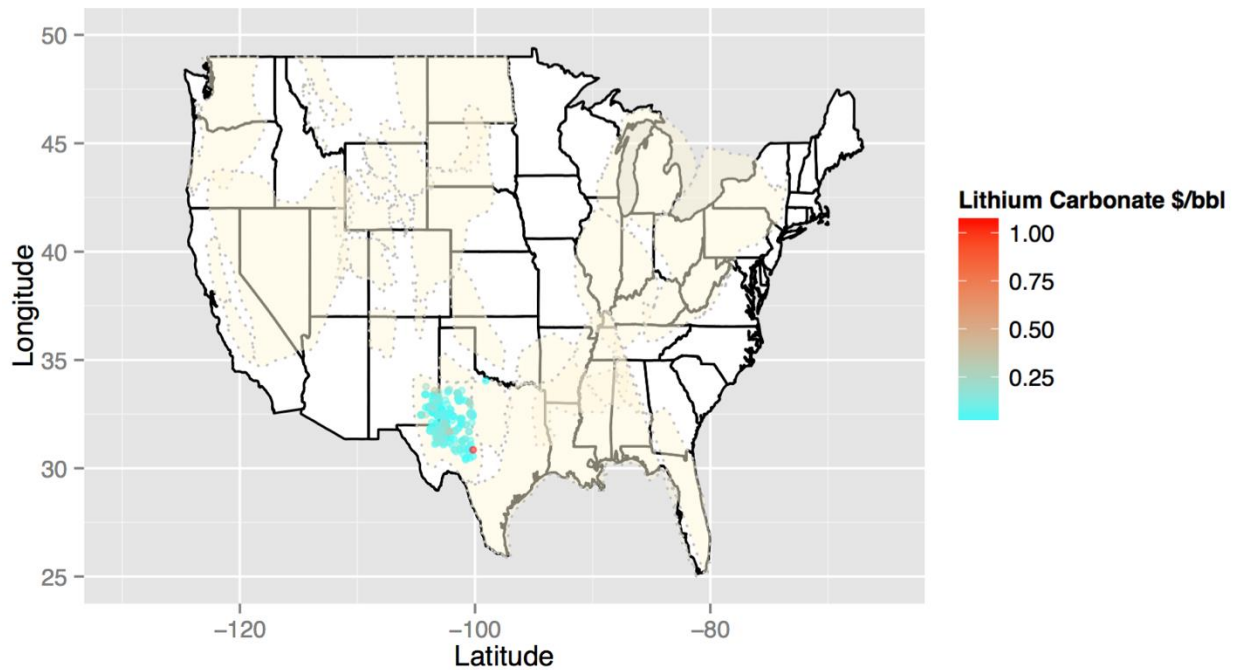


Figure 128: Permian Basin economic map for lithium carbonate identifying highest areas of interest.

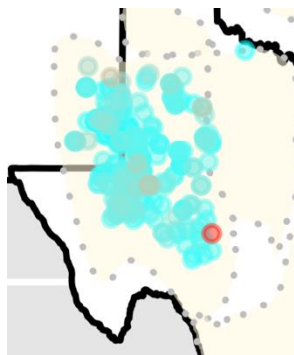


Figure 129: Magnified economic lithium carbonate Permian Basin concentration map identifying highest areas of interest.

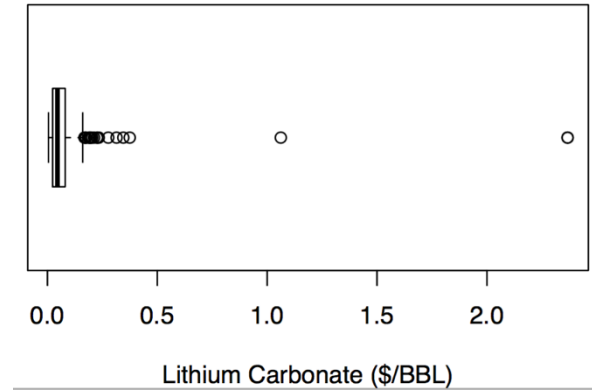


Figure 130: Tukey boxplot of economic values for identifying lithium carbonate in Permian Basin produced waters.

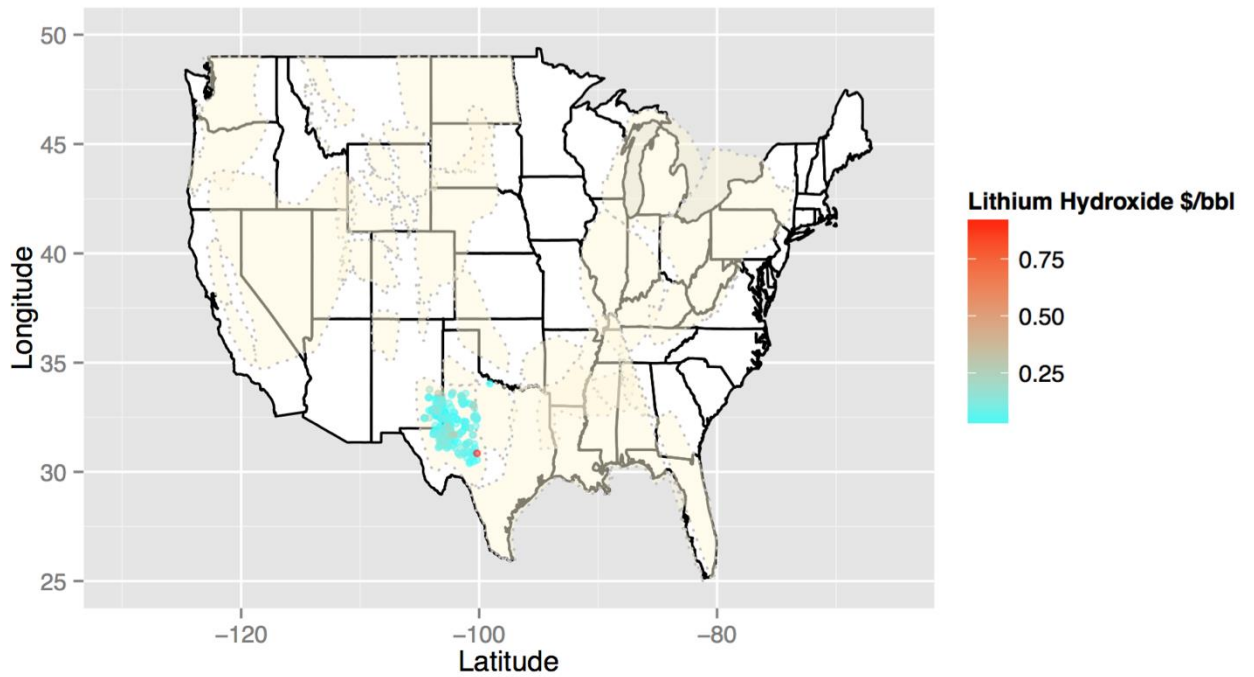


Figure 131: Economic concentration map identifying highest areas of interest.

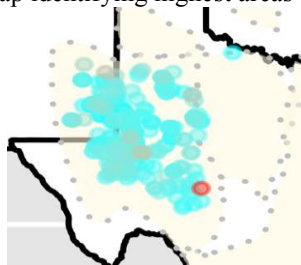


Figure 132: Magnified economic lithium hydroxide Permian Basin concentration map identifying highest areas of interest.

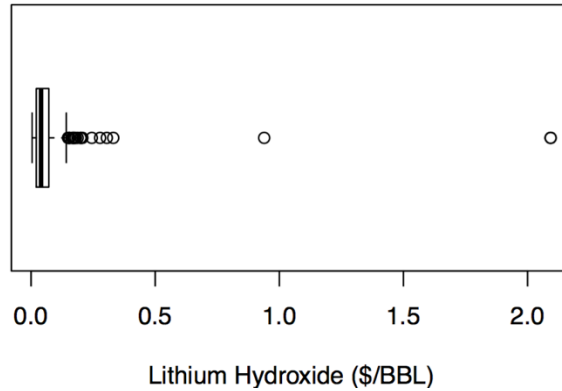


Figure 133: Tukey boxplot of economic values for identifying lithium hydroxide in Permian Basin produced waters.

Lithium commodities are divided into two commodities: lithium carbonate at \$5.64 per kilogram ( $3.02\text{E-}05$  per milligram per liter) and lithium hydroxide at \$7.43 per kilogram ( $2.56\text{E-}05$  per milligram per liter). Economic results show the potential for future lithium extraction is moderate; lithium carbonate and lithium hydroxide values approximates between \$0.25/bbl to \$0.50/bbl, with a few high outliers. These values near disposal costs and should be considered with other commodity extractions.

#### 7.4.3 Summary:

Development in produced waters for lithium commodities is currently produced in the Smackover Formation. Given the data coverage and range in values, potential for exploration of lithium in Permian Basin produced waters is moderate. To increase revenue, lithium could be combined with other co-associated commodities such as bromine, iodine, and potassium.

### **7.5 Magnesium in the Permian Basin**

Magnesium is often recovered from seawater, brines, dolomites and magnesite. According to Platts Metals Week, annual average price in 2013 was \$2.17 per pound. In 2013, there was a higher demand for magnesium hydroxides than magnesium sulfates. U.S production price averages are proprietary information and are withheld. Magnesium Investing News projects a “gradual increase” in global demand for the year 2015. Magnesium has an array of uses, ranging from the medical field to construction of metals

### 7.5.1 Geochemical Statistics:

Magnesium concentrations were examined using two types of plots (Figure 134): that include a combination of a histogram, density trace, boxplot, and one-dimensional scatterplot (left side) and Empirical Cumulative Distribution Function (ECDF)-plot (right side) (Reimann et al., 2008). Interpretation of the EDCF-plot (Figure 134) has a progressive distribution and shows a variance indicated by sub populations with breaks near 50 mg/L, 100mg/L, 400 mg/L, and 5000 mg/L. The density plots, histograms, boxplots and scatterplot suggest that Mg concentration are left skewed, on a log-scale.

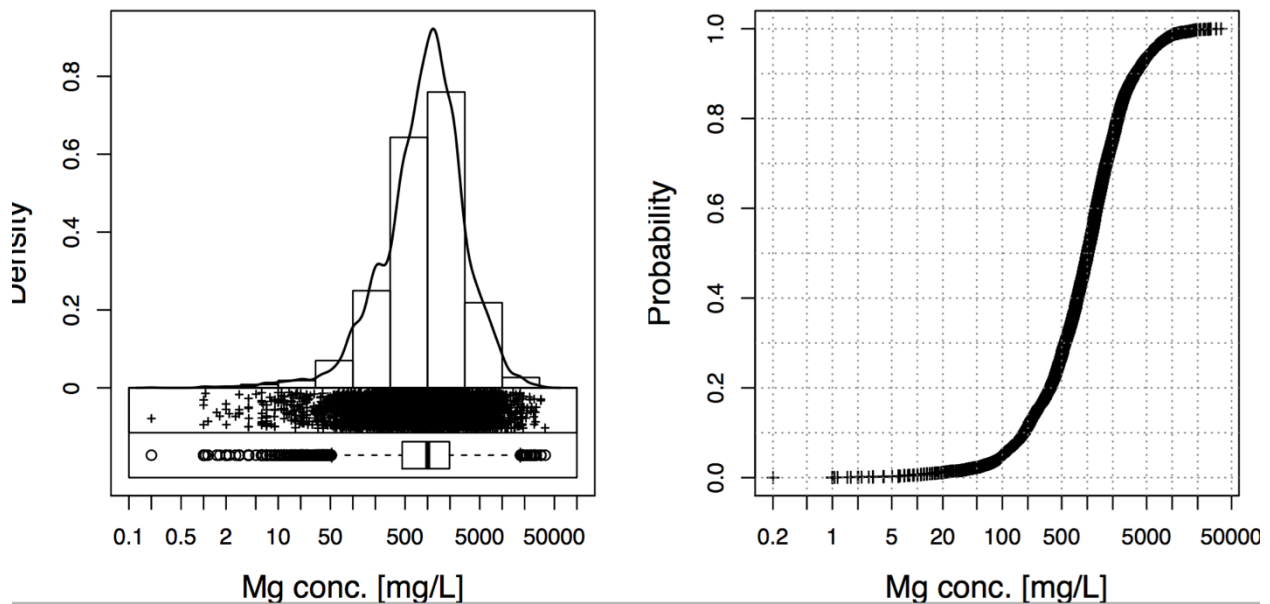


Figure 134: Permian Basin EDA-plot in log scale, which includes a combination of a histogram, density trace, boxplot, and one-dimensional scatterplot (left side) and Empirical Cumulative Distribution Function (ECDF)-plot (right side). Magnesium concentrations are left skewed and the graph shows a multiple distribution.

## 7.5.2 Maps:

### 7.5.2.1 Spatial Distribution:

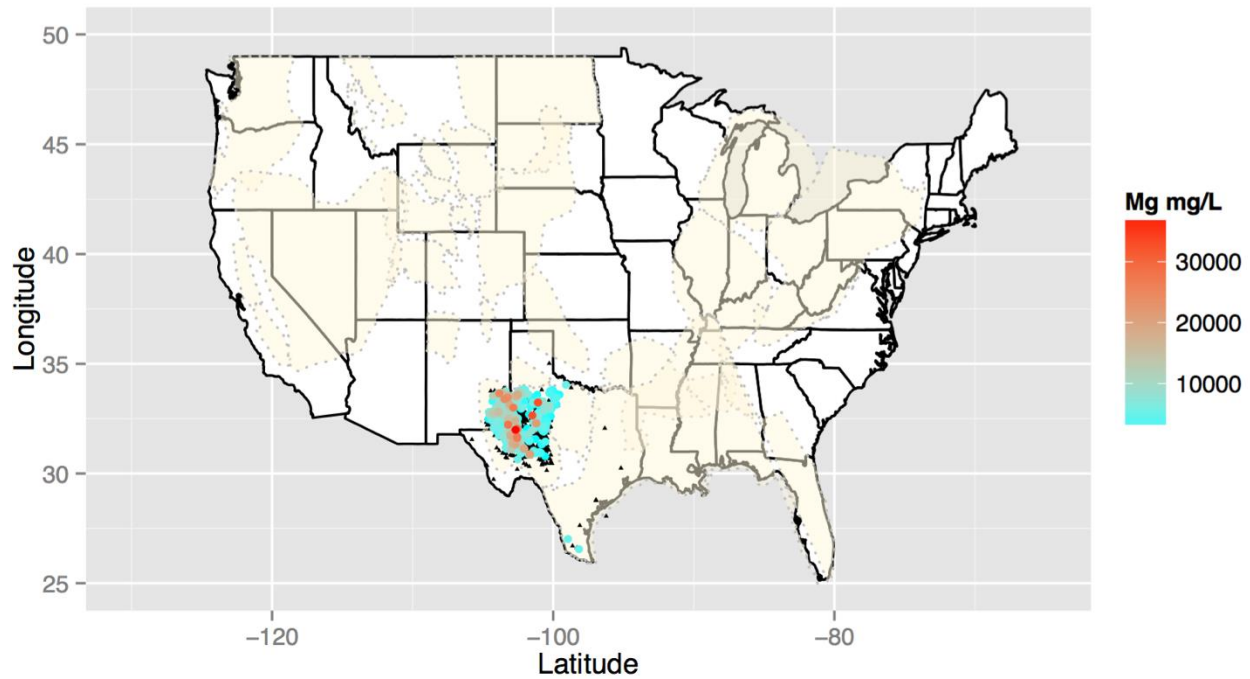


Figure 135: Permian Basin spatial concentration map for magnesium. Black triangles identify locations where Mg concentration data exist but are below the 75th percentile. Color ramped symbols applied to the sites where concentrations exceed the 75th percentile.

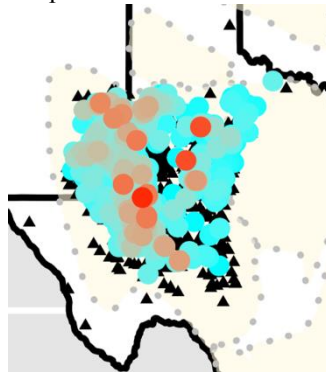


Figure 136: Magnified view of the Permian Basin spatial concentration map for magnesium. Black triangles identify locations where Br concentration data exist but are below the 75th percentile. Color ramped symbols applied to the sites where concentrations exceed the 75th percentile.

The spatial distribution of magnesium data is well established with minimal data gaps (Figure 135). Areas with the highest Mg concentrations also exhibit high TDS (Figure 1). Magnesium concentrations in some samples exceed 30,000 mg/L.

#### 7.5.2.2 Estimated Economic Values:

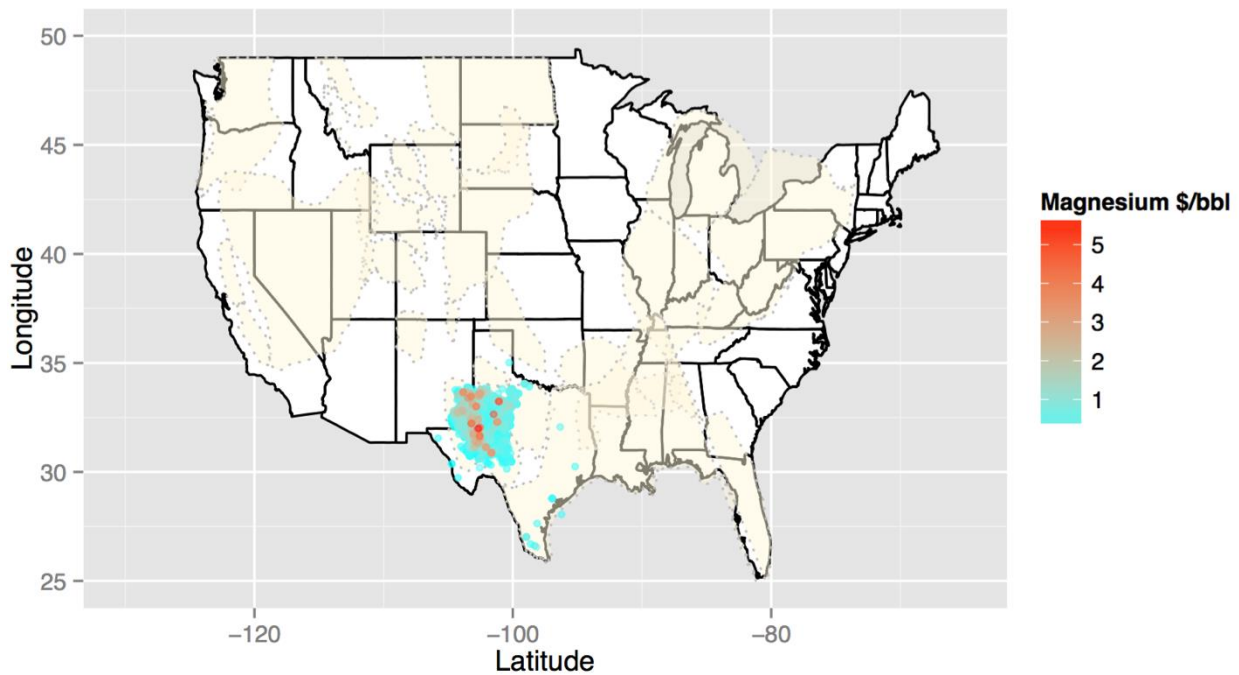


Figure 137: Permian Basin economic map for magnesium identifying highest areas of interest.

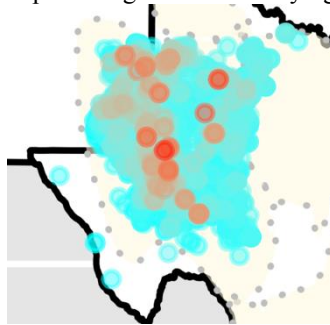


Figure 138: Magnified economic magnesium Permian Basin concentration map identifying highest areas of interest.

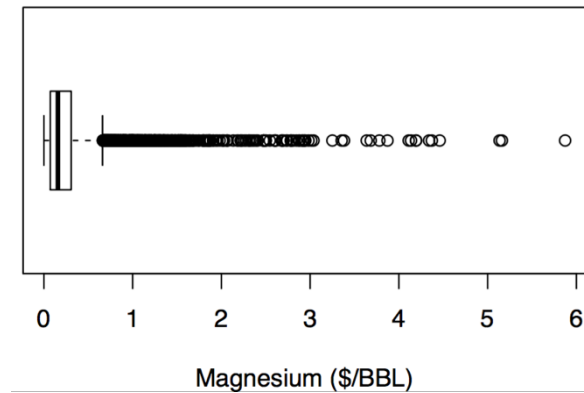


Figure 139: Tukey boxplot of economic values for identifying magnesium in Permian Basin produced waters.

Magnesium hydroxide, the primary mineral commodity produced from Mg, is valued at \$2.17 per pound (\$9.82E-07 per milligram per liter). Applied to the concentration results shown in Figure 57, Mg at \$1.00/bbl exceeds disposal costs for the Permian Basin. Magnesium extraction production is currently processed during desalination as salt products (MgCl<sub>2</sub>).

### 7.5.3 Summary:

The exploration for spatial coverage is minimal, however exploration for product extraction is high due to the availability of Mg. Development in produced waters for magnesium commodity products has a high potential and is highly probable. Magnesium can also be combined with other commodities such as bromine, iodine, and lithium, or co-produced with NaCl; many other constituents correlate well with Mg. Disposal costs become negligible when producing Mg as a commodity as it easily exceeds the expense. Magnesium chloride can be precipitated out during evaporation as a byproduct and could be considered as an additional commodity that is not identified as a commodity in the USGS Minerals Commodity.

## **7.6 Potash in the Permian Basin**

The potassium concentration in the Permian Basin makes potash a primary target for commodity production. Potash is largely produced from sylvite and langbeinite ores from underground mines and deep-well solution mining. Sylvite is crystalized using solar evaporation from brine solution and a flotation process separated the potassium chloride from byproduct sodium chloride. Potash is valued at \$350 per metric ton (\$1.07E-06 per milligram per liter). Potash is used primarily in the agriculture industry for crop and soil amendments.

### 7.6.1 Geochemical Statistics:

Potassium concentrations were examined using two types of plots (Figure 140) that include a combination of a histogram, density trace, boxplot, and one-dimensional scatterplot (left side) and Empirical Cumulative Distribution Function (ECDF)-plot (right side) (Reimann et al., 2008). Interpretation of the ECDF-plot (Figure 140) shows a variance indicated by subpopulations with breaks near 50 mg/L, 100 mg/L and 2500 mg/L. The density plots, histograms, boxplots and scatterplot suggest that potassium concentration data are slightly left skewed, on a log-scale.

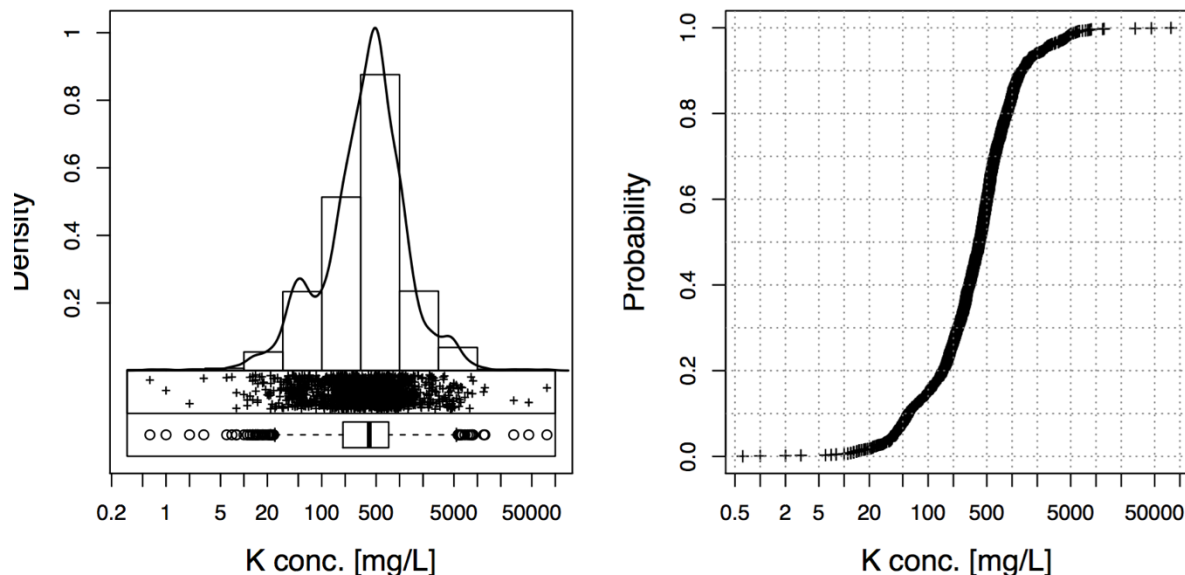


Figure 140: Permian Basin EDA-plot in log scale, which includes a combination of a histogram, density trace, boxplot, and one-dimensional scatterplot (left side) and Empirical Cumulative Distribution Function (ECDF)-plot (right side). Potassium concentrations are slightly left skewed.

## 7.6.2 Maps:

### 7.6.2.1 Spatial Distribution:

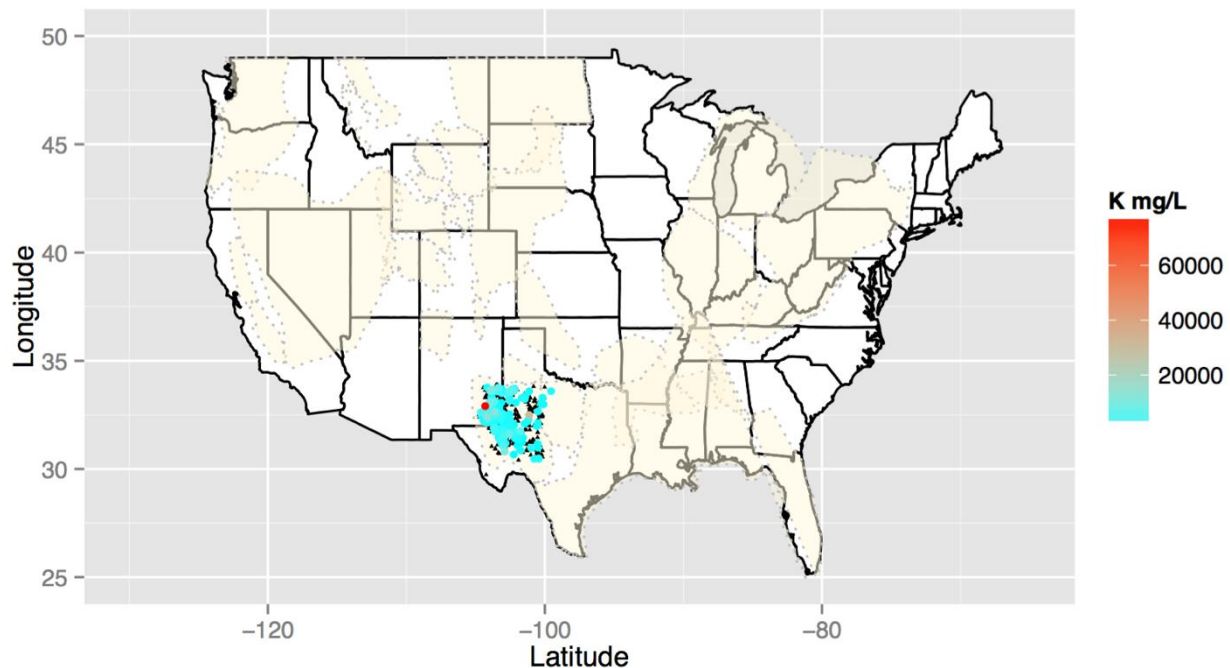


Figure 141: Permian Basin spatial concentration map for potassium. Black triangles identify locations where K concentration data exist but are below the 75th percentile. Color ramped symbols applied to the sites where concentrations exceed the 75th percentile.

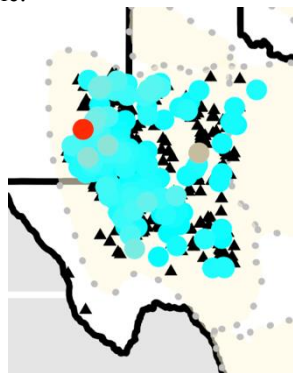


Figure 142: Magnified view of the Permian Basin spatial concentration map for potassium. Black triangles identify locations where Br concentration data exist but are below the 75th percentile. Color ramped symbols applied to the sites where concentrations exceed the 75th percentile.

The coverage for potassium is well established with a few high concentrated areas in the Delaware Basin. Moderate concentration values are found throughout the Permian Basin. Exploration for spatial data is low, exploration in extraction for other potassium based products that is not potash ash is high.

### 7.6.2.2 Estimated Economic Values:

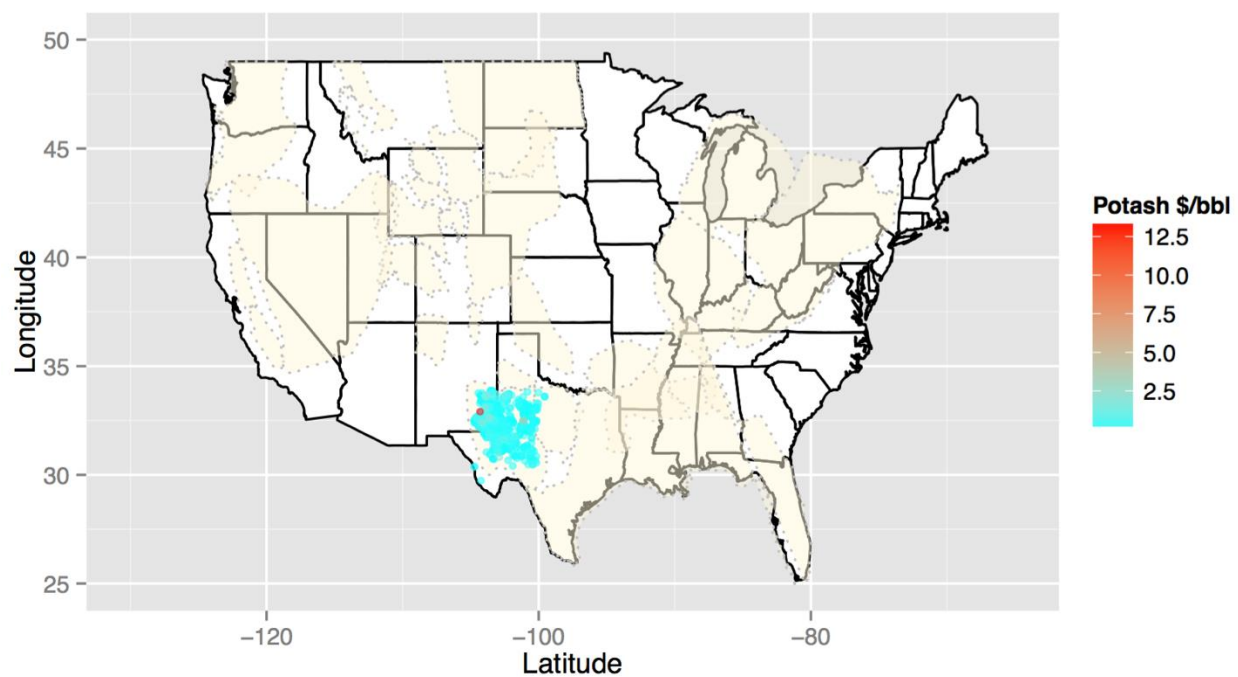


Figure 143: Permian Basin economic map for potassium identifying highest areas of interest.

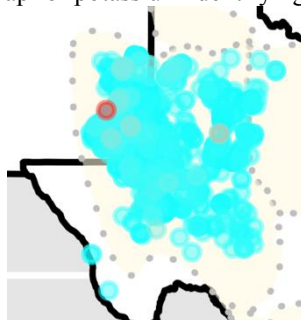


Figure 144: Magnified economic potash Permian Basin concentration map identifying highest areas of interest.

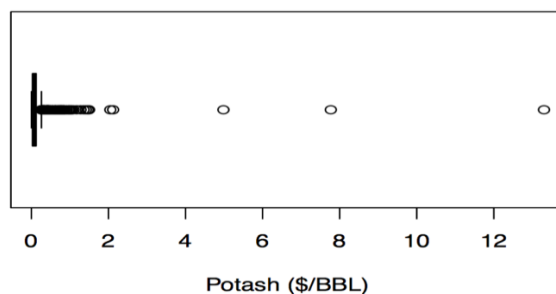


Figure 145: Tukey boxplot of economic values for identifying potash in Permian Basin produced waters.

Potash is valued at \$350 per metric ton (\$1.07E-06 per milligram per liter). Applied to the concentration results shown in Figure 141, there is potential for development. The potential value in potash exceeds even the higher range of the local disposal costs (\$0.30-\$4.00) in this region. Potash production is currently processed during deep-well solution mining from brines. Potassium chloride (KCl) can be precipitated out during evaporation as a byproduct and could be considered as an additional commodity that is not identified as a commodity in the USGS Minerals Commodity Yearbook.

### **7.6.3 Summary:**

The exploration for spatial data is low, the extraction potential is high for development in produced waters for potash and other potassium based products. Sylvite, a potassium mineral is naturally precipitation in the Delaware Basin, explaining the higher localized concentrations. To increase revenue K could be combined with other commodities such as bromine, iodine, and lithium. Potassium chloride (KCl) can be precipitated out during evaporation.

## 7.7 Maximizing Potential

To maximize the development potential in the Permian Basin, it is suggested to group the commodities together. An early statistical analysis included a Kendall Tau correlation, the results concluded the geochemical similarities between the elements within each group (thus similar methods for removal) are highly correlated. Co-extraction of associated commodities has potential to increase economic value of produced waters, given that the disposal costs are assumed constant regardless of the number of commodities removed. Any combination of the grouped commodities can prove beneficial, for the purpose of the case study it will be demonstrated with the maximum potential. In this case, the groups of commodities include alkali metals (Li, K), alkaline earth elements (Mg), and halogens (Br, I).

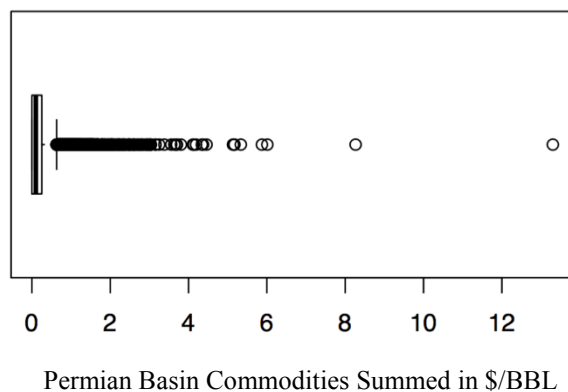


Figure 142: Boxplot of economic values for identifying bromine, iodine, lithium, magnesium, and potash values in Permian Basin produced waters.

In addition to individual maps and economic box plots, an economic box plot for the gross grouped commodity values was completed. The economic box plot (Figure 142) is a sum of all identified mineral commodities (Br, I, Li, Mg, and Potash) available in the Permian Basin. The value for these grouped commodities meets and exceeds the disposal costs for most of the Permian Basin. It is not unreasonable to anticipate profits when grouped together to exceed \$2.00/BBL,

which not only exceeds most disposals costs but also can eliminate additional costs for purchasing water by using recycled brines for other drilling operations. These groups are chosen, because of geochemical similarities between the elements within each group (thus similar methods for removal) and because, in most cases, the elements are highly correlated.

## 7.8 Regulation and Policies

The Rule of Capture governs the solution and barrier in the case of mineral commodity removal from produced waters. The State of Texas regards groundwater rights as real estate, in that groundwater can be leased or sold. Once water is produced from a well, it becomes personal property. The landowner may sever the oil and gas estate, either by a conveyance of the oil and gas estate, or by conveyance of the surface realty reserving or excepting from the conveyance the oil and gas estate. In their severed states, the oil and gas estate is considered to be the "dominant estate" and the surface the "servient estate." As the dominant estate, the owner of the oil and gas estate, in the absence of some expressed restriction or limitation to the contrary, is entitled to use as much of the premises of the surface estate "as is reasonably necessary to effectuate the purposes of the [oil and gas] lease." This right includes the right to use water from the leased premises, i.e., the groundwater in place beneath the surface (44 Tex. Tech L. Rev. 883, 922). In 1983, Texas instituted sixteen ground water conservation districts, intended for regulation and greater transparency (Texas Water Development Board, 1991). At present there are 100 of these districts. In 2011 SB 332, a provision reaffirming the landowner's rights to groundwater, while introducing the district's ability to regulate ground water production using permits (Tex. Gen. Laws 3224, 2011). The Rule of Capture asserts that a land owner attempting to extract water from beneath the property could do so even if it interferes with a neighbor's access to the resource (Tex. Water Code Ann. § 36.002 (West)).

State regulation curtails production if harm is done to the reservoir, surface owners may produce as much water as they like without exposure to surrounding landowners who might complain their aquifers are being depleted (Kulander, 2014). In 2013, the state legislature added legally binding clarifications to the previous laws of liability. The new explanations exempt

recycling companies from being held responsible for tort damages occurring from the use of their products (Whitmore, 2014).

The Rule of Capture and the case study's originality creates vulnerability due to the lack of jurisprudence addressing produced water recycling coupled with elemental extraction. As the state and federal governments seek to create clearer guidelines for the field, the case study will be subject to potential reforms from mineral extraction laws and water regulations. The state of Texas allows property owners to sell or lease their stakes in mineral rights. As a result of this, mineral rights need to be evaluated on a case by case basis. An individual can sell a property but maintain the mineral rights (Blythe and Tintera, 2014). The case study faces legal exposure that is both direct and indirect with a potential redaction to the Energy Policy Act of 2005.

The Texas Railroad Commission (RRC) ensures compliance of Texas state law with regards to the oil and gas industry. The RRC issues five types of permits based on the facility's mobility, location and a commercial behavior (Whitmore, 2014). So far the RRC has only issued nine permits to mobile recyclers of produced and/or flow back water (Railroad Commission, 2015). A commercial facility is defined as one whose owner or operator receives compensation for services (Rule 78). Rule§ 4.274(c) and §4.290(c) of Texas State law define a commercial venture as having "legitimate commercial use". State law dictates that if the operator proposes to haul fluids to off-site locations, the operator must provide written authorization from those agencies or companies involved in the trucking activity. The RRC requires permits WH-1, WH-2 and WH-3.

In New Mexico, the Oil Conservation Department (OCD) under the New Mexico Minerals and Natural Resources Department enforces state field regulations. The OCD also collects

industrial data and issues most mining permits. The New Mexico Environmental Department oversees the regulation of petroleum storage tanks and manages legislation rules and policy. New Mexico law 19.15.34.8 requires a mobile facility to obtain a permit for the transportation of produced waters (NMAC. 19.15.34.8). On March 31st of 2015, the state of New Mexico implemented a new amendment authorizing recycling of produced waters, only registration is required (19.15.34,9 B,5) (NMAC, §19.15.34,9). This new amendment provides opportunities towards environmental sustainability. State law (19.15.34 NMAC) requires a C-133 permit that provides authorization to move produced waters between locations. In the state of New Mexico all records of ownership pertaining to federal land can be obtained from the Bureau of Land Management (BLM) (Bureau of Land Management, 2015).

## 7.9 Permian Basin Summary

By utilizing mineral commodities in produced waters that are often overlooked, this case study has the ability to diversify and strengthen a local economy. The potential for success is due to the flexibility of combining mineral commodities as needed. One of the case studies greatest strength is the potential to extract valuable mineral commodities from both active and inactive injection wells. The removal of mineral commodities also has the potential to generate opportunity for employment and indirect revenue sources that gives flexibility to the energy industry making it more resilient to economic changes. It should also noteworthy, in the national evaluation rubidium and cesium are valuable commodities. There are 3 data points for Rb and none for Cs in the Permian Basin, making an economic assessment for these commodities inconclusive. Due to the geochemical relationship between K, Rb and Cs; exploration for both data and development should be included for mineral commodity extraction (Rb and Cs exceed \$20.00/bbl) in the Permian Basin.

There were 10,966 drilling and re-entry permits issued in 2014 in the Permian Basin alone (Railroad Commission of Texas, 2015). The strong presence of the Oil and Gas Industry and supporting businesses means the local population has experience or skillset that would be valuable to developing commodity products. By tapping into the regional labor pool, a proposal of this magnitude has the ability to diversify the economy through the generation of jobs. These positions are only partially contingent on the health of the energy sector because the project can operate on marginally economic wells.

The evaluation of produced waters for economic exploration and development in the Permian Basin suggests potential economic viability. The expenditures for water treatment and mining are primary drivers of capital cost and operation investments. To minimize expenses and

maximize revenues, a geochemical analyses of individual wells would be conducted to ascertain individual characteristics of mineral commodity extraction. The uniqueness of the proposal subjects the operations to potential legal exposure. The interpretation of the legal description to lease owners or operators and water right owners would need to be predetermined on a case by case basis prior to treatment or extraction. The operation could result in recycled waters and products from the commodity extraction. This combination supports local economies through job growth, product sales and the revenue that indirectly returns to the community and investment potential while being environmentally friendly in recycling produced waters. In summary, water, energy and mineral commodity portfolios for operations in the Permian Basin, in Texas has high potential for profit and ultimately recycling produced waters.

## Chapter 8. Conclusion

The most voluminous byproduct from the oil and gas industry is produced water, water that is co-generated from hydrocarbon wells. To minimize or offset disposal costs that are generated every day, this thesis evaluated the U.S Geological Survey geochemical database for mineral resource potential and exploration. Extraction of mineral resources from produced waters has beneficial reuse properties: financial revenue, commodity extraction, and waste water treatment, thus potentially decreasing volumes of wasted water. Bromine, iodine and lithium are currently generated as mineral commodities from basinal brines in the United States. However, as shown in this thesis, many constituents in produced waters have enough economic value to exceed disposal costs suggesting that the waters are potential sources for domestic mineral commodities (Figure 137). This thesis used disposal costs as the minimal criteria in determining the potential in a commodity, as values below this cutoff would consist of a net loss. Determining disposal costs is a complex issue; there is clear divisibility in what defines disposal costs as there are variety of options which are impacted by location and regulations. Moreover, commodity values are subject to the rise and fall of the worldwide economics. The value is partly determined by the industry trades, removal processing and/or availability for the commodity. The “true” value of any commodity is variable and dependent upon its final form and market.

In an attempt to quantify the relative commodity value and exploration potential of individual mineral commodities, the upper range (75<sup>th</sup>-99.9<sup>th</sup> percentiles) for the economic values (\$/bbl basis) are compared against data coverage (Figure 137). The economic values (x-axis) were taken directly from the statistics for the individual commodities. The data coverage parameter is calculated as the proportion of disposal costs areas (Table 1), wherein the number of data with reported concentrations exceed 1000 points. Although arbitrary, this proxy for data coverage

prevented high numbers of samples from individual basins from suggesting that data coverage on a national basis was adequate for characterizing concentrations. Thus, the y-axis values range from 0-1, where 0 is defined as poor data availability and values of 1 suggesting relative good data coverage. To avoid over-printing in the figure, a small amount of scatter was added along this axis. For comparative purposes, grouped disposal costs from each of the regions are provided. I identified the following constituents as being found in concentrations at some locations which exceeded disposal costs: bromine, cesium, iodine, lithium carbonate, lithium chloride, magnesium, potash, rubidium formate, rubidium chloride, and soda ash. From these identified commodities, those with the greatest potential for further data exploration are rubidium formate, rubidium chloride and cesium. These commodities are valued higher than the others, but have the least data coverage, suggesting that areas with the highest concentrations may not yet have been discovered. Those commodities with moderate coverage and with the greatest potential for development are bromine, iodine, lithium hydroxide and lithium carbonate. Because these commodities have moderate data coverage more economically advantageous areas might be defined with further geochemical exploration. It is of note that these commodities are being produced from brines from the Smackover Formation and/or Anadarko Basin. However, based on results from this study, economically feasible production of these constituents might be able expand to other basins (e.g. Permian and Appalachian) as the commodity in general exceeds most disposal costs in these basins. For magnesium, potash, and soda ash, these commodities may be found in economic concentrations and data are complete enough that there is little need for further exploration. Constituents with the lowest potential for development are the transition metals: cobalt, copper, nickel, molybdenum, zinc and mercury. The total number of data points available for these elements is <1000 data points, they are valued less than \$0.50/bbl and, in most regions, fall below

disposal costs minimums.

The greatest potential for development of produced waters is through grouping mineral commodities that already have been identified individually as targets. In the case of the Permian Basin and the Smackover Formation, revenue is maximized when grouping bromine, lithium and iodine (\$3.00/bbl to over \$5.00/bbl). There is even greater potential when other commodities can be added to these groups, such as potash, soda ash and magnesium. For basins such as the Anadarko Basin and Williston Basin, grouping cesium, rubidium, potash, soda ash and magnesium would potentially have a greater impact for revenue (\$1.00/bbl to over \$10.00/bbl; rubidium and cesium over \$20.00/bbl). Similar results may also exist in other basins, but a dearth of data for rubidium and cesium concentrations prevents extrapolation.

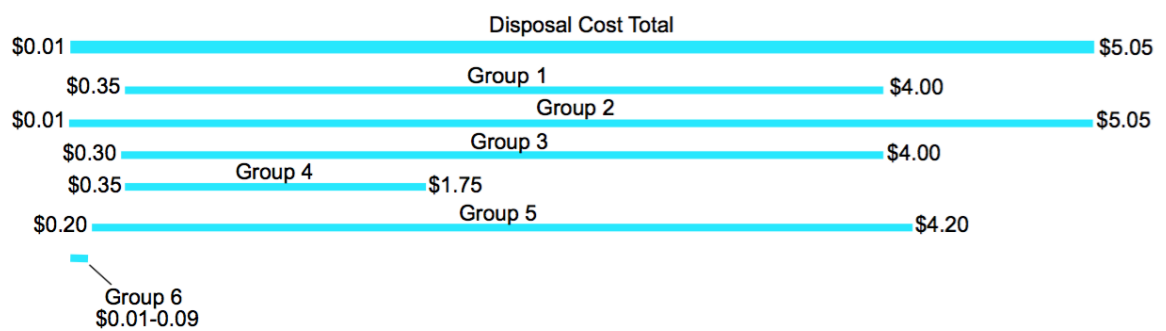
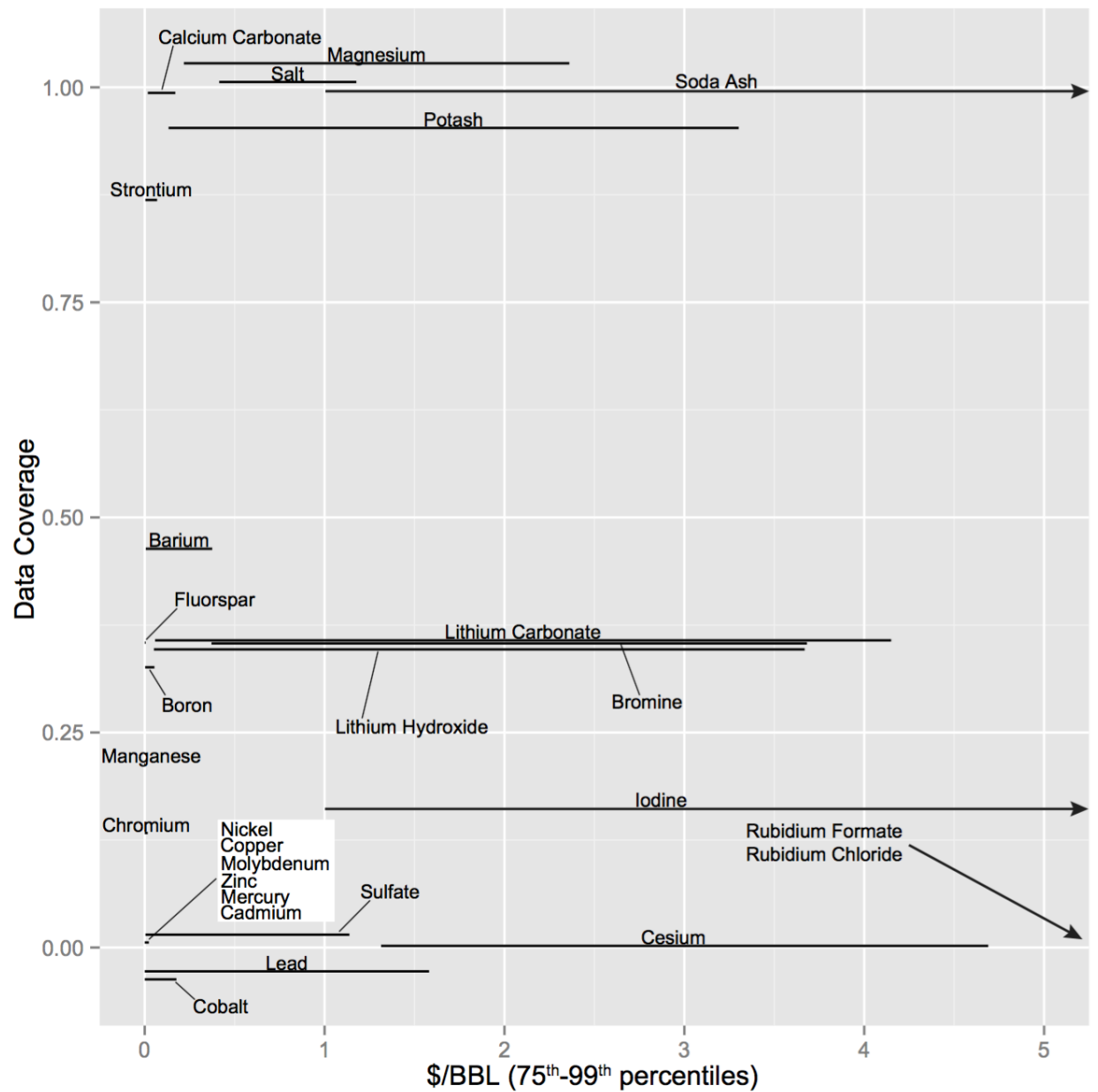


Figure 137. Complete analysis of available commodities in produced water compared to disposal costs.

In addition to mineral commodities extraction, there is both intrinsic and extrinsic value in water; desalination of produced water for re-use or recycling combined with removing mineral commodities from produced waters provides dual benefits (National Research Council., 2008). Improving water management practices and costs depend on produced water composition, geologic constraints, regulations control costs, availability for commercial treatment facilities, agricultural application, chemical production, injection to maintain reservoir pressure, and other beneficial uses (Guerra et al., 2011). When combined with water treatment and mineral commodity removal from produced waters, revenue can exceed disposal and operation costs with marketable water and a product from mineral recovery. An assessment would require a detailed analysis from an engineering team to complete and can be modified per basin and per commodity desired.

A case study for the Permian Basin was provided to determine the viability of mineral commodity extraction and combining benefits with water treatment technologies. The case study showed when commodities can be grouped, the revenue potential greatly increases relative to individual extractions. The study also demonstrated the local economy could also benefit from the introduction to a new product operation creating economic diversity within a local community. There was also an introduction to possible state or regional-level legal constraints that would have to be addressed for any regional development. There is also identification to the Permian Basin where exploration for other potential commodities can be explored for further development. Above all, in localized region, where disposal costs are at a minimum and would otherwise be easier to dispose of produced waters, profits can still be made and should be emphasized.

At the time of completing this evaluation, we were able to identify some valuable commodities, spatial data gaps that need to be completed and areas for increased development. The biggest identifiable problem that would be addressed in future work would be further exploration for

commodities where data are absent or exceptionally sparse, such as uranium and the rare earth elements (REE). The data coverage for uranium consisted of 3 data points, not enough to make an assessment, but uranium is considered a USGS commodity. Data from produced waters outside the United States have found quantifiable concentrations of REEs in produced waters. Rare earth elements are highly valuable commodities, but with a complete lack of data for the U.S., exploration is needed. In addition, future work needs to be completed for other identifiable commodities that are not inclusive of the USGS Mineral Yearbook, such as potassium chloride. An examination would also need to be completed to determine if or how extensive the chemical treatment would be for commodities such as iodine or bromine to be considered for medical grade quality for the pharmaceutical industry. In some cases, for example salt or potassium based products, it may provide useful to look for local product manufactures in determining other manufacturing needs based on local available commodities in produced waters.

## References

- Alley, B., Beebe, A., Rodgers, J., Castle, J.W., 2011. Chemical and physical characterization of produced waters from conventional and unconventional fossil fuel resources. *Chemosphere* 85, 74–82. doi:10.1016/j.chemosphere.2011.05.043
- Angino, E.E., 1970. Selective Element Recovery from Oil Field Brines. *Water Resour. Res.* 6, 1501–1504. doi:10.1029/WR006i005p01501
- Arthur, J.D., Langhus, B.G., Patel, C., Technical Summary of Oil and Gas Produced Water Treatment Technologies, Produced Water Treatment Technology 2005.
- Blondes, Madalyn S., Gans, Kathleen D., Rowan, Elisabeth L., Thordsen, James J., Reidy, Mark E., Engle, Mark A., Kharaka, Yousif K., Thomas, Burt., 2016. U.S. Geological Survey National Produced Waters Geochemical Database v2.2 (PROVISIONAL). <http://eerscmap.usgs.gov/pwapp/>
- Bots, P., Benning, L.G., Rickaby, R.E.M., Shaw, S., 2011. The role of SO<sub>4</sub> in the switch from calcite to aragonite seas. *Geol.* 39, 331–334. doi:10.1130/G31619.1
- Boggs, S.J., 2006. Principles of Sedimentology and Stratigraphy, 4th ed, J. Chem. Info. and Model. Pearson.
- Boysen, D.B., J.E. Boysen, and J.A. Boysen, 2002, Strategic Produced Water Management and Disposal Economics in the Rocky Mountain Region, presented at the 2002 Ground Water Protection Council Produced Water Conference, Colorado Springs, CO, Oct. 16-17.
- Boysen, J.E., D.B. Boysen, T. Larson and J.A. Sorensen, 2002. Field Application of the Freeze-Thaw Evaporation (FTE) Process for the Treatment of Natural Gas Produced Water in Wyoming, GRI Publication #02-0221.
- Boschee, P., 2014. Produced and Flowback Water Recycling and Reuse. *Oil Gas Facili.*, February, 17–21.

- Bray, R.B., Hanor, J.S., 1988. Spatial Variations in Subsurface Pore Fluid Properties in a Portion of Southeast of Louisiana: Implications for Regional Fluid Flow and Solute Transport. *Gulf Coast Assoc. Geol. Soc.* XL, 53–64.
- Brownstein, D., 2009 *Iodine: Why You Need It, Why You Can't Live Without It*. 4th ed. West Bloomfield, Mich.: Medical Alternatives, 2009. Ebook.
- Clark, C., Veil, J., 2009. Produced Water Volumes and Management Practices in the United States, Argonne National Laboratory Report, 64 p.
- Coday, B.D., Miller-Robbie, L., Beaudry, E.G., Munakata-Marr, J., Cath, T.Y., 2015. Life cycle and economic assessments of engineered osmosis and osmotic dilution for desalination of Haynesville shale pit water. *Desal.* 369, 188–200. doi:10.1016/j.desal.2015.04.028
- Collins, A.G., 1975. *Geochemistry of Oilfield Waters*, *Developments in Petroleum Science* 1, Elsevier, New York, 496 p.
- Collins, A.G., 1970. Finding profits in oil-well waste waters. *Chemical Engineering* 77, 165-168.
- Coumou, D., Driesner, T., Weis, P., Heinrich, C., 2009. Phase separation, brine formation, and salinity variation at Black Smoker hydrothermal systems. *J. Geophys. Res.* 114. doi:10.1029/2008JB005764
- Engle, M.A., Bern, C.R., Healy, R.W., Sams, J.I., Zupancic, J.W., Schroeder, K.T., 2011. Tracking solutes and water from subsurface drip irrigation application of coalbed methane–produced waters, Powder River Basin, Wyoming. *Environ. Geosci.* 18, 169–187.
- Engle, M.A., Reyes, F.R., Varonka, M.S., Orem, W.H., Ma, L., Ianno, A.J., Schell, T.M., Xu, P., Carroll, K.C., 2016. Geochemistry of formation waters from the Wolfcamp and “Cline” shales: Insights into brine origin, reservoir connectivity, and fluid flow in the Permian Basin, USA. *Chem. Geol.* 425, 76–92.
- Frank T.D., Gui Z. (2010) Cryogenic origin for brine in the subsurface of southern McMurdo Sound. *Antarc. Geol.* 38: 587–590.

- Guerra, K., Dahm, K., Dunderf, S., 2011. Oil and Gas Produced Water Management and Beneficial Use in the Western United States, U.S. Bureau of Reclamation Science and Technology Program Report No. 157, 113p.
- Herut, B., Starinsky, A., Katz, A., Bein, A., 1990. The role of seawater freezing in the formation of subsurface brines. *Geochim. Cosmochim. Acta* 54, 13–21. doi:10.1016/0016-7037(90)90190-V
- Hem, J.D., 1989. Study and Interpretation of the Chemical Characteristics of Natural Water, Third Edition, Water-Supply Paper 2254. Washington, D.C.
- Horner, J.E., Castle, J.W., Rodgers, J.H., 2011. A risk assessment approach to identifying constituents in oilfield produced water for treatment prior to beneficial use. *Ecotox. Environ. Safety* 74, 989–99. doi:10.1016/j.ecoenv.2011.01.012
- ICF Consulting, 2000. Overview of exploration and production waste volumes and waste management practices in the United States, 74 p.
- Johnson, K.S., 1994. Iodine. *Industrial Minerals and Rocks*, 6th edition, Society for Mining, Metallurgy, and Exploration, 583-587.
- Jones, B.F., Hanor, J.S., Evans, W.R., 1994. Sources of dissolved salts in the central Murray Basin, Australia. *Chem. Geol.* 111, 135–154. doi:10.1016/0009-2541(94)90087-6
- J.D. Arthur, B.G. Langhus, C. Patel, Technical Summary of Oil and Gas Produced Water Treatment Technologies, Produced Water Treatment Technology 2005.
- Kharaka, Y., Hanor, J., 2007. Deep fluids in the continents: I. Sedimentary basins, in: *Treatise on Geochemistry*. pp. 1–48.
- Kobelski, B, 2003, communication between Kobelski, U.S. Environmental Protection Agency, Washington, DC, and M. Puder, Argonne National Laboratory, Washington, DC, Oct. 16, 2003.

- Krauskopf, K.B., Bird, D.K., 1995. Introduction to Geochemistry 3rd Edition, 3rd ed. McGraw-Hill Companies, Inc., New York, N.Y.
- Krukowski, S.T., 2008. Iodine Production from Morrow Sandstones, Anadarko Basin. Oklahoma Geological Survey Circular 111, 39-48.
- Kurkowski, S., 2010. Iodine. Mining Engineering, 62(6), 56-56. Retrieved April 22, 2015, from EBSCO Host Connection.
- Kulander, C., 2014. 2014 Oil & Gas Case Law Update.
- Lowenstien, T.K., Hardie, L.A., Timofeeff, M.N., Demicco, R. V., 2003. Secular variation in seawater chemistry and the origin of calcium chloride basinal brines. Geol. 31, 857–760.
- Lyons, B., Tintera, J.J., 2014. Sustainable Water Management in the Texas Oil and Gas Industry. Atl. Counc. Energy Environ. Progr.
- Mackenzie, D.L., 2010. Water and Wastewater Engineering, 2nd ed, Zhurnal Eksperimental'noi i Teoreticheskoi Fiziki. McGraw-Hill Companies, Inc.
- Mantell, M., 2011. EPA Hydraulic Fracturing Study Technical Workshop #4 Water Resources Management Produced Water Reuse and Recycling Challenges and Opportunities Across Major Shale Plays, Alexandria, Virginia, March 29-30.
- Matich, Terisa,. 2014. "Magnesium Outlook 2015: Demand to Increase Gradually." Magnesium Investing News. N.p., 17
- National Research Council, 2008. Minerals, Critical Minerals, and the U.S. Economy. The National Academies Press, Washington, DC.
- Odu, S.O., Van Der Ham, A.G.J., Metz, S., Kersten, S.R.A., 2015. Design of a Process for Supercritical Water Desalination with Zero Liquid Discharge. Ind. Eng. Chem. Res. 54, 5527–5535.
- Rassenfoss, S., 2011. From Flowback to Fracturing: Water Recycling Grows in the Marcellus Shale. J. Pet. Technol. 2014 63, 48–51.

- Skalak, K.J., Engle, M.A., Rowan, E.L., Jolly, G.D., Conko, K.M., Benthem, A.J., Kraemer, T.F., 2014. Surface disposal of produced waters in western and southwestern Pennsylvania: Potential for accumulation of alkali-earth elements in sediments. *Int. J. Coal Geol.* 126, 162–170.
- Stackpole, T., 2013. A Small Part of Ohio has Secured the Ignominious Honor of Becoming the Most Successful Frackwater Dumping Ground in the State.
- Stewart, B. W., Chapman, E. C., Capo, R. C., Johnson, J. D. (2015). Origin of brines, salts and carbonate from shales of the Marcellus Formation: Evidence from geochemical and Sr isotope study of sequentially extracted fluids. *Appl. Geochem.*, 60, 78–88. <http://doi.org/10.1016/j.apgeochem.2015.01.004>
- Tao, F.T., Curtice, S., Hobbs, R.D., Sides, J.L., Wieser, J.D., Dyke, C.A., Tuohey, D., Pilger, P.F., 1993. Reverse osmosis process successfully converts oil field brine into freshwater. *Oil Gas J.* 91, 88–91.
- Theodori, G.L., Wynveen, B.J., Fox, W.E., Burnett, D.B., 2007. Public perception of desalinated water from oil and gas field operations: Data from Texas. *Society Nat. Resour.* 22, 674–685. doi:10.1080/08941920802039804
- U.S. Geological Survey, 2012. Metal Prices in the United States Through 2010, U.S. Geological Survey Scientific Investigations Report 2012-5188, 204 p.
- U.S. Geological Survey, 2014. Mineral Commodity Summaries 2014, U.S. Geological Survey, 196 p.
- U.S. Geological Survey, 2015, Mineral Commodity Summaries 2015: U.S. Geological Survey, 196 p.
- Warren, B.S., 2000. A New Bromide: Brine Is Much Better Than Oil in Arkansas --- State Is Rich in Vital Element That Can Curl Your Boots, But Dead Sea Looms Large. *Wall Street Journal*, February, 14, p. A1.

- Whitmore., 2015. Oilfield Recycling in Texas: Why Command and Control Regulations Are Stifling the End Goal. *Texas Environ. Law J.*, 44(287).
- Wilson, T.P. and Long, D.T., 1993. Geochemistry and isotope chemistry of Michigan Basin brines: Devonian formations, *Appl. Geochem.* 8, 81–100.
- Veil, J., 2015. U.S. Produced Water Volumes and Management Practices in 2012, *Veil Environmental Report*, 119 p.

## Appendix A- Potential Mineral Commodities of Produced Waters

Mineral Commodity	Defense Logistics Agency Strategic Materials	USGS Produced Waters Database	Mineral Commodity	Defense Logistics Agency Strategic Materials	USGS Produced Waters Database
Abrasives			Magnesium	X	X
Aluminum	X	X	Manganese	X	X
Antimony	X		Mercury	X	X
Arsenic		X	Mica		
Asbestos			Molybdenum	X	
Barite		X, as barium	Neodymium	X	
Bauxite	X		Nickel	X	X
Beryllium	X	X	Niobium / Tantalum		
Bismuth	X		Nitrogen		
Boron	X	X	Oxygen		
Bromine		X	Peat		
Cadmium	X	X	Perlite		
Calcium		X	Phosphate Rock		
Carbon		X, as alkalinity	Phosphorus		X, as phosphate
			Platinum and Platinum Groups		
Cement			Metals	X	
Cerium	X		Potash		
Cesium		X	Potassium		X
Chlorine		X	Praseodymium	X	
Chromium	X	X	Promethium		
Clay			Pumice		
Coal Combustion Products			Quartz	X	
Cobalt			Rare Earths		
Copper	X	X	Rhenium	X	X
Crushed Stone			Rubidium		X
Diamond			Salt (sodium chloride)		X, as ions
Diatomite			Samarium	X	
Dimension Stone			Sand and Gravel		
Dysprosium	X		Scandium	X	
Erbium	X		Selenium	X	X
Europium	X		Silica	X	X

Feldspar			Silicon	X	
Fluorspar	X	X	Silver	X	X
Gadolinium			Soda Ash		
Gallium	X		Sodium sulfate		X, as ions
Garnet			Stone		
Gemstones			Strontium	X	X
Germanium	X		Sulfur		X
Gold			Talc	X	
Graphite			Tantalum	X	
Gypsum			Tellurium	X	
Hafnium	X		Terbium	X	
Helium			Thallium		
Holmium	X		Thorium		
Indium	X		Thulium	X	
Iodine		X	Tin		
Iron and Steel			Titanium	X	X
Iron Ore		X, as total iron	Tungsten	X	
Iron Oxide Pigments			Vanadium	X	X
Kyanite			Vermiculite		
Lanthanum	X		Wollastonite		
Lead	X	X	Ytterbium	X	
Lime			Yttrium	X	
Lithium	X	X	Zeolites		
Lutetium	X		Zinc	X	X
			Zirconium	X	

The potential mineral commodities of produced water appendix were created to help identify strategic commodities between the Defense Logistics Agency and United States Geological Survey.

Appendix B- Kendall Tau Correlation Table

The Kendall Tau Correlation Table is the complete statistical analysis of all previously discussed constituents found in the USGS Geochemical Produced Waters database that were used to analyze each individual commodity. The individual statistics can be found in each chapter.

#1	TDSUSGS	As	B	BO3	Ba	Be	Br	HCO3	Ca	Cd	Cl	Co	Cr	Cs	Cu	F	FeTot	FeIII	FeII	FeI	FeAl	FeAl2O3	Hg	I	K	Kna	Li	Mg	Mn	Mo	Na	Ni	P	Pb	Rb	S	SO4	Se	Si	Sn	Sr	Th	Ti	Tl	U	V	Zn	TOC							
TDSUSGS	1	0.27	0.50	-0.06	0.37	0.59	0.73	-0.37	0.72	0.39	0.94	0.55	0.43	0.25	0.54	0.30	0.29	0.27	0.31	0.27	0.27	0.30	-0.16	0.20	0.70	0.65	0.63	0.66	0.6	0.49	0.92	0.53	0	0.58	0.53	-0.24	0.05	0.62	-0.10	0.19	0.69	0.27	0.18	0.36	-0.33	0.33	0.48	0.03							
As	0.27	1	0.58		0.13	0.02	0.26	0.17	-0.15	0.29	0.36	0.32	0.28	0.69	0.34	0.39	0.17						0.13	-0.11	0.39	0.17	0.39	-0.05	0.16	0.53	0.39	0.24		0.29	0.35	0.02	0.25	0.34	0.38	0.39	0.16	0.16	0.32	0.27	1	0.38	0.14	0.09							
B	0.50	0.58	1		0.40	0.14	0.53	0.13	0.29	0.28	0.50	0.44	0.49	0.31	0.41	0.41	0.39					-0.42	0.01	0.36	0.53	0.27	0.44	0.29	0.38	0.58	0.53	0.43		0.38	0.39	0.08	0.18	0.54	0.23	-0.08	0.5	0.10	0.18	0.05	-0.33	0.41	0.37	0.01							
BO3	-0.06		1	1	0.07		0.36	0.05	0.03		-0.08			0.23	-0.67		0.03					-0.10		0.00	0.09		0.37	-0.19	-0.06		-0.07			0.48		-0.26		0.03		0.07				-0.09	0.48										
Ba	0.37	0.13	0.40	0.07	1	0.58	0.48	-0.13	0.34	0.33	0.37	0.58	0.52	0.33	0.37	0.19	0.31	0.16	0.18			-0.25	-0.07	-0.01	0.41	1	0.55	0.32	0.53	0.10	0.36	0.38		0.45	0.23	-0.02	-0.24	0.34	-0.01	0.18	0.50	0.18	0.16	0.26	0.33	0.02	0.35	-0.09							
Be	0.59	0.02	0.14		0.58	1	0.61	-0.28	0.46	0.48	0.59	0.46	0.52	1	0.67	-0.1	0.59						0.16	-0.42	0.38		0.54	0.43	0.51	0.36	0.59	0.61		0.75	0.13	-0.02	-0.30	0.55	0.17	0.87	0.57	-0.91	0.05	0.54		0.45	0.49	0.05							
Br	0.73	0.26	0.53	0.36	0.48	0.61	1	-0.21	0.77	0.52	0.74	0.63	0.47	0.25	0.53	0.39	0.57					-0.07	-0.22	0.28	0.64	0.09	0.59	0.65	0.63	0.42	0.66	0.49		0.64	0.42	-0.22	0.13	0.56	-0.20	0.14	0.75	0.22	0.20	0.35	-0.33	0.14	0.52	0.10							
HCO3	-0.37	0.17	0.13	0.05	-0.13	-0.28	-0.21	1	-0.47	0.08	-0.38	0.31	0.11	0.05	-0.01	0.16	-0.12	-0.19	-0.21	-0.10		-0.30	-0.02	0.08	-0.19	-0.25	-0.12	-0.44	-0.09	0.26	-0.35	0.26	0.41	0.16	-0.20	0.27	0.00	0.25	0.19		-0.31	0.35		1	0.23	-0.10	-0.10								
Ca	0.72	-0.15	0.29	0.03	0.34	0.46	0.77	-0.47	1	0.41	0.71	0.60	0.34	0.20	0.49	0.00	0.30	0.34	0.30	0.22	0.29	-0.16	0.18	0.61	0.38	0.53	0.76	0.55	0.19	0.65	0.52	1	0.52	0.49	-0.31	0.06	0.52	-0.04	0.12	0.73	0.20	0.22	0.34	-0.33	0.07	0.45	0.03								
Cd	0.39	0.29	0.28		0.33	0.48	0.52	0.08	0.41	1	0.35	0.61	0.62	0.15	0.63	0.26	0.22					-0.08	-0.16	0.35		0.39	0.38	0.41	0.48	0.34	0.55		0.62	0.37	0.04	0.15	0.63	-0.46	0.29	0.35	0.02	0.14	-0.12	0.23	0.57	-0.02									
Cl	0.94	0.36	0.50	-0.08	0.37	0.59	0.74	-0.38	0.71	0.35	1	0.54	0.43	0.26	0.49	0.29	0.30	0.27	0.30	0.27	0.30		-0.13	0.21	0.69	0.64	0.62	0.65	0.56	0.46	0.90	0.46	-0.55	0.54	0.53	-0.24	0.04	0.60	-0.10	0.14	0.69	0.22	0.20	0.36	-0.33	0.32	0.45	0.03							
Co	0.55	0.32	0.44		0.58	0.46	0.63	0.31	0.60	0.61	0.54	1	0.53	0.54	0.48	0.36	0.47					0.25	-0.19	0.46	0.58	0.54	0.61	0.44	0.46	0.70	0.65	0.39	0.04		0.65	0.39	0.04	0.20	0.59	0.12	0.32	0.64	0.23	0.13	0.41		-0.05	0.51	-0.16						
Cr	0.43	0.28	0.49		0.52	0.52	0.47	0.11	0.34	0.62	0.43	0.53	1	0.56	0.52	0.29	0.11					-0.14	0.36	0.36	-0.11	0.56	0.29	0.43	0.47	0.44	0.52		0.60	0.44	-0.01	0.36	0.51	0.04	0.30	0.41	-0.47	-0.02	0.07		-1	0.21	0.36	0.04							
Cs	0.25	0.69	0.31	0.23	0.33	1	0.25	0.05	0.20	0.15	0.26	0.54	0.56	1	0.04	0.01	0.17						0.03	0.27			0.32	0.10	0.37	0.03	0.21	0.18			0.14	0.46		-0.19	0.47	-0.11		0.27		-1	0.80	0.26	0.19								
Cu	0.54	0.34	0.41	-0.67	0.37	0.67	0.53	-0.01	0.49	0.63	0.49	0.48	0.52	0.04	1	0.25	0.4						-0.09	0.04	0.50	-0.09	0.55	0.46	0.43	0.39	0.51	0.53		0.55	0.16	0.44	0.31	0.63	-0.47	0.46	0.49	-0.07	0.02	0.33		0.21	0.60	0.10							
F	0.30	0.39	0.41		0.19	-0.1	0.39	0.16	0.00	0.26	0.29	0.36	0.29	0.01	0.25	1	0.25						0.08	-0.05	0.34		0.38	-0.02	0.15	0.35	0.39	0.35	0.33	0.32	0.21	0.08	0.23	0.31	0.13	0.17	0.23	0.16	0.11	0.23	-1	0.14	0.12	0.07							
FeTot	0.29	0.17	0.39	0.03	0.31	0.59	0.57	-0.12	0.30	0.22	0.30	0.47	0.11	0.17	0.40	0.25	1	-1	-0.33			0.91	-0.19	0.13	0.41	-0.13	0.56	0.28	0.60	0.26	0.33	0.33	0.49	0.11	-0.27	-0.04	0.46	-0.02	0.15	0.52	0.49	0.22	0.17	0.31	1	0.14	0.44	0.06							
FeIII	0.27				0.16			-0.19	0.34		0.27						-1.00	1	0.51																																				
FeII	0.31				0.18			-0.21	0.30		0.30						0.33	0.51	1																																				
FeAl	0.27							-0.10	0.22		0.27									1																																			
FeAl2O3	0.30		-0.42	-0.10	-0.25		-0.07	-0.30	0.29		0.30						0.91					1		-0.27	0.49		1	0.33																											
Hg	-0.16	0.13	0.01		-0.07	0.16	-0.22	-0.02	-0.16	-0.08	-0.13	0.25	-0.14		-0.09	0.08	-0.19						1		0.09	-0.08		-0.12	-0.13	-0.22	0.10	-0.15	0.10			0.24	0.14	0.05	0.12		0	0.01	0.45	-0.19		0.06	0.42		-0.01	-0.04	-0.04				
I	0.20	-0.11	0.36	0.00		-0.01	-0.42	0.28	0.08	0.18	-0.16	0.21	-0.19	0.36	0.03	0.04	-0.05	0.13				-0.27	0.09	1	0.2		0.12	0.12	0.27	0.13	0.20	-0.37	0.14	-0.04		0.14	-0.04		0.11		0.27			0.38	0.09	0.21									
K	0.70	0.39	0.53	0.09	0.41	0.38	0.64	-0.19	0.61	0.35	0.69	0.46	0.27	0.50	0.34	0.41	0.26	0.18				0.49	-0.08	0.20		1	0.16	0.66	0.57	0.51	0.44	0.67	0.46	0	0.53	0.66	-0.13	0.21	0.53	-0.03		0	0.60	0.28	0.26	0.19	-0.33	0.36	0.45	0.08					
Kna	0.65		0.27		1		0.09	-0.25	0.38		0.64		-0.11		-0.09		-0.13								1				0.55	-0.26																									
Li	0.63	0.39	0.44	0.37	0.55	0.54	0.59	-0.12	0.53	0.39	0.62	0.58	0.56	0.32	0.55	0.38	0.56					1	-0.12	0.12	0.66		1	0.53	0.58	0.43	0.61	0.56			0.51	0.64	-0.04	0.17	0.57	-0.15	0.14	0.68	0.27	0.12	0.37	-0.33	0.20	0.51	0.00						
Mg	0.66	-0.05	0.29	-0.19	0.32	0.43	0.65	-0.44	0.76	0.38	0.65	0.54	0.29	0.10	0.46	-0.02	0.28	0.29	0.25	0.20	0.33	-0.13	0.12	0.57	0.55	0.53	1	0.53	0.20	0.61	0.47	0.33	0.49	0.42	-0.30	0.09	0.46	-0.11	0.08	0.62	0.33	0.22	0.31	-0.33	0.13	0.44	0.00								
Mn	0.60	0.16	0.38	-0.06	0.53	0.51	0.63	-0.09	0.55	0.41	0.56	0.61	0.43	0.37	0.43	0.15	0.60					-0.22	0.27	0.51	-0.26	0.58	0.53	1	0.36	0.59	0.43	-1	0.58	0.35	-0.21	0.17	0.43	0.01	0.14	0.64	0.04	0.16	0.34	-1	0.26	0.48	0.06								
Mo	0.49	0.53	0.58		0.10	0.36	0.42	0.26	0.19	0.48	0.46	0.44	0.47	0.03	0.39	0.35	0.26					0.10	0.13	0.44		0.43	0.20	0.36	1	0.57	0.39		0.54	0.02	0.12	0.42	0.43	0.39	0.31	0.31	0.03	0.17	0.38		0.45	0.37	0.12								
Na	0.92	0.39	0.53	-0.07	0.36	0.59	0.66	-0.35	0.65	0.34	0.90	0.46	0.44	0.21	0.51	0.39	0.26	0.22	0.27	0.28	0.28	-0.15	0.2	0.67	0.38	0.61	0.61	0.59	0.57	1	0.43	-0.55	0.56	0.51	-0.23	0.05	0.58	-0.12	0.15	0.63	0.17	0.17	0.36	-0.33	0.40	0.47	0.00								
Ni	0.53	0.24	0.43		0.38	0.61	0.49	0.26	0.52	0.55	0.46	0.70	0.52	0.18	0.53	0.35	0.33					0.10	-0.37	0.46		0.56	0.47	0.43	0.39	0.43	1		0.65	0.27	-0.02	0.26	0.59	-0.11	0.42	0.52	0.11	0.12	0.51		0.05	0.46	-0.09								
P	0.00						0.41	1		-0.55						0.33	0.33																																						

## Appendix C - Comparison of available treatment technologies

Treatment	Advantages	Disadvantages	Oil and gas produced water applications
<b>Corrugated plate separator</b>	No energy required, cheaper, effective for bulk oil removal and suspended solid removal, with no moving parts, this technology is robust and resistant to breakdowns in the field	Inefficient for fine oil particles, requirement of high retention time, maintenance	Oil recovery from emulsions or water with high oil content prior to discharge. Produced water from water-driven reservoirs and water flood production are most likely feed stocks. Water may contain oil and grease in excess of 1000 mg/L.
<b>Centrifuge</b>	Efficient removal of smaller oil particles and suspended solids, lesser retention time high-throughput	Energy requirement for spinning, high maintenance cost	
<b>Hydroclone</b>	Compact modules, higher efficiency and throughput for smaller oil particles	Energy requirement to pressurize inlet, no solid separation, fouling, higher maintenance cost	
<b>Gas floatation</b>	No moving parts, higher efficiency due to coalescence, easy operation, robust and durable	Generation of large amount of air, retention time for separation, skim volume	
<b>Extraction</b>	No energy required, easy operation, removes dissolved oil	Use of solvent, extract handling, regeneration of solvent	Oil removal from water with low oil and grease content (<1000 mg/L) or removal of trace quantities of oil and grease prior to membrane processing. Oil reservoirs and thermogenic natural gas reservoirs usually contain trace amounts of liquid hydrocarbons.
<b>Ozone</b>	Easy operation, efficient for primary treatment of soluble constituents	On-site supply of oxidizer, separation of precipitate, byproduct CO <sub>2</sub> , etc.	
<b>Adsorption</b>	Compact packed bed modules, cheaper, efficient	High retention time, less efficient at higher feed concentration	
<b>Lime softening</b>	Cheaper, accessible, can be modified	Chemical addition, post-treatment necessary	These technologies typically require less power and less pretreatment than membrane technologies. Suitable produced waters will have TDS values between 10,000 and 1000 mg/L. Some of the treatments remove oil and grease contaminants and some of them require oil and grease contaminants to be treated before these operations
<b>Ion-exchange</b>	Low energy required, possible continuous regeneration of resin, efficient, mobile treatment possible	Pre- and post-treatment require for high efficiency, produce effluent concentrate	
<b>Rapid spray evaporation</b>	High quality treated water, higher conversion efficiency	High energy required for heating air, required handling of solids	
<b>Freeze-thaw evaporation</b>	No energy required, natural process, cheaper	Lower conversion efficiency, long operation cycle	
<b>Microfiltration</b>	Higher recovery of fresh water, compact modules	High energy required, less efficiency for divalent, monovalent salts, viruses, etc.	Removal of trace oil and grease, microbial, soluble organics, divalent salts, acids, and trace solids.
<b>Ultrafiltration</b>	Higher recovery of fresh water, compact modules, viruses and organics, etc. removal	High energy, membrane fouling, low MW organics, salts, etc	Contaminants can be targeted by the selection of Ultrafiltration Membrane removes ultraparticles the membrane.
<b>Reverse osmosis</b>	Removes monovalent salts, dissolved contaminants, etc., compact modules	High pressure requirements, even trace amounts of oil and grease can cause membrane fouling	Removal of sodium chloride, other monovalent salts, and other organics. Some organic species may require pretreatment. While energy costs increase with higher TDS, RO is able to efficiently remove salts in excess of 10,000 mg/L.
<b>Activated sludge</b>	Cheaper, simple and clean technology	Oxygen requirement, large dimensions of the filter	Removal of suspended and trace solids, ammonia, boron, metals, etc. Post-treatment is normally required to separate biomass, precipitated solids, Constructed dissolved gases, etc.
<b>Constructed wetland treatment</b>	Cheaper, efficient removal of dissolved and suspended contaminants	Retention time requirement, maintenance, temperature and pH effects	

## Appendix D– National Summary Statistics

	MIN	Q_0.05	Q1	MEDIAN	MEAN-log	MEAN	Q3	Q_0.95	MAX	SD	MAD	Pseudosigma	CV %	CVR %
TDSUSGS	2	1644	10020	50120	34950	93510	155000	308600	528700	101300	68690	107400	108.3	137
As	1.00E-06	0.00135	0.006	0.024	0.04047	0.4335	0.41	2.325	13	0.8484	0.03262	0.2995	195.7	135.9
B	0.007	0.075	0.37	5.1	3.157	19.83	23	72	650	43.48	7.366	16.78	219.3	144.4
BO3	1	10	93.8	152.2	113.2	152.3	217.2	282	377	85.34	95.21	91.48	56.05	62.56
Ba	0	0.042	2	14	8.53	93.89	69	401.2	13600	343.5	20.61	49.67	365.8	147.2
Be	4.00E-05	6.00E-04	0.002	0.01	0.007524	0.02366	0.04	0.054	0.3	0.037	0.01396	0.02817	156.4	139.6
Br	0.01	0.04	3.45	117.9	37.77	538.5	667	2220	10600	966.9	174.7	491.9	179.5	148.2
HCO3	0	37.3	146	342	346.2	820.1	905.2	2611	241600	2445	375.2	562.8	298.1	109.7
Ca	0	16	168	1405	982.5	5580	7530	23660	170600	9476	2035	5457	169.8	144.9
Cd	0	2.00E-05	1.00E-04	0.0012	0.001514	0.03103	0.016	0.05	1.38	0.1293	0.001735	0.01179	416.7	144.6
Cl	0.01	27.13	2203	23110	9959	52450	89940	185000	364000	61450	34010	65040	117.1	147.2
Co	1.30E-05	3.22E-05	1.29E-04	7.53E-04	1.76E-03	0.4383	0.011	2.5	40	2.654	1.03E-03	8.06E-03	605.5	137.2
Cr	4.00E-04	0.002	0.05	1	0.3448	8.277	1	29	2204	57.68	1.186	0.7042	696.8	118.6
Cs	0	0.02	0.1	0.4	0.3865	1.738	1.4	5.406	87	5.94	0.5041	0.9637	341.8	126
Cu	0	3.00E-04	0.002	0.01	0.01683	0.7359	0.14	1	130	6.689	0.01453	0.1023	908.9	145.3
F	0.003	0.1	0.3	0.9	0.9024	2.303	2.44	9.1	320	7.067	1.038	1.586	306.9	115.3
FeTot	0	0.03	2.007	14	8.622	69.91	55.5	270	10000	265.1	20.27	39.65	379.2	144.8
Fell	0	0.2	0.3	1	1.901	92.51	6.5	167.5	8800	560.6	1.186	4.596	606	118.6
Fell	0.01	0.4	2	10.85	11.66	112.4	55	414.3	4150	406.6	15.05	39.29	361.8	138.7
Hg	2.20E-05	6.40E-05	0.0001275	2.00E-04	0.0003018	0.001554	0.0005475	0.003065	0.107	0.008444	0.0001483	0.0003113	543.4	74.13
I	0	0.0321	3.26	11	6.568	23.86	22	80	2080	67.58	13.14	13.89	283.3	119.4
K	0	3.6	20	98	119.4	922.4	780	4700	78200	2123	136.4	563.4	230.1	139.2
KNa	1	2.412	30	144.5	155.4	3243	1192	12480	67060	10360	209.8	861.7	319.5	145.2
Li	3.00E-04	0.025	1.05	4	3.175	20.52	12	80.3	1730	69.07	5.271	8.117	336.6	131.8
Mg	0	5	42	339	220.5	969.6	1394	3568	137100	1632	487.8	1002	168.3	143.9
Mn	1.00E-04	0.001	0.023	0.2	0.2067	6.598	1.605	46.9	440.5	20.45	0.2933	1.173	310	146.6
Mo	2.00E-04	0.001	0.0044	0.0143	0.01759	0.3628	0.04	1.4	28	1.98	0.01809	0.02639	545.7	126.5
Na	0.04	292	3096	15810	10000	28360	47470	93200	204300	30360	21950	32900	107.1	138.8
Ni	5.00E-05	0.000289	0.001	0.003	0.00519	0.1741	0.01365	0.4	18.6	1.097	0.003366	0.009377	630	112.2
Pb	4.00E-05	7.00E-05	0.001	0.005	0.01192	21.4	0.05	37.6	8187	368.9	0.007339	0.03632	1724	146.8
Rb	0	0.02	0.121	0.3505	0.4399	3.03	1.6	15.65	80	8.539	0.4159	1.096	281.8	118.7
S	0.1	0.2	1.6	3	3.137	32.55	3.2	99.95	1440	151.7	1.583	1.186	466.2	52.78
SO4	0	8	76.5	378.4	296.2	1123	1426	4751	60000	1821	525.5	1000	162.1	138.9
Se	2.00E-04	4.00E-04	0.001	0.002	0.004281	0.04367	0.0165	0.1	4.3	0.2326	0.001927	0.01149	532.7	96.37
Si	0	3	8.578	19	20.82	61.43	49.02	152.8	5555	247.7	19.27	29.98	403.2	101.4
Sn	0.0037	0.01749	0.5	1	0.4941	0.8485	1	1.85	2	0.4788	0	0.3706	56.43	0
Sr	0	0.29	12.16	107	58.24	391	448.9	1730	13100	726.3	156.4	323.8	185.7	146.2
Th	2.00E-05	2.00E-05	3.00E-05	7.00E-05	0.0001055	0.0004264	0.00026	0.002298	0.0054	0.001052	7.41E-05	0.0001705	246.8	105.9
Tl	0.0042	0.01111	0.04025	0.1	0.08869	0.1612	0.2	0.5	1	0.1874	0.1042	0.1184	116.3	104.2
V	2.00E-04	0.00143	0.00605	0.011	0.01304	0.04773	0.0298	0.187	1.5	0.1402	0.01038	0.01761	293.7	94.35
Zn	1.00E-04	0.0017	0.01	0.06	0.09668	7.271	0.951	18.04	575	37.26	0.08436	0.6976	512.5	140.6
TOC	2.98	20.5	48	120	123	270.6	260	1044	5680	507.3	127.5	157.2	187.5	106.3

## **Vita**

Stephanie Ray earned her Bachelor of Science in Geological Sciences from The University of Texas at El Paso in 2014. Stephanie has a broad set of experiences stemming from service in the Coast Guard, to ship-based expeditions in the South Pacific, to leading an interdisciplinary team at the Texas Innovation Challenge in Austin, Texas. Her master's thesis program consisted of analyzing brine water geochemical data analysis in support of the USGS Energy Resource Division.

Stephanie would like to continue and expand her research in produced water and operations to improve waste water management and resource recovery. She is interested in developing technology as part of an interdisciplinary team to maximize the potential for produced water recycling and reuse.

Contact Information: [slray@miners.utep.edu](mailto:slray@miners.utep.edu)

This thesis/dissertation was typed by Stephanie L. Ray